

School of Molecular and Life Sciences

**Macromolecular Engineering with Tailor-made Functional
Fluoropolymers via RAFT Polymerization and Diels-Alder Reaction**

Siva Ponnupandian

**This thesis is presented for the Degree of
Doctor of Philosophy
of
Curtin University**

January 2021

Macromolecular Engineering with Tailor-made Functional Fluoropolymers via RAFT Polymerization and Diels-Alder Reaction

*Thesis submitted to the
Indian Institute of technology, Kharagpur
and
Curtin University, Perth, Western Australia
for the award of the degree*

Doctor of Philosophy

Submitted by

Siva P

Under the Guidance of

**Prof. Nikhil K. Singha, IIT Kharagpur
Prof. Andrew B. Lowe, Curtin University**



**Rubber Technology Centre
Indian Institute of Technology
Kharagpur
West Bengal, India**



**School of Molecular and Life Sciences
Curtin University
Perth, Western Australia,
Australia**

January 2021

© 2021 Siva P. All rights reserved.

Dedicated to My Supervisors

Prof. Nikhil K. Singha

Prof. Andrew B. Lowe

Dedicated to My Brother
Prof. M. Rajesh Kannan

***Dedicated to
All My Teachers, Family
members and Friends***

APPROVAL OF THE VIVA-VOCE BOARD

28/01/2021

This is to certify that the thesis entitled “**Macromolecular Engineering with Tailor-made Functional Fluoropolymers via RAFT Polymerization and Diels-Alder Reaction**” submitted by **Mr. Siva P** to the Indian Institute of Technology, Kharagpur, India and Curtin University, Perth, Western Australia, under the Dual Doctoral Degree Program (DDDP) for the award of the degree **Doctor of Philosophy** has been accepted by the external examiners and that the student has successfully defended the thesis in the viva-voce examination held on **January 28, 2021** at Rubber Technology Centre, Indian Institute of Technology Kharagpur.

Prof. Susanta Banerjee
(Member of the DSC)

Prof. Dipak K. Maity
(Member of the DSC)

Prof. Kinsuk Naskar
(Member of the DSC)

Prof. Nikhil K. Singha
(Supervisor – IIT Kharagpur)

Prof. Andrew B. Lowe
(Supervisor - Curtin University)

Dr. Prakash P. Wadgaonkar
(External Examiner)

Prof. Santanu Chattopadhyay
(Chairman and Head of the Centre)



डॉ. निखिल कुमार सिंह, एफ.आर.एस.सि.

प्राध्यापक

Dr. Nikhil Kumar Singha, FRSc

Professor

भारतीय प्रौद्योगिकी संस्थान

रबड़ प्रौद्योगिकी केन्द्र

खड़गपुर-721 302, भारत

**Indian Institute of Technology
Rubber Technology Centre**

Kharagpur - 721302, India

CERTIFICATE

This is to certify that the thesis entitled "**Macromolecular Engineering with Tailor-made Functional Fluoropolymers via RAFT Polymerization and Diels-Alder Reaction**" submitted by **Mr. Siva P** to Indian Institute of Technology Kharagpur, Kharagpur, India and Curtin University, Perth, Western Australia is a record of bonafide research work done under the joint supervision of myself and Prof. Andrew B. Lowe from Curtin University under the Dual Doctoral Degree Program (DDDP) and I consider it worthy of consideration for the award of the degree of Doctor of Philosophy of the Indian Institute of Technology Kharagpur and Curtin University.

Date:

(Prof. Nikhil K. Singha)
Rubber Technology Centre
IIT Kharagpur

Phone (दूरभाष) : Office (कार्यालय) +91-3222-283178 / 282291, Residence (आवास) : +91-3222-283179

Fax (फैक्स) : +91-3222-255303 / 282700, Email (ई-मेल) : nks@rtc.iitkgp.ac.in / nks@rtc.iitkgp.ernet.in / nks8888@yahoo.com



Andrew B. Lowe
Professor of Polymer Science &
Director, Curtin Institute of Functional
Molecules and Interfaces

Discipline of Chemistry
School of Molecular & Life Sciences
Faculty of Science & Engineering

Telephone +61 8 9266 9281
Email andrew.b.lowe@curtin.edu.au

CERTIFICATE

This is to certify that the thesis entitled “**Macromolecular Engineering with Tailor-made Functional Fluoropolymers via RAFT Polymerization and Diels-Alder Reaction**” submitted by **Mr. Siva P** to Indian Institute of Technology Kharagpur, Kharagpur and Curtin University, Perth, Western Australia is a record of bonafide research work under the joint supervision of myself and Prof. Nikhil K Singha from Indian Institute of Technology Kharagpur under the Dual Doctoral Degree Program and I consider it worthy of consideration for the award of the degree of Doctor of Philosophy of the Indian Institute of Technology Kharagpur and Curtin University.

Date: 28th January 2021

(Prof. Andrew B. Lowe)
Curtin University, Perth
Western Australia

Acknowledgements

First, I take this exorbitantly euphoric opportunity to express my overwhelming sense of gratitude to my Supervisors, *Prof. Nikhil K. Singha* and *Prof. Andrew B. Lowe*.

It was indeed an honour, pride and privilege working under the meticulous supervision of Prof. Singha. The friendly guidance of my supervisor from day one till hitherto enabled me to develop an understanding of the current area of research and helped me inculcating the scientific bent of mind in solving the research problems. I also thank him for the personal and moral support during tough times during my research life.

My ineffable and humble greetings to *Prof. Lowe* for allowing me to work in his laboratory. I am grateful to him for his ardent and ablest guidance, continued interest, and incessant encouragement throughout my tenure.

I am very much thankful to the present Head of the Centre, *Prof. Santanu Chattopadhyay*, for providing me facilities and official supports during my research program.

I would also like to express my sincere thanks to all the faculty members of our centre, *Prof. Kinsuk Naskar*, *Prof. Narayan Chandra Das*, *Prof. Titash Mondal* and *Prof. Soumyadip Chowdury* for their timely help, supports and encouragement during my research work.

I am also thankful to the former faculties of our centre, *Prof. Dipak Khastgir*, *Prof. Tapan Kumar Chaki*, *Prof. Golok B. Nando* and *Prof. Anil Kumar Bhowmick* for their support in the early carrier of my research at IIT Kharagpur.

I am very much thankful to my DSC members, *Prof. Susanta Banerjee*, *Prof. Dipak Kumar Maiti* and *Prof. Kinsuk Naskar* for their valuable comments and suggestions during all my seminars, generous co-operation and constant inspiration to carry out the research work.

I thank IIT Kharagpur-Curtin University Dual Doctoral Degree Program co-ordinators, *Prof Barghab Maitra* (IIT Kharagpur) and *Prof Abhijit Mukherjee* (Curtin University) for all their effort and support for this collaborative Ph.D. Program.

I would like to acknowledge the help and co-operation of my senior and present lab mates, *Dr. Arindam Chakkraborty*, *Dr. Bishnu P. Koiry*, *Dr. Prithwiraj Mandal*, *Dr. Souvik Ata*, *Dr. Nabendu B. Pramanik*, *Dr. Prasanta K. Behera*, *Dr. Sovan lal Banerjee*, *Dr. Prantik Mondal*, *Mr. Girish Mirchandani*, *Mr. Arunjunai Raja Shankar*, *Mr. Sarthik Samanta*, *Mr. Koushik Bhattacharya*, *Mr. Uddhab Kalita*, *Ms. Shrabana Sarkar*, *Mr. Sagar Kumar Raut*, *Mr. Ritabarata Ganguly* *Mr. Tuhin Subhra Pal*, *Ms. Bhavya Parameswaran*.

I thank the constant help and support from colleagues and friends of our centre especially, *Dr. Selvakumar M*, *Dr. Padmanaban*, *Dr. Vijayalekshmi*, *Dr. Drupita*, *Dr. Sudipta Panja*, *Mrs. Anagha*, *Mrs. Laksmi M Mukhundhan*, *Mrs. Ashwathi*, *Ms. Sreethu*, *Mr. Sanjay Remanan*, *Mr. Jeevanantham*, *Mr. Sanjay Pal*, *Mr. Abhay Kumar*, and scholars from other departments *Dr. Vasudevan Subramaniam*, *Dr. Melvin Samuel*, *Dr. Vasudevan B*, *Dr. Janakiraman*, *Ms. Jayita Chakrobarty* and *Mr. R. Rajesh Kumar*, *Mr. Kishore*, and *Mr. Sudhakar*.

I would like to express my gratitude to all my colleagues and friends in building 500, Curtin University especially Prof. Lowe's lab members *Mr. Nicholas Shen Loong Tan*, *Mr. Harry Jepson*, *Ms. Ellena Dallerba* for their valuable help and encouragement during my stay at Curtin University. I also extend my thanks to the other friends at Curtin University, *Ms. Shagraf*, *Dr. Barani*, *Dr. Mrunmai*, *Dr. Sanket*,

Dr. Adirath, Dr. Subra, Dr. Sambhu, Dr. Subrata, Mr. Hari, Mr Herald, Mr. Raturaj, Mr. Krushna, Ms. Asha, Ms. Sakshi, Ms. Deepali, and Ms. Rofia for their support.

Special thanks to *Dr. Prantik Mondal, Mr. Sarthik Samanta, and Mr. Sanjay Remanan* for their extensive support during my thesis preparation.

I wish to thank all the instrument operators in CRF and all the non-teaching staff of RTC, especially *Mr. Syed Musthaq and Mr. Rajesh De*, for their extensive co-operation during the conduct of research.

I would like to thank *Mr. Satya Sadhan Datta, Mr. Anubhab Das and Mr. Ramu Lingam* for their help and support in handling my official documents during my entire tenure and thesis submission.

I thank *Prof. Anbarasan Ramasamy and Dr. Meenarathi Anbarasan*, my undergraduate and postgraduate research mentors for their continuous motivation and support. I thank all the faculties of Department of Polymer Technology, Kamaraj College of Engineering and Technology, Virudhunagar, Tamilnadu for their constant support till date. Special thanks to *Dr. Agathian, Mr. Sivakuamravel, Mr. Selva Kumar, Dr. Sribala, Dr. Jeyapriya, Dr. Kannamal, and Dr. Palani Kumar*, for their support.

I thank my school and college friends *Mr. Kamesh, Mr. Siva Guru, Mr. Adithya Harsha, Mr. Lena Kannan, Mr. Mithun*, for their constant support and encouragement. Thanks to my friends in Australia *Mr. Syed Rafeek, Mr. Sheik Fareeth, Mr. Rahul Anand, Mrs. Molly and Ms. Thisarie* for their support and help during my stay in Australia. Thanks to all my friends gang specially *Annanchi Kootam, Bijili Gang, Our Own ADDA, N 207, ZH samayal Arai and IITKGP Tamil Sangam* for their help and warm friendship which will be cherished forever.

I am obligated to *Prof. Rajesh Kannan M and Prof. Ganesh Venkatraman* for their valuable help and moral support during the lockdown days.

I wish to acknowledge *CSIR, New Delhi*, for providing me financial assistance to carry out my research work. I am also very much thankful to *IIT Kharagpur and MHRD* for providing me fellowship during my stay at Kharagpur, and I extend my thanks to Curtin University for providing me scholarship during my stay at Perth.

I am thankful to Hybrid Plastics, USA for providing the POSS materials.

It is indeed an agony with an abundance of happiness at the end to express my feelings towards my family for their consistent support and sacrifice in different parts of my life. My sincere indebtedness, love and gratitude to my beloved father *Mr. Ponnupandian*, my Mother *Mrs. Vijayalakshmi*, my wife *Mrs. Eniya*, all my niece and nephews, my elder brother *Mr. Kaniarasan*, my sisters *Mrs. Durga, Mrs. Kanimozhi, Mrs. Kanipriya*, my brothers-in-law *Mr. Paulraj, Mr. Rajkumar, Mr. Gajendra Kumar*, and my uncle *Mr. Ramakarishnan*. Special thanks to my uncle *Dr. Murugesan Mariappan* for being my role model and motivating me since my childhood to pursue a research career. Special mention to all the cute littles.

Finally, this acknowledgement would be incomplete without specifically thanking my brother, well-wisher and cycling partner *Prof. Rajesh Kannan*, Department of mathematics, IIT Kharagpur who allowed me to stay with him and been supportive during the tough times and the entire lonely days of the pandemic situation. Special thanks for his inspiring support, motivation, fruitful discussions, and positive thoughts. I am also thankful to his family especially master Advait Kanna for their unconditional kindness and support.

(Siva P)

DECLARATION

I certify that

- The work contained in the thesis is original and has been done by myself under the general supervision of my supervisors.
- The work has not been submitted to any other Institute for any degree or diploma.
- I have followed the guidelines provided by the Institute in writing the thesis.
- I have conformed to the norms and guidelines given in the Ethical Code of Conduct of the Institute.
- Whenever I have used materials (data, theoretical analysis, and text) from other sources, I have given due credit to them by citing them in the text of the thesis and giving their details in the references.
- Whenever I have quoted written materials from other sources, I have put them under quotation marks and given due credit to the sources by citing them and giving required details in the references.

(Siva P)

List of Abbreviations

4VP	4-vinyl pyridine
ABCVA	4,4'-azobis(4-cyanovaleric acid)
ACA	9-anthracene carboxylic acid
ACM	n-acryloyl morpholine
AE	Alder-ene
AFM	Atomic Force Microscopy
AIBN	2,2'-azobisisobutyronitrile
ATRP	Atom transfer radical polymerization
BA	Butyl acrylate
BCP	Block copolymers
bisTAD	(4,4'-(4,4'-diphenylmethylene)-bis-(1,2,4-triazoline-3,5-dione))
CA	Contact angle
CDTSPA	4-Cyano-4-[(dodecylsulfanylthiocarbonyl)sulfanyl]pentanoic acid
CHCl ₃	Chloroform
CPDTC	2-cyano-2-propyl dodecyl trithiocarbonate
CRP	Controlled radical polymerization
CSIRO	Commonwealth Scientific and Industrial Research Organization
CTA	Chain transfer agents
DA	Diels-Alder
DCC	N,N'-dicyclohexylcarbodiimide
DCM	Dichloromethane
DMAEMA	2-(dimethylamino)ethyl methacrylate
DMAP	4-dimethylaminopyridine
DMF	N, N-dimethylformamide
DMSO-d ₆	Dimethyl sulfoxide-d ₆
DSC	Differential scanning calorimetry
EC	Ethyl carbazate
EDX	Energy dispersive X-ray
F ₆ BMA	2,2,3,4,4,4-hexafluorobutyl methacrylate
FA	Fluorinated acrylates
FDA	1H,1H,2H,2H-perfluorodecyl acrylate

FESEM	Field emission scanning electron microscope
FHEMA	Perfluorohexylethyl methacrylate
FMA	Fluorinated methacrylates
FOEMA	2-(perfluorooctyl)ethyl methacrylate
FRP	Free radical polymerization
FT-IR	Fourier transform infrared
GMA	Glycerol monomethacrylate
GPC	Gel permeation chromatography
HCR	High Consistency Rubber
HDFDMA	Heptadecafluorodecyl methacrylate
HEMA	2-hydroxyethyl methacrylate
HFBA	2,2,3,3,4,4,4-heptafluorobutyl acrylate
KPS	Potassium persulfate
LAMs	Less activated monomers
MAePOSS	Methacryloethyl POSS
MA _{ib} POSS	Methacryloisobutyl POSS
MAMs	More activated monomers
MMA	Methyl methacrylate
NMP	Nitroxide-mediated polymerization
NMR	Nuclear magnetic resonance
NVP	N-vinyl pyrrolidone
OM	Optical Microscopy
PET	Poly(ethylene terephthalate)
PFPMA	Pentafluorophenyl methacrylate
PISA	Polymerization-induced self-assembly
POSS	Polyhedral Oligomeric Silsesquioxane
POSS-M	POSS-maleimide isobutyl
PTFE	Polytetrafluorethylene
RAFT	Reversible Addition Fragmentation Chain Transfer Polymerization
RDRP	Reversible-Deactivation Radical Polymerization
SAXS	Small Angle X-ray Scattering
SFEP	Surfactant free emulsion polymerization
SHP	Self-healing Polymer

SMP	Shape memory polymers
SS	Sodium 4-vinylbenzene sulfonate
TAD	1,2,4-triazoline-3,5-dione
TBCP	Triblock block copolymer
TEM	Transmission Electron Microscopy
TFEA	2,2,2-trifluoroethyl acrylate
TFEMA	2,2,2-trifluoroethyl methacrylate
TGA	Thermogravimetric analysis
THF	Tetrahydrofuran
WCA	Water contact angle
XPS	X-ray photoelectron spectroscopy

Table of Contents

	Content	Page No.
	Title Page	i
	Approval of the Viva-Voce Board	ix
	Certificate from Prof. Nikhil K. Singha	xi
	Certificate from Prof. Andrew B. Lowe	xiii
	Acknowledgement	xv
	Declaration	xxi
	List of abbreviations	xxi-xxiii
	Table of Contents	xxv-xxix
	Abstract	xxx
Chapter-1	Introduction and Literature Review	01-48
1.1	Polymers	01
1.2	Polymerization	01
1.3	Polymerization Techniques	03
1.4	Reversible-Deactivation Radical Polymerization (RDRP)	04
1.4.1	Reversible Addition Fragmentation Chain Transfer Polymerization (RAFT)	06
1.5	Fluoropolymers	09
1.6	Organic/inorganic hybrid polymers	11
1.6.1	Polyhedral Oligomeric Silsesquioxane (POSS)	14
1.7	Hydrophobic Polymers	15
1.8	Self-healing Polymer (SHP)	16
1.9	Self-assembly in polymers	21
1.10	Polymerization-induced self-assembly (PISA) in polymers	21
1.11	Literature Review	23
1.12	Scope and Objectives of the Work	29
	References	30
Chapter-2	Experimental and Characterization Techniques	49-56
2.1	Materials	49
2.1.1	Monomers	49

2.1.2	RAFT agents	49
2.1.3	Thermal initiators	50
2.1.4	Solvents and other reagents	50
2.1.5	Cross-linker (Dienophile)	51
2.2	Characterization Techniques	51
2.2.1	Gel permeation chromatography (GPC) analysis	51
2.2.2	Nuclear magnetic resonance (NMR) spectroscopy	52
2.2.3	Fourier transform infrared (FT-IR) spectroscopy	52
2.2.4	Differential scanning calorimetry (DSC)	52
2.2.5	Thermogravimetric analysis (TGA)	53
2.2.6	Optical Microscopy (OM)	53
2.2.7	Field Emission Scanning Electron Microscopy (FE-SEM)	53
2.2.8	Transmission Electron Microscopy (TEM)	53
2.2.9	Atomic Force Microscopy (AFM)	54
2.2.10	Small Angle X-ray Scattering (SAXS) Analysis	54
2.2.11	X-ray photoelectron spectroscopy (XPS) Analysis	54
2.2.12	Contact angle analysis	54
2.2.13	Mechanical Properties	55
2.2.14	Dielectric Study	55
2.2.15	Self-healing study	55
Chapter-3	POSS and Fluorine Containing Nanostructured Block Copolymer; Synthesis via RAFT Polymerization and its Application as Hydrophobic Coating Material	57-86
	Abstract	57
3.1	Introduction	58
3.2	Experimental	61
3.2.1	Preparation of PMAibPOSS via RAFT Polymerization	61
3.2.2	Preparation of PTFEMA via RAFT Polymerization	61
3.2.3	PMAibPOSS- <i>block</i> -PTFEMA preparation using PMAibPOSS as a macro-RAFT agent	62
3.2.4	Preparation of fabric and metal surfaces for coating with BCP	62
3.3.	Results and discussion	63

3.3.1	Preparation of PMAibPOSS and PTFEMA Block Copolymers	63
3.3.2	¹ H NMR spectroscopy	63
3.3.3	GPC Analysis	65
3.3.4	FTIR Analysis	68
3.3.5	Thermal Analysis	68
3.3.6	Morphology Study	70
3.3.7	SAXS Analysis	74
3.3.8	XPS Analysis	75
3.3.9	Water Contact Angle (WCA) Analysis	76
3.3.10	Preparation of PMAibPOSS- <i>b</i> -PTFEMA coated Hydrophobic Surfaces	78
3.4	Conclusion	79
	References	80
Chapter-4	Self-healing Ultrahydrophobic POSS-Functionalized Fluorinated Copolymer via RAFT Polymerization and Dynamic Diels-Alder Reaction	87-112
	Abstract	87
4.1	Introduction	88
4.2	Experimental section	90
4.2.1	Synthesis of PTFEMA ₄₅ - <i>rand</i> -PFMA ₃₈ (P1) via RAFT polymerization	90
4.2.2	Modification of P1 copolymer with POSS maleimide via DA reaction	91
4.3	Results and discussion	91
4.3.1	Synthesis of furfuryl bearing tailor-made fluorocopolymer and DA reaction between POSS-M and the furfuryl group in the copolymer	91
4.3.2	¹ H NMR Spectroscopic analysis	92
4.3.3	GPC analysis	97
4.3.4	FTIR analysis of copolymer and DA-modified copolymer	98
4.3.5	Differential Scanning Calorimetry (DSC) analysis	99
4.3.6	TGA analysis of Polymers	101
4.3.7	Self-healing analysis of polymers	102
4.3.8	Hydrophobicity and surface morphology of the polymers	105

4.4	Conclusion	107
	References	108
Chapter-5	A Multifunctional Triblock Copolymer Based on Fluoroacrylate via Polymerization-Induced Self-Assembly (PISA); Synthesis and Application as A Thin Film Dielectric Material	113-138
	Abstract	113
5.1	Introduction	114
5.2	Experimental section	117
5.2.1	Synthesis of macro-RAFT (PSS) via RAFT polymerization	118
5.2.2	Synthesis of the diblock copolymer (PSS- <i>b</i> -PBA) via surfactant-free RAFT polymerization	118
5.2.3	Synthesis of the triblock copolymer (PSS- <i>b</i> -PBA- <i>b</i> -PTFEA) (TBCP) via surfactant-free RAFT emulsion polymerization	119
5.3	Results and discussion	119
5.3.1	Synthesis of PSS- <i>b</i> -PBA- <i>b</i> -PTFEA triblock copolymer (TBCP) via PISA	119
5.3.2	¹ H NMR Spectroscopic analysis	120
5.3.3	FTIR analysis of polymers	123
5.3.4	Differential scanning calorimetry (DSC) analysis	123
5.3.5	TGA analysis	124
5.3.6	Transmission electron microscopy (TEM) analysis	125
5.3.7	Dynamic light scattering (DLS) study	126
5.3.8	Analysis of Tensile properties of TBCP	127
5.3.9	Water contact angle (WCA) analysis	128
5.3.10	AC impedance spectroscopy	129
5.4	Conclusions	131
	References	132
Chapter-6	Self-Healable Hydrophobic Anthracenyl Functionalized Fluorous Block Copolymer via RAFT Polymerization and Diels-Alder Reaction using 1,2,4-triazoline-3,5-dione (TAD) Derivative	139-158
	Abstract	139

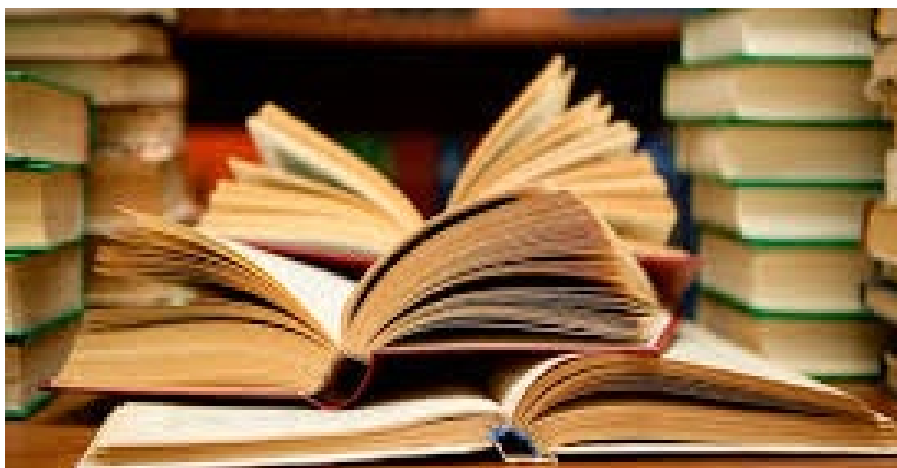
6.1	Introduction	140
6.2	Experimental section	142
6.2.1	Preparation of (4,4'-(4,4'-diphenylmethylene)-bis-(1,2,4-triazoline-3,5-dione)) (bisTAD)	142
6.2.2	Preparation of poly(HEMA- <i>block</i> -TFEMA) using CDTSPA as the RAFT agent	143
6.2.3	Modification of PHEMA- <i>block</i> -PTFEMA using anthracenecarboxylic acid (ACA) and crosslinking using TAD compound	144
6.2.4	Crosslinking reaction of anthracenyl modified BCP using TAD Compound	145
6.3	Results and discussion	145
6.3.1	Preparation of PHEMA- <i>block</i> -TFEMA and modification of BCP with anthracenyl unit and further crosslinking using bisTAD	147
6.3.2	¹ H NMR spectroscopic analysis	146
6.3.3	FTIR analysis of polymers	149
6.3.4	Differential scanning calorimetry (DSC) analysis	151
6.3.5	Water contact angle (WCA) analysis	152
6.3.6	Self-healing analysis	153
6.4	Conclusion	154
	References	155
Chapter-7	Summary and Conclusions	159-167
7.1	Summary and Conclusions	159
7.2	Contribution of thesis	162
7.3	Future scope of the thesis	163
	List of Publications	
	Curriculum Vitae	

Abstract

Fluoropolymers, since its serendipitous discovery in 1930 has attained enormous research and technological importance and important marketplace in the development of advanced materials having interesting structural and functional properties. Owing to the unique properties of fluoropolymers such as excellent water and oil resistance, chemical resistance and thermal stability they have been widely used in developing speciality coatings. This thesis reports on the preparation of well-defined functional fluoropolymers such as block and random copolymers based on fluoroacrylates and fluoromethacrylates along with different comonomers via reversible addition-fragmentation chain-transfer (RAFT) polymerization. The potential application of these fluoropolymers mainly as a coating material along with other different properties such as self-healing behaviour was studied. The functional copolymers bearing fluoroalkyl groups and other reactive groups were further modified by post polymerization modification using Diels-Alder chemistry to prepare polymers with self-healing property. The functional copolymers prepared were characterized using FT-IR, ¹H-NMR, GPC, TGA, DSC, SAXS, XPS and AFM analyses. The self-healing property was studied by scratch-and-heal analysis, which was monitored using optical microscopy (OM) and AFM analyses. At first, block copolymers comprising hybrid polyhedral oligomeric silsesquioxane (POSS) and 2,2,2-trifluoroethyl methacrylate (TFEMA) were prepared via RAFT polymerization. The morphological behaviour of the BCPs was studied in different solvents. The BCP thin films demonstrated core-shell type morphology when deposited from chloroform and lamellar type morphology when deposited from THF as the solvent. Further, the potential application of the BCPs as a hydrophobic coating material was studied by coating the BCPs over different substrates such as glass, cotton fabric and an aluminium metal plate via dip-coating. Interestingly, the BCPs showed hydrophobicity up to ~135° over cotton fabric. To develop a fluoropolymer with self-healing functionality along with the excellent hydrophobicity, random copolymer consisting of PTFEMA and poly(furfuryl methacrylate) (PFMA) was synthesized by RAFT polymerization. Further, the furfuryl moieties of this copolymer were modified via Diels-Alder (DA) reaction using varied content of POSS-maleimide (POSS-M). In addition, to increase in hydrophobicity the copolymers exhibited good self-healing efficiency (~78 %) due to dynamic DA covalent bonds between the reactive furan group in the copolymer and the maleimide group in POSS-M. Further, to prepare fluoropolymers with fast crosslinking efficiency BCPs comprising TFEMA and 2-hydroxyethyl methacrylate (HEMA) was prepared via RAFT polymerization. Then the hydroxyl groups of the BCP were modified with anthracenyl moiety and were crosslinked using 1,2,4-triazoline-3,5- dione (TAD) derivatives which led to faster dynamic conjugation with anthracenyl moiety. Interestingly, the hydrophobicity of the BCP was not changed even after incorporation of hydrophilic TAD moiety and the self-healing property was studied using AFM analysis. A multifunctional triblock copolymer (TBCP) comprising sodium 4-vinylbenzene sulfonate (SS), butyl acrylate (BA), and 2,2,2-trifluoroethyl acrylate (TFEA) was prepared via the polymerization induced self-assembly (PISA) process using RAFT polymerization. The TBCP film showed interesting mechanical properties with remarkable high elongation of 1500%. Moreover, the TBCP exhibits excellent hydrophobicity having a water contact angle (WCA) ~122°. The dielectric properties of the prepared copolymer were studied using AC-impedance analysis.

Keywords: *Fluoropolymers, RAFT, Diels-Alder Reaction, hydrophobicity, self-healing.*

INTRODUCTION AND LITERATURE REVIEW



This chapter presents the basics of different methods of polymerization, an introduction to fluoropolymers, POSS-based hybrid materials, RAFT polymerization, click chemistry, self-healing polymers, hydrophobic coating materials and the corresponding literature review. This chapter also includes the objectives and scope of the work.

1.1 Polymers

Polymers, once criticized by the scientist community as a "Schmierenchemie" (greasy chemistry) in the early 20th century, have become an essential aspect of research and innovation over a century after the introduction of the "macromolecular concept" by Herman Staudinger in 1920. [1] The name polymer (πολύς – polus meros) is coined from the Greek phrases "polus-poly-many + meros-mer-parts." Polymers, as per the IUPAC definition are defined as "A molecule of relatively high molecular mass, the structure of which essentially comprises the multiple repetitions of units derived, actually or conceptually, from molecules of low relative molecular mass." [2] Polymers, based on their ultimate form, usage, and the basic properties are broadly classified as "thermosets," "thermoplastics," or "elastomers." Research curiosity in the arena of polymer science and engineering has evolved significantly from its inception leading to amazing discoveries and made a massive revolution towards the development of cost-effective and durable materials and also led to the development of impressive advanced functional materials including liquid crystalline polymers, hydrogels, self-healing polymers (SHPs) and shape memory polymers.

1.2 Polymerization

The process of synthesizing polymers from monomer(s) is termed 'polymerization.' Generally, a polymerization process is broadly classified as an addition or step-growth polymerization. Step growth polymerization involves step by step process and monomers with functional groups like -COOH, -OH and -COCl. and generally, involves the elimination of small molecules like water as a condensate. The polymers obtained from several heterocyclic monomers, polyethers, polycaprolactones, and polyurethanes are generally produced via step-growth polymerization. [3-6] Chain growth or radical addition polymerization mostly uses

vinyl monomers and involves the sequential addition of monomer to the growing polymer chains by a chain growth process via an active centre. There is no elimination of small molecules, as in the case of step-growth polymerization. Chain-growth polymerization is broadly categorized as 1) ionic polymerization, 2) coordination chain polymerization, and 3) radical chain polymerization. In ionic polymerization, an ionic species is generated to act as the active center. [7, 8] They are further classified based on the charge of the activating ion as anionic and cationic polymerization. Anionic polymerization is also referred to as "living polymerization" as the chain-termination process is stopped, and a polymer with a living end or active end group can be synthesized. [7] This active chain can be used further to react with another monomer to produce block copolymers (BCP). Ionic polymerization is challenging commercially given its stringent reaction conditions. [9] Coordination chain polymerization (CCP) employs a metal catalytic system. CCP is commonly employed for the industrial production of olefinic polymers. One widely known CCP is that based on Ziegler-Natta catalysts, invented by the renowned scientists K. Ziegler and G. Natta in 1963, which led to the award of the Noble Prize. [10-13] Despite the commercial production usage for olefinic monomers, the catalysts are susceptible to moisture and oxygen and fail to polymerize heteromolecular monomers viz., functional acrylates or acrylamides. The catalysts can also undergo side reaction with the reactive groups of specialty functional monomers leading to usage limitations. Radical chain polymerization (RP), where a free radical with lone pair of electrons generated by the decomposition of the initiator acts as an active center. RP involves three main steps i) initiation, where the primary radicals are generated by decomposition of initiators and the first radical-monomer adduct is formed ii) propagation, where the radicals react with monomer and the majority of chain growth

takes place, and iii) termination, where the active radicals are deactivated via chain transfer or disproportionation reaction or coupling reaction. [3-6, 14-16] RP is the most extensively utilized process for the industrial production of commodity polymers with high molecular weight. RP is one of the feasible methods that can be adapted to synthesize a wide range of polymers. Despite of its advantages, there are several drawbacks to the RP process, like the polymers produced by this technique have very broad molecular weight distributions and high molecular weight. This uncontrollable molecular weight becomes a drawback hindering the functional properties of the polymer, making it difficult to process and to find a suitable solvent for the synthesized polymer. Preparing polymers with controlled architecture, as well as with well-defined topology, is very difficult via RP. For example, it is very challenging to prepare block, star, and brush-like copolymers via conventional RP. Reversible-deactivation radical polymerization (RDRP) overcomes this drawback by helping in controlling the molecular weight and in making tailor-made polymers with desired properties. The detailed explanation about the RDRP is described in the following sections.

1.3 Polymerization Techniques

Based on the physical aspects, a polymerization process can be classified broadly as a bulk, solution, suspension, or emulsion polymerization. [5, 6, 16] The factors like the nature of the monomer, output physical form of the polymer required, the type of polymerization mechanism it undergoes, and notably, the viability of the process for commercial production of polymers helps in deciding the polymerization technique required for polymer synthesis. In the case of bulk polymerization, the monomer in the liquid form and the initiator dissolved in the monomer in a reactor are polymerized. [17] It is a simple process and gives high purity product as there are no

other ingredients. But they produce high molecular weight polymers and sometimes lead to gelation as a result of poor heat conduction in the reactor. Solution polymerization involves the use of a suitable inert solvent where the monomer and the initiator are dissolved, and the polymerization proceeds. The drawbacks of poor heat conduction and gelation in bulk polymerization can be overcome by this method. Still, the achievement of high molecular weight can be hindered due to chain transfer to solvent and removal of solvent traces in the end product makes it a tedious process. Suspension polymerization involves suspending monomer and the monomer soluble initiator in water in the form of droplets and stabilized with stabilizing agents, followed by the polymerization reaction. In this process, the product is obtained in the form of beads or pearls and can be used directly for molding after drying. But this technique is limited to water-insoluble monomer(s) and polymer(s). Emulsion polymerization involves forming a uniform emulsion of monomer in water and stabilizing the emulsion with surfactants. Polymerization in this technique takes place in micelles formed by the surfactants. The product polymer is in the form of latex, which can be used directly or precipitated to obtain a polymer. This is one of the most widely used techniques in industry.

1.4 Reversible-Deactivation Radical Polymerization (RDRP)

After the introduction of "reversible-deactivation radical polymerization (RDRP)," previously called living or controlled radical polymerization (CRP) in the 1990s, RDRP has been an essential synthetic tool for the synthesis of functional polymers. RDRP leads to the development of polymers with controlled molecular weights along with low dispersity (D). The presence of an active end group in the synthesized polymer shows living nature, and it can be further used to prepare complex macromolecular architectures like block, star, or graft copolymers, or other

complex architectures. [18-21] **Figure 1.1** illustrates the architectures that can be accessed using RDRP techniques. The RDRP techniques, like nitroxide-mediated polymerization (NMP), atom transfer radical polymerization (ATRP), and reversible addition-fragmentation chain transfer polymerization (RAFT) are of great interest. They are used to synthesize polymers with well-defined architectures and tailor-made properties. Among the available RDRP methods known, ATRP and RAFT are the two most widely employed for the synthesis of functional (co)polymers under a wide range of experimental conditions. ATRP involves the use of transition metal halides based on Cu, Fe or Ru as a catalyst in combination with suitable amine containing ligands. [22, 23] It was observed that there are some issues when ATRP is used for specific monomers. Metal catalysts and their complexes are not soluble in monomers which have low surface energy. Importantly metals have to be separated from the polymers via a tedious separating process. [24] RAFT polymerization involves RP in the presence of certain thiocarbonyl chain transfer agents. This polymerization produces a polymer with an active end group that can be further exploited to form block copolymers. As this thesis involves the RAFT polymerization process, a more comprehensive perspective on RAFT polymerization is emphasized in the subsequent section.

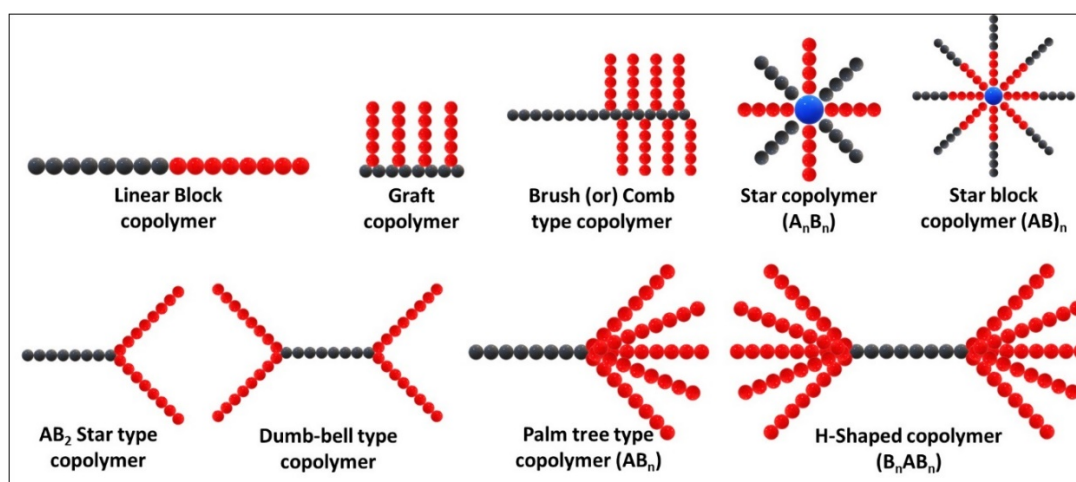


Figure 1.1 Complex architectures that can be achieved utilizing RDRP techniques

1.4.1. Reversible Addition Fragmentation Chain Transfer Polymerization (RAFT)

The RAFT polymerization process was developed in 1998 by the Commonwealth Scientific and Industrial Research Organization (CSIRO) in Melbourne, Australia. [25-31] Soon after the introduction of the concept of RAFT polymerization, it became the focus of intensive research in the development of tailor-made macromolecules. Among all the RDRP techniques, the RAFT process is a highly versatile method that has been exploited for the preparation of polymers with tailored architectures such as linear block copolymers, [27, 32, 33] star-branched, [34, 35] shell-cross-linked micelles, [36, 37] core-cross-linked materials, [38] and many other systems. [39-41]

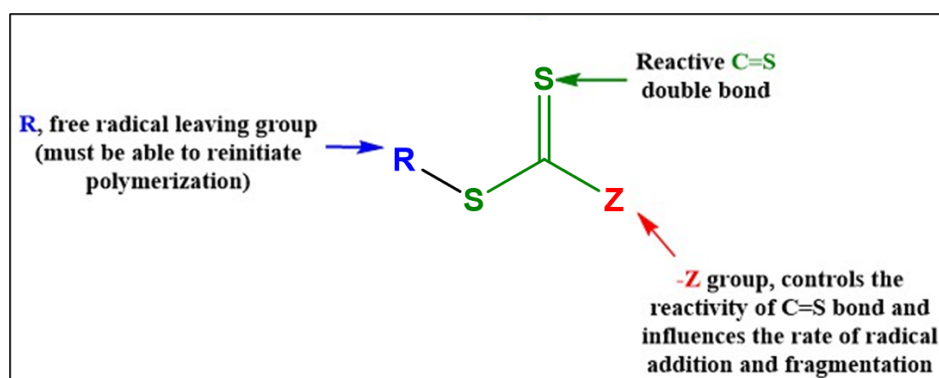


Figure 1.2a. The general structure of a RAFT agent

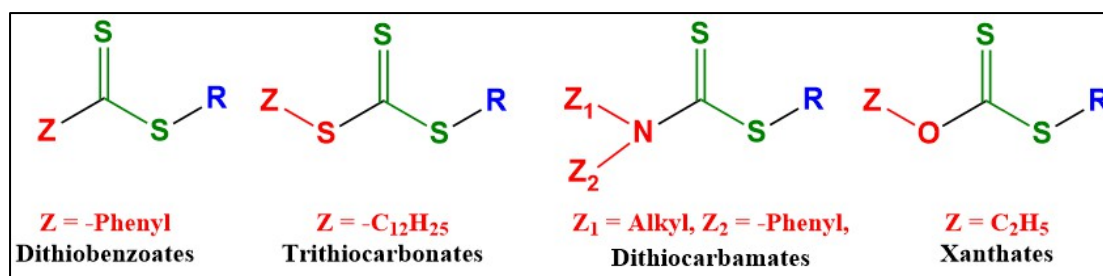


Figure 1.2b. Types of RAFT agents

As mentioned earlier, the RAFT process is based on the degenerative chain transfer phenomena with specifically designed chain transfer agents (CTA). The presence of a suitable RAFT agent is mandatory to attain a controlled polymerization

via the RAFT process. **Figure 1.2a** shows the general structure of a RAFT agent. The $-R$ and $-Z$ groups are the critical components of a RAFT agent. In this case, the $-R$ group is a free-radical leaving group that can reinitiate polymerization. During the polymerization, the propagating radicals add to the $C=S$ and fragments the $-R$ group as a free radical. The $-Z$ groups are responsible for influencing the bulk reactivity of the $C=S$ bond toward radical addition [26, 29, 30, 42-44]. Based on the $-Z$ group, the RAFT agents are categorized into dithiobenzoates, trithiocarbonates, dithiocarbamates, and xanthates. **Figure 1.2b** shows the basic chemical structures of different classes of RAFT agents.

Figure 1.3 illustrates the mechanism of the RAFT polymerization based on a dithioester type RAFT agent. In this case, the polymerization proceeds through a series of steps. The initial step is similar to the initiation step in conventional RP, i.e. the primary radicals are generated from thermal decomposition of suitable initiators. The radicals generated then add to monomer forming the $I-M^*$ propagating radicals. In the next step, the propagating radical attacks the $C=S$ bond in the RAFT agent (1) forming a pre-equilibrium intermediate radical species (2). The intermediate radical then fragments, forming a new propagating radical that with the concurrent formation of a new chain transfer species, (3). In this case, a rapid equilibrium exists between dormant species and active radicals. This enables the active radical concentration to remain low and offers equal probability for all chains to grow, and an equilibrium is established with the leaving group radical (R^*). In the third step, reinitiation occurs where the radical (R^*) reacts with monomer and generates oligomeric radicals (P_m^*), or it can react back to the RAFT agent (1). This macro RAFT agent may undergo chain equilibration (step 4) with another oligomeric species (P_m^*). The overall reactivity of the RAFT agents depends on the activating group (Z) and leaving group

(R[•]). Compared to the propagating polymeric radicals, R[•] should be a stable free radical leaving group and must have the capability to reinitiate polymerization reaction by reacting with monomers to produce new propagating polymeric chains. [26, 31]

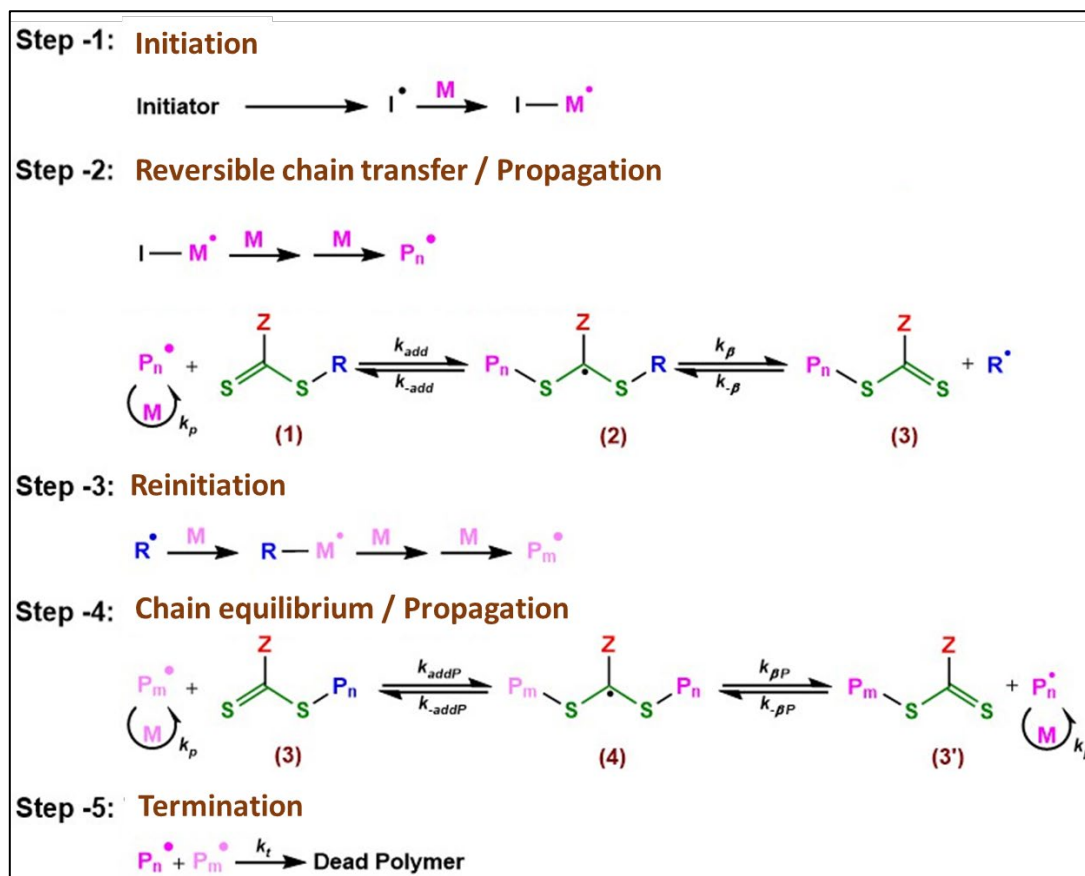


Figure 1.3. Mechanism of RAFT Polymerization (Adapted from Moad et al. [26])

RAFT polymerization is compatible with a wide array of monomers as well as solvents. RAFT can be conducted in bulk, solution, suspension, and via emulsion polymerization techniques. This makes RAFT polymerization more versatile compared to any other RDRP process. Despite having these many advantages, there are a few drawbacks like selective RAFT agent works only for a particular set of monomers. Because of the presence of sulphur containing moiety RAFT polymers are often colored and have foul odor and the synthesis of RAFT agents involves multiple steps for which there have been a few drawbacks of the RAFT system. [44, 45]

As stated earlier in this section, a set of RAFT agents works only with a group of monomers. Based on this, monomers are categorized into i) less activated monomers (LAMs) and ii) more activated monomers (MAMs). The monomers that contain C=C bond in conjugation with another C=C bond adjacent to a carbonyl group or an aromatic ring comes under MAMs. Acrylic and methacrylic monomers, acrylamide and methacrylamide based monomers, maleic anhydride, maleimide, and acrylonitrile-based monomers are examples of MAMs. Monomers containing C=C bond alongside heteroatoms such as oxygen, nitrogen and sulfur are LAMs. Vinyl acetate, N-vinylpyrrolidone and vinyl chloride are typical examples. Generally, trithiocarbonates and dithiobenzoates are suitable for MAMs, whereas xanthates and dithiocarbamates are suitable for LAMs. **Figure 1.4** shows a schematic representation of guidelines for the selection of suitable RAFT agents for different monomers based on the -Z and the -R group of the RAFT agents.

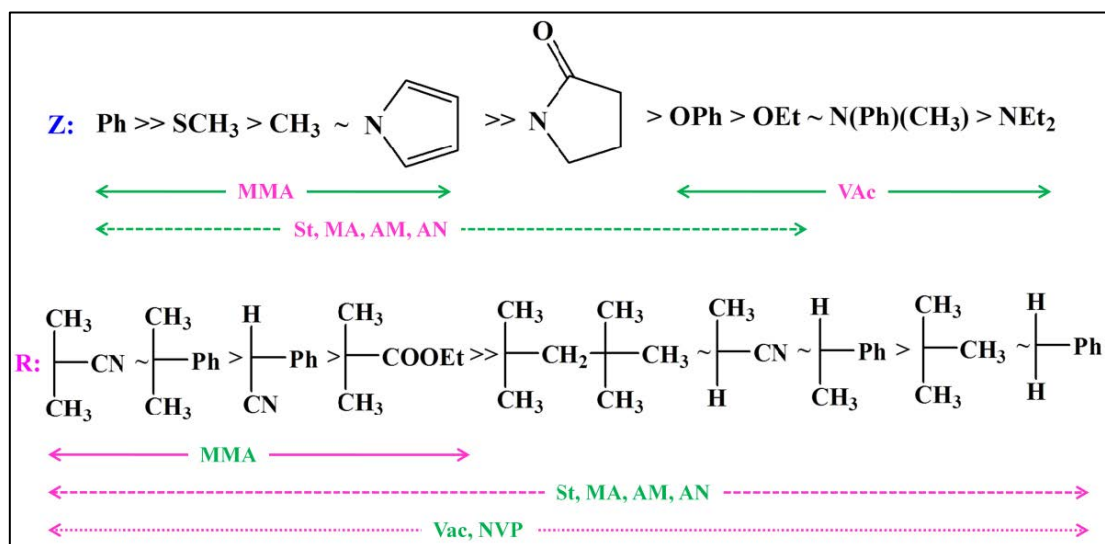


Figure 1.4. Guideline for suitable RAFT reagents selection based on the -R and -Z group for different monomers. (Adapted from Kowollik et al. [29])

1.5 Fluoropolymers

The fluorine atom, by its high electronegativity and high bond strength with carbon, can be used to construct compounds with remarkable properties. In the early

years, there is numerous histories of traumatic incidents that happened in the fluorine chemistry laboratory, and at times, challenges in synthesizing fluorine-containing materials remain daunting. However, fortuitously, subduing both the hazards and synthetic ambiguities were overcome by technological development and advanced facilities.

Fluorine containing polymers have advanced properties and they have been utilized in high-performance applications. Fluoropolymers contain the highly polar and strongest C-F bond (bond dissociation energy = 485 KJmol^{-1}) and have unique properties. [46] The technological importance and the marketplace of fluoropolymers have attained an excellent reputation and reached a different level since the serendipitous discovery of polytetrafluorethylene (PTFE) (marketed as Teflon) by Roy J. Plunkett at the E.I. du Pont Nemours & Company, Jackson Laboratory in 1930. [47] The accelerating growth in fluoropolymers with exceptional properties achieved through the fluorine atoms present has paved the way for the development of new synthetic fluorine chemistry, new processes, and a wide array of applications. Fluorinated polymers have high thermal stability, excellent low-temperature properties, resistance to fuels and corrosive chemicals, low moisture absorption, non-flammability in air, good electrical properties such as low dielectric strength and high dielectric constant, high optical clarity, and low surface energy, providing low friction and high lubricity. [48] As such fluoropolymers are used in various fields such as water repellent coatings, chemical proof coating, lubricant, anti-thermal, electric insulation materials, in the making of oil seals, O-rings and cables. **Figure 1.5** shows the general classifications of fluorinated vinyl monomers that can be polymerized via RP [46, 48-51]. Other than the commercially available fluoropolymers, the development of specialty fluoropolymers like fluorosilicates, fluorinated

polyurethanes, fluorinated thermoplastic elastomers have become key research area, and a significant number of new materials have been developed in the last two decades. In the class of fluorinated polymers, generally, fluoroacrylates are more important, as their properties can be tuned by altering the count of fluorine units in the chain. [52-57]

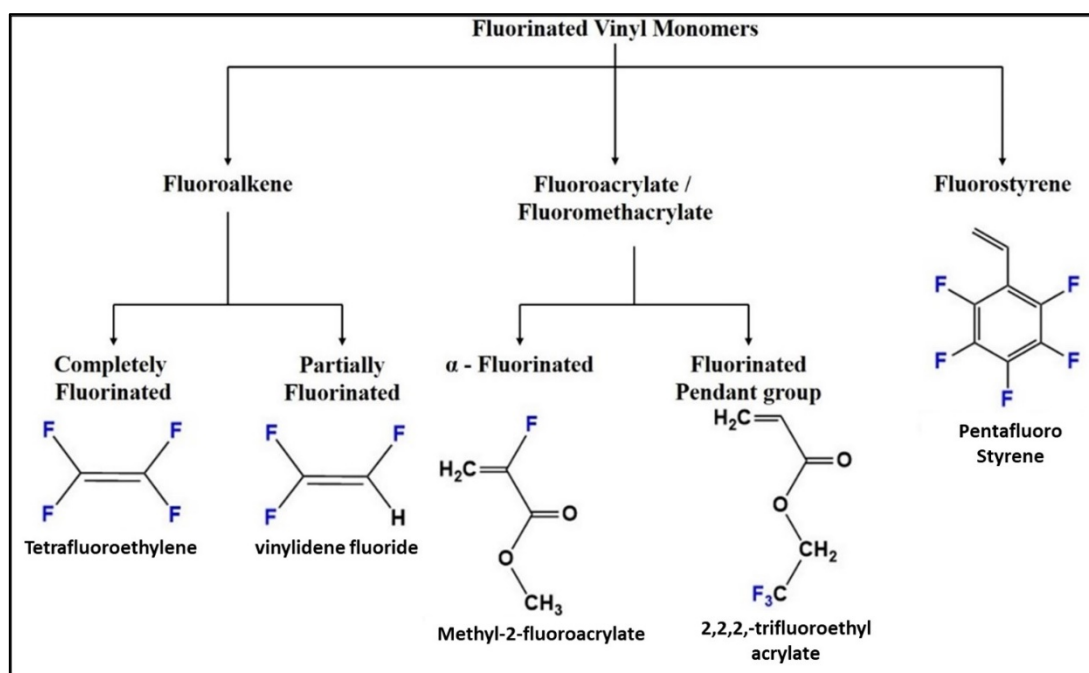


Figure 1.5. Classification of fluorinated vinyl monomers.

Highly fluorine rich backbone containing polyfluoroalkenes exhibit outstanding properties like high thermal resistance, excellent resistance towards chemicals, ageing and weather resistance and have remarkable inertness towards a wide range of solvents, acids, hydrocarbons, less moisture absorption, and have low flammability, refractive index, dielectric constants. Due to these incomparable properties of polyfluoroalkenes, they are used in many high-tech applications. They have profound usage in producing various automobile parts [58]; in battery applications like the development of fuel cell components and lithium-ion batteries; in the production of parts like seals/O-rings/gaskets which are used in the fuel tanks for the storage of liquid hydrogen in space shuttles [59]; in pipes and coatings as liners in

the petrochemical industry; in microelectronics; in the development of high-performance membranes in chemical engineering [60]; UV-resistant paints and coatings for buildings; in textile treatment [61], and in optical fiber cables [62].

Despite this impressive application base, polyfluoroalkenes suffer from certain limitations: i) the production, handling, and purification of gaseous monomers is difficult; ii) complicated experimental setup; iii) the produced polymer has a high melting temperature, very high crystallinity (for example, PTFE is 95% crystalline) and low solubility in most common organic solvents leading to difficulty in processability. [63] Fluoropolymers based on fluorinated acrylates/methacrylates (FA/FMA) having pendant fluorine atoms help in surmounting the shortcomings of the polyfluoroalkenes and have governed significant interest in recent years. They are mostly amorphous, soluble in common organic solvents, resilient to chemicals, oil, and water. Furthermore, the properties of polyfluoroacrylates/methacrylates (PFA/PFMA) can be tailored by varying the alkyl chain length and number of fluorine atoms in the pendent group. The self-stratification of the fluoropolymer segment, i.e., the tendency to aggregate at the film-air interface because of the pendant $-CF_2-$ and $-CF_3-$ units in PFA/PFMA helps in enriching the fluoro segments towards the surface than to the bulk. [64-68] This interesting phenomenon attracted researchers to formulate fluorinated random and BCPs with lower fluorine content and made them an important class of materials from a commercial point of view. [69] Acrylic and methacrylic based fluorinated polymers and copolymers have been used in a large array of application, explicitly in anti-graffiti and easy-clean coatings, release coatings/liners in pressure-sensitive adhesives, treatments for paper, paperboard, and leather, as penetrating sealers for porous surfaces and as protective coatings for electronic applications. Generally, PFA/PFMA is prepared via the RP technique. But

the preparation of tailor-made fluorinated copolymers with precise architectures and controlled incorporation of fluorinated segments is challenging. Also, as discussed earlier, the limitations of RP, like uncontrolled molecular weight, high dispersity, gel fraction, and dead polymer chains makes it difficult to polymerize fluorinated acrylates/methacrylates. In this perspective, the RDRP technique helps in preparing fluorinated copolymers with controlled incorporation of fluoropolymer segments. The advent of the RDRP technique started an era in the fabrication of fluoropolymers with well-defined architectures. Fluorinated homopolymers, random copolymers, and block copolymers based on FA/FMA can be successfully prepared by adopting RDRP techniques. These techniques were also successful in preparing fluoropolymers in bulk, solution as well as in emulsion polymerization. [56, 57, 68, 70, 71]

1.6 Organic/inorganic hybrid polymers

Organic-inorganic hybrid polymeric materials comprise an organic polymer building block that provides bonding between the inorganic building blocks, which helps in attaining excellent properties like enhanced mechanical properties and improved thermal properties. Organic-inorganic hybrid materials have excellent properties like excellent toughness, strength, hardness, and functionalities. Hybrid materials in nature like nacre shell, crustacean carapaces, and bone or teeth tissues, which constitutes calcium carbonate platelets and organic proteins, inspired material chemists to develop synthetic smart nature-mimetic hybrid materials.[72-77] Organic-inorganic hybrid polymers are broadly classified based on the nature of the inner interface between the inorganic and the organic moiety. They are divided into two classes viz., of materials in which the cohesion between the two parts is achieved through weak bonds (such as van der Waals' forces, hydrogen bonding), and the other category of materials where the organic blocks are covalently attached to the

inorganic units. There are several methods adopted in the development of these hybrid materials. [72, 78-81] Depending upon where it is used, and the essential properties required, different kinds of inorganic materials are used, including iron nanoparticles, [82] titanium oxide, [83-85] silicon nanoparticles, [86-88] and metal alkoxides. [89, 90] Recently, polyhedral oligomeric silsesquioxane (POSS), the smallest member in the silicon family, has received attention in the development of smart hybrid polymeric materials. [68, 76, 77, 91, 92]

1.6.1. Polyhedral Oligomeric Silsesquioxane (POSS)

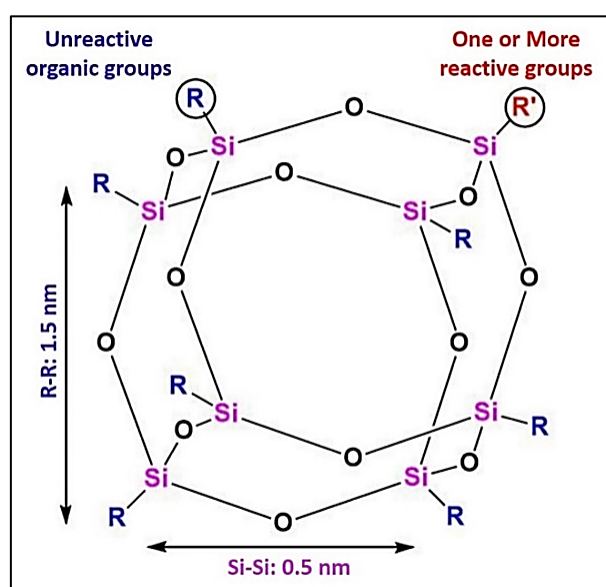


Figure 1.6. General structure of POSS. (Adapted from Cordes et al. [93])

Polyhedral Oligomeric Silsesquioxane (POSS), also formed "molecule silica," is a category of organo-silicone compounds with a nanoscale cubic structure (~1-3 nm). Chemically, the structure of POSS comprises the elemental composition of $(\text{RSiO}_{1.5})_n$, usually $n = 8$. [93] The main structure of POSS has an inorganic siloxane cage as the core and is externally covered by an organic substituent. By varying the organic substituent, the compatibility and dispersion of POSS in an organic polymer system can be regulated. [94, 95] **Figure 1.6.** general POSS cage structure.

POSS, due to its non-toxicity, inertness towards a broad range of chemicals, thermal and mechanical stability, and its nano-size, means it has become an attractive material in the development of organic-inorganic hybrid materials for numerous applications. The incorporation of POSS into polymeric systems enhances the macroscopic properties of the polymer such as the thermal stability, mechanical strength, flame retardancy, hydrophobicity and surface texture, by influencing the segment mobility, molecular conformations, and molecular interactions, which dominates those properties of the polymer. [76, 93, 96-98] The distinctive structural morphology of POSS makes it applicable in a wide range of applications, especially in the coating industry, because of its hydrophobicity, low surface energy, and high thermostability. [99, 100] POSS based hybrid polymeric materials can be produced by using POSS as an initiator, or as a monomer, or as a crosslinking agent. Hybrid polymers comprising POSS with tailor-made architectures like block copolymers, star-shaped polymers and dendrimers have been prepared via RDRP techniques. [68, 76, 95, 101-103]

1.7 Hydrophobic Polymers

The scientific concept of water repellency dates to the early 19th century. [104, 105] In coatings application, hydrophobicity of a solid surface is an essential property of the material and it depends on the surface roughness and surface energy. The surface, whether it is hydrophobic or hydrophilic, can be determined by the value of the water contact angle (WCA). [104-106] If a water droplet is placed on a solid surface, the angle through the droplet between the surface and the water meniscus close to the line of contact is defined as the WCA. A surface is said to be hydrophilic when the WCA is less than 90°. A hydrophobic surface has the WCA greater than 90°. When the WCA is greater than 150°, the surface is termed superhydrophobic.

The lotus leaf is the best example of a natural superhydrophobic surface (SHS) . [107, 108] . **Figure 1.7** shows the nature of water droplets on different surfaces concerning the WCA. There is a correlation between hydrophobicity and surface energy of a solid surface. A hydrophilic surface always has very high surface energy, whereas a surface with low surface energy shows good hydrophobic properties. The chemistry of SHS involves a nanoscale roughness with trapped air inside. As a result, a water-drop rolls off in the surface showing the superhydrophobic and self-cleaning property.

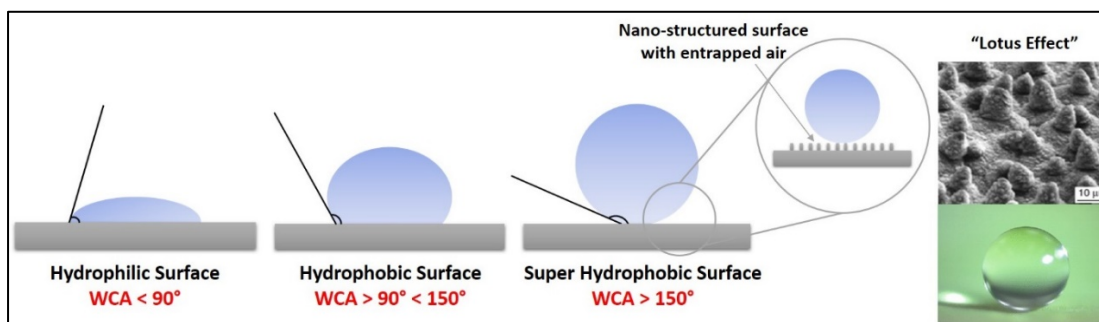


Figure 1.7. Nature of water droplets on different surfaces and "Lotus effect."
(Adapted from Barthlott et al. [107])

1.8 Self-healing Polymer (SHP)

Several environmental factors, like heat, moisture, and physical damage, hamper the stability and endurance of materials. Polymeric materials are also prone to these harmful effects from the environmental and physical factors. Several effects like discoloration, degradation, delamination, crazing, scratch, ablation, puncture, development of cracks, or fractures either externally or internally limit the usage and ultimately reduce the lifetime of the products. **Figure 1.8.** shows the damages occur in a polymeric material.

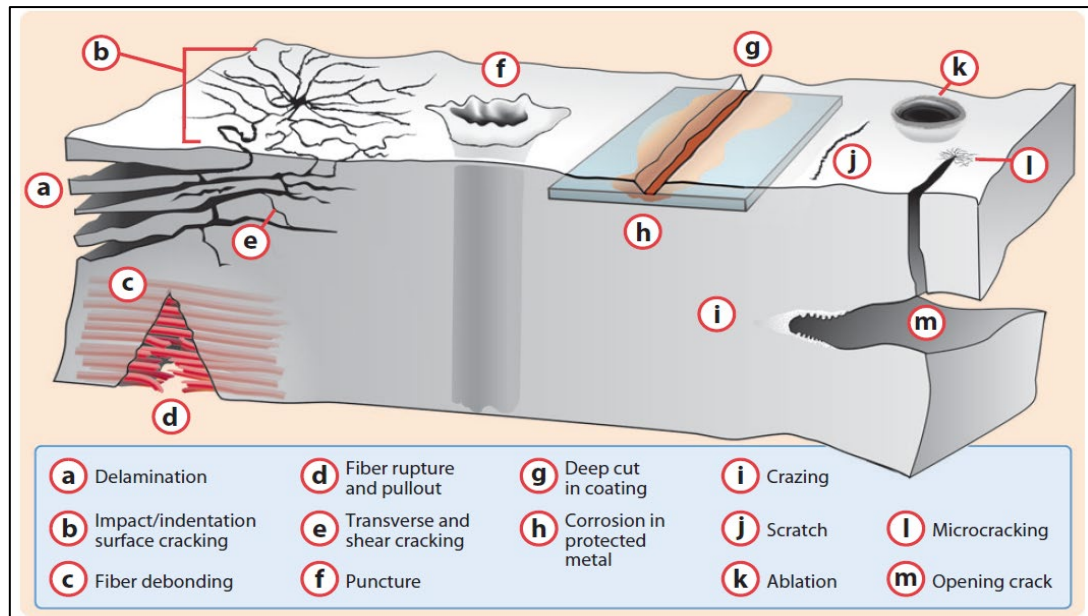


Figure 1.8. Various damage occurred in a hybrid polymeric material (reprinted from Blaiszik et al. [109])

Effects like discoloration or degradation can be reduced or rectified by adding a filler or modifier or by application of an external coating. Recent advances like modification of the materials by incorporation or chemical modification with additives can also overcome these issues. But the physical damage, either internally or externally like puncture, microcracking, open crack, or rupture, either require replacement as a whole or of the part damaged. The development of smart materials by the polymer research community has become an alternative approach to address this issue without replacement. The naturally occurring phenomenon, like built-in repairing mechanisms in biological systems *e.g.*, self-repairing of DNA or damaged blood vessels, self-healing of human skin or macroscopic repair in a damaged plant stem, has inspired the development of smart self-healing materials. SHPs have become of great interest in the polymer research community and has resulted in the development of a wide array of novel smart polymers. [109-113] Self-healing materials can repair on their own and recover back to their functionality using the inherently available healing agents with them. The process of repairing damage either

occurs automatically or can be externally assisted by triggering them using stimuli like heat, light or pH. Generally, based on the approach towards the healing process, self-healing materials can be sub-divided into two distinct categories *viz.*, extrinsic healing and intrinsic healing materials. The extrinsic healing of a material is achieved by using an external healing agent filled in capsules (microencapsulation approach) or hollow cylinders (microvascular approach) and are incorporated into the material. [109, 110, 114] **Figure 1.9** shows the schematic depiction of the extrinsic self-healing approach. In the case of the microencapsulation approach, healing agents are encapsulated in isolated capsules. The self-healing mechanism is triggered by the release of the healing agent when the capsules are ruptured by damage. [114] After the capsule is ruptured, the healing agent inside the capsule is depleted, leading to a one-time healing event, whereas the microvascular approach involves encapsulating the healing agents within capillaries, or hollow channels, interconnected either by one-dimensionally (1D), two-dimensionally (2D), or three-dimensionally (3D) interconnected polymer networks (IPNs). The self-healing action again is triggered by damage. [115-117]. Unlike the microencapsulation approach, the healing agents can be refilled from an external source. Disadvantageously, the extrinsic healing approaches fail to execute multiple healing behaviors. Unless new capsules are employed, or the hollow channels are refilled, repeated healing is difficult due to thermosetting interaction with the polymer material.

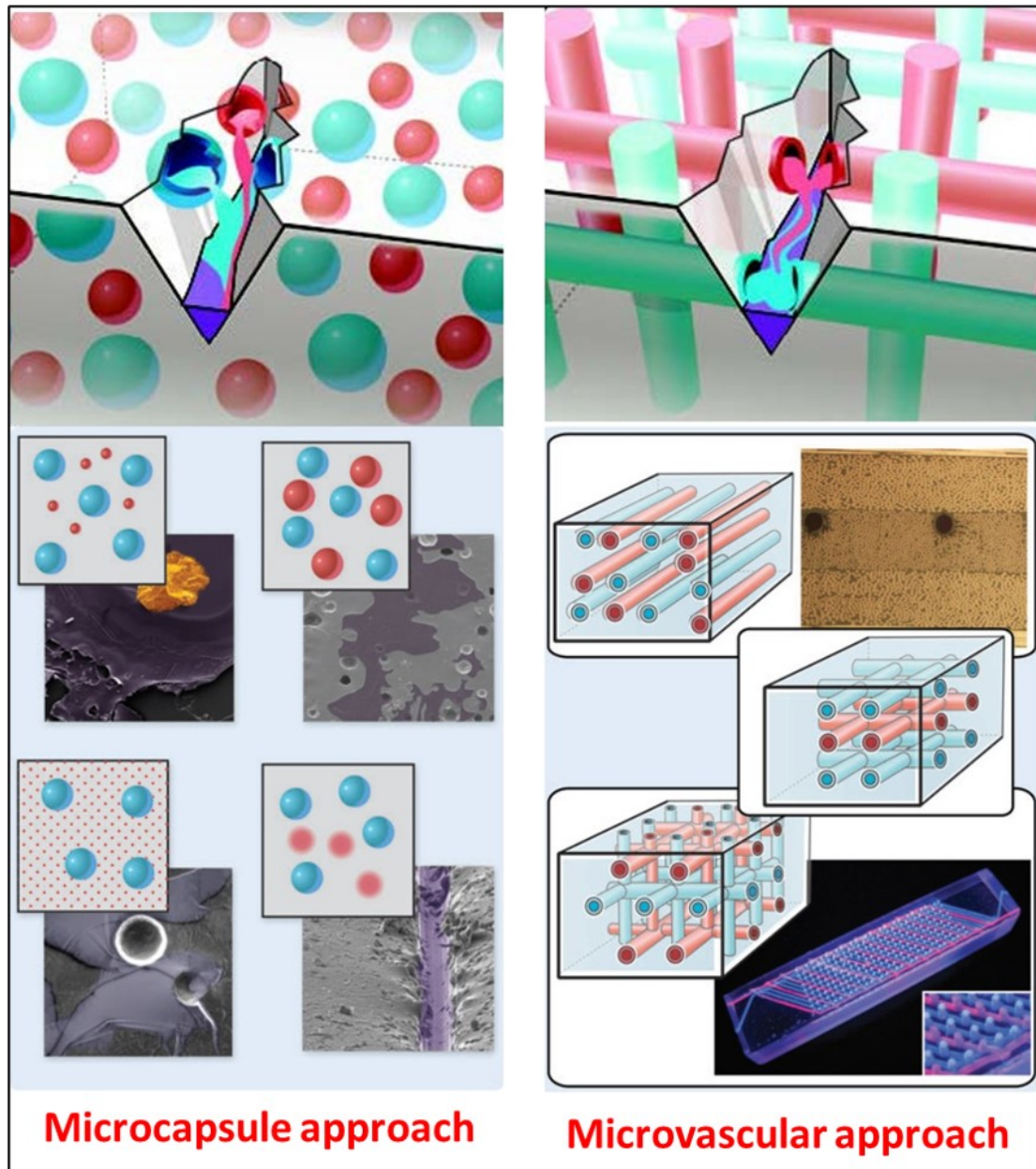


Figure 1.9. Extrinsic self-healing approach (adopted from Blaiszik et al. [109])

Self-healing via an intrinsic approach is achieved based on varied physical or chemical interactions either by a dynamic covalent interaction or noncovalent interaction. **Figure 1.10** shows a schematic representation of various intrinsic approaches involved in the development of smart SHPs. The dynamic covalent interaction can be achieved via disulfide linkages, boronate ester bonding, imine bonding, coordination bonding or the Diels-Alder (DA) reaction. [118-125] The noncovalent interactions can be attained by different mechanisms such as host-guest

interaction, hydrogen bonding, ionic interaction, electrostatic interaction, and π - π interactions. [126-134]

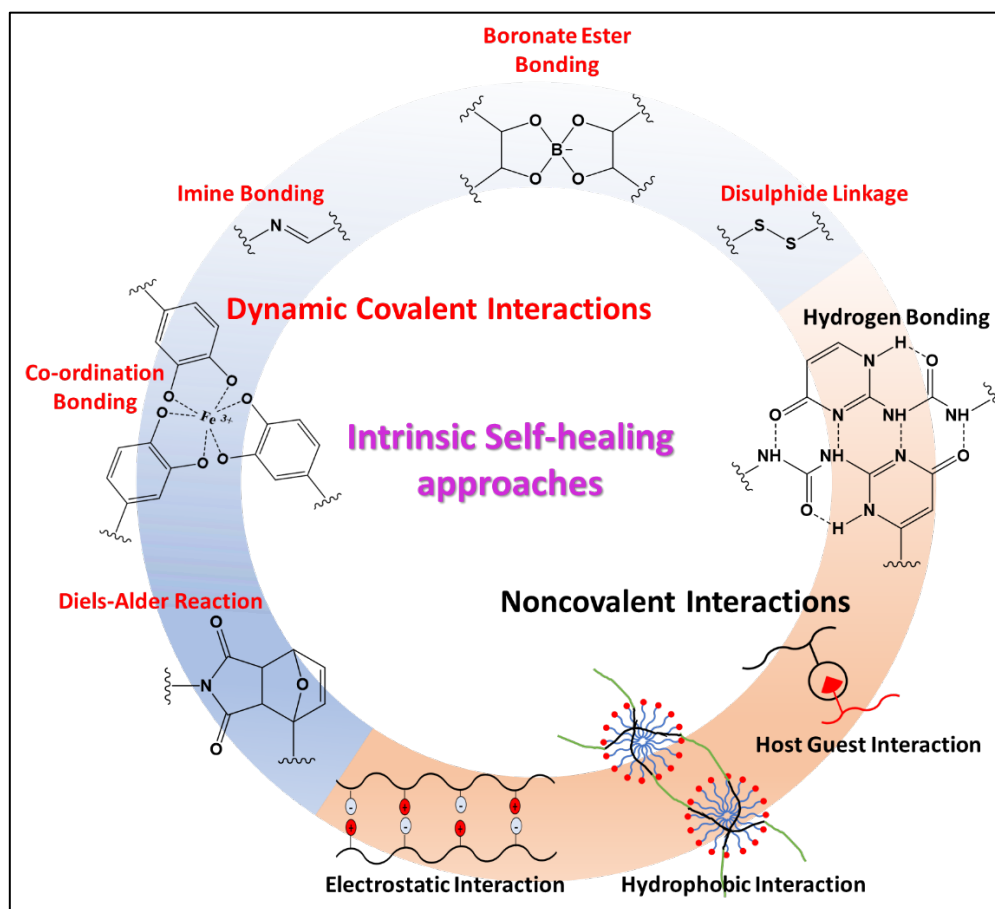


Figure 1.10. Various intrinsic self-healing approaches

Unlike the extrinsic approaches, intrinsic healing mechanisms can exhibit multiple healing characteristics. The dynamic DA/ retro-DA covalent approach has been substantially recognized in the development of numerous self-healing materials. The highly chemo selective process proceeds with significant conversion and high yields, which makes it more attractive to the macromolecular research community. Especially, functional moieties such as furan or anthracene, have been proven to be the suitable reactive partners for DA cycloaddition with maleimides. [119, 135-138] Recently, 1,2,4-triazoline-3,5-dione (TAD) chemistry has achieved a significant attention in producing ultrafast self-healing materials. [112, 113]

1.9 Self-assembly in polymers

Controlled polymerization of a monomer followed by chain extension with another monomer produces a macromolecular architecture which is called a block copolymer (BCP). The structural nature and chemical disparity of different blocks makes BCP an exciting material. The difference in solubility of different blocks, in a given solvent, in a BCP leads to self-assembly, producing various nano-objects like micelles, vesicles or lamellae. [56, 68, 139-143]. In this case, the BCPs to be self-assembled should be amphiphilic, having one hydrophilic segment and another hydrophobic segment. RDRP technique is a powerful tool to prepare BCPs in a stepwise process. At first, one polymer block is prepared that is further used as a macro-initiator or macro-CTA to prepare another block. Self-assembled morphologies in a BCP can be observed taking it in a solvent where the solubilities of the blocks in that solvent are different. However, an amphiphilic BCP can self-assemble in its non-solvent during the formation of the second block. This concept of *in situ* self-assembly during the formation of BCP is called as 'polymerization-induced self-assembly (PISA).' This instead allows producing nano-objects of BCP using one polymer in one step [144].

1.10 Polymerization-induced self-assembly (PISA) in polymers

PISA allows the formation nano-objects of BCP using one polymer in one step [144]. Amphiphilic BCPs are often used as a stabilizer instead of conventional surfactants in emulsion polymerization [145, 146]. In this case, they self-assemble in water to produce micelles where the polymerization of a water-immiscible monomer takes place to create a surfactant-free emulsion. Sometimes, it is challenging to prepare the aqueous solution of the BCP containing a long hydrophobic segment. The PISA process provides significant advances in this regard. As this process is

associated with the *insitu* self-assembly of amphiphilic BCP during its synthesis, it can be used to stabilize an emulsion devoid of conventional surfactants. In this process, a water-soluble polymer synthesized via a RDRP technique is taken together with a water-immiscible monomer in a surfactant-free emulsion. **Figure 1.11** shows the pathway of surfactant-free emulsion polymerization with the help of the PISA process. At the preliminary stage of polymerization, the chain extension of the living hydrophilic polymer with few molecules of hydrophobic monomer takes place, producing an amphiphilic propagating species. Then, the propagating species self-assembles to stabilize the emulsion because of their amphiphilic nature and help to polymerize the rest of the monomer. Thus, a water-immiscible monomer is polymerized in a surfactant-free emulsion. The rate of conversion is slower at the early stage of polymerization, because of the formation and self-assembly of amphiphilic propagating units. Once they are self-assembled, a large fraction of the monomer is transported to the core of the self-assembled propagating species. Thus, an ideal condition of emulsion polymerization is framed, and the polymerization takes place at a faster rate. Surfactant free emulsion polymerization (SFEP) via the PISA process has several advantages over conventional emulsion polymerization. Highly stable emulsion with very high conversion (~100%) can be achieved within a short time, which is beneficial from an industrial perspective [147, 148]. In most cases, depending on the concentration of hydrophilic living polymer, the resulting latex particles have a narrow size distribution with a core-shell morphology [149, 150]. This process offers a better alternative to the RDRP of specific monomers like vinyl acetate, which is challenging to polymerize via conventional emulsion [151]. These self-assembled polymers produced can have different morphology, as shown in **Figure 1.11**, based on the concentration and chain length of the monomers.

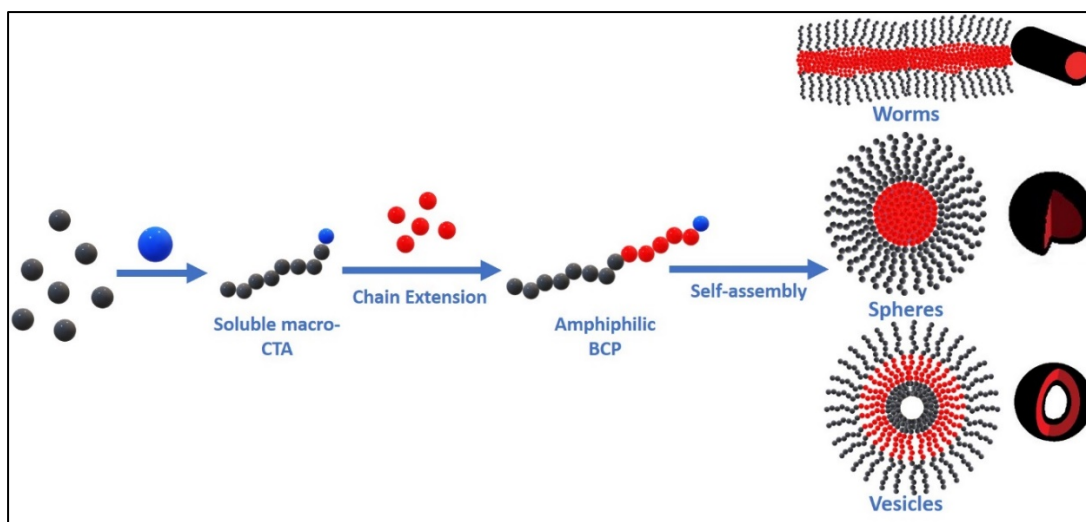


Figure 1.11. self-assembled polymer particles and its morphology obtained via PISA

1.11 Literature Review

Fluoropolymers based on fluorinated acrylates/methacrylates (FA/FMA) having pendant fluorine atoms have governed substantial research interest in recent years. FA/FMA based fluoropolymers with tailor-made properties and well-defined architecture can be prepared via RDRP techniques. As stated earlier, the RDRP process comprises of three important techniques, NMP, ATRP, and RAFT. Extensive literature survey shows that literature on RDRP of FA/FMA is scarce. There are only a few instances where the NMP process is used to polymerize FA/FMA. In 2012 Barth et al. reported NMP of 1H,1H, 2H, 2H-tridecafluorooctyl methacrylate in bulk polymerization [152]. Lacroix-Desmazes et al. and Grignard et al. successfully demonstrated the preparation of fluorinated block copolymer composed of 1H,1H,2H,2H-tetrahydroperfluorodecyl acrylate and styrene or methyl methacrylate via NMP [153, 154]. Because of its amphiphilic nature, this block copolymer was used as a stabilizer for dispersion polymerization in supercritical carbon dioxide. ATRP was successfully used to prepare tailor-made fluoropolymers based on FA/FMA. There are several reports on the preparation of homopolymers of FA/FMA viz., 2,2,2-trifluoroethyl methacrylate (TFEMA) [155], and pentafluorophenyl

methacrylate (PFPMA). [156] ATRP has also been used to prepare BCPs containing FA/FMA viz., 1H,1H-dihydroperfluorooctyl methacrylate [157], 2,2,3,4,4,4-hexafluorobutyl methacrylate (F₆BMA) [158], perfluorohexylethyl methacrylate (FHEMA) [159] and 2-(perfluorooctyl)ethyl methacrylate (FOEMA) [160]. This process also offered the scope to prepare fluoropolymer brushes by the polymerization of dodecafluoroheptyl methacrylate [161] or 2,2,3,3,4,4,4-heptafluorobutyl methacrylate (HFBMA) on nanosilica [162]; TFEMA, HFBMA and FOEMA on silicon wafer [163]; and TFEMA on poly(ethylene terephthalate) (PET) [164] surfaces. In most instances, the polymer showed exceptional surface properties essential for application as coatings.

Even though NMP and ATRP can be used for preparing homopolymers and copolymers, RAFT polymerization is widely used to polymerize FA/FMA. Many reports have taken benefit of the hydrophobic and oleophobic nature of the fluorinated segment to prepare amphiphilic BCPs under a range of RAFT conditions including polymerization of fluoro monomers using bulk, solution, and emulsion polymerization process Markin and co-workers reported the bulk polymerization of 1H,1H,5H-octafluoropentyl acrylate [165]. Koiry et al. reported the solution polymerization of 2,2,3,3,4,4,4-heptafluorobutyl acrylate (HFBA) [166]. Gibson and co-workers adopted the RAFT to polymerize pentafluoropropyl methacrylate (PFPMA) [167]. In this case, the authors got the scope for post-polymerization modification with primary amines and opened the route to synthesize libraries of water-soluble functional polymers. Zaitsev et al. reported the preparation of fluorinated alternating copolymers via RAFT polymerization [168]. In this case, the copolymerization of 1,1,1,3,3,3-hexafluoroisopropyl- α -fluoroacrylate with *N*-vinyl pyrrolidone (NVP) was carried out in tetrahydrofuran (THF). The copolymerization

of electron-rich NVP with electron-deficient FPFA produced an alternating copolymer. RAFT copolymerization of butyl acrylate with 2,2,3,3,4,4,4-heptafluorobutyl acrylate was reported by Koiry et al. In this, their reactivity ratios were determined using different models. Guo et al. reported one pot synthesis of amphiphilic BCPs of methacrylic acid (MAA) and TFEMA (PMAA-*b*-PTFEMA) using RAFT polymerization via PISA process using water-soluble PMAA as the macro-RAFT agent [169]. Li and co-workers used RAFT polymerization to prepare PMMA-*b*-PTFEMA [170]. Chakraborty et al. reported the synthesis of tailor-made FA and its BCP by RAFT polymerization in miniemulsion. Based on the above literature survey, RAFT polymerization is found to be a feasible and versatile approach for the polymerization of FA/FMA. This dissertation delineates the synthesis of various block copolymers based on FA/FMA via RAFT polymerization and their properties and different application.

As noted earlier, the properties of a polymer can be enhanced by the incorporation of a tailor-made inorganic cluster into the organic polymer matrix. This facilitates development nanostructured materials with significant improvement in the mechanical properties, [97, 171] thermal stability, [172] flammability and oxidation resistance, [161, 173, 174] and excellent oil and water resistance. [175] Polyhedral oligomeric silsesquioxane (POSS) being a unique inorganic component with definite hybrid nanostructure is used to prepare hybrid polymers with well-defined architectures like block copolymers (BCPs), star-shaped polymers and dendrimers via RDRP. [94, 102, 176]. As stated in the earlier sections, FA/FMA based polymers have excellent chemical resistance, thermal stability, and low surface energy. So polyfluoroacrylates have gained attention in the development of hydrophobic/superhydrophobic surfaces. [46, 50, 53, 55, 71, 177, 178]. Combining

the organic fluoropolymers and the inorganic hybrid POSS material substantially enhances the properties of the materials and leads to a broad application base. The coatings and films based on these hybrid BCPs exhibit outstanding thermal stability and excellent chemical stability. BCPs bearing POSS moieties receive special attention as they can undergo microphase separation and self-assembly with long-range structural ordering. [179] Fluorinated block copolymers are materials with special properties like anti-fogging, anti-icing, and anti-wetting coatings owing to their active self-migration and self-orientation to the surfaces. [180] There are not many reports on the synthesis of hybrid BCPs based on POSS and fluoroacrylate. BCPs based on POSS and fluoroacrylate have been prepared via ATRP. Pan *et al.* prepared POSS-tethered fluorinated BCPs using octakis(dibromoethyl) POSS (POSS-(Br)₁₆), aminopropyl isobutyl POSS (ap-POSS), and dodecafluoroheptyl methacrylate (DFHM). [181] Qiang *et al.* synthesized star-shaped POSS fluorinated acrylates via ATRP and used them for hydrophobic honeycomb porous film application [182] These hybrid polymers based on POSS and FA find potential application as a coating material. [181-184] Preparation of hybrid BCPs based on fluoroacrylate and methacryloethyl POSS (MAePOSS) via RAFT polymerization was reported by Nakatani *et al.* [185] There are only a few studies on BCPs based on FA/FMA and POSS via RAFT polymerization. Chapter-3 of this dissertation focuses on the preparation, and comprehensive morphological studies of BCPs based on fluoroacrylate and POSS functionalized acrylate *via* RAFT.

Developing a SHP based on fluoropolymer is challenging, and conspicuously, there has been little work done in the field of fluoropolymers. For the development of SHPs via an intrinsic approach, the use of click chemistry is the most apparent. The Diels-Alder (DA) reaction is used in polymer chemistry for the synthesis of a range of

functional polymers. The polymers modified by the DA reaction showed thermoresponsive properties due to the reversible nature of the DA reaction. The main advantage of the DA reaction is that this reaction takes place in the absence of a metal catalyst. As mentioned earlier, there are only a few reports on fluoropolymer-based SHPs. Henderson et al. fabricated vascular grafts based on polytrifluoroethylene. Wang et al. reported polymer and protein repellent antifouling coatings based on self-healing fluoropolymer brushes prepared via ATRP. [186, 187] Li et al. reported sulfonated poly(ether ether ketone) and 1H,1H,2H,2H-perfluorooctyltriethoxysilane based superhydrophobic self-healing coatings. [188] Wang and co-workers developed fluorinated decyl POSS and hydrolyzed fluorinated alkylsilane based self-healing superhydrophobic and superoleophobic surfaces. [189] Fluoroalkylsilane and modified silica nanoparticles based robust self-healing super amphiphilic fabrics was reported by Zhou et al. [190] Although a tremendous effort has been recently devoted to developing self-repairing fluoropolymers based on FA/FMA, the number of related articles based on dynamic DA 'click chemistry' is low. So far, Padhan et al. [191] and Banerjee et al. [192] successfully utilized dynamic covalent chemistry based on furfuryl and bis-maleimide DA cycloaddition in developing self-healing fluoropolymers. Chapter-4 of this thesis delineates the synthesis of SHPs based on copolymers bearing fluorinated functional groups and reactive furan groups and the dynamic clicking of POSS maleimide via DA 'click chemistry'. This approach helps in developing hybrid polymer along with self-healing behaviour and improvement in surface properties.

Fluoropolymers, as delineated earlier, have excellent electrical properties and high resistance to chemicals and water. They are used widely in chemical repellent coatings, fuel cell membranes and as insulators in battery applications. The presence

of surfactant in emulsion-based fluoropolymers used for these applications deteriorates their performance. It is, therefore of interest to develop surfactant-free emulsion formulations. In recent years, several interesting approaches for surfactant-free emulsion polymerization (SFEP) have been reported. Xu and co-worker adopted the SFEP process to prepare an amphiphilic FBCP [193]. Here, they adopted the RAFT polymerization technique to prepare PMAA, which was used as a macro-RAFT agent in the PISA process in the surfactant-free emulsion polymerization of DFHMA producing PMAA-b-PDFHMA. The water-resistance of the amphiphilic FBCP largely depends on the polymer chain orientation towards the film-air interface. A complete rearrangement in that orientation can be caused by heat treatment. A similar approach was also adopted by Guo and co-workers to prepare PMAA-b-PTFEMA by SFEP in 1,4-dioxane/water (1:4) via the PISA approach. [169] There are reports on the preparation of fluorinated copolymer via SFEP using polymerizable emulsifiers like 4-styrenesulfonic acid [194], ammonium allyloxymethylate nonylphenol ethoxylates sulphate [195, 196], sodium 3-allyloxy-2-hydroxypropanesulfonate [197] and maleic acid double ester-octadecyl poly(ethyleneoxy) ether-ethylene trimethyl ammonium chloride [198]. In most of the cases, seeded emulsion polymerization was carried out to obtain core-shell latex particles where the shell was enriched with fluorinated segments. An amphiphilic RAFT agent was successfully used to prepare a fluorinated gradient copolymer via SFEP under starved feed conditions [199, 200]. The films prepared from the copolymer emulsion had good resistance to acid, alkali, and salt. Chapter-5 of this thesis emphasizes the preparation of thin films based on fluoropolymer, styrene sulfonate, and butyl acrylate prepared via the PISA process. The dielectric properties, mechanical, and thin-film surface properties of the multifunctional material have been studied.

1.12 Scope and Objectives of the Work

Based on the literature reviewed, the need for the development of new range of materials for wide range of applications leads to a broad scope to prepare new classes of FA/FMA based fluoropolymers and study their properties to use effectively in different applications like hydrophobic coatings, self-healing coatings, and thin films for electrical applications. The objectives of the thesis are presented precisely below:

- Preparation of a hybrid polymer system based on POSS and fluoromethacrylate block copolymers to study its properties and to explore its use as an effective hydrophobic coating material.
- Development of hydrophobic self-healing polymers based on POSS functionalized fluoropolymers and POSS derived by Diels-Alder chemistry and RAFT polymerization.
- Synthesis of a multifunctional copolymer based on fluoroacrylate via polymerization-induced self-assembly (PISA) and to study their properties as thin-film coating materials and their potential in electrical applications.
- Development of a new class of hydrophobic self-healing BCPs based on fluoropolymer and anthracene functionality via TAD chemistry.

References

- [1] H. Staudinger, Concerning polymerization, Ber. Dtsch. Chem. Ges 53 (1920) 1073-1085.
- [2] A.D. McNaught, A. Wilkinson, The IUPAC Compendium of Chemical Terminology, Royal Society of Chemistry, Cambridge, UK, 1997.
- [3] P.J. Flory, Principles of polymer chemistry, Cornell University Press, New York, 1953.
- [4] F.W. Billmeyer, Textbook of polymer science, John Wiley & Sons, Singapore, 1984.
- [5] V.R. Gowariker, N. Viswanathan, J. Sreedhar, Polymer science, New Age International, New Delhi, 1986.
- [6] G. Odian, Principles of polymerization, John Wiley & Sons, New Jersey, 2004.
- [7] M. Szwarc, 'Living' polymers, Nature 178(4543) (1956) 1168-1169.
- [8] M. Szwarc, M. Van Beylen, Ionic polymerization and living polymers, Springer Science & Business Media, Dordrecht, 1993.
- [9] R.O. Ebewele, Polymer science and technology, CRC press, Florida, 2000.
- [10] K. Ziegler, E. Holzkamp, H. Breil, H. Martin, Das mülheimer normaldruck-polyäthylen-verfahren, Angewandte Chemie 67(19-20) (1955) 541-547.
- [11] G. Natta, I. Pasquon, The kinetics of the stereospecific polymerization of α -olefins, Advances in catalysis, Elsevier, 1959, pp. 1-66.
- [12] J. Boor, J. Boor, Ziegler-Natta catalysts and polymerizations, Academic Press Inc., New York, 1979.
- [13] H. Sinn, W. Kaminsky, Ziegler-Natta catalysis, Advances in Organometallic Chemistry, Elsevier, 1980, pp. 99-149.
- [14] T.P. Davis, Handbook of radical polymerization, Wiley-Interscience, Hoboken, 2002.
- [15] K. Matyjaszewski, T.P. Davis, Handbook of radical polymerization, John Wiley & Sons, Hoboken, 2003.
- [16] J.M.G. Cowie, V. Arrighi, Polymers: chemistry and physics of modern materials, Third ed., CRC press, Florida, 2007.
- [17] S. Balke, A. Hamielec, Bulk polymerization of methyl methacrylate, Journal of applied Polymer science 17(3) (1973) 905-949.

- [18] D. Bertin, B. Boutevin, Controlled radical polymerization, *Polymer Bulletin* 37(3) (1996) 337-344.
- [19] K. Matyjaszewski, P.J. Miller, E. Fossum, Y. Nakagawa, Synthesis of block, graft and star polymers from inorganic macroinitiators, *Applied organometallic chemistry* 12(10-11) (1998) 667-673.
- [20] K. Matyjaszewski, J. Spanswick, Controlled/living radical polymerization, *Materials Today* 8(3) (2005) 26-33.
- [21] L. Mespouille, M. Vachaudéz, F. Suriano, P. Gerbaux, W. Van Camp, O. Coulembier, P. Degée, R. Flammang, F. Du Prez, P. Dubois, Controlled synthesis of amphiphilic block copolymers based on polyester and poly (amino methacrylate): Comprehensive study of reaction mechanisms, *Reactive and Functional Polymers* 68(5) (2008) 990-1003.
- [22] J.-S. Wang, K. Matyjaszewski, Controlled/" living" radical polymerization. atom transfer radical polymerization in the presence of transition-metal complexes, *Journal of the American Chemical Society* 117(20) (1995) 5614-5615.
- [23] M. Kato, M. Kamigaito, M. Sawamoto, T. Higashimura, Polymerization of methyl methacrylate with the carbon tetrachloride/dichlorotris-(triphenylphosphine) ruthenium (II)/methylaluminum bis (2, 6-di-tert-butylphenoxide) initiating system: possibility of living radical polymerization, *Macromolecules* 28(5) (1995) 1721-1723.
- [24] M. Ding, X. Jiang, L. Zhang, Z. Cheng, X. Zhu, Recent progress on transition metal catalyst separation and recycling in ATRP, *Macromolecular rapid communications* 36(19) (2015) 1702-1721.
- [25] J. Chiefari, Y. Chong, F. Ercole, J. Krstina, J. Jeffery, T.P. Le, R.T. Mayadunne, G.F. Meijs, C.L. Moad, G. Moad, Living free-radical polymerization by reversible addition- fragmentation chain transfer: the RAFT process, *Macromolecules* 31(16) (1998) 5559-5562.
- [26] G. Moad, R.T. Mayadunne, E. Rizzardo, M. Skidmore, S.H. Thang, Kinetics and mechanism of RAFT polymerization, *Polymer Preprints America* 43(2) (2002) 114-115.
- [27] V. Jitchum, S. Perrier, Living radical polymerization of isoprene via the RAFT process, *Macromolecules* 40(5) (2007) 1408-1412.
- [28] R.T. Mayadunne, E. Rizzardo, J. Chiefari, Y.K. Chong, G. Moad, S.H. Thang, Living radical polymerization with reversible addition-fragmentation chain transfer

(RAFT polymerization) using dithiocarbamates as chain transfer agents, *Macromolecules* 32(21) (1999) 6977-6980.

[29] C. Barner-Kowollik, *Handbook of RAFT polymerization*, John Wiley & Sons, Weinheim, 2008.

[30] G. Moad, E. Rizzardo, S.H. Thang, Radical addition–fragmentation chemistry in polymer synthesis, *Polymer* 49(5) (2008) 1079-1131.

[31] C. Barner-Kowollik, M. Buback, B. Charleux, M.L. Coote, M. Drache, T. Fukuda, A. Goto, B. Klumperman, A.B. Lowe, J.B. Mcleary, Mechanism and kinetics of dithiobenzoate-mediated RAFT polymerization. I. The current situation, *Journal of Polymer Science Part A: Polymer Chemistry* 44(20) (2006) 5809-5831.

[32] D.S. Germack, K.L. Wooley, RAFT-Based Synthesis and Characterization of ABC versus ACB Triblock Copolymers Containing tert-Butyl Acrylate, Isoprene, and Styrene Blocks, *Macromolecular Chemistry and Physics* 208(23) (2007) 2481-2491.

[33] C.S. Gudipati, M.B. Tan, H. Hussain, Y. Liu, C. He, T.P. Davis, Synthesis of Poly (glycidyl methacrylate)-block-Poly (pentafluorostyrene) by RAFT: Precursor to Novel Amphiphilic Poly (glyceryl methacrylate)-block-Poly (pentafluorostyrene), *Macromolecular Rapid Communications* 29(23) (2008) 1902-1907.

[34] X. Hao, C. Nilsson, M. Jesberger, M.H. Stenzel, E. Malmström, T.P. Davis, E. Östmark, C. Barner-Kowollik, Dendrimers as scaffolds for multifunctional reversible addition–fragmentation chain transfer agents: Syntheses and polymerization, *Journal of Polymer Science Part A: Polymer Chemistry* 42(23) (2004) 5877-5890.

[35] J. Bernard, A. Favier, L. Zhang, A. Nilasaroya, T.P. Davis, C. Barner-Kowollik, M.H. Stenzel, Poly (vinyl ester) star polymers via xanthate-mediated living radical polymerization: from poly (vinyl alcohol) to glycopolymer stars, *Macromolecules* 38(13) (2005) 5475-5484.

[36] Y. Li, A.E. Smith, B.S. Lokitz, C.L. McCormick, In Situ Formation of Gold-“Decorated” Vesicles from a RAFT-Synthesized, Thermally Responsive Block Copolymer §, *Macromolecules* 40(24) (2007) 8524-8526.

[37] N. Suchao-in, S. Chirachanchai, S. Perrier, pH-and thermo-multi-responsive fluorescent micelles from block copolymers via reversible addition fragmentation chain transfer (RAFT) polymerization, *Polymer* 50(17) (2009) 4151-4158.

[38] L. Zhang, J. Bernard, T.P. Davis, C. Barner-Kowollik, M.H. Stenzel, Acid-Degradable Core-Crosslinked Micelles Prepared from Thermosensitive

Glycopolymers Synthesized via RAFT Polymerization, *Macromolecular rapid communications* 29(2) (2008) 123-129.

[39] A.M. Granville, S.G. Boyes, B. Akgun, M.D. Foster, W.J. Brittain, Thermoresponsive behavior of semifluorinated polymer brushes, *Macromolecules* 38(8) (2005) 3263-3270.

[40] H.P. Yap, X. Hao, E. Tjipto, C. Gudipati, J.F. Quinn, T.P. Davis, C. Barner-Kowollik, M.H. Stenzel, F. Caruso, Synthesis, multilayer film assembly, and capsule formation of macromolecularly engineered acrylic acid and styrene sulfonate block copolymers, *Langmuir* 24(16) (2008) 8981-8990.

[41] D. Hua, J. Tang, J. Jiang, X. Zhu, Synthesis of phenylphosphinic acid-containing amphiphilic homopolymers by reversible addition-fragmentation transfer (RAFT) polymerization and its aggregation in water, *Polymer* 50(24) (2009) 5701-5707.

[42] G. Moad, Y. Chong, A. Postma, E. Rizzardo, S.H. Thang, Advances in RAFT polymerization: the synthesis of polymers with defined end-groups, *Polymer* 46(19) (2005) 8458-8468.

[43] G. Moad, E. Rizzardo, S.H. Thang, Living radical polymerization by the RAFT process—a first update, *Australian Journal of Chemistry* 59(10) (2006) 669-692.

[44] G. Moad, E. Rizzardo, S.H. Thang, Living radical polymerization by the RAFT process—a second update, *Australian journal of chemistry* 62(11) (2009) 1402-1472.

[45] K. Skrabania, A. Miasnikova, A.M. Bivigou-Koumba, D. Zehm, A. Laschewsky, Examining the UV-vis absorption of RAFT chain transfer agents and their use for polymer analysis, *Polymer Chemistry* 2(9) (2011) 2074-2083.

[46] G.G. Hougham, P.E. Cassidy, K. Johns, T. Davidson, *Fluoropolymers 1: synthesis*, Kluwer Academic Publishers, New York, 2006.

[47] R.J. Plunkett, The history of polytetrafluoroethylene: discovery and development, *High Performance Polymers: Their Origin and Development*, Springer, New York, 1986, pp. 261-266.

[48] G.G. Hougham, P.E. Cassidy, K. Johns, T. Davidson, *Fluoropolymers 2: properties*, Kluwer Academic Publishers, New York, 2006.

[49] J. Scheirs, *Modern fluoropolymers: high performance polymers for diverse applications*, Wiley, New York, 1997.

[50] B. Ameduri, B. Boutevin, *Well-architected fluoropolymers: synthesis, properties and applications*, Elsevier, Amsterdam, 2004.

- [51] S. Ebnesajjad, Fluoroplastics, volume 2: Melt processible fluoropolymers-the definitive user's guide and data book, William Andrew Publishing, New York, 2015.
- [52] F. Ciardelli, M. Aglietto, L.M. di Mirabello, E. Passaglia, S. Giancristoforo, V. Castelvetro, G. Ruggeri, New fluorinated acrylic polymers for improving weatherability of building stone materials, *Progress in Organic Coatings* 32(1) (1997) 43-50.
- [53] P. Graham, M. Stone, A. Thorpe, T.G. Nevell, J. Tsibouklis, Fluoropolymers with very low surface energy characteristics, *Journal of Fluorine Chemistry* 104(1) (2000) 29-36.
- [54] M. Antonietti, S. Oestreich, Novel fluorinated block copolymers, *Fluoropolymers 1: Synthesis*, Kluwer Academic Publishers, New York, 2002, pp. 151-166.
- [55] V. Malshe, N.S. Sangaj, Fluorinated acrylic copolymers: Part I: Study of clear coatings, *Progress in Organic Coatings* 53(3) (2005) 207-211.
- [56] B.P. Koiry, S. Ponnupandian, S. Choudhury, N.K. Singha, Syntheses and morphologies of fluorinated diblock copolymer prepared via RAFT polymerization, *Journal of Fluorine Chemistry* 189 (2016) 51-58.
- [57] A. Chakrabarty, S. Ponnupandian, K. Naskar, N.K. Singha, Nanoclay stabilized Pickering miniemulsion of fluorinated copolymer with improved hydrophobicity via RAFT polymerization, *RSC Advances* 6(41) (2016) 34987-34995.
- [58] A.L. Moore, J.G. Drobny, *Fluoroelastomers handbook: the definitive user's guide and databook*, William Andrew Publishing, New York, 2006.
- [59] B. Ameduri, B. Boutevin, G. Kostov, *Fluoroelastomers: synthesis, properties and applications*, *Progress in Polymer Science* 26(1) (2001) 105-187.
- [60] Z. Cui, E. Drioli, Y.M. Lee, Recent progress in fluoropolymers for membranes, *Progress in Polymer Science* 39(1) (2014) 164-198.
- [61] M. Licchelli, M. Malagodi, M.L. Weththimuni, C. Zanchi, Water-repellent properties of fluoroelastomers on a very porous stone: Effect of the application procedure, *Progress in Organic Coatings* 76(2-3) (2013) 495-503.
- [62] F. Mikes, H. Teng, G. Kostov, B. Ameduri, Y. Koike, Y. Okamoto, Synthesis and characterization of perfluoro-3-methylene-2, 4-dioxabicyclo [3, 3, 0] octane: Homo-and copolymerization with fluorovinyl monomers, *Journal of Polymer Science Part A: Polymer Chemistry* 47(23) (2009) 6571-6578.

- [63] A. Taguet, B. Ameduri, B. Boutevin, Crosslinking of vinylidene fluoride-containing fluoropolymers, *Crosslinking in Materials Science*, Springer2005, pp. 127-211.
- [64] E. Barbu, R.A. Pullin, P. Graham, P. Eaton, R.J. Ewen, J.D. Smart, T.G. Nevell, J. Tsibouklis, Poly (di-1H, 1H, 2H, 2H-perfluoroalkylitaconate) films: surface organisation phenomena, surface energy determinations and force of adhesion measurements, *Polymer* 43(6) (2002) 1727-1734.
- [65] J. Tsibouklis, P. Graham, P.J. Eaton, J.R. Smith, T.G. Nevell, J.D. Smart, R.J. Ewen, Poly (perfluoroalkyl methacrylate) film structures: surface organization phenomena, surface energy determinations, and force of adhesion measurements, *Macromolecules* 33(22) (2000) 8460-8465.
- [66] I.J. Park, S.-B. Lee, C.K. Choi, K.-J. Kim, Surface properties and structure of poly (perfluoroalkylethyl methacrylate), *Journal of colloid and interface science* 181(1) (1996) 284-288.
- [67] S. Sheiko, E. Lermann, M. Möller, Self-dewetting of perfluoroalkyl methacrylate films on glass, *Langmuir* 12(16) (1996) 4015-4024.
- [68] S. Ponnupandian, A. Chakrabarty, P. Mondal, R. Hoogenboom, A.B. Lowe, N.K. Singha, POSS and fluorine containing nanostructured block copolymer; Synthesis via RAFT polymerization and its application as hydrophobic coating material, *European Polymer Journal* (2020) 109679-109689.
- [69] R.R. Thomas, D.R. Anton, W.F. Graham, M.J. Darmon, B.B. Sauer, K.M. Stika, D.G. Swartzfager, Preparation and surface properties of acrylic polymers containing fluorinated monomers, *Macromolecules* 30(10) (1997) 2883-2890.
- [70] N.M. Hansen, K. Jankova, S. Hvilsted, Fluoropolymer materials and architectures prepared by controlled radical polymerizations, *European Polymer Journal* 43(2) (2007) 255-293.
- [71] B.P. Koiry, H.-A. Klok, N.K. Singha, Copolymerization of 2, 2, 3, 3, 4, 4, 4-heptafluorobutyl acrylate with butyl acrylate via RAFT polymerization, *Journal of Fluorine Chemistry* 165 (2014) 109-115.
- [72] C. Sanchez, B. Julián, P. Belleville, M. Popall, Applications of hybrid organic–inorganic nanocomposites, *Journal of Materials Chemistry* 15(35-36) (2005) 3559-3592.
- [73] D.J. Haloi, S. Ata, N.K. Singha, Synthesis and characterization of all acrylic block copolymer/clay nanocomposites prepared via surface initiated atom transfer

radical polymerization (SI-ATRP), *Industrial & engineering chemistry research* 51(29) (2012) 9760-9768.

[74] N.K. Singha, A. Kavitha, D.J. Haloi, P. Mandal, A. Janke, D. Jehnichen, H. Komber, B. Voit, Effect of nanoclay on in situ preparation of “all acrylate” ABA triblock copolymers via ATRP and their morphology, *Macromolecular Chemistry and Physics* 213(19) (2012) 2034-2043.

[75] Z. Zhang, H.T.H. Nguyen, S.A. Miller, S.M. Cohen, polyMOFs: a class of interconvertible polymer-metal-organic-framework hybrid materials, *Angewandte Chemie International Edition* 54(21) (2015) 6152-6157.

[76] S. Ata, P. Dhara, R. Mukherjee, N.K. Singha, Thermally amendable and thermally stable thin film of POSS tethered Poly (methyl methacrylate)(PMMA) synthesized by ATRP, *European Polymer Journal* 75 (2016) 276-290.

[77] S. Ata, S.L. Banerjee, N.K. Singha, Self-assembly behavior of POSS based ABA type amphiphilic tri-block copolymer prepared via ATRP, *European Polymer Journal* 118 (2019) 10-16.

[78] D.A. Loy, K.J. Shea, Bridged polysilsesquioxanes. Highly porous hybrid organic-inorganic materials, *Chemical Reviews* 95(5) (1995) 1431-1442.

[79] P. Judeinstein, C. Sanchez, Hybrid organic–inorganic materials: a land of multidisciplinary, *Journal of Materials Chemistry* 6(4) (1996) 511-525.

[80] C. Sanchez, G.d.A. Soler-Illia, F. Ribot, T. Lalot, C.R. Mayer, V. Cabuil, Designed hybrid organic– inorganic nanocomposites from functional nanobuilding blocks, *Chemistry of Materials* 13(10) (2001) 3061-3083.

[81] G. Kickelbick, Concepts for the incorporation of inorganic building blocks into organic polymers on a nanoscale, *Progress in polymer science* 28(1) (2003) 83-114.

[82] K. Zhang, W. Wu, K. Guo, J.-F. Chen, P.-Y. Zhang, Magnetic polymer enhanced hybrid capsules prepared from a novel Pickering emulsion polymerization and their application in controlled drug release, *Colloids and Surfaces A: Physicochemical and Engineering Aspects* 349(1-3) (2009) 110-116.

[83] B.F. Urbano, I. Villenas, B.L. Rivas, C.H. Campos, Cationic polymer–TiO₂ nanocomposite sorbent for arsenate removal, *Chemical Engineering Journal* 268 (2015) 362-370.

[84] W. Tong, Y. Zhang, L. Yu, F. Lv, L. Liu, Q. Zhang, Q. An, Amorphous TiO₂-coated reduced graphene oxide hybrid nanostructures for polymer composites with low dielectric loss, *Chemical Physics Letters* 638 (2015) 43-46.

- [85] V. Rybalko, A. Nikityuk, E. Pisarenko, T. Kuznetsova, P. D'yachenko, S.L. Guseinov, A. Malashin, A. Korchmarek, V. Kireev, Effect of inorganic nanopowders on properties of acrylic composites, *Russian Journal of Applied Chemistry* 88(5) (2015) 826-832.
- [86] D. Zhang, X. Wang, Z.-a. Qiao, D. Tang, Y. Liu, Q. Huo, Synthesis and characterization of novel lanthanide (III) complexes-functionalized mesoporous silica nanoparticles as fluorescent nanomaterials, *The Journal of Physical Chemistry C* 114(29) (2010) 12505-12510.
- [87] G. Zhang, M. Chen, J. Zhang, B. He, H. Yang, B. Yang, Effective increase in the refractive index of novel transparent silicone hybrid films by introduction of functionalized silicon nanoparticles, *RSC Advances* 5(76) (2015) 62128-62133.
- [88] A. Chakrabarty, S. Ponnupandian, N.G. Kang, J.W. Mays, N.K. Singha, Designing superhydrophobic surface based on fluoropolymer–silica nanocomposite via RAFT-mediated polymerization-induced self-assembly, *Journal of Polymer Science Part A: Polymer Chemistry* 56(3) (2018) 266-275.
- [89] Q. Tang, J. Duan, Y. Duan, B. He, L. Yu, Recent advances in alloy counter electrodes for dye-sensitized solar cells. A critical review, *Electrochimica Acta* 178 (2015) 886-899.
- [90] Y.-Y. Yu, T.-J. Huang, W.-Y. Lee, Y.-C. Chen, C.-C. Kuo, Highly transparent polyimide/nanocrystalline-zirconium dioxide hybrid materials for organic thin film transistor applications, *Organic Electronics* 48 (2017) 19-28.
- [91] P.K. Behera, P. Mondal, N.K. Singha, Self-Healable and Ultrahydrophobic Polyurethane-POSS Hybrids by Diels–Alder “Click” Reaction: A New Class of Coating Material, *Macromolecules* 51(13) (2018) 4770-4781.
- [92] C. Saha, P.K. Behera, S.K. Raut, N.K. Singha, Polyurethane–POSS hybrid materials: by solution blending and in-situ polymerization processes, *Bulletin of Materials Science* 43(1) (2020) 1-8.
- [93] D.B. Cordes, P.D. Lickiss, F. Rataboul, Recent developments in the chemistry of cubic polyhedral oligosilsesquioxanes, *Chem. Rev* 110(4) (2010) 2081-2173.
- [94] S.-W. Kuo, F.-C. Chang, POSS related polymer nanocomposites, *Progress in Polymer Science* 36(12) (2011) 1649-1696.
- [95] W. Zhang, A.H. Müller, Architecture, self-assembly and properties of well-defined hybrid polymers based on polyhedral oligomeric silsesquioxane (POSS), *Progress in Polymer Science* 38(8) (2013) 1121-1162.

- [96] E.T. Kopesky, T.S. Haddad, R.E. Cohen, G.H. McKinley, Thermomechanical properties of poly (methyl methacrylate) s containing tethered and untethered polyhedral oligomeric silsesquioxanes, *Macromolecules* 37(24) (2004) 8992-9004.
- [97] E.T. Kopesky, G.H. McKinley, R.E. Cohen, Toughened poly (methyl methacrylate) nanocomposites by incorporating polyhedral oligomeric silsesquioxanes, *Polymer* 47(1) (2006) 299-309.
- [98] J. Wu, P.T. Mather, POSS polymers: physical properties and biomaterials applications, *Polymer Reviews* 49(1) (2009) 25-63.
- [99] Q. Hong, X. Ma, Z. Li, F. Chen, Q. Zhang, Tuning the surface hydrophobicity of honeycomb porous films fabricated by star-shaped POSS-fluorinated acrylates polymer via breath-figure-templated self-assembly, *Materials & Design* 96 (2016) 1-9.
- [100] H. Zhou, Q. Ye, J. Xu, Polyhedral oligomeric silsesquioxane-based hybrid materials and their applications, *Materials Chemistry Frontiers* 1 (2017) 212-230.
- [101] J. Pyun, K. Matyjaszewski, The synthesis of hybrid polymers using atom transfer radical polymerization: homopolymers and block copolymers from polyhedral oligomeric silsesquioxane monomers, *Macromolecules* 33(1) (2000) 217-220.
- [102] F. Wang, X. Lu, C. He, Some recent developments of polyhedral oligomeric silsesquioxane (POSS)-based polymeric materials, *Journal of Materials Chemistry* 21(9) (2011) 2775-2782.
- [103] Z.-W. Yu, S.-X. Gao, K. Xu, Y.-X. Zhang, J. Peng, M.-C. Chen, Synthesis and characterization of silsesquioxane-cored star-shaped hybrid polymer via “grafting from” RAFT polymerization, *Chinese Chemical Letters* 27(11) (2016) 1696-1700.
- [104] R.N. Wenzel, Resistance of solid surfaces to wetting by water, *Industrial & Engineering Chemistry* 28(8) (1936) 988-994.
- [105] A. Cassie, S. Baxter, Wettability of porous surfaces, *Transactions of the Faraday society* 40 (1944) 546-551.
- [106] T. Onda, S. Shibuichi, N. Satoh, K. Tsujii, Super-water-repellent fractal surfaces, *Langmuir* 12(9) (1996) 2125-2127.
- [107] W. Barthlott, C. Neinhuis, Purity of the sacred lotus, or escape from contamination in biological surfaces, *Planta* 202(1) (1997) 1-8.
- [108] C. Neinhuis, W. Barthlott, Characterization and distribution of water-repellent, self-cleaning plant surfaces, *Annals of botany* 79(6) (1997) 667-677.

- [109] B.J. Blaiszik, S.L. Kramer, S.C. Olugebefola, J.S. Moore, N.R. Sottos, S.R. White, Self-healing polymers and composites, *Annual review of materials research* 40 (2010) 179-211.
- [110] S.R. White, N.R. Sottos, P.H. Geubelle, J.S. Moore, M.R. Kessler, S. Sriram, E.N. Brown, S. Viswanathan, Autonomic healing of polymer composites, *Nature* 409(6822) (2001) 794-797.
- [111] V.K. Thakur, M.R. Kessler, Self-healing polymer nanocomposite materials: A review, *Polymer* 69 (2015) 369-383.
- [112] P. Mondal, P.K. Behera, N.K. Singha, A healable thermo-reversible functional polymer prepared via RAFT polymerization and ultrafast ‘click’ chemistry using a triazolinedione derivative, *Chemical Communications* 53(62) (2017) 8715-8718.
- [113] P. Mondal, S.K. Raut, N.K. Singha, Thermally amendable tailor-made acrylate copolymers via RAFT polymerization and ultrafast alder-ene “click” chemistry, *Journal of Polymer Science Part A: Polymer Chemistry* 56(20) (2018) 2310-2318.
- [114] E.N. Brown, S.R. White, N.R. Sottos, Microcapsule induced toughening in a self-healing polymer composite, *Journal of Materials Science* 39(5) (2004) 1703-1710.
- [115] K.S. Toohey, N.R. Sottos, J.A. Lewis, J.S. Moore, S.R. White, Self-healing materials with microvascular networks, *Nature materials* 6(8) (2007) 581-585.
- [116] K. Toohey, N. Sottos, S. White, Characterization of microvascular-based self-healing coatings, *Experimental Mechanics* 49(5) (2009) 707-717.
- [117] S. Olugebefola, A. Aragón, C. Hansen, A. Hamilton, B. Kozola, W. Wu, P.H. Geubelle, J. Lewis, N.R. Sottos, S.R. White, Polymer microvascular network composites, *Journal of composite materials* 44(22) (2010) 2587-2603.
- [118] A.A. Kavitha, N.K. Singha, Smart “all acrylate” ABA triblock copolymer bearing reactive functionality via atom transfer radical polymerization (ATRP): demonstration of a “click reaction” in thermoreversible property, *Macromolecules* 43(7) (2010) 3193-3205.
- [119] Y.-L. Liu, T.-W. Chuo, Self-healing polymers based on thermally reversible Diels–Alder chemistry, *Polymer Chemistry* 4(7) (2013) 2194-2205.
- [120] N.B. Pramanik, G.B. Nando, N.K. Singha, Self-healing polymeric gel via RAFT polymerization and Diels–Alder click chemistry, *Polymer* 69 (2015) 349-356.

- [121] O.R. Cromwell, J. Chung, Z. Guan, Malleable and self-healing covalent polymer networks through tunable dynamic boronic ester bonds, *Journal of the American Chemical Society* 137(20) (2015) 6492-6495.
- [122] R. Guo, Q. Su, J. Zhang, A. Dong, C. Lin, J. Zhang, Facile access to multisensitive and self-healing hydrogels with reversible and dynamic boronic ester and disulfide linkages, *Biomacromolecules* 18(4) (2017) 1356-1364.
- [123] C.H. Li, J.L. Zuo, Self-Healing Polymers Based on Coordination Bonds, *Advanced Materials* (2019) 1903762-1903791.
- [124] L. Zhai, A. Narkar, K. Ahn, Self-healing polymers with nanomaterials and nanostructures, *Nano Today* 30 (2020) 100826-100843.
- [125] P. Wang, L. Yang, B. Dai, Z. Yang, S. Guo, G. Gao, L. Xu, M. Sun, K. Yao, J. Zhu, A self-healing transparent polydimethylsiloxane elastomer based on imine bonds, *European Polymer Journal* 123 (2020) 109382-109389.
- [126] S.J. Kalista Jr, T.C. Ward, Thermal characteristics of the self-healing response in poly (ethylene-co-methacrylic acid) copolymers, *Journal of the royal society interface* 4(13) (2007) 405-411.
- [127] P. Cordier, F. Tournilhac, C. Soulié-Ziakovic, L. Leibler, Self-healing and thermoreversible rubber from supramolecular assembly, *Nature* 451(7181) (2008) 977-980.
- [128] S. Burattini, H.M. Colquhoun, J.D. Fox, D. Friedmann, B.W. Greenland, P.J. Harris, W. Hayes, M.E. Mackay, S.J. Rowan, A self-repairing, supramolecular polymer system: healability as a consequence of donor-acceptor π - π stacking interactions, *Chemical communications* (44) (2009) 6717-6719.
- [129] S. Burattini, H.M. Colquhoun, B.W. Greenland, W. Hayes, A novel self-healing supramolecular polymer system, *Faraday discussions* 143 (2009) 251-264.
- [130] A.P. Vogt, B.S. Sumerlin, Temperature and redox responsive hydrogels from ABA triblock copolymers prepared by RAFT polymerization, *Soft Matter* 5(12) (2009) 2347-2351.
- [131] G. Deng, F. Li, H. Yu, F. Liu, C. Liu, W. Sun, H. Jiang, Y. Chen, Dynamic hydrogels with an environmental adaptive self-healing ability and dual responsive sol-gel transitions, *ACS Macro Letters* 1(2) (2012) 275-279.
- [132] F. Herbst, D. Döhler, P. Michael, W.H. Binder, Self-healing polymers via supramolecular forces, *Macromolecular rapid communications* 34(3) (2013) 203-220.

- [133] W. Pu, F. Jiang, P. Chen, B. Wei, A POSS based hydrogel with mechanical robustness, cohesiveness and a rapid self-healing ability by electrostatic interaction, *Soft Matter* 13(34) (2017) 5645-5648.
- [134] J. Yang, L. Yi, X. Fang, Y. Song, L. Zhao, J. Wu, H. Wu, Self-healing and recyclable biomass aerogel formed by electrostatic interaction, *Chemical Engineering Journal* 371 (2019) 213-221.
- [135] J.S. Park, T. Darlington, A.F. Starr, K. Takahashi, J. Riendeau, H.T. Hahn, Multiple healing effect of thermally activated self-healing composites based on Diels–Alder reaction, *Composites Science and Technology* 70(15) (2010) 2154-2159.
- [136] P.A. Pratama, M. Sharifi, A.M. Peterson, G.R. Palmese, Room temperature self-healing thermoset based on the Diels–Alder reaction, *ACS applied materials & interfaces* 5(23) (2013) 12425-12431.
- [137] G. Fortunato, V. Marroccoli, F. Corsini, S. Turri, G. Griffini, A facile approach to durable, transparent and self-healing coatings with enhanced hardness based on Diels-Alder polymer networks, *Progress in Organic Coatings* 147 (2020) 105840-105852.
- [138] K. Yasuda, K. Sugane, M. Shibata, Self-healing high-performance thermosets utilizing the furan/maleimide Diels-Alder and amine/maleimide Michael reactions, *Journal of Polymer Research* 27(1) (2020) 18-29.
- [139] L. Zhang, A. Eisenberg, Multiple morphologies of " crew-cut" aggregates of polystyrene-b-poly (acrylic acid) block copolymers, *Science* 268(5218) (1995) 1728-1731.
- [140] D.E. Discher, A. Eisenberg, Polymer vesicles, *Science* 297(5583) (2002) 967-973.
- [141] S. Jain, F.S. Bates, On the origins of morphological complexity in block copolymer surfactants, *Science* 300(5618) (2003) 460-464.
- [142] F. D'Agosto, J. Rieger, M. Lansalot, RAFT-Mediated Polymerization-Induced Self-Assembly, *Angewandte Chemie International Edition* 59(22) (2020) 8368-8392.
- [143] S. Krause, Dilute solution properties of a styrene—methyl methacrylate block copolymer, *The Journal of Physical Chemistry* 68(7) (1964) 1948-1955.
- [144] B. Charleux, G. Delaittre, J. Rieger, F. D'Agosto, Polymerization-induced self-assembly: from soluble macromolecules to block copolymer nano-objects in one step, *Macromolecules* 45(17) (2012) 6753-6765.

- [145] A. Munoz-Bonilla, S.I. Ali, A. Del Campo, M. Fernández-García, A.M. van Herk, J.P. Heuts, Block copolymer surfactants in emulsion polymerization: Influence of the miscibility of the hydrophobic block on kinetics, particle morphology, and film formation, *Macromolecules* 44(11) (2011) 4282-4290.
- [146] B.P. Koiry, A. Chakrabarty, N.K. Singha, Fluorinated amphiphilic block copolymers via RAFT polymerization and their application as surf-RAFT agent in miniemulsion polymerization, *RSC Advances* 5(20) (2015) 15461-15468.
- [147] M. Manguian, M. Save, B. Charleux, Batch Emulsion Polymerization of Styrene Stabilized by a Hydrophilic Macro-RAFT Agent, *Macromolecular rapid communications* 27(6) (2006) 399-404.
- [148] J. Rieger, W. Zhang, F. Stoffelbach, B. Charleux, Surfactant-free RAFT emulsion polymerization using poly (N, N-dimethylacrylamide) trithiocarbonate macromolecular chain transfer agents, *Macromolecules* 43(15) (2010) 6302-6310.
- [149] N. Yeole, D. Hundiwale, Effect of hydrophilic macro-RAFT agent in surfactant-free emulsion polymerization, *Colloids and Surfaces A: Physicochemical and Engineering Aspects* 392(1) (2011) 329-334.
- [150] N. Yeole, S.R. Kutcherlapati, T. Jana, Tunable core-shell nanoparticles: macro-RAFT mediated one pot emulsion polymerization, *RSC advances* 4(5) (2014) 2382-2388.
- [151] S. Binauld, L. Delafresnaye, B. Charleux, F. D'Agosto, M. Lansalot, Emulsion polymerization of vinyl acetate in the presence of different hydrophilic polymers obtained by RAFT/MADIX, *Macromolecules* 47(10) (2014) 3461-3472.
- [152] J. Barth, R. Siegmann, S. Beuermann, G.T. Russell, M. Buback, Investigations Into Chain-Length-Dependent Termination in Bulk Radical Polymerization of 1H, 1H, 2H, 2H-Tridecafluorooctyl Methacrylate, *Macromolecular Chemistry and Physics* 213(1) (2012) 19-28.
- [153] P. Lacroix-Desmazes, P. Andre, J.M. Desimone, A.V. Ruzette, B. Boutevin, Macromolecular surfactants for supercritical carbon dioxide applications: Synthesis and characterization of fluorinated block copolymers prepared by nitroxide-mediated radical polymerization, *Journal of Polymer Science Part A: Polymer Chemistry* 42(14) (2004) 3537-3552.
- [154] B. Grignard, T. Phan, D. Bertin, D. Gigmes, C. Jérôme, C. Detrembleur, Dispersion nitroxide mediated polymerization of methyl methacrylate in supercritical

carbon dioxide using in situ formed stabilizers, *Polymer Chemistry* 1(6) (2010) 837-840.

[155] G. He, G. Zhang, J. Hu, J. Sun, S. Hu, Y. Li, F. Liu, D. Xiao, H. Zou, G. Liu, Low-fluorinated homopolymer from heterogeneous ATRP of 2, 2, 2-trifluoroethyl methacrylate mediated by copper complex with nitrogen-based ligand, *Journal of Fluorine Chemistry* 132(9) (2011) 562-572.

[156] N.K. Singha, M.I. Gibson, B.P. Koiry, M. Danial, H.-A. Klok, Side-chain peptide-synthetic polymer conjugates via tandem “Ester-Amide/Thiol–Ene” post-polymerization modification of poly (pentafluorophenyl methacrylate) obtained using ATRP, *Biomacromolecules* 12(8) (2011) 2908-2913.

[157] M.Y. Lee, Y.T. Jeong, K.T. Lim, B.-C. Choi, H.G. Kim, Y.S. Gal, Multiple morphologies of self-assembled amphiphilic Poly (FOMA-b-EO) diblock copolymers, *Molecular Crystals and Liquid Crystals* 508(1) (2009) 173/[535]-182/[544].

[158] B. Jiang, L. Zhang, B. Liao, H. Pang, Self-assembly of well-defined thermo-responsive fluoropolymer and its application in tunable wettability surface, *Polymer* 55(21) (2014) 5350-5357.

[159] W. Guo, X. Tang, J. Xu, X. Wang, Y. Chen, F. Yu, M. Pei, Synthesis, characterization, and property of amphiphilic fluorinated abc-type triblock copolymers, *Journal of Polymer Science Part A: Polymer Chemistry* 49(7) (2011) 1528-1534.

[160] M. Rabnawaz, G. Liu, Preparation and application of a dual light-responsive triblock terpolymer, *Macromolecules* 45(13) (2012) 5586-5595.

[161] J.-c. Huang, C.-b. He, Y. Xiao, K.Y. Mya, J. Dai, Y.P. Siow, Polyimide/POSS nanocomposites: interfacial interaction, thermal properties and mechanical properties, *Polymer* 44(16) (2003) 4491-4499.

[162] H.J. Yu, Z.H. Luo, Novel superhydrophobic silica/poly (siloxane-fluoroacrylate) hybrid nanoparticles prepared via two-step surface-initiated ATRP: Synthesis, characterization, and wettability, *Journal of Polymer Science Part A: Polymer Chemistry* 48(23) (2010) 5570-5580.

[163] N.S. Bhairamadgi, S.P. Pujari, C.J. van Rijn, H. Zuilhof, Adhesion and friction properties of fluoropolymer brushes: On the tribological inertness of fluorine, *Langmuir* 30(42) (2014) 12532-12540.

- [164] C.-H. Xue, X.-J. Guo, J.-Z. Ma, S.-T. Jia, Fabrication of robust and antifouling superhydrophobic surfaces via surface-initiated atom transfer radical polymerization, *ACS applied materials & interfaces* 7(15) (2015) 8251-8259.
- [165] A.V. Markin, S.D. Zaitsev, O.S. Zotova, N.N. Smirnova, Thermodynamic Properties of Poly-1 H, 1 H, 5 H-octafluoropentyl Acrylate, *Journal of Chemical & Engineering Data* 58(11) (2013) 3201-3206.
- [166] B.P. Koiry, M. Moukwa, N.K. Singha, Reversible addition–fragmentation chain transfer (RAFT) polymerization of 2, 2, 3, 3, 4, 4, 4-heptafluorobutyl acrylate (HFBA), *Journal of Fluorine Chemistry* 153 (2013) 137-142.
- [167] M.I. Gibson, E. Fröhlich, H.A. Klok, Postpolymerization modification of poly (pentafluorophenyl methacrylate): Synthesis of a diverse water-soluble polymer library, *Journal of Polymer Science Part A: Polymer Chemistry* 47(17) (2009) 4332-4345.
- [168] S. Zaitsev, Y.D. Semchikov, E. Chernikova, Controlled radical copolymerization of N-vinylpyrrolidone with 1, 1, 1, 3, 3, 3-hexafluoroisopropyl- α -fluoroacrylate, *Polymer Science Series B* 51(3-4) (2009) 84-88.
- [169] L. Guo, Y. Jiang, T. Qiu, Y. Meng, X. Li, One-pot synthesis of poly (methacrylic acid)-b-poly (2, 2, 2-trifluoroethyl methacrylate) diblock copolymers via RAFT polymerization, *Polymer* 55(18) (2014) 4601-4610.
- [170] G. Li, A. Xu, B. Geng, S. Yang, G. Wu, S. Zhang, Synthesis and characterization of fluorinated diblock copolymer of 2, 2, 2-trifluoroethyl methacrylate and methyl methacrylate based on RAFT polymerization, *Journal of Fluorine Chemistry* 165 (2014) 132-137.
- [171] W. Zhang, X. Li, X. Guo, R. Yang, Mechanical and thermal properties and flame retardancy of phosphorus-containing polyhedral oligomeric silsesquioxane (DOPO-POSS)/polycarbonate composites, *Polymer Degradation and Stability* 95(12) (2010) 2541-2546.
- [172] H. Xu, S.-W. Kuo, J.-S. Lee, F.-C. Chang, Preparations, thermal properties, and T_g increase mechanism of inorganic/organic hybrid polymers based on polyhedral oligomeric silsesquioxanes, *Macromolecules* 35(23) (2002) 8788-8793.
- [173] Z. Zhang, A. Gu, G. Liang, P. Ren, J. Xie, X. Wang, Thermo-oxygen degradation mechanisms of POSS/epoxy nanocomposites, *Polymer Degradation and Stability* 92(11) (2007) 1986-1993.

- [174] E. Devaux, M. Rochery, S. Bourbigot, Polyurethane/clay and polyurethane/POSS nanocomposites as flame retarded coating for polyester and cotton fabrics, *Fire and Materials* 26(4-5) (2002) 149-154.
- [175] I. Jerman, M. Koželj, B. Orel, The effect of polyhedral oligomeric silsesquioxane dispersant and low surface energy additives on spectrally selective paint coatings with self-cleaning properties, *Solar Energy Materials and Solar Cells* 94(2) (2010) 232-245.
- [176] J. Wu, P.T. Mather, POSS polymers: physical properties and biomaterials applications, (2009).
- [177] A. Bruno, Controlled radical (co) polymerization of fluoromonomers, *Macromolecules* 43(24) (2010) 10163-10184.
- [178] G. Hougham, *Fluoropolymers 2: Properties*, Kluwer Academic Publishers, New York, 1999.
- [179] L. Matějka, M. Janata, J. Pleštil, A. Zhigunov, M. Šlouf, Self-assembly of POSS-containing block copolymers: Fixing the hierarchical structure in networks, *Polymer* 55(1) (2014) 126-136.
- [180] A. Pan, S. Yang, L. He, POSS-tethered fluorinated diblock copolymers with linear-and star-shaped topologies: synthesis, self-assembled films and hydrophobic applications, *RSC Advances* 5(68) (2015) 55048-55058.
- [181] A. Pan, L. He, L. Wang, N. Xi, POSS-based Diblock Fluoropolymer for Self-assembled Hydrophobic Coatings, *Materials Today: Proceedings* 3(2) (2016) 325-334.
- [182] X. Qiang, X. Ma, Z. Li, X. Hou, Synthesis of star-shaped polyhedral oligomeric silsesquioxane (POSS) fluorinated acrylates for hydrophobic honeycomb porous film application, *Colloid and Polymer Science* 292(7) (2014) 1531-1544.
- [183] H. Araki, K. Naka, Syntheses of Dumbbell-Shaped Trifluoropropyl-Substituted POSS Derivatives Linked by Simple Aliphatic Chains and Their Optical Transparent Thermoplastic Films, *Macromolecules* 44(15) (2011) 6039-6045.
- [184] J. Hao, Y. Wei, B. Chen, J. Mu, Polymerization of polyhedral oligomeric silsequioxane (POSS) with perfluoro-monomers and a kinetic study, *RSC Advances* 7(18) (2017) 10700-10706.
- [185] R. Nakatani, H. Takano, L. Wang, A. Chandra, Y. Tanaka, R. Maeda, N. Kihara, S. Minegishi, K. Miyagi, Y. Kasahara, Precise synthesis of fluorine-

containing block copolymers via RAFT, *J. Photopolym. Sci. Technol.* 29(5) (2016) 705-708.

[186] Z. Wang, H. Zuilhof, Self-healing fluoropolymer brushes as highly polymer-repellent coatings, *Journal of Materials Chemistry A* 4(7) (2016) 2408-2412.

[187] Z. Wang, H. Zuilhof, Self-healing superhydrophobic fluoropolymer brushes as highly protein-repellent coatings, *Langmuir* 32(25) (2016) 6310-6318.

[188] Y. Li, L. Li, J. Sun, Bioinspired self-healing superhydrophobic coatings, *Angewandte Chemie* 122(35) (2010) 6265-6269.

[189] H. Wang, Y. Xue, J. Ding, L. Feng, X. Wang, T. Lin, Durable, self-healing superhydrophobic and superoleophobic surfaces from fluorinated-decyl polyhedral oligomeric silsesquioxane and hydrolyzed fluorinated alkyl silane, *Angewandte Chemie* 123(48) (2011) 11635-11638.

[190] H. Zhou, H. Wang, H. Niu, A. Gestos, T. Lin, Robust, self-healing superamphiphobic fabrics prepared by two-step coating of fluoro-containing polymer, fluoroalkyl silane, and modified silica nanoparticles, *Advanced Functional Materials* 23(13) (2013) 1664-1670.

[191] A.K. Padhan, D. Mandal, Thermo-reversible self-healing in a fluoruous crosslinked copolymer, *Polymer Chemistry* 9(23) (2018) 3248-3261.

[192] S. Banerjee, B.V. Tawade, B. Améduri, Functional fluorinated polymer materials and preliminary self-healing behavior, *Polymer Chemistry* 10(16) (2019) 1993-1997.

[193] S. Xu, W. Liu, Synthesis and surface characterization of an amphiphilic fluorinated copolymer via emulsifier-free emulsion polymerization of RAFT, *Journal of Fluorine Chemistry* 129(2) (2008) 125-130.

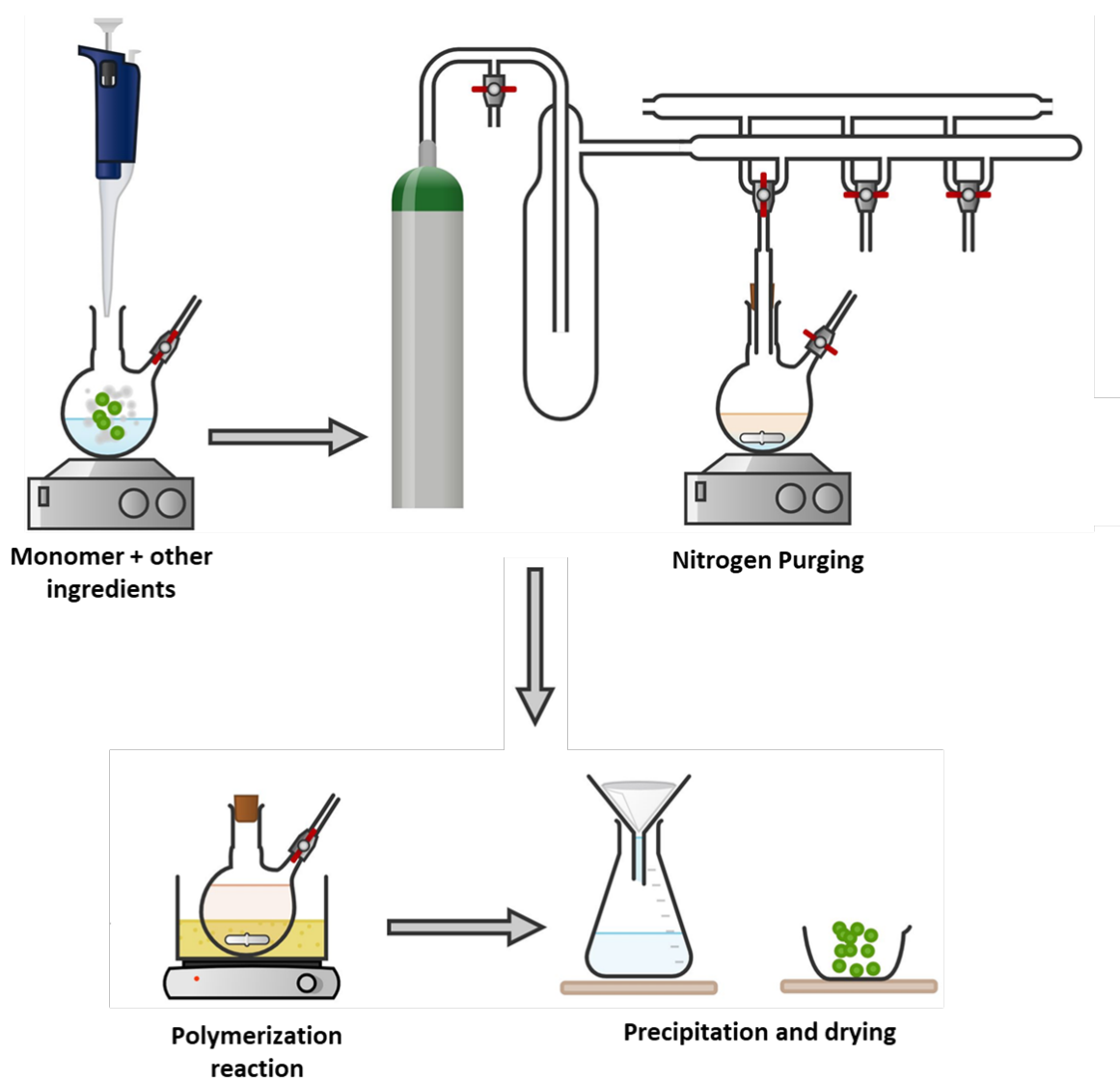
[194] X. Cui, S. Zhong, Y. Gao, H. Wang, Preparation and characterization of emulsifier-free core-shell interpenetrating polymer network-fluorinated polyacrylate latex particles, *Colloids and Surfaces A: Physicochemical and Engineering Aspects* 324(1-3) (2008) 14-21.

[195] L. Hao, Q. An, W. Xu, D. Zhang, M. Zhang, Effect of polymerizable emulsifier and fluorine monomer on properties of self-crosslinking fluorinated polyacrylate soap-free latexes, *Journal of Polymer Research* 20(7) (2013) 174-183.

[196] W. Xu, Q. An, L. Hao, D. Zhang, M. Zhang, Synthesis and characterization of self-crosslinking fluorinated polyacrylate soap-free latices with core-shell structure, *Applied surface science* 268 (2013) 373-380.

- [197] Y. Chen, C. Zhang, X. Chen, Emulsifier-free latex of fluorinated acrylate copolymer, *European polymer journal* 42(3) (2006) 694-701.
- [198] W. Xu, Q. An, L. Hao, Z. Sun, W. Zhao, Synthesis of cationic core-shell fluorine-containing polyacrylate soap-free latex and its application on cotton substrate, *Fibers and Polymers* 14(6) (2013) 895-903.
- [199] H. Wang, H. Zhou, Y. Chen, C. Zhang, Synthesis of fluorinated gradient copolymers by RAFT emulsifier-free emulsion polymerization and their compatibilization in copolymer blends, *Colloid and Polymer Science* 292(11) (2014) 2803-2809.
- [200] Y. Chen, W. Luo, Y. Wang, C. Sun, M. Han, C. Zhang, Synthesis and self-assembly of amphiphilic gradient copolymer via RAFT emulsifier-free emulsion polymerization, *Journal of colloid and interface science* 369(1) (2012) 46-51.

EXPERIMENTAL AND CHARACTERIZATION TECHNIQUES

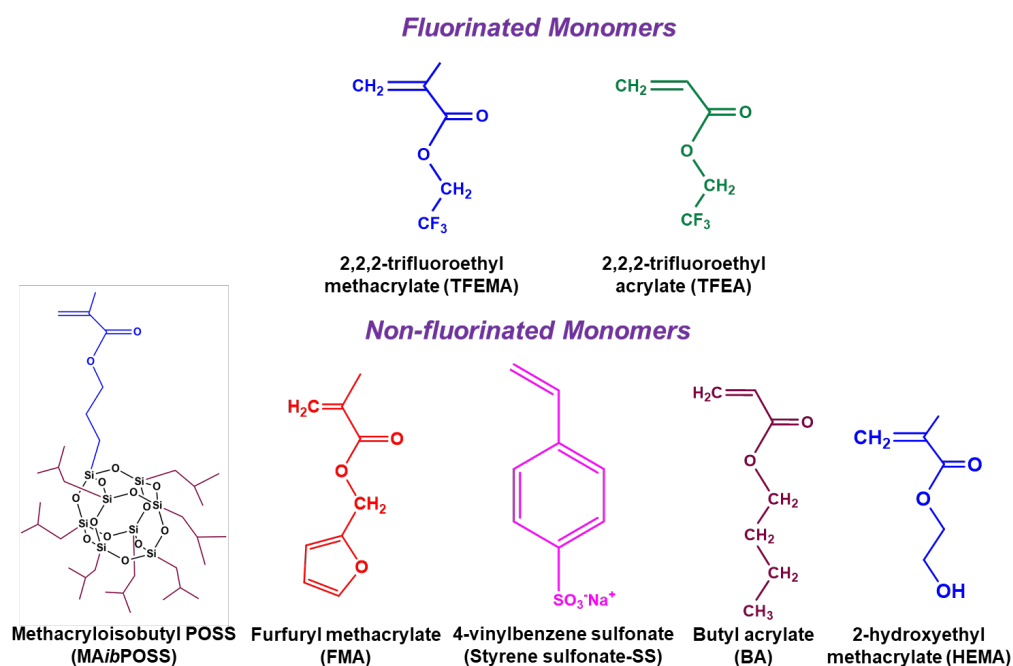


This chapter delineates the details of the materials used in this thesis work. The details of the characterization techniques adapted in the studies are also elaborated here.

2.1. Materials

2.1.1. Monomers

The fluorinated monomers, 2,2,2-trifluoroethyl acrylate (TFEA), and 2,2,2-trifluoroethyl methacrylate (TFEMA) were procured from Sigma-Aldrich, USA and used as received. The non-fluorinated functional co-monomers, furfuryl methacrylate (FMA), butyl acrylate (BA) and 2-hydroxyethyl methacrylate (HEMA) were purchased from Sigma-Aldrich, USA and were purified by passing through a basic alumina column. Styrene sulfonate (SS) was procured from Sigma-Aldrich and was used as received. The organic hybrid monomer containing POSS moiety, methacryloisobutyl POSS (MAibPOSS), was obtained from Hybrid Plastics, USA, and was used as received. **Scheme 2.1.** shows the chemical structures of the fluorinated and the non-fluorinated monomers used in this thesis work.

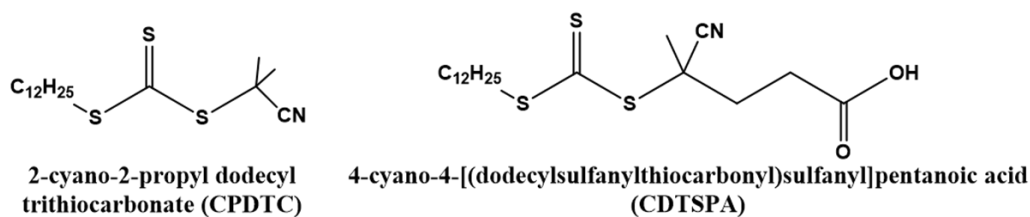


Scheme 2.1. Chemical structures of various fluorinated and non-fluorinated monomers used.

2.1.2. RAFT agents

The RAFT agents, 2-cyano-2-propyl dodecyl trithiocarbonate (CPDTC), and 4-cyano-4-[(dodecylsulfanylthiocarbonyl)sulfanyl]pentanoic acid (CDTSPA) were

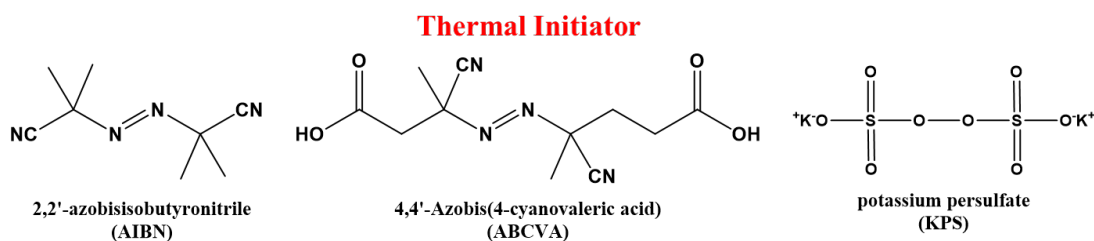
purchased from Sigma-Aldrich, USA and used as received. **Scheme 2.2.** Chemical structures of RAFT agents used in this thesis work.



Scheme 2.2. Chemical structure of various RAFT agents used.

2.1.3. Thermal initiators

2,2'-Azobisisobutyronitrile (AIBN), 4,4'-azobis(4-cyanovaleric acid) (ABCVA), and potassium persulfate (KPS) were used as initiators. The initiators, ABCVA and KPS, were purchased from Sigma-Aldrich and used as received. The initiator, AIBN, was purchased from Merck, India, and was purified by recrystallization from ethanol prior to use. **Scheme 2.4.** shows the chemical structures of thermal initiators used in this thesis work.



Scheme 2.4. Chemical structure of various initiators used.

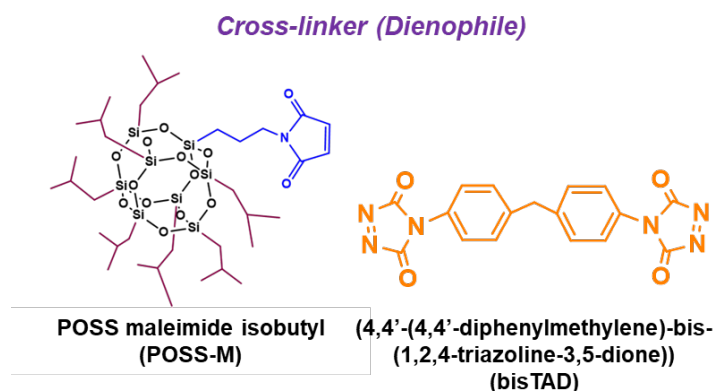
2.1.4. Solvents and other reagents

Typical organic solvents like acetone, tetrahydrofuran (THF), N,N-dimethylformamide (DMF), toluene, chloroform (CHCl₃), methanol, ethyl acetate, and dichloromethane (DCM) were purchased from Merck, India and purified by vacuum distillation over CaH₂. HPLC grade THF for gel permeation chromatography (GPC) analysis was purchased from Spectrochem, India, and used as received.

Deuterated solvents for NMR analysis viz., DMSO-D₆, CDCl₃, D₂O were purchased from Sigma-Aldrich and used as received.

2.1.5. Cross-linker (Dienophile)

POSS-maleimide isobutyl (POSS-M) was purchased from Hybrid Plastics, USA, and was used as received. The (4,4'-(4,4'-diphenylmethylene)-bis-(1,2,4-triazoline-3,5-dione)) (bisTAD) was prepared following the reaction procedure mentioned in section 6.2.1 of Chapter-6. **Scheme 2.3.** shows the chemical structure of POSS-maleimide isobutyl and bisTAD. This POSS-M and bisTAD were used as a dienophile in Diels-Alder chemistry.



Scheme 2.3. Chemical structure of POSS-M.

2.2. Characterization Techniques

2.2.1. Gel permeation chromatography (GPC) analysis

The molecular weights (M_n) and the dispersity (D) of the prepared polymers were determined at ambient temperature by GPC analysis. Samples for GPC analysis were prepared by dissolving the polymers in HPLC grade THF at a concentration of 2.0 mg/mL. A VISCOTEK GPC instrument equipped with two ViscoGel mixed bed columns connected in series with a RI detector (model VE 3580) and UV detector (model VE 3210) was used. THF was used as the eluent at a flow rate of 1 mL/min. A set of poly(methyl methacrylate) (PMMA) and polystyrene (PS) standards of low

dispersity were used as the calibration standards. Data were processed by using OmniSEC 4.6 software.

2.2.2. Nuclear magnetic resonance (NMR) spectroscopy

The chemical structure of the prepared homopolymers, BCPs, and the modified polymers were studied by using NMR analysis. The ¹HNMR spectra of the polymers were recorded on Bruker 400 MHz and Varian VNMRs 500 MHz spectrometers. The samples for the NMR analysis were prepared using CDCl₃, DMSO-D₆, and D₂O as solvents. Tetramethylsilane (TMS) was used as an internal standard.

2.2.3. Fourier transform infrared (FT-IR) spectroscopy

The chemical and structural properties of the prepared polymers were studied using FTIR analysis. FTIR spectra were recorded on a Fourier transform infrared spectrophotometer (Perkin Elmer, model spectrum 2). The samples were analyzed in attenuated total reflection (ATR) mode. The spectra, over the range 400 cm⁻¹ - 4000 cm⁻¹, were recorded and plotted.

2.2.4. Differential scanning calorimetry (DSC)

The thermal properties of the prepared polymers were studied via differential scanning calorimetry (DSC) using a TA Instrument (Model Discovery DSC 25). The thermal transitions were recorded for the temperature range of -30 °C to 200 °C at a 10 °C/min heating rate, under a nitrogen atmosphere. Around 5-6 mg of samples were taken in the Tzero aluminum pan for the analysis. The samples were initially quenched to liquid nitrogen temperature then heated to +200 °C at the rate of 10 °C/min. After an equilibration time of 1 min, the samples were cooled to -80 °C at the cooling rate of 10 °C/min followed by reheating to +200 °C. The heat flow with

respect to temperature was recorded. The inflection point in the second heating scan is taken as the glass transition temperature (T_g).

2.2.5. Thermogravimetric analysis (TGA)

The thermal properties, like the degradation behavior and the stability of the prepared polymers, were studied using thermogravimetric analysis (TGA). TGA analysis was carried out on a Shimadzu TGA-50 model instrument. Approximately 10 mg of sample was taken in a platinum pan and heated from 30 °C to 600 °C temperature range under the nitrogen atmosphere at a heating rate of 20 °C/min. The weight loss with respect to the temperature is recorded.

2.2.6. Optical Microscopy (OM)

Optical images of thin films of the prepared polymers were observed and recorded using an optical microscope (Leica, DM2500). Polymers dissolved in desired solvents were cast into uniform thin films on a cleaned glass substrate. The samples were then dried overnight at 40 °C in a vacuum oven.

2.2.7. Field Emission Scanning Electron Microscopy (FE-SEM)

The morphology of the prepared polymers was observed with a field emission scanning electron microscope (FESEM) (Supra 40, Carl ZEISS Pvt. Ltd.). For this analysis, polymers were dissolved in the desired solvent and were cast as films on small glass plates or on silicon wafers. Before analysis, the samples were gold coated. The energy dispersive X-ray (EDX) setup fitted with the SEM instrument was used to identify the elemental composition of the polymer samples.

2.2.8. Transmission Electron Microscopy (TEM)

The particle size and morphology of the prepared homopolymers, block copolymers and the polymer latex were studied using an analytical TEM instrument

(Tecnai G2 20 S-TWIN TEM, USA) operated at an accelerated voltage of 120 kV. The samples were prepared by drop-casting the diluted polymer solution in the desired solvent on a 300 mesh Cu grid and air dried for 3-4 days.

2.2.9. Atomic Force Microscopy (AFM)

Surface topography and morphology of the prepared polymers were studied using an atomic force microscope (Agilent 5100, USA). The samples for the AFM analysis were prepared by dissolving the polymer in the desired solvent, the polymer solution was then cast as thin films by either drop-casting or spin coating over a cleaned glass slide or silicon wafer followed by drying in air for 3-4 days. The AFM samples were scanned using a silicon cantilever (PPP-NCL, Nanosensors) operating under intermittent contact mode (tapping mode).

2.2.10. Small Angle X-ray Scattering (SAXS) Analysis

SAXS analysis was carried out on a Xeuss 2.0, Xenocs, France instrument with $\text{CuK}\alpha$ radiation ($\alpha = 1.542 \text{ \AA}$) as the source and Pilatus 300K (Dectris) two-dimensional area detector with a sample-to-detector distance of 2500 mm. Silver behenate was used as a reference specimen for calibration.

2.2.11. X-ray photoelectron spectroscopy (XPS) Analysis

The surface chemical composition of the prepared copolymers was analyzed using XPS analysis. The XPS analysis was carried out using K-AlphaTM + X-ray photoelectron spectrometer with a monochromatic Al K α X-ray source.

2.2.12. Contact angle analysis

The surface properties of the prepared polymers were studied by measuring the contact angle (CA) using a Goniometer (Rame-Hart instrument co., USA Model no.- 260F4). Samples were prepared by casting the polymer solution on a glass slide

or on a metal surface as required for the study and dried in air for 2-3 days. The static contact angle was measured by placing a drop of about 0.5 μL drop on the sample, and DROPimage advanced CA software was used to measure the angle.

2.2.13. Mechanical Properties

The mechanical properties of the prepared polymers films were studied according to ASTM D412 using Universal Testing Machine (Zwick Roel Z10). The tensile strength, modulus, and elongation at break of the samples were measured. The tensile specimens were cut using a standard die and the speed of testing was kept at 500 mm/min.

2.2.14. Dielectric Study

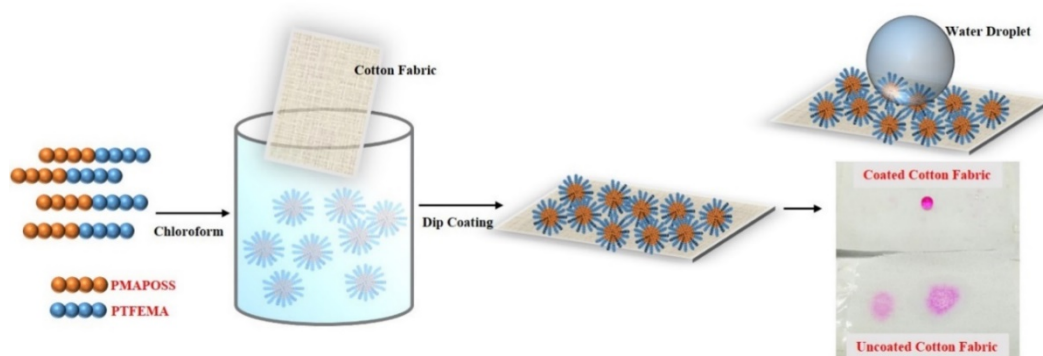
The dielectric properties viz., ionic conductivity, dielectric constant, and loss tangent of the prepared polymer film based on fluoropolymer was studied using A.C. impedance spectroscopy (model HIOKI 3532–50 LCR meter, Japan) over a frequency range of 42 Hz to 100 kHz at room temperature.

2.2.15. Self-healing study

The healing efficiency was analyzed by monitoring the reduction of the deliberately created scratch width using an optical microscope (OM) (Leica DMLM, made in Germany). The scratch test related healing efficiency (E_H) was calculated using the following equation.

$$E_H (\%) = \frac{(\text{Initial scratch width}) - (\text{healed scratch width})}{(\text{Initial scratch width})} \times 100$$

POSS AND FLUORINE CONTAINING NANOSTRUCTURED BLOCK COPOLYMER; SYNTHESIS VIA RAFT POLYMERIZATION AND ITS APPLICATION AS HYDROPHOBIC COATING MATERIAL



This chapter delineates the synthesis, characterization, and application of organic-inorganic hybrid block copolymers (BCPs) of POSS and fluorinated acrylic polymers via RAFT polymerization. This chapter also describes the self-assembly conduct of BCPs in different solvent and the potential application of the POSS fluorinated hybrid polymers as a coating material.

Abstract

In this Chapter, the nanostructured BCPs of POSS-methacrylate and fluorinated methacrylate were prepared via RAFT polymerization. In this case, methacryloisobutyl polyhedral oligomeric silsesquioxane (MA*ib*POSS) was first polymerized using 2-cyano-2-propyl dodecyl trithiocarbonate (CPDTC) as a RAFT agent. Later, 2,2,2-trifluoroethyl methacrylate (TFEMA) monomer was polymerized using the PMA*ib*POSS as a macro-RAFT agent. The BCPs were characterized via FT-IR, ¹H-NMR and GPC analyses. The BCPs, when cast using different organic solvents exhibited core-shell and lamellar type nanostructures. The nanostructured morphology of the BCPs was studied using SEM, AFM, TEM, and SAXS analyses. The potential application of the prepared BCPs as an efficient coating material was studied by coating the BCPs over different substrates and their hydrophobicity was measured using water contact angle analysis. The coated substrates exhibited improved hydrophobicity with the water contact angle values as high as ~135°.

3.1. Introduction

Organic-inorganic hybrid polymers have excellent properties, combining the desirable properties from both the organic and inorganic components. [1, 2] Incorporation of nanoscale inorganic materials, such as silica, nano clay, metal, or metal oxide nanoparticles, into the polymer matrix can lead to the development of these hybrid polymeric materials. [3-5] However, the aggregation propensity of the inorganic component in the organic polymeric matrix encounters problems while processing as well as in applications of these hybrid materials. This drawback can be overcome by an approach like functionalizing these materials with reactive functional groups or attaching them covalently onto the polymer chains. In conjunction with this, the physical properties of the material like the mechanical strength, thermal stability, and surface properties can be improved by tailoring the architectures, such as the preparation of block copolymers, star-shaped polymer, branched polymers, or brush-like polymers. This enhancement in properties can lead to high application potential of these hybrid materials as prosthetics, medical implants, drug carriers, sensors, self-healing, and self-cleaning surfaces.[6-8] Another shortcoming of these types of materials is that it is very challenging to have controlled molecular weights and design the polymer architecture through conventional radical polymerization. This can be surmounted by employing reversible deactivation radical polymerization (RDRP) techniques, like nitroxide mediated polymerization (NMP), [9, 10] atom transfer radical polymerization (ATRP), [11-13], and RAFT polymerization [14, 15]. RDRP enables both the well-defined architecture and tailoring of the properties of hybrid polymeric materials. [16-19]

Polyhedral oligomeric silsesquioxane (POSS), also named "molecule silica," is a unique inorganic component with definite hybrid nanostructure of organo-silicone

compounds with a nanoscale cubic structure (~1-3 nm). [20-22] Incorporation of POSS into an organic polymer matrix can substantially improve the properties like mechanical strength, [23, 24] thermal stability, [25] flammability and oxidation resistance, [26-28] and resistance towards oil and water, etc. [29] also it gives rise to nanostructured materials with well-defined architecture. POSS-containing nanostructured materials can be prepared by using POSS either as an initiator, or monomer or as a crosslinking agent. [30, 31] Adopting the RDRP technique helps in preparing hybrid POSS containing polymers with well-defined architectures like block copolymers (BCPs), star-shaped polymers, dendrimers, etc. The advances in the synthesis of hybrid material based on POSS via RDRP techniques was reviewed by Zhang *et al.* [32] Recently, Tajbaksh *et al.* prepared methacryloisobutyl POSS (MA*ib*POSS) based homopolymers and copolymers via NMP using the miniemulsion technique.[33] Ullah *et al.* prepared BCPs containing MA*ib*POSS and n-acryloyl morpholine (ACM) (PMA*ib*POSS-*b*-PACM) via NMP. [34] ATRP is most commonly used for the synthesis of random and block copolymers using POSS as monomers [27, 30, 35-37]. Matyjaszewski and Pyun reported the first-ever BCP based on methacryloyl POSS (MAPOSS) as a monomer along with butyl acrylate (PMAPOSS-*b*-PBA-*b*-PMAPOSS). [30] Recently, Ata *et al.* prepared POSS tethered poly(methyl methacrylate) (PMMA) based thin films via ATRP technique, and studied its self-healing behavior was reported by [38] Equivalent to ATRP, RAFT polymerization has also been used to synthesize well-defined POSS containing block copolymers Zhang and co-workers pioneered the preparation of POSS based hybrid copolymers via RAFT polymerization [39, 40]. They reported POSS containing BCPs based on *N*-isopropyl acrylamide and deliberated their thermal properties and self-assembly behavior. Mya *et al.* reported the preparation and reaction kinetics of POSS containing BCPs based polyacrylates [41]. They noted that the steric

hindrance of the silsesquioxane cage in the macro-monomer leads to a limiting degree of polymerization on POSS based BCPs. POSS and PMMA based BCPs prepared *via* RAFT, their self-assembly behavior, and their use as a modifier for epoxy-based thermosets were reported by Deng and co-workers. [42]. Exploration of the interesting self-assembling nanostructures and different patterns of POSS-based materials have attained great interest and led to the development of a wide range of hybrid materials and utilize them as potential drug carriers, lithographic substrates, surface patterning, etc. [43, 44] Zhang *et al.* have reviewed the self-assembly behavior and architecture of POSS based BCPs. [45, 46]

Fluorinated polymers, especially polyfluoroacrylates, provide remarkable properties like excellent thermal stability, good resistance towards a wide range of chemicals, and low surface energy. [47-49] Owing to these exceptional properties, they are used widely in preparing surfaces with a hydrophobic/superhydrophobic nature. [50-53] Substantial enhancement in property can be achieved further by combining this hybrid POSS material and fluoropolymers. These combined organic-inorganic hybrid polymers have improved properties leading to the development of various applications. Coatings and films based on these hybrid BCPs show great thermal stability and excellent resistance to chemicals. The ability of the POSS containing BCPs to endure self-assembly and microphase separation leading to long-range structural ordering because of the presence of POSS moiety has attained great interest in developing these hybrid polymers. [54] The self-orientation and self-migration of the fluoro blocks in the fluorinated block copolymers can help in developing coatings with unique properties like anti-wetting, anti-fogging, and anti-icing. [55] BCPs based of a fluoroacrylate and methacryloethyl POSS (MAePOSS) via RAFT polymerization was reported Nakatani *et al.*. [56] There are only a few studies related for the preparation of

hybrid BCPs based on POSS and fluoroacrylate. [57-60] Most of these BCPs based on POSS and fluoroacrylate were prepared *via* ATRP.

This chapter delineates the RAFT polymerization of MA*ib*POSS and TFEMA for the preparation of BCP, PMA*ib*POSS-*block*-PTFEMA, using PMA*ib*POSS as the macro-RAFT agent. The self-assembled morphology of the BCPs varying the solvents was studied. Their potential application as coating material was analyzed by coating the BCPs over different substrates like cotton, metal, and glass surface.

3.2. Experimental

3.2.1. Preparation of PMA*ib*POSS via RAFT Polymerization

In a typical polymerization reaction, the monomer, MA*ib*POSS (1 g, 1.0 mmol), and the RAFT agent CPDTC (34.5 mg, 0.1 mmol) were taken in 1 ml toluene in a Schlenk tube. Then the initiator AIBN (4.1 mg, 0.025 mmol) is added to the above mixture, followed by purging of nitrogen for 15 min to remove the oxygen in the reaction medium. The polymerization reaction was carried out for 8 h at 70 °C. The reaction was terminated by quenching the reaction tube in an ice bath. Methanol/ethyl acetate mixture (80:20 v/v) is used to precipitate the final polymer product and dried in a vacuum oven at 45°C overnight. Later, TFEMA is polymerized using the prepared poly(methacryloisobutyl POSS) (PMA*ib*POSS) as a macro-RAFT agent.

3.2.2. Preparation of PTFEMA via RAFT Polymerization

Following the similar procedure adapted for preparing PMA*ib*POSS, a homopolymer of TFEMA was prepared for comparative studies. In a typical reaction, the monomer TFEMA (1 g, 5.95 mmol) and the RAFT agent, CPDTC (34.5 mg, 0.1 mmol), were solubilized in 1 ml toluene in a Schlenk tube. Then the initiator, AIBN (4.1 mg, 0.025 mmol), was put into the mixture and stirred for 15 mins under nitrogen purging to make an oxygen-free environment for the reaction. The polymerization

reaction was carried out at 70°C for 8 h. The reaction was terminated by quenching the reaction tube in an ice bath. The final product was dissolved in THF and precipitated in methanol and then dried in a vacuum oven at 45 °C overnight.

3.2.3. PMAibPOSS-*block*-PTFEMA preparation using PMAibPOSS as a macro-RAFT agent

A homogenous mixture of the macro-RAFT agent PMAibPOSS (0.18 g, 0.025 mmol) and TFEMA (0.5 g, 2.97 mmol) in toluene was taken in a Schlenk tube. Followed by the addition of the initiator, AIBN (1 mg, 0.001 mmol), the reaction tube was sealed and made inert by purging nitrogen for 15 min under constant stirring. The polymerization reaction was then carried out for 8 h at 70°C. The final product was precipitated in *n*-hexane and dried overnight in a vacuum oven at 45 °C. Following the same procedure, block copolymers (BCPs) with a different block length of fluoropolymer were prepared, keeping the ratio of [initiator]:[macro-RAFT] at 1:4.

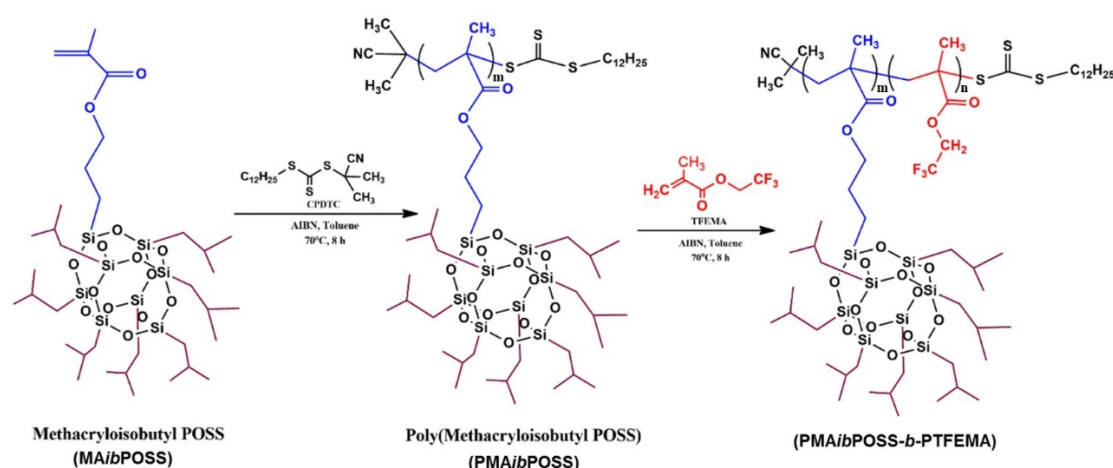
3.2.4. Preparation of fabric and metal surfaces for coating with BCP

To explore the potential application of the PMAibPOSS-*block*-PTFEMA as an efficient coating material, the BCPs were coated over different surfaces like glass, fabric, and metal surfaces. A piece of cotton fabric washed with distilled water for 3 h, followed by acetone for 1 h, was used to prepare the hydrophobic fabric surface. The pre-washed fabric is dipped into the BCP polymer solution with a concentration of 0.2 g/mL for about two to three minutes, and it was dried in air overnight. Following the same procedure, a piece of aluminum metal plate cut from a sheet was also prepared before coating the BCP over the metallic surfaces. The metal plate is then dipped into the polymer solution and dried in air overnight.

3.3. Results and discussion

3.3.1. Preparation of PMA*ib*POSS and PTFEMA Block Copolymers

Scheme 3.1 shows the schematic representation of the preparation of PMA*ib*POSS and PTFEMA block copolymers. As explained earlier, the homopolymer of MA*ib*POSS was prepared via RAFT polymerization using CPDTC as a RAFT agent and AIBN as the initiator ($[AIBN]:[CPDTC] = 1:4$). Then the BCPs were prepared by the subsequent polymerization of TFEMA monomer using PMA*ib*POSS as a macro-RAFT agent led to the formation of BCPs of PMA*ib*POSS-*b*-PTFEMA. The details about the homopolymers and the BCPs prepared are shown in **Table 3.1**. About 80% conversion is achieved in 8 h for the homopolymerization of MA*ib*POSS whereas, ~60% conversion during the preparation of BCPs.



Scheme 3.1. Schematic representation of the preparation of PMA*ib*POSS and using it as a macro-RAFT agent for the preparation of PMA*ib*POSS-*b*-PTFEMA

3.3.2. ¹H NMR spectroscopy

¹H NMR spectroscopy of the PMA*ib*POSS polymerized via RAFT process is shown in **Figure 3.1**.

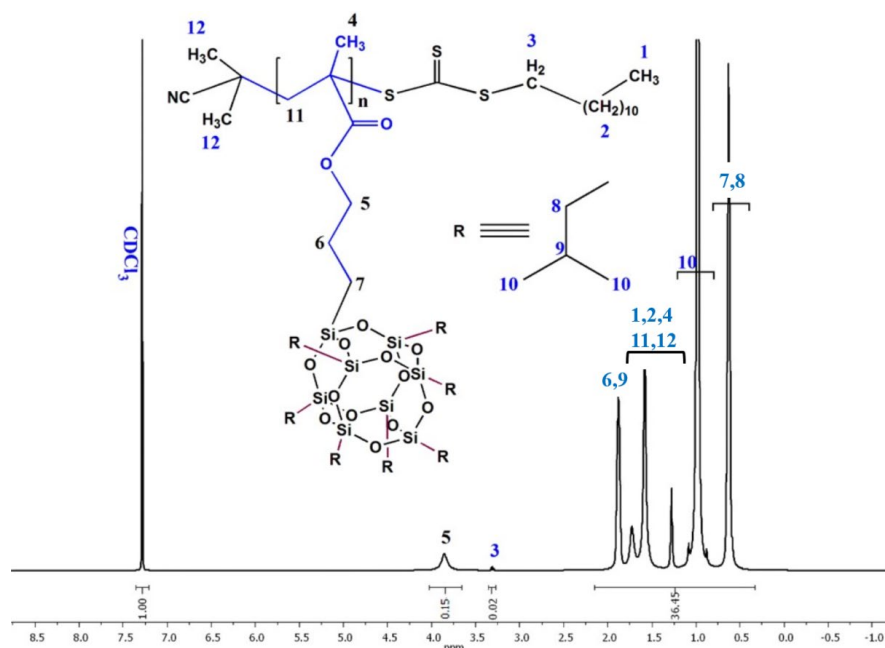


Figure 3.1. ^1H NMR spectrum of PMAibPOSS homopolymer in the CDCl_3 solvent.

The methylene protons ($-\text{O}-\text{CH}_2$) in the pendant POSS unit emerged at $\delta = 3.9$ ppm (designated as **5**). At the same time, the remaining methylene, methyl, and methine protons of the POSS unit emerged at $\delta = 0.6$ ppm (designated as **7** and **8**), 1.0 ppm (designated as **10**), and 1.8 ppm (designated as **6** and **9**) respectively. The peak at $\delta = 3.3$ ppm (designated as **3**) is attributed to the methylene protons ($-\text{S}-\text{CH}_2-$) of the RAFT-end group. The molecular weight of the PMAibPOSS homopolymer was calculated from the integral areas of peaks **5** and **3** using the following equation.

$$M_{\text{PMAibPOSS}} = M_{\text{RAFT}} + [(I_5/2)/(I_3/2)] \times M_{\text{MAibPOSS}}$$

Where M_{RAFT} and M_{MAibPOSS} stand for the molecular weights of RAFT agent and the monomer MAibPOSS, respectively, and I_5 and I_3 are the integral areas of peak **5** and **3** respectively in **Figure 3.1**. The molecular weight of PMAibPOSS from the NMR spectrum was calculated to be 7400 g/mol.

^1H NMR spectroscopy of the BCP, PMAibPOSS-*b*-PTFEMA, is shown in **Figure 3.2**. The chemical shift at $\delta = 4.0$ ppm attributes to the $-\text{O}-\text{CH}_2$ protons present in the MAibPOSS, whereas the chemical shift at $\delta = 4.6$ ppm corresponds to the $-\text{O}-\text{CH}_2$

protons present in the TFEMA side chain. The chemical shift at $\delta = 3.3$ ppm is attributed to the RAFT end group. The molar composition of the individual blocks of PMA*ib*POSS and PTFEMA in the BCP was calculated from the integrals of the chemical shifts mentioned above, and the PMA*ib*POSS: PTFEMA ratio is found to be 1:5. The molecular weight of the BCP from the NMR was determined to be $M_{n, NMR} = 13100$ g/mol.

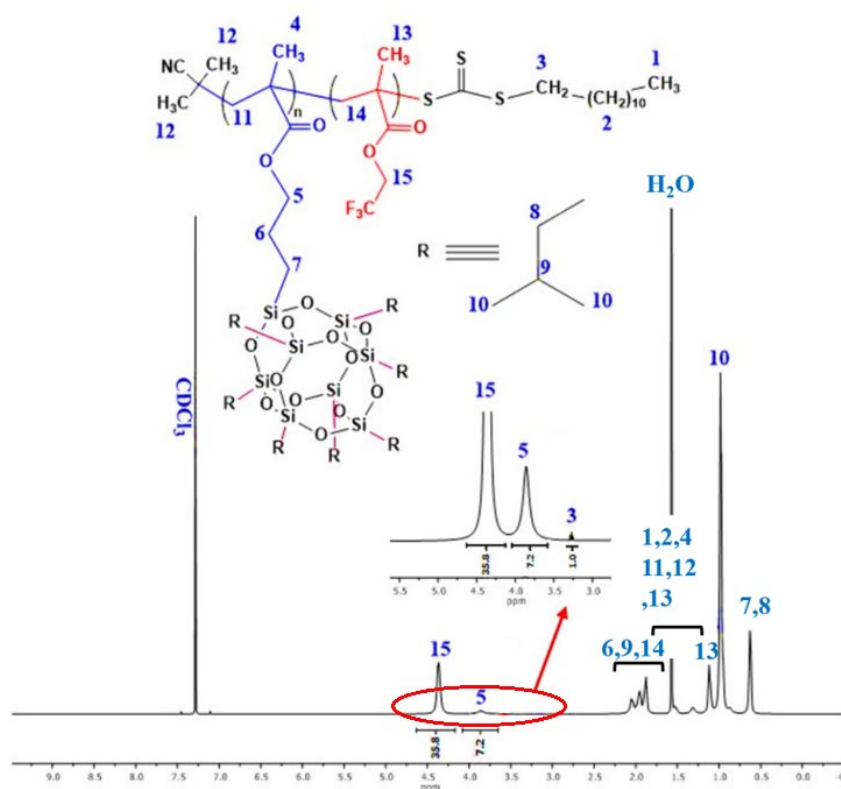


Figure 3.2. ^1H NMR spectrum of PMA*ib*POSS-*b*-PTFEMA polymer in the CDCl_3 solvent.

3.3.3. GPC Analysis

The BCPs, PMA*ib*POSS-*b*-PTFEMA was prepared by using the homopolymer, PMA*ib*POSS as a macro-RAFT agent for the polymerization of the TFEMA monomer. By varying the TFEMA monomer to the macro-RAFT concentration, BCPs with a different block length of PTFEMA were prepared. **Figure 3.3** shows the GPC traces of the macro-RAFT agent and both the BCPs. The complete shift of the GPC traces

denotes the significant increase in molecular weights of the BCPs compared to the macro-RAFT agent, and this demonstrates the successful formation of the block copolymer.

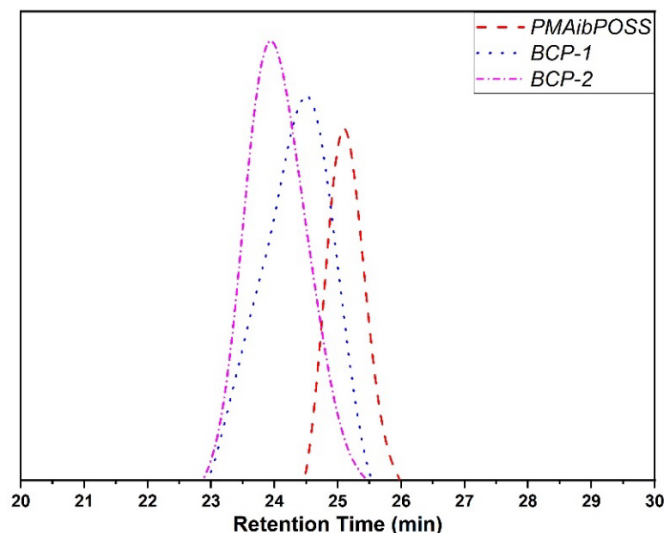


Figure 3.3. SEC traces of macro-RAFT (PMAibPOSS) agent and BCP (PMAibPOSS-*b*-PTFEMA the block copolymer).

Table 3.1 shows the details of the homopolymer and BCPs prepared. Both the macro-RAFT agent and the BCPs show low D values and controlled molecular weights. A decent correlation amongst the values of molecular weight derived theoretically and the molecular weight obtained from GPC and NMR analyses can be observed. In the case of BCPs, the compositions of different blocks in terms of the degree of polymerization were calculated from the molecular weights obtained from the GPC analysis. In this study, two distinct BCPs (BCP-1 and BCP-2) with different length of PTFEMA segments (36 units and 68 units respectively) and 8 units of PMAibPOSS segment in both the BCPs were prepared. The subscript to the polymer in **Table 3.1** denotes the respective value of the degree of polymerization.

Table 3.1. Summary of PMA*ib*POSS and PMA*ib*POSS-*b*-PTFEMA polymers prepared via RAFT polymerization. *

Sample Code	[M]:[R]:[I] [§]	Conv. ^a (%)	$M_{n,theo}^b$ (g/mol)	$M_{n,SEC}$ (g/mol)	$M_{n,NMR}$ (g/mol)	Dispersity (\bar{D})	Composition ^c	POSS Content (wt%)	Fluorine Content (wt%)
PMA <i>ib</i> POSS	10:1:0.25	80	7900	7200	7400	1.09	PMA <i>ib</i> POSS ₈	39.2	-
BCP-1	60:1:0.25	60	13300	13200	13100	1.30	PMA <i>ib</i> POSS ₈ - PTFEMA ₃₆	21.4	15.5
BCP-2	120:1:0.25	56	18600	18700	-	1.25	PMA <i>ib</i> POSS ₈ - PTFEMA ₆₈	15.1	20.7

[§] [M]:[R]:[I] = [Monomer]:[RAFT]:[Initiator]

*BCPs were prepared using PMA*ib*POSS₈ ($M_{n,SEC} = 7200$ g/mol) as a macro-RAFT agent
#Time = 8 h; Temp = 70 °C

^a Calculated gravimetrically.

$$^b M_{n,theo} = \left(\frac{[M]_0}{[RAFT]} \times M_{monomer} \times X \right) + M_{RAFT}$$

Where,

$[M]_0$ = Initial monomer concentration; [RAFT] = RAFT concentration.

$M_{monomer}$ = Molecular weight of monomer; M_{RAFT} = Molecular weight of RAFT agent / $M_{n,SEC}$ of the macro-RAFT agent.

X = % monomer conversion

^c Calculated from GPC analysis results.

3.3.4. FTIR Analysis

Figure 3.4 shows the FTIR spectra of the homopolymers, PMA*ib*POSS and PTFEMA, and the BCP, PMA*ib*POSS-*b*-PTFEMA [BCP-1]. The presence of the absorption band at 1105 cm^{-1} attributes to the Si-O group present in the POSS moiety and the C-F bond of TFEMA appeared at 1280 cm^{-1} . The presence of both these bands in the FTIR spectra of the BCP confirms the presence of both the blocks in the BCP.

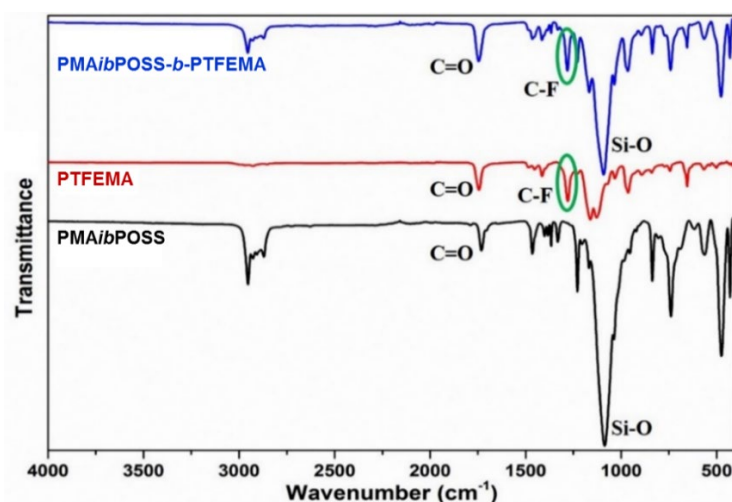


Figure 3.4. FTIR spectra of a) PMA*ib*POSS b) PTFEMA c) PMA*ib*POSS-*b*-PTFEMA

3.3.5. Thermal Analysis

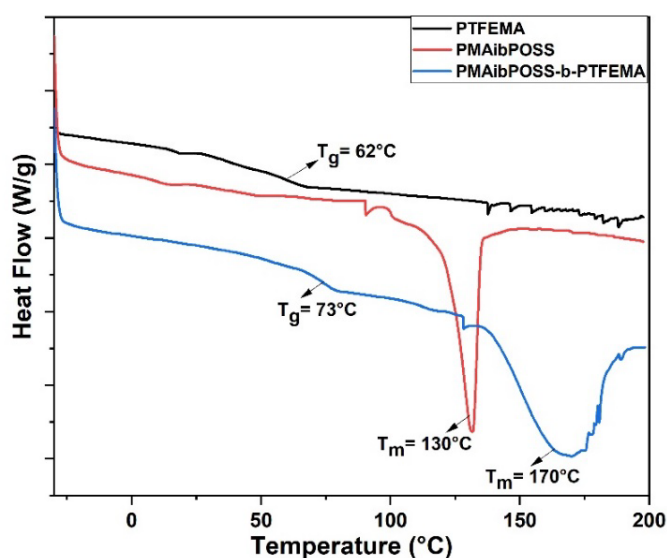


Figure 3.5. DSC thermogram of PTFEMA, PMA*ib*POSS and PMA*ib*POSS-*b*-PTFEMA.

The DSC and TGA analyses were used to study the thermal properties of the homopolymer and the block copolymer. The DSC traces of the homopolymers, PMA*ib*POSS and PTFEMA, and the BCP [BCP-1] are shown in **Figure 3.5**. The T_g of the homopolymer PTFEMA is observed at 62°C. The sharp melting peak at around 130 °C in the DSC thermogram of the homopolymer, PMA*ib*POSS, showed its crystalline nature. The BCP showed a T_g peak at 73°C, which attributes to the PTFEMA block and an endothermic melting peak at ~170 °C of the PMA*ib*POSS block. The shift in the T_g of the PTFEMA occurred as a result of the presence of the crystalline POSS block in the polymer chain. This again confirms the formation of the block copolymer, and it can be inferred from these separate transitions that the two blocks are immiscible.

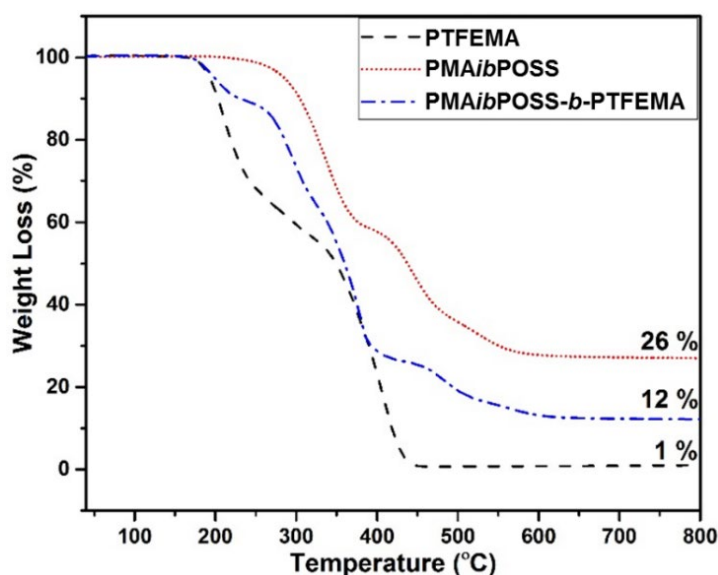


Figure 3.6. TGA thermogram of PTFEMA, PMA*ib*POSS, and PMA*ib*POSS-*b*-PTFEMA

The TGA results of the homopolymers and the BCP are shown in **Figure 3.6**. From the TGA thermogram, it can be observed that even after heating at 800 °C, there is not much char residue in the PTFEMA homopolymer. In contrast, the PMA*ib*POSS homopolymer showed large char residue (26%) owing to the presence of POSS moiety. The presence of 12% char residue in the BCP concerning almost no char residue in PTFEMA indicates the presence of POSS moieties in the BCP. It can also be observed

that the TGA thermogram of BCP follows a combination of individual traces of PTFEMA and PMA*ib*POSS homopolymer. The influence of PTFEMA units in the BCP can be inferred by the decrease in the initial degradation of BCP compared to the PMA*ib*POSS homopolymer.

3.3.6. Morphology Study

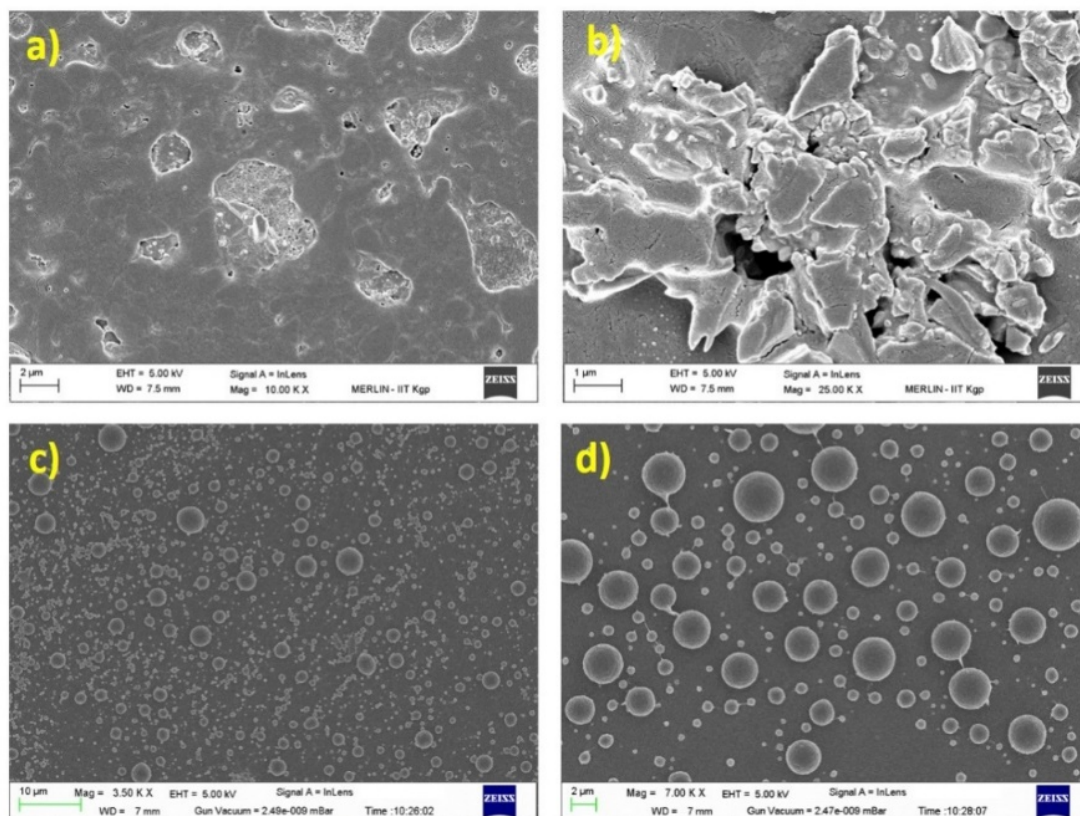


Figure 3.7. SEM images of PMA*ib*POSS (a,b) and PMA*ib*POSS-*b*-PTFEMA (BCP-1) (c,d) at different magnifications.

The structural morphology of the BCP [BCP-1] was analyzed by SEM, TEM, and AFM analyses. **Figure 3.7** shows the SEM images of the homopolymer, PMA*ib*POSS, and the BCP-1 at different magnifications. The samples for SEM analysis were prepared by drop-casting the polymer solution in chloroform to form a thin film over a glass slide. The aggregation of the POSS molecules can be observed from the SEM image of the PMA*ib*POSS homopolymer. At the same time, the BCP showed core-shell type morphology, which was further confirmed by TEM analysis.

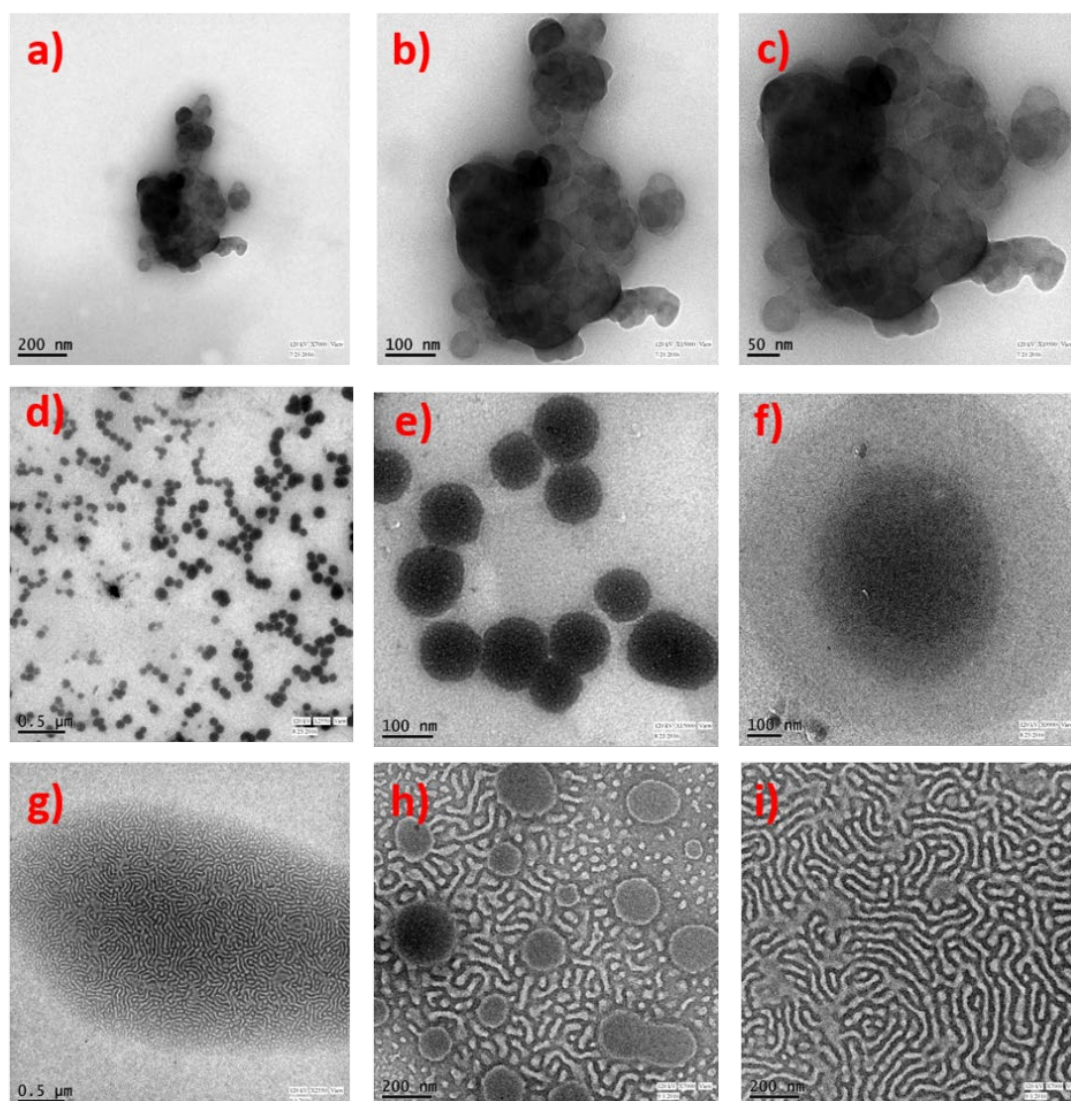


Figure 3.8. TEM images (at different magnifications and in a different location after evaporation of the solvent) of a-c) PMAibPOSS homopolymer d-f) BCP-1 prepared from chloroform g-i) BCP-1 prepared from THF

The observation from the DSC and SEM analyses infers the incompatibility of both the PMAibPOSS and the PTFEMA blocks in the BCP. Generally, the BCPs obtained from the incompatible homopolymers have the ability to phase separate into different nano and microstructures in different solvent which is due to various factors like solubility parameter, interaction, and polarity of the solvent.[61, 62] In this case, the nanostructured morphology of the BCPs were studied by dissolving the BCPs in different solvents like chloroform and THF. The samples were then drop-cast over the TEM grid and were analyzed by TEM analysis. The polymer solution concentration is

maintained as 1 mg/ml in all the cases. The TEM images of the homopolymer PMA*ib*POSS and the hybrid block copolymers of MA*ib*POSS and TFEMA are shown in **Figure 3.8**.

The aggregation of PMA*ib*POSS can be observed from the TEM images of the homopolymer (**Figure 3.8 (a-c)**); this goes in accordance with the images of the homopolymer in SEM analysis earlier. The difference in surface energy and the immiscibility of the two blocks, viz. PMA*ib*POSS and PTFEMA facilitated different morphology of the BCP when the samples for TEM analyses were prepared using different solvents. **Figure 3.8 (d-f)** shows the TEM images at different magnifications of the samples prepared by using chloroform as a solvent. **Figure 3.8 (g-i)** shows the TEM images of the samples prepared using THF as a solvent. It can be observed from the TEM images that the samples prepared from chloroform clearly shows the core-shell type morphology [**Figure 3.8 (d-f)**]. Whereas the samples prepared using THF as solvent indicated predominantly lamellar type morphology together with some core-shell particles [**Figure 3.8 (g-i)**]. The presence of core-shell particles in combination with the lamellar structures can be clearly seen from **Figure 3.8 (g-i)**. It can also be observed that the lamellar morphology predominates over the core-shell type morphology. The *d*-spacing in the lamellar morphology was calculated to be 22-28 nm. The difference in the solubility parameter of the individual blocks in the BCPs is the prime factor that facilitates this difference in the morphology of using a different solvent. The solubility parameter of PTFEMA (16.4 – 17.3 (MPa)^½) is slightly lesser than that of PMA*ib*POSS (19.30 to 20.58 (MPa)^½). [63, 64]. THF being more polar compared to chloroform (Dielectric constant values of THF=7.58; Chloroform=4.81), PMA*ib*POSS tends to have preferential solubility in THF compared to PTFEMA, as polyfluoroacrylates have low solubility parameter. The difference in morphology has a

slight impact on the hydrophobicity of the BCP, as it can be seen by the difference in the water contact angle shown in **Table 3.2**.

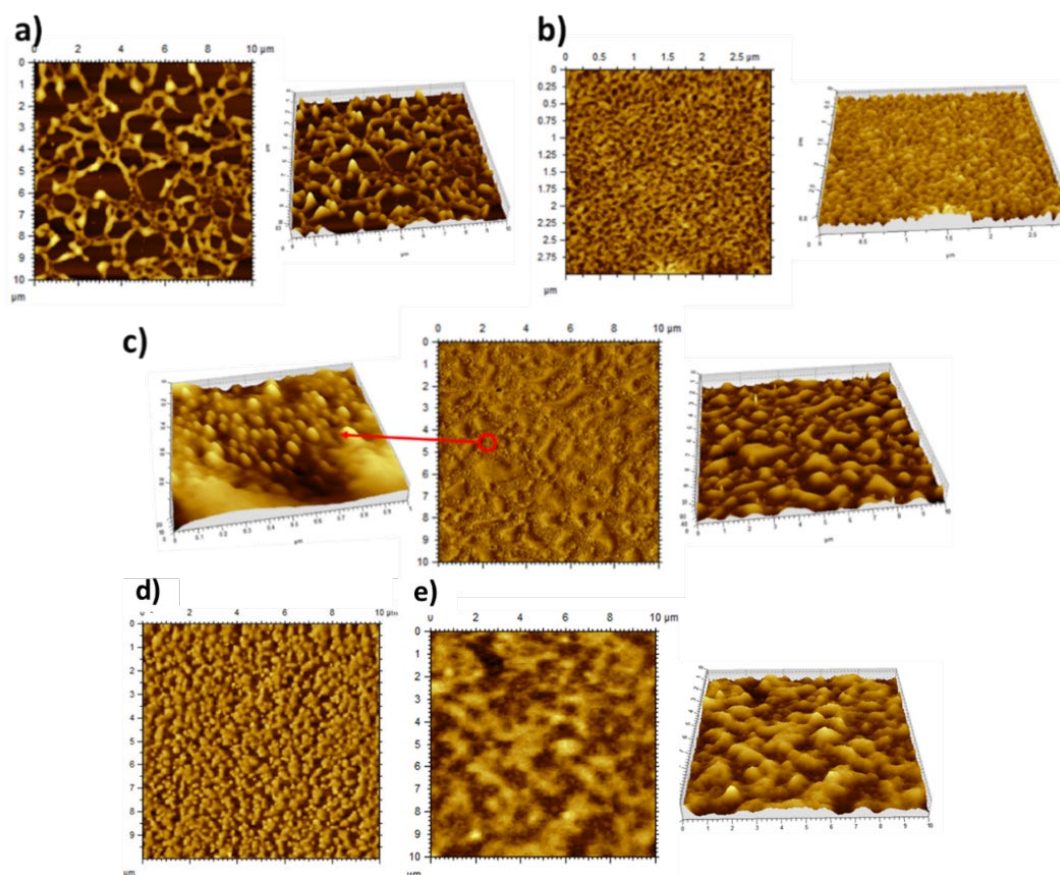


Figure 3.9. AFM images of a) PMAibPOSS; b, c) BCP-1 before annealing and after annealing; d, e) BCP-2 before annealing and after annealing

The phase and 3D AFM images of the homopolymer, PMAibPOSS, and the BCPs, were shown in **Figure 3.9**. The samples for AFM analyses were prepared by dissolving the polymers in THF, and a thin film was cast over a glass substrate by spin coating. The aggregation of POSS into crystalline domains and rapid evaporation of the solvent led to the formation of holes in the films, as seen in the AFM images of the PMAibPOSS. A complete surface coverage with a finer structure can be observed in the AFM images of the BCP (**Figure 3.9b**), which can be ascribed to a phase-separated lamellar type morphology. The lamellar phase separation was further confirmed by SAXS analysis. The morphological change in the BCPs with respect to the effect of

temperature was studied by annealing the coated substrate. The BCP films were annealed for 24 h at 120 °C. **Figure 3.9c** depicts the AFM images of the annealed samples, a phase-separated morphology with increased surface roughness can be observed. The surface roughness values found a steep increase from 2.89 nm before annealing to 10.5 nm after annealing, which can be attributed to the crystallization of the POSS moiety. [65, 66]. The rise in surface roughness also boosts the hydrophobicity of the polymer; this can be ascribed to the increase in contact angle value given in **Table 3.2** before and after annealing. **Figure 3.9(d-e)** shows the AFM images of BCP-2 before and after annealing. It can be noted that there is no substantial change in the morphology between both the BCPs, but the change in the chain length of the fluorinated block shows a clear phase difference before and after annealing of the BCPs. The roughness values increased to 13nm, attributing to the increase in the hydrophobicity of the BCP-2, as shown in **Table 3.2**.

3.3.7. SAXS Analysis

The SAXS profile of the PMA*ib*POSS and BCP-1 is shown in **Figure 3.10**. A single broad peak at around 0.025 \AA^{-1} is observed in the scattering vector (q) versus scattering intensity (log-log scale). This is attributed to the presence of a microphase separation between the two matrices. In contrast, no such peaks were found in the PMA*ib*POSS homopolymer that infers that there is no phase separation. The inter-domain spacing (d) between the phases was determined from the equation, $d = 2\pi/q_{\text{max}}$, to be around 25 nm, which agrees with the d -spacing measured from TEM analysis.

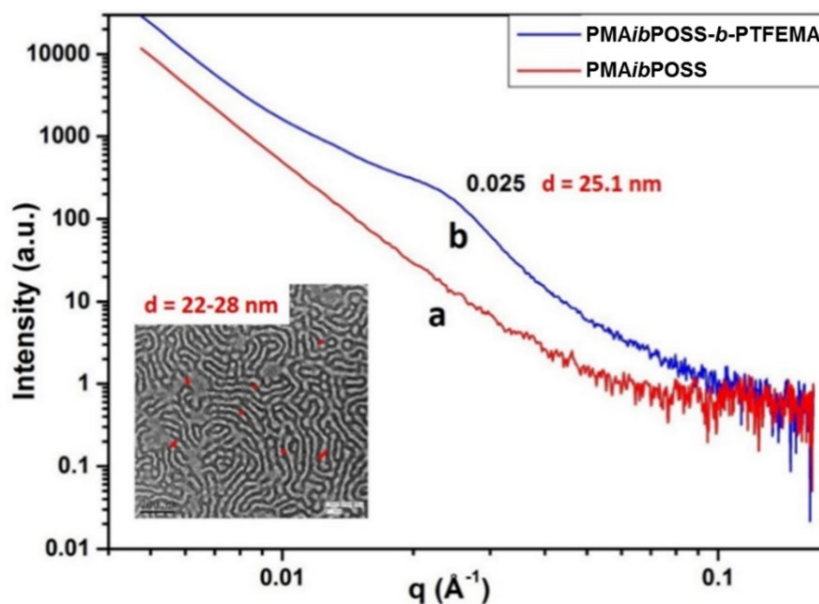


Figure 3.10. SAXS profile of a) PMAibPOSS and b) BCP-1. (Inset: TEM image of BCP (Figure 3.8i) and d-spacing measured from TEM analysis)

3.3.8. XPS Analysis

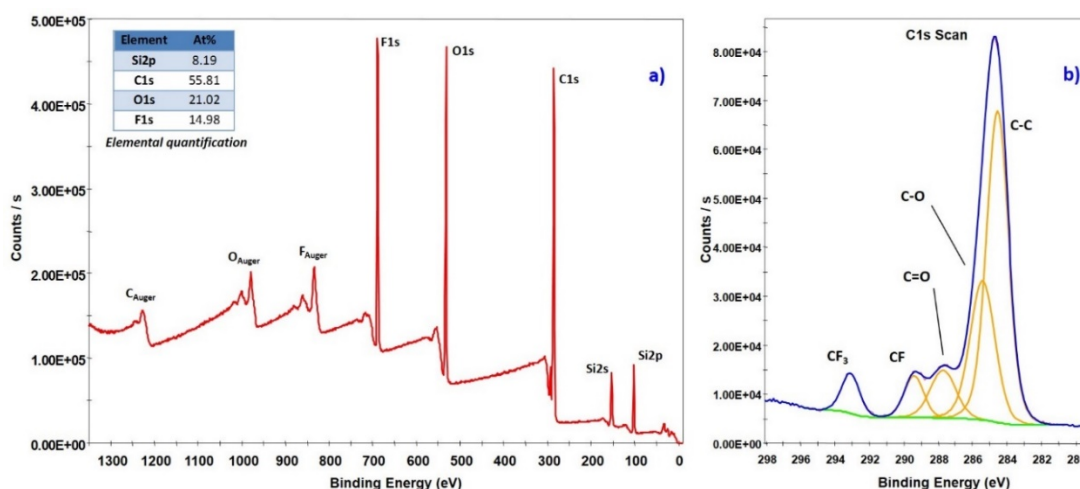


Figure 3.11. XPS analysis of BCP-1; a) Wide-scan spectrum b) C 1s Scan spectrum

The surface chemical composition of the BCP-1 was analyzed by XPS analysis (Figure 3.10). Figure 3.10a shows the full scan spectrum of all the elements in the BCP. The peaks corresponding to Si 2s, Si 2p, C 1s, O 1s, and F 1s peaks were identified at around 150, 100, 295, 535, and 690 eV, respectively. The high-resolution XPS spectrum of carbon 1s is shown in Figure 3.10b, which was fitted with sub-peaks corresponding to $-\text{CF}_3$ at 293 eV, $-\text{CF}$ at 290 eV, $-\text{C}=\text{O}$ at 288 eV, $\text{C}-\text{O}$ at 286 eV, $\text{C}-\text{C}$ at 284 eV.

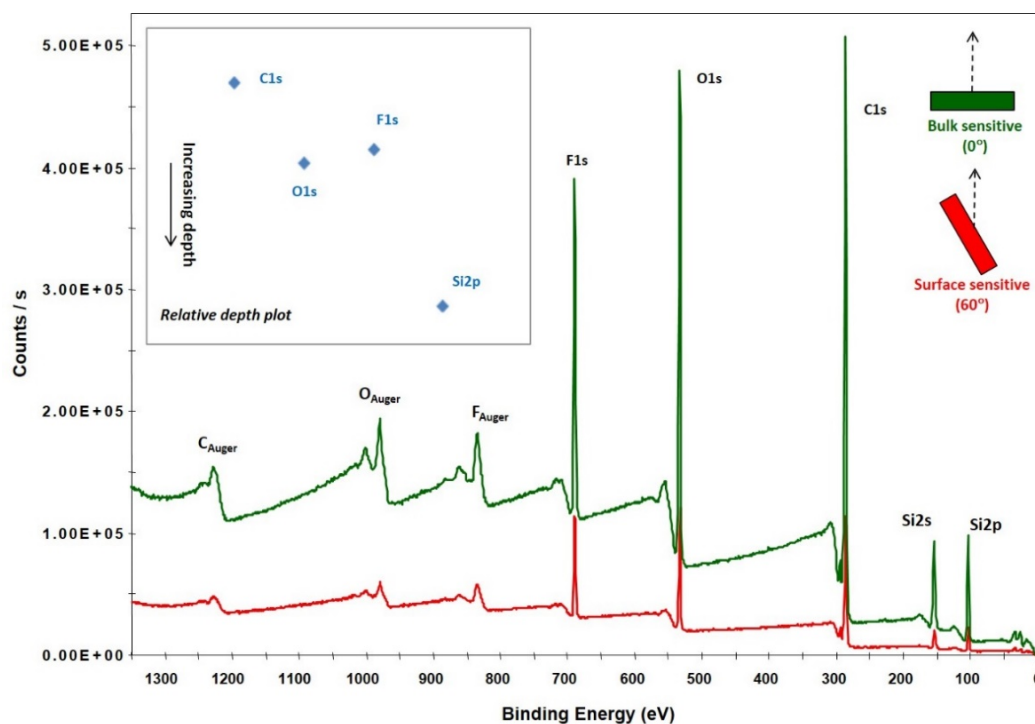


Figure 3.12. Cluster profile data of XPS analysis of PMAibPOSS-*b*-PTFEMA

The SEM analyses (**Figure 3.7**) and TEM analyses (**Figure 3.8**) show that the BCP forms core-shell type morphology when casting from chloroform as solvent. Cluster profiling analysis in XPS for the dried BCP is analyzed to understand what is in the core and what is in the shell. The XPS cluster profile data are shown in **Figure 3.12**. The values from the surface and the bulk are calculated, as shown in **Figure 3.12**. The relative depth plot (shown as an inset in **Figure 3.12**) is plotted by calculating $-\ln(I_{\text{bulk}}/I_{\text{surface}})$ for each element. The relative depth plot indicates that the PTFEMA segment (on average) is closer to the surface, whereas PMAibPOSS segments (on average) towards the bulk. This is because of the better interaction between chloroform with PTFEMA than with PMAibPOSS segments.

3.3.9. Water Contact Angle (WCA) Analysis

The hydrophobicity of the BCP films was explored by contact angle analysis. The homo and block copolymers were dissolved in chloroform and THF and coated on different substrates viz., glass, metal, and cotton fabric. The water contact angle (WCA)

values are shown in **Table 3.2**. There was a slight increase in WCA in the BCPs compared to the constituent homopolymers. The WCA also increased slightly in BCP-2 than BCP-1, i.e., on increasing the length of the fluorinated segment in the BCP. In order to improve the hydrophobicity, the coated substrates were annealed at 120 °C for 24 h under vacuum. The WCA value increased to about 125° after annealing. The increase in this WCA is due to the increase in roughness of the surface resulting from PMA*ib*POSS crystallization, as noted in the AFM analysis.

Table 3.2. Water contact angle values.

Sample	Solvent to Dissolve	Surface Coated	Water Contact Angle (°)
PMA <i>ib</i> POSS	THF	Glass	100°
PTFEMA	THF	Glass	95°
		Glass	104°
BCP-1	CHCl ₃	Cotton fabric	130°
		Metal	112°
		Glass	110°
	THF	Glass, followed by thermal annealing	126°
BCP-2	CHCl ₃	Glass	110°
		Cotton Fabric	135°
	THF	Glass	115°
		Glass, followed by thermal annealing	128°

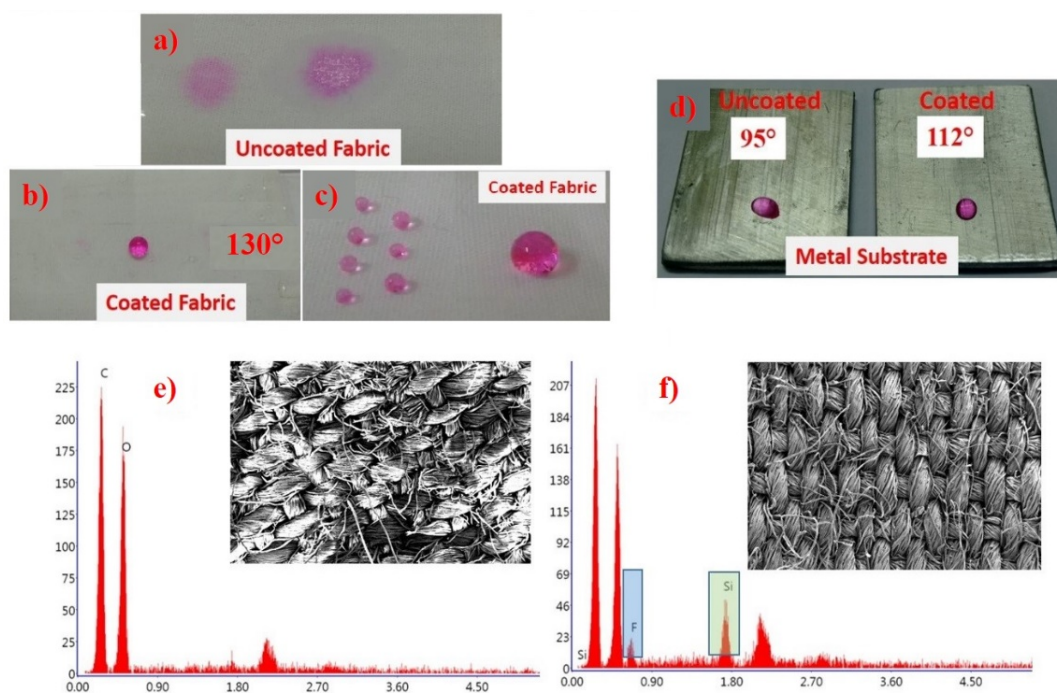
3.3.10. Preparation of PMAibPOSS-*b*-PTFEMA coated Hydrophobic Surfaces

Figure 3.13. Images of water droplet over (a) uncoated cotton fabric (b, c) coated cotton fabric at different locations (d) uncoated and coated aluminium metal plates (e, f) FESEM and EDAX images of uncoated (e) and coated fabric (f)

In order to study the practical application of the synthesized BCP as a potential coating material, various hydrophobic surfaces viz., hydrophobic fabric, and metal surfaces were prepared. The hydrophobic surfaces were prepared by coating the BCPs on a piece of woven cotton fabric and on an aluminium metal surface. The BCP solution in chloroform is coated over the treated substrates via the dip-coating process. **Figure 3.13 (a-d)** shows the picture of a water droplet (colored using a dye to have better visibility) placed on top of the coated and uncoated cotton fabric and aluminium metal plates. It can be observed that the uncoated fabric is exceptionally hydrophilic, whereas the coated fabric resists water absorption. The contact angle value of the coated fabric is very high, around 135° . **Figure 3.13 (e and f)** shows the SEM images and the EDAX analysis of the uncoated and the coated cotton fabric, respectively. It offers a uniform coating over the fabric, and the presence of silica and fluorine in the EDX spectrum depicts the coating of BCP over the fabric.

3.4. Conclusion

Diblock copolymers (AB-type) comprising hybrid POSS moiety (MA*ib*POSS) and fluorinated moiety (TFEMA) were successfully synthesized via RAFT polymerization. The BCPs were characterized by ¹H NMR, FT-IR, and SEC analyses. The prepared homopolymers and the BCPs had controlled molecular weight with narrow dispersity. The structural morphology of the BCPs in different solvents was studied by SEM and TEM analyses. The BCP thin films demonstrated core-shell type morphology when deposited from chloroform and lamellar type morphology when deposited from THF as the solvent. The cluster profiling data from XPS analysis revealed that the PTFEMA segments are towards the shell, and the PMA*ib*POSS segments are towards the core. The AFM analysis showed that the surface roughness of the coated BCP film increased from 2.89 nm before annealing to 10.5 nm after annealing at 120 °C owing to the crystallization of the PMA*ib*POSS block. The water contact angle of the BCP also increased to 128°. The BCPs were coated on cotton fabric and an aluminium metal plate via dip-coating. The resulting BCP coated substrates showed significantly improved hydrophobicity as determined by WCA measurements. These tailor-made fluorinated BCP containing POSS moieties can have potential application as the hydrophobic coating material.

References

- [1] M. Rehamn, Organic/inorganic hybrid polymers, *Acta polymerica* 49(5) (1998) 201-224.
- [2] K.-H. Haas, K. Rose, Hybrid inorganic/organic polymers with nanoscale building blocks: precursors, processing, properties and applications, *Reviews on Advanced Materials Science* 5(1) (2003) 47-52.
- [3] A. Chakrabarty, S. Ponnupandian, K. Naskar, N.K. Singha, Nanoclay stabilized Pickering miniemulsion of fluorinated copolymer with improved hydrophobicity via RAFT polymerization, *RSC Advances* 6(41) (2016) 34987-34995.
- [4] H. Zou, S. Wu, J. Shen, Polymer/silica nanocomposites: preparation, characterization, properties, and applications, *Chem. Rev* 108(9) (2008) 3893-3957.
- [5] R.B. Grubbs, Hybrid metal-polymer composites from functional block copolymers, *Journal of Polymer Science Part A: Polymer Chemistry* 43(19) (2005) 4323-4336.
- [6] K. Inoue, Functional dendrimers, hyperbranched and star polymers, *Progress in Polymer Science* 25(4) (2000) 453-571.
- [7] H.-i. Lee, J. Pietrasik, S.S. Sheiko, K. Matyjaszewski, Stimuli-responsive molecular brushes, *Progress in polymer science* 35(1) (2010) 24-44.
- [8] N. Hadjichristidis, S. Pispas, G. Floudas, Block copolymers: synthetic strategies, physical properties, and applications, John Wiley & Sons, New Jersey, 2003.
- [9] C.J. Hawker, A.W. Bosman, E. Harth, New polymer synthesis by nitroxide mediated living radical polymerizations, *Chemical reviews* 101(12) (2001) 3661-3688.
- [10] J. Nicolas, Y. Guillaneuf, C. Lefay, D. Bertin, D. Gigmes, B. Charleux, Nitroxide-mediated polymerization, *Progress in Polymer Science* 38(1) (2013) 63-235.
- [11] T.E. Patten, J. Xia, T. Abernathy, K. Matyjaszewski, Polymers with very low polydispersities from atom transfer radical polymerization, *Science* 272(5263) (1996) 866.
- [12] N.K. Singha, B. de Ruyter, U.S. Schubert, Atom transfer radical polymerization of 3-ethyl-3-(acryloyloxy) methyloxetane, *Macromolecules* 38(9) (2005) 3596-3600.
- [13] H. Datta, N.K. Singha, Atom transfer radical polymerization of hexyl acrylate and preparation of its "all-acrylate" block copolymers, *Journal of Polymer Science Part A: Polymer Chemistry* 46(11) (2008) 3499-3511.
- [14] G. Moad, Y. Chong, A. Postma, E. Rizzardo, S.H. Thang, Advances in RAFT polymerization: the synthesis of polymers with defined end-groups, *Polymer* 46(19) (2005) 8458-8468.

- [15] B.P. Koiry, S. Ponnupandian, S. Choudhury, N.K. Singha, Syntheses and morphologies of fluorinated diblock copolymer prepared via RAFT polymerization, *Journal of Fluorine Chemistry* 189 (2016) 51-58.
- [16] J. Pyun, K. Matyjaszewski, Synthesis of nanocomposite organic/inorganic hybrid materials using controlled/"living" radical polymerization, *Chemistry of Materials* 13(10) (2001) 3436-3448.
- [17] N.J. Warren, S.P. Armes, Polymerization-induced self-assembly of block copolymer nano-objects via RAFT aqueous dispersion polymerization, *Journal of the American Chemical Society* 136(29) (2014) 10174-10185.
- [18] H. Gao, K. Matyjaszewski, Synthesis of star polymers by a combination of ATRP and the "click" coupling method, *Macromolecules* 39(15) (2006) 4960-4965.
- [19] R.G. Lopez, F. D'Agosto, C. Boisson, Synthesis of well-defined polymer architectures by successive catalytic olefin polymerization and living/controlled polymerization reactions, *Progress in polymer science* 32(4) (2007) 419-454.
- [20] J. Wu, P.T. Mather, POSS polymers: physical properties and biomaterials applications, *Polymer Reviews* 49(1) (2009) 25-63.
- [21] S.-W. Kuo, F.-C. Chang, POSS related polymer nanocomposites, *Progress in Polymer Science* 36(12) (2011) 1649-1696.
- [22] F. Wang, X. Lu, C. He, Some recent developments of polyhedral oligomeric silsesquioxane (POSS)-based polymeric materials, *Journal of Materials Chemistry* 21(9) (2011) 2775-2782.
- [23] E.T. Kopesky, G.H. McKinley, R.E. Cohen, Toughened poly (methyl methacrylate) nanocomposites by incorporating polyhedral oligomeric silsesquioxanes, *Polymer* 47(1) (2006) 299-309.
- [24] W. Zhang, X. Li, X. Guo, R. Yang, Mechanical and thermal properties and flame retardancy of phosphorus-containing polyhedral oligomeric silsesquioxane (DOPO-POSS)/polycarbonate composites, *Polymer Degradation and Stability* 95(12) (2010) 2541-2546.
- [25] H. Xu, S.-W. Kuo, J.-S. Lee, F.-C. Chang, Preparations, thermal properties, and T_g increase mechanism of inorganic/organic hybrid polymers based on polyhedral oligomeric silsesquioxanes, *Macromolecules* 35(23) (2002) 8788-8793.
- [26] J.-c. Huang, C.-b. He, Y. Xiao, K.Y. Mya, J. Dai, Y.P. Siow, Polyimide/POSS nanocomposites: interfacial interaction, thermal properties and mechanical properties, *Polymer* 44(16) (2003) 4491-4499.

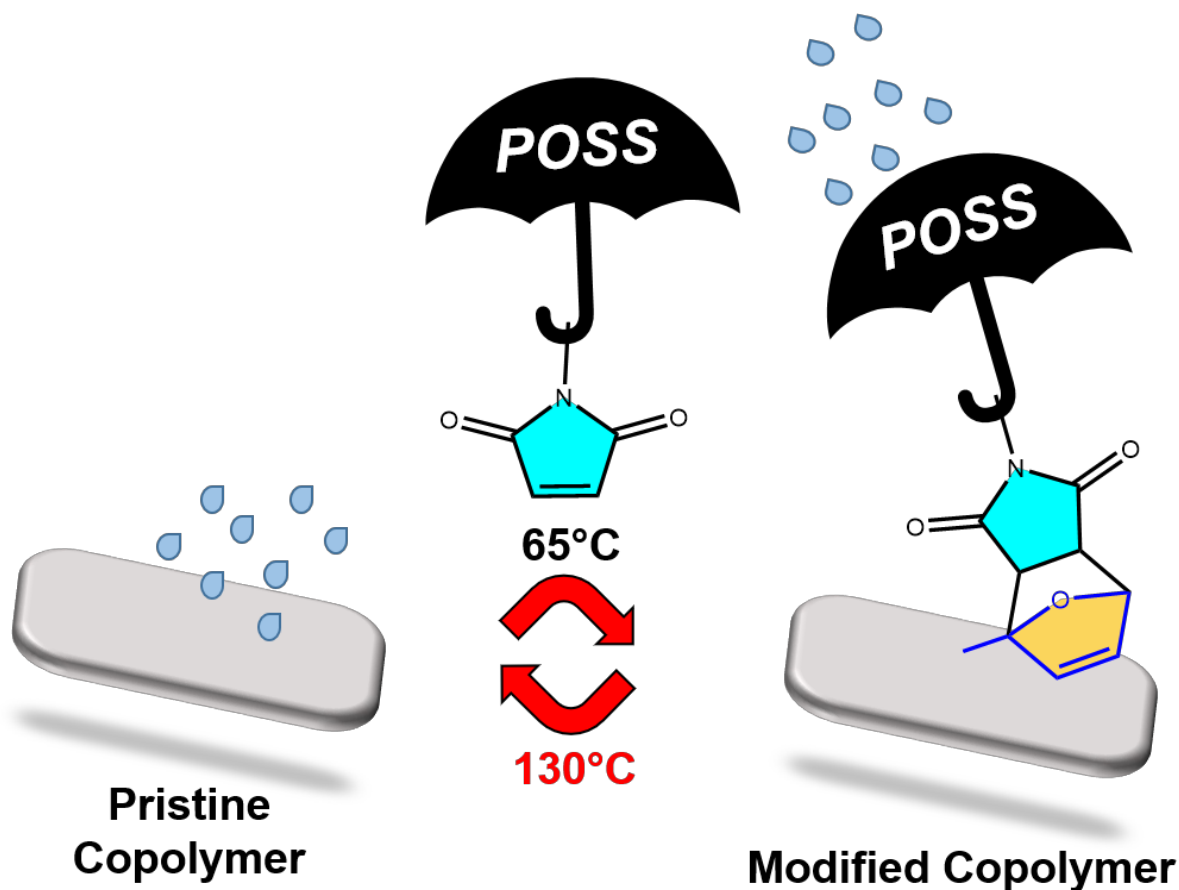
- [27] Z. Zhang, A. Gu, G. Liang, P. Ren, J. Xie, X. Wang, Thermo-oxygen degradation mechanisms of POSS/epoxy nanocomposites, *Polymer Degradation and Stability* 92(11) (2007) 1986-1993.
- [28] E. Devaux, M. Rochery, S. Bourbigot, Polyurethane/clay and polyurethane/POSS nanocomposites as flame retarded coating for polyester and cotton fabrics, *Fire and Materials* 26(4-5) (2002) 149-154.
- [29] I. Jerman, M. Koželj, B. Orel, The effect of polyhedral oligomeric silsesquioxane dispersant and low surface energy additives on spectrally selective paint coatings with self-cleaning properties, *Solar Energy Materials and Solar Cells* 94(2) (2010) 232-245.
- [30] J. Pyun, K. Matyjaszewski, Synthesis of hybrid polymers using atom transfer radical polymerization: homopolymers and block copolymers from polyhedral oligomeric silsesquioxane monomers, *Macromolecules* 33(1) (2000) 217-220.
- [31] Z.-W. Yu, S.-X. Gao, K. Xu, Y.-X. Zhang, J. Peng, M.-C. Chen, Synthesis and characterization of silsesquioxane-cored star-shaped hybrid polymer via “grafting from” RAFT polymerization, *Chinese Chemical Letters* 27(11) (2016) 1696-1700.
- [32] Z. Zhang, P. Zhang, Y. Wang, W. Zhang, Recent advances in organic–inorganic well-defined hybrid polymers using controlled living radical polymerization techniques, *Polymer Chemistry* 7(24) (2016) 3950-3976.
- [33] S. Tajbakhsh, M. Marić, Nitroxide mediated miniemulsion polymerization of methacryloisobutyl POSS: Homopolymers and copolymers with alkyl methacrylates, *Journal of Polymer Science* 58(19) (2020) 2741-2754.
- [34] A. Ullah, S.M. Shah, A. Hassan, M. Maric, H. Hussain, Nitroxide-mediated radical polymerization of methacryloisobutyl POSS and its block copolymers with poly (n-acryloylmorpholine), *Journal of Polymer Science* 58(3) (2020) 428-437.
- [35] J. Pyun, K. Matyjaszewski, J. Wu, G.-M. Kim, S.B. Chun, P.T. Mather, ABA triblock copolymers containing polyhedral oligomeric silsesquioxane pendant groups: synthesis and unique properties, *Polymer* 44(9) (2003) 2739-2750.
- [36] H. Hussain, B. Tan, G.L. Seah, Y. Liu, C. He, T.P. Davis, Micelle formation and gelation of (PEG–P (MA-POSS)) amphiphilic block copolymers via associative hydrophobic effects, *Langmuir* 26(14) (2010) 11763-11773.
- [37] B. Tan, H. Hussain, C. He, Tailoring micelle formation and gelation in (PEG–P(MA-POSS)) amphiphilic hybrid block copolymers, *Macromolecules* 44(3) (2011) 622-631.

- [38] S. Ata, P. Dhara, R. Mukherjee, N.K. Singha, Thermally amendable and thermally stable thin film of POSS tethered Poly (methyl methacrylate)(PMMA) synthesized by ATRP, *European Polymer Journal* 75 (2016) 276-290.
- [39] W. Zhang, L. Liu, X. Zhuang, X. Li, J. Bai, Y. Chen, Synthesis and self-assembly of tadpole-shaped organic/inorganic hybrid poly (N-isopropylacrylamide) containing polyhedral oligomeric silsesquioxane via RAFT polymerization, *Journal of Polymer Science Part A: Polymer Chemistry* 46(21) (2008) 7049-7061.
- [40] W. Zhang, X. Zhuang, X. Li, J. Bai, Y. Chen, Preparation and characterization of organic/inorganic hybrid polymers containing polyhedral oligomeric silsesquioxane via RAFT polymerization, *Reactive and Functional Polymers* 69(2) (2009) 124-129.
- [41] K.Y. Mya, E.M. Lin, C.S. Gudipati, L. Shen, C. He, Time-dependent polymerization kinetic study and the properties of hybrid polymers with functional silsesquioxanes, *The Journal of Physical Chemistry B* 114(28) (2010) 9119-9127.
- [42] Y. Deng, J. Bernard, P. Alcouffe, J. Galy, L. Dai, J.F. Gérard, Nanostructured hybrid polymer networks from in situ self-assembly of RAFT-synthesized POSS-based block copolymers, *Journal of Polymer Science Part A: Polymer Chemistry* 49(20) (2011) 4343-4352.
- [43] E. Tegou, V. Bellas, E. Gogolides, P. Argitis, Polyhedral oligomeric silsesquioxane (POSS) acrylate copolymers for microfabrication: properties and formulation of resist materials, *Microelectronic engineering* 73 (2004) 238-243.
- [44] Z. Su, B. Yu, X. Jiang, J. Yin, Hybrid core-shell microspheres from coassembly of anthracene-containing POSS (POSS-AN) and anthracene-ended hyperbranched poly (ether amine)(hPEA-AN) and their responsive polymeric hollow microspheres, *Macromolecules* 46(9) (2013) 3519-3528.
- [45] W. Zhang, A.H. Müller, Architecture, self-assembly and properties of well-defined hybrid polymers based on polyhedral oligomeric silsesquioxane (POSS), *Progress in Polymer Science* 38(8) (2013) 1121-1162.
- [46] F. Liu, Y. Zhang, L. Xu, W. Zhang, Morphology-Controlled Self-Assembly of an Organic/Inorganic Hybrid Porphyrin Derivative Containing Polyhedral Oligomeric Silsesquioxane (POSS), *Chemistry—A European Journal* 21(14) (2015) 5540-5547.
- [47] B. Ameduri, B. Boutevin, *Well-architected fluoropolymers: synthesis, properties and applications*, Elsevier, Amsterdam, 2004.
- [48] A. Bruno, Controlled radical (co) polymerization of fluoromonomers, *Macromolecules* 43(24) (2010) 10163-10184.

- [49] B.P. Koiry, H.-A. Klok, N.K. Singha, Copolymerization of 2, 2, 3, 3, 4, 4, 4-heptafluorobutyl acrylate with butyl acrylate via RAFT polymerization, *Journal of Fluorine Chemistry* 165 (2014) 109-115.
- [50] P. Graham, M. Stone, A. Thorpe, T.G. Nevell, J. Tsibouklis, Fluoropolymers with very low surface energy characteristics, *Journal of Fluorine Chemistry* 104(1) (2000) 29-36.
- [51] G. Hougham, *Fluoropolymers 2: Properties*, Kluwer Academic Publishers, New York, 1999.
- [52] G.G. Hougham, P.E. Cassidy, K. Johns, T. Davidson, *Fluoropolymers 1: Synthesis*, Kluwer Academic Publishers, New York, 2006.
- [53] V. Malshe, N.S. Sangaj, Fluorinated acrylic copolymers: Part I: Study of clear coatings, *Progress in Organic Coatings* 53(3) (2005) 207-211.
- [54] L. Matějka, M. Janata, J. Pleštil, A. Zhigunov, M. Šlouf, Self-assembly of POSS-containing block copolymers: Fixing the hierarchical structure in networks, *Polymer* 55(1) (2014) 126-136.
- [55] A. Pan, S. Yang, L. He, POSS-tethered fluorinated diblock copolymers with linear- and star-shaped topologies: synthesis, self-assembled films and hydrophobic applications, *RSC Advances* 5(68) (2015) 55048-55058.
- [56] R. Nakatani, H. Takano, L. Wang, A. Chandra, Y. Tanaka, R. Maeda, N. Kihara, S. Minegishi, K. Miyagi, Y. Kasahara, Precise synthesis of fluorine-containing block copolymers via RAFT, *J. Photopolym. Sci. Technol.* 29(5) (2016) 705-708.
- [57] X. Qiang, X. Ma, Z. Li, X. Hou, Synthesis of star-shaped polyhedral oligomeric silsesquioxane (POSS) fluorinated acrylates for hydrophobic honeycomb porous film application, *Colloid and Polymer Science* 292(7) (2014) 1531-1544.
- [58] A. Pan, L. He, L. Wang, N. Xi, POSS-based Diblock Fluoropolymer for Self-assembled Hydrophobic Coatings, *Materials Today: Proceedings* 3(2) (2016) 325-334.
- [59] H. Araki, K. Naka, Syntheses of Dumbbell-Shaped Trifluoropropyl-Substituted POSS Derivatives Linked by Simple Aliphatic Chains and Their Optical Transparent Thermoplastic Films, *Macromolecules* 44(15) (2011) 6039-6045.
- [60] J. Hao, Y. Wei, B. Chen, J. Mu, Polymerization of polyhedral oligomeric silsesquioxane (POSS) with perfluoro-monomers and a kinetic study, *RSC Advances* 7(18) (2017) 10700-10706.

- [61] W.-H. Huang, P.-Y. Chen, S.-H. Tung, Effects of annealing solvents on the morphology of block copolymer-based supramolecular thin films, *Macromolecules* 45(3) (2012) 1562-1569.
- [62] Y. Tada, H. Yoshida, Y. Ishida, T. Hirai, J.K. Bosworth, E. Dobisz, R. Ruiz, M. Takenaka, T. Hayakawa, H. Hasegawa, Directed self-assembly of POSS containing block copolymer on lithographically defined chemical template with morphology control by solvent vapor, *Macromolecules* 45(1) (2012) 292-304.
- [63] H.W. Milliman, D. Boris, D.A. Schiraldi, Experimental determination of Hansen solubility parameters for select POSS and polymer compounds as a guide to POSS–polymer interaction potentials, *Macromolecules* 45(4) (2012) 1931-1936.
- [64] S.K. Papadopoulou, C. Panayiotou, Assessment of the thermodynamic properties of poly (2, 2, 2-trifluoroethyl methacrylate) by inverse gas chromatography, *Journal of Chromatography A* 1324 (2014) 207-214.
- [65] T. Hirai, M. Leolukman, T. Hayakawa, M.-a. Kakimoto, P. Gopalan, Hierarchical nanostructures of organosilicate nanosheets within self-organized block copolymer films, *Macromolecules* 41(13) (2008) 4558-4560.
- [66] K. Tsuchiya, Y. Ishida, A. Kameyama, Synthesis of diblock copolymers consisting of POSS-containing random methacrylate copolymers and polystyrene and their cross-linked microphase-separated structure via fluoride ion-mediated cage scrambling, *Polym. Chem.* 8(16) (2017) 2516-2527.

SELF-HEALING ULTRAHYDROPHOBIC POSS-FUNCTIONALIZED
FLUORINATED COPOLYMER VIA RAFT POLYMERIZATION AND
DYNAMIC DIELS-ALDER REACTION



This chapter describes the synthesis of a hydrophobic self-healing fluoropolymer based on POSS derived dynamic covalent chemistry and RAFT polymerization. This work includes the synthesis of copolymers containing fluoropolymer and furfuryl methacrylate via RAFT polymerization. Further, the copolymers are modified with maleimide containing POSS. The healing behavior and the hydrophobic characteristics of the copolymers are analyzed.

Abstract

This chapter reports the preparation of a tailor-made copolymer of furfuryl methacrylate (FMA) and trifluoroethyl methacrylate (TFEMA) via RAFT polymerization. The furfuryl groups of the copolymer were modified via the Diels-Alder (DA) reaction using different molar content of polyhedral oligomeric silsesquioxane maleimide (POSS-M), yielding hydrophobic fluorinated copolymers with varying POSS content. The chemical composition, molecular weights, and extent of grafting of POSS moieties were measured by ^1H NMR spectroscopy, size exclusion chromatography (SEC), and FTIR analyses. Interestingly, compared to the parent fluoro copolymer with a water contact angle (WCA) of $\approx 101^\circ$, the DA modification with hydrophobic POSS molecules significantly improved the surface hydrophobicity of the modified DA polymers leading to a WCA of 135° . Moreover, as evidenced by DSC, AFM, and OM analyses, the thermoreversible behaviour of the dynamic covalent furan-POSS-M linkages facilitated the self-healing ability of these functional hybrid polymethacrylates. The developed self-healing ultra hydrophobic POSS modified DA fluoropolymers are interesting materials that can find promising applications as speciality paints and coatings.

4.1. Introduction

Fluoropolymers have received significant attention in the field of paints and coatings [1, 2] due to their excellent thermal stability, chemical and physical properties, and hydrophobicity. On account of displaying remarkable barrier properties and chemical inertness, fluoropolymers are widely used as preventive coatings of fuel cells in photovoltaic devices, lithium batteries, aerospace, O-rings, gaskets, and medical devices.[3] Nevertheless, due to unprecedented environmental stimuli, such polymers are prone to eventual damage and degradation via in situ generation of micro-cracks that ultimately lead to catastrophic failure.[4] To prolong their service life, the inclusion of self-healing characteristics in such advanced fluoro materials is desirable. Self-healing materials are an exciting class of macromolecules with the ability to self-repair in situ generated micro-cracks similar to naturally occurring phenomena, e.g., repairing human skin cuts. Following the initial report of White et al. in the early 21st century, the area of self-healing materials flourished within the material research community.[4-6] Consequently, in 2013, the Global Agenda Council and the World Economic Forum announced self-healing materials as one of the top 10 evolving materials. Self-healing materials can be engineered via incorporation of mechanical[6] or photoactivated healing agents,[7, 8] dynamic covalent,[9-11] and non-covalent interactions,[12, 13] such as host-guest interactions[14] or ionic interactions.[15] Nevertheless, the exploitation of dynamic covalent bonds to develop self-healing materials is notably broad.[16] Several dynamic covalent reactions viz., Diels-Alder (DA),[17, 18] Alder-ene (AE),[19] and disulfide metathesis reactions,[20] have been well-explored for the development of numerous self-healing (bio) materials. However, due to the high selectivity and exceptional tolerance to a wide range of chemicals, the DA cycloaddition reaction between furfuryl and maleimide groups has been widely used to

develop self-healing materials.[21] Although tremendous efforts have been devoted to developing self-healable functional polymers, the number of articles dealing with self-healing fluoropolymers based on dynamic DA chemistry is rather limited. Recently, Padhan et al.[22] and Banerjee et al.[23] reported the preparation of self-healable fluoropolymers based on the furfuryl-maleimide DA cycloaddition reaction. However, in both systems, the furfuryl pendant containing copolymers were synthesized via conventional radical polymerization (RP) and crosslinked with an aromatic bismaleimide derivative. It is known that FRP of furfuryl containing monomers leads to uncontrolled molecular weights and, in several cases, was reported to lead to gelation due to side reactions during the radical polymerization.[24, 25] Tailor-made functional copolymers bearing the furfuryl pendants have been successfully prepared via different RDRP techniques viz., ATRP and RAFT polymerization. [26, 27]

This Chapter reports a new class of self-healing ultra-hydrophobic functional fluoropolymers bearing pendant polyhedral oligomeric silsesquioxane (POSS) units via RAFT polymerization and dynamic DA cycloaddition chemistry of furfuryl and maleimide functionalities. In this work, a copolymer of furfuryl methacrylate (FMA) and 2,2,2-trifluoroethyl methacrylate (TFEMA) was synthesized via RAFT polymerization and, subsequently, modified with POSS maleimide (POSS-M) molecules via a DA reaction. As one of the most interesting nanostructured inorganic-organic building blocks, POSS molecules are widely exploited in developing hybrid polymer nanocomposites with improved mechanical properties, thermal stability, and hydrophobicity.[28-31] A POSS molecule, represented as $(\text{RSiO}_3/2)_n$, is composed of an inner silsesquioxane core encircled by organic functionalities (R) covalently bonded to the Si atoms.[32, 33] Recently, Behera et al. utilized POSS-M molecules to synthesize a new class of ultra-hydrophobic self-healable polyurethane-POSS hybrids

based on the furan-maleimide dynamic DA reaction.[34] However, the utilization of POSS-M in developing a self-healable tailor-made fluoropolymer associated with excellent hydrophobicity is yet to be explored. In our system, the incorporation of hybrid POSS molecules not only improves the hydrophobicity of the resultant polymers but also endows the self-healing feature within the POSS derived fluorinated polymethacrylates.

This chapter as delineated earlier describes the development of self-healable hydrophobic fluoropolymethacrylate prepared via RAFT polymerization and the POSS-M derived DA cycloaddition reaction whose dynamic conjugation leads to efficient self-healing characteristics.

4.2. Experimental section

4.2.1. Synthesis of PTFEMA₄₅-*rand*-PFMA₃₈ (P1) via RAFT polymerization

The typical RAFT copolymerization of FMA and TFEMA monomers was carried out using CDTSPA as the RAFT agent and ABCVA as a thermal initiator. In this case, the monomers, TFEMA (1.0 g, 6.0 mmol) and FMA (0.659 g, 4 mmol), were added to a 100 mL round-bottomed flask (RBF) and dissolved in DMF (2.0 ml). Then, CDTSPA (0.04 g, 0.1 mmol) and ABCVA (4.1 mg, 0.025 mmol) were added to the mixture and stirred. The flask was sealed with a silicone rubber septum, and the reaction solution was made oxygen-free by purging with nitrogen for 45 min. The RBF was placed in an oil bath preheated to 85°C and the polymerization reaction was continued for 12 h. The reaction was terminated by placing the reaction flask in an ice bath and exposed to air. The polymer was dissolved in a minimum volume of DMF solvent and precipitated into cold methanol. The precipitation process was performed several times to ensure the product polymer was free of any unreacted monomer. Finally, the polymer was dried in a vacuum oven at 40°C overnight.

4.2.2. Modification of P1 copolymer with POSS maleimide via DA reaction

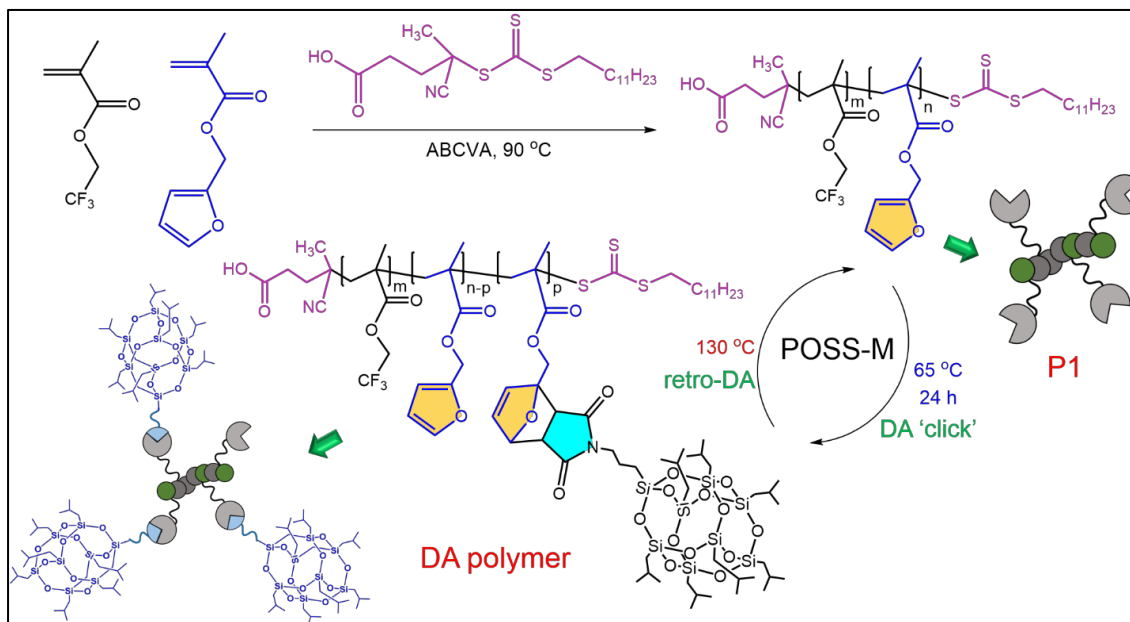
In a typical post-DA-modification reaction, initially, the random copolymer **P1** (1.0 g, 0.065 mmol) and POSS-M (0.63 g, 0.65 mmol) were taken in a 10 ml RBF and dissolved by adding 1.0 mL of DMF to the flask. The P1 copolymer modification was carried out using different molar contents of POSS-M (as shown in **Table 4.1**) at 65°C for 24 h under a nitrogen atmosphere. At the end of the reaction, the POSS-M derived individual DA polymers were further diluted with a small volume (≈ 0.5 mL) of DMF and precipitated into an excess volume of cold methanol to remove the unreacted POSS-M. The re-precipitation process was repeated several times. Although the re-precipitation process was continued several times, as evidenced by the ^1H NMR spectroscopy, removing a trace amount of unreacted POSS-M from a copolymer system was relatively strenuous.[35] Finally, the polymer was dried under a vacuum at 60°C.

4.3. Results and discussion

4.3.1. Synthesis of furfuryl bearing tailor-made fluorocopolymer and DA reaction between POSS-M and the furfuryl group in the copolymer

The synthesis of the POSS-M derived **P1** random copolymer is outlined in **Scheme 4.1**. Initially, the tailor-made copolymer with a narrow dispersity was prepared via RAFT polymerization of FMA and TFEMA monomers using CDTSPA as the RAFT agent and ABCVA as the thermal initiator at 85 °C (as shown in **Table 4.1**). The copolymer was readily soluble in common organic solvents including, DMF, chloroform, acetone, and THF. Further, the pendant reactive furfuryl groups of the **P1** copolymer were modified via a DA reaction with various molar contents of POSS-M, as shown in **Scheme 4.1**. The POSS-M acts as a dienophile reaction partner to the furfuryl (diene) functionality. The proportion of POSS-M feed was such that the ratio of reactive furfuryl:

maleimide groups in the individual mixtures was 38:10 in **P1A**, 38:20 in **P1B**, and 38:40 in **P1C**. During the DA modification with POSS-M, the temperature of the reaction system was kept constant at 65°C.



Scheme 4.1. Preparation of a random copolymer of FMA and TFEMA and its POSS-M modification via a dynamic DA reaction

4.3.2. ^1H NMR Spectroscopic analysis

The ^1H NMR spectrum of the **P1** copolymer is shown in **Figure 4.1**. The characteristic broad resonances at δ (ppm) 4.34 (H^{11}), 4.98 (H^5), 6.37 (H^6), 6.41 (H^7), and 7.44 (H^8) indicate the successful polymerization of the comonomers. The presence of the RAFT agent within the **P1** copolymer was unambiguously observed from the resonance at δ (ppm) 3.23 (H^2) attributed to the $-\text{S}-\text{CH}_2-$ methylene protons. The M_{n} , NMR and copolymer composition were calculated from the peak integral ratios of the H^5 protons of the PFMA chain, H^{11} protons of the PTFEMA segment, and H^2 protons of the terminal RAFT group (**Figure 4.1**). As depicted in **Table 4.1**, the $M_{\text{n, NMR}}$ value of **P1** copolymer was consistent with its $M_{\text{n, SEC}}$ and $M_{\text{n, Theo.}}$ values.

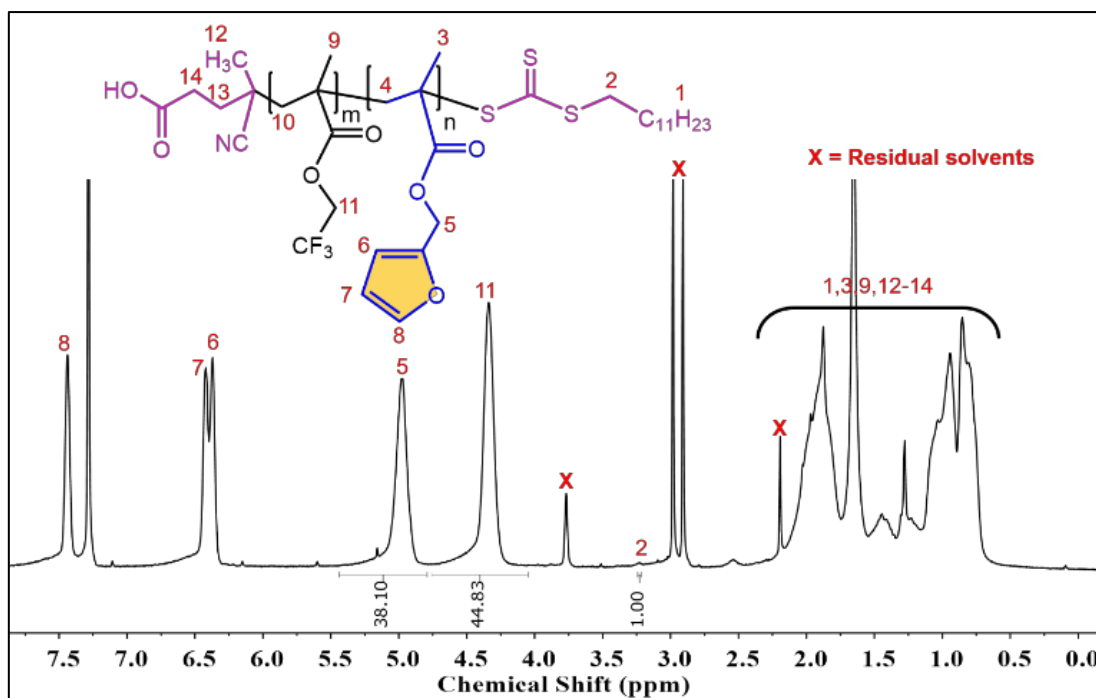


Figure 4.1. ^1H NMR spectrum of **P1** copolymer in CDCl_3 solvent.

The molar composition of the copolymer was determined from the ^1H NMR spectrum of the **P1** copolymer using **Equation 4.1**. The degree of polymerization (DP) of FMA and TFEMA within the **P1** copolymer was calculated using the integral area of the $-\text{CH}_2$ protons of FMA (H^5) and TFEMA (H^{11}) with respect to the $-\text{CH}_2$ proton of the RAFT end group (H^2) and found to be 38 and 45, respectively (*vide infra* **Table 4.1**).

$$\text{Composition of FMA } (M_{\text{FMA}})(\%) = \frac{M_{\text{FMA}/2}}{M_{\text{FMA}/2} + M_{\text{TFEMA}/2}} \times 100 \quad \text{Equation 4.1}$$

Where, M_{FMA} and M_{TFEMA} are the integrated areas of H^5 and H^{11} .

Later, the pendant reactive furfuryl groups of **P1** copolymer were DA ‘clicked’ with varied molar content of POSS-M. The POSS-M acts as a dienophile ‘click’ partner to furfuryl (diene) functionality. The proportion of POSS-M fed was such that the ratio of reactive furfuryl: maleimide groups in the individual mixture was 38: 1 (**P1A**), 19: 1 (**P1B**), and 9.5: 1 (**P1C**). It can be expected that **P1C** was fourfold as much DA modified as **P1A** provided the conversions were quantitative. Consequently, **P1B** was

supposed to be twice as much DA modified as **P1A** with POSS-M molecules. During the DA modification with POSS-M, the temperature of the reaction system was not exceeded beyond 65 °C. An overview of DA modification of P1 copolymer with varied molar content of POSS-M has been shown in **Table 4.1**.

Figure 4.2 (a-c) shows the ^1H NMR spectrum of the **P1A**, **P1B** and **P1C** DA-modified polymers, the resonances for the H^{5-8} protons of the PFMA segments of the **P1** copolymer were substantially reduced after the DA reaction with POSS-M. Notably, the incorporation of POSS-M was confirmed from the presence of the distinct $-\text{Si}-\text{CH}_2-$ ($\text{H}^{17,18}$, $\delta = 0.62$ ppm), methine ($-\text{CH}-$, H^{20}), methylene ($-\text{CH}_2-$, H^{16}) at δ (ppm) 1.88, and $-\text{CH}_3$ (H^{20} , $\delta = 0.96$ ppm) protons. The occurrence of new characteristic peaks at δ (ppm) 3.44 (H^{15}), 4.63 ($\text{H}^{5'}$), 5.27 ($\text{H}^{8'}$), 6.25 ($\text{H}^{6'}$), and 6.58 ($\text{H}^{7'}$) also confirms the formation of the furan-maleimide DA cycloadduct.

Table 4.1. An overview of all polymers

Sample code	Feed molar ratio (P1: POSS-M)	Number of reactive furan units in a copolymer chain: POSS-M	$M_{n, \text{theo}}$	$M_{n, \text{NMR}}$	SEC ^d		Number of furfuryl unit per copolymer chain ^e		% of grafting w.r.t furfuryl unit	POSS-M grafting efficiency (%)
					M_n	D (M_w/M_n)	Before DA modification	After DA modification		
P1^a	-	-	13500 ^b	13800	15200	1.35	38	-	-	-
P1A	1:10	38:10	24700 ^c	21900	21600	1.48	38	30	21	80
P1B	1:20	38:20	34200 ^c	25700	24700	1.62	38	26	32	70
P1C	1:40	38:40	53600 ^c	29500	30200	1.75	38	22	42	40

^a Monomer feed ratio of TFEMA: FMA = 60:40; copolymer composition (mol%) [TFEMA: FMA = 55:45] was calculated from the ¹H NMR spectrum.

^b The values in the bracket indicates the ratio of reactive furfuryl (FMA): maleimide units in the respective mixture.

^c The theoretical molecular weight of P1 polymer was calculated from the extent of conversion achieved by gravimetric analysis.

^d The theoretical molecular weight of DA copolymers were calculated using the following formula:

$$M_n(P1) + (Z \times \text{Molecular weight of POSS-M})$$

Where, Z is the molar ratio of POSS-M incorporated while DA modification of P1 copolymer.

^e Using PMMA standards.

4.3.3. GPC analysis

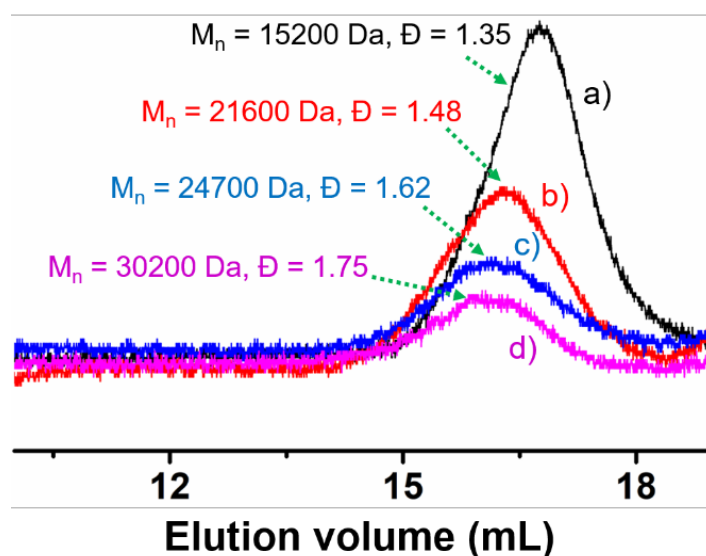


Figure 4.3. SEC analysis of a) **P1** copolymer, b) **P1A**, c) **P1B**, d) **P1C** DA polymers.

The SEC traces of **P1** and its DA modified polymers are shown **Figure 4.3**. The extent of DA conversion is accompanied by an apparent increase in the molecular weight of the POSS-M derived polymers. As the molar content of POSS-M was increased, the SEC traces of the individual DA polymers concomitantly shifted towards lower elution volume. Importantly, in all the cases, the SEC trace of the respective copolymers are monomodal with low dispersity (\bar{D}). With lower feed content of POSS-M molecules in **P1A** and (somewhat in) **P1B**, the extent of DA POSS grafting efficiency was 70-80% (*vide supra* **Table 4.1**). However, a significantly lower DA POSS grafting efficiency of 40% was observed when the molar feed content of POSS-M was increased in **P1C**. This can be related to the bulkier size of (already grafted) POSS molecules after a specific limit of DA modification, which sterically impedes the further conversion of the copolymer.[36] Furthermore, the gradual increase in the \bar{D} of DA polymers with increased molar content of POSS-M indicates that not all the macromolecular chains were uniformly grafted.

4.3.4. FTIR analysis of copolymer and DA-modified copolymer

The DA modification of the furfuryl pendants of the P1 polymer with POSS-M was further confirmed by comparing the FTIR spectrum of the pristine P1 and the DA POSS-M modified polymers.

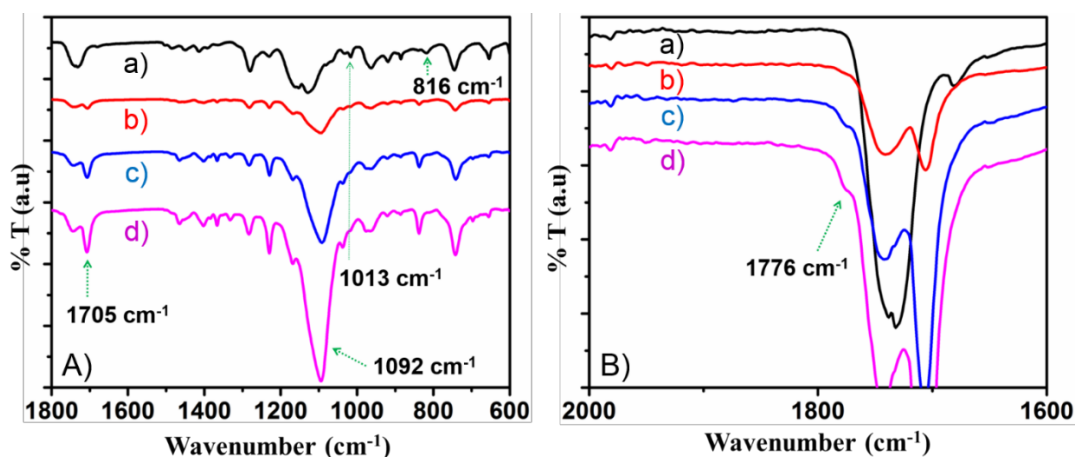


Figure 4.4. FTIR analysis of A) a) **P1**, b) **P1A**, c) **P1B**, d) **P1C** polymers; B) amplified spectrum of A).

Figure 4.4 shows that the intensity of the furan symmetric C-O-C stretching vibration, $\nu_{\text{C-O-C}}$ (1013 cm^{-1}), and out-of-plane C-H bending vibration, $\nu_{\text{C-H}}$ (816 cm^{-1}), of the **P1** polymer were significantly reduced after the DA modification with POSS-M. Also, the emergence of new bands at 1092 cm^{-1} (-Si-O- bond), 1705 cm^{-1} (asymmetric stretching of succinimide $> \text{C}=\text{O}$ of the DA adduct), and 1776 cm^{-1} (symmetric stretching of succinimide $> \text{C}=\text{O}$ of DA adduct) for the DA polymers confirms the successful attachment of the POSS-M species. As the molar content of POSS-M was increased, a higher number of furfuryl functionalities in the **P1** polymer underwent the DA reaction that eventually resulted in a greater extent of furan-POSS-M DA conjugates. Consequently, in the respective DA-modified polymers, the peak intensities associated with the POSS species intensify with a simultaneous decrease of the furan peaks. Indeed, the extent of reduction and intensification of furan and POSS-M absorption peaks, respectively, are the greatest in **P1C** DA polymer (with the highest molar content of POSS-M), followed by **P1B** and **P1A** DA polymers.

4.3.5. Differential Scanning Calorimetry (DSC) analysis

Figure 4.5 shows the DSC thermogram of the pristine copolymer and the POSS-M modified polymer. Compared to the pristine **P1** copolymer with a glass transition temperature (T_g) of 57 °C (**Figure 4.5a**), the T_g of the POSS-M derived DA copolymers are higher. The modification of the **P1** copolymer with bulky POSS-functionalities enhances the rigidity of the macromolecular chains in the resultant DA polymers.

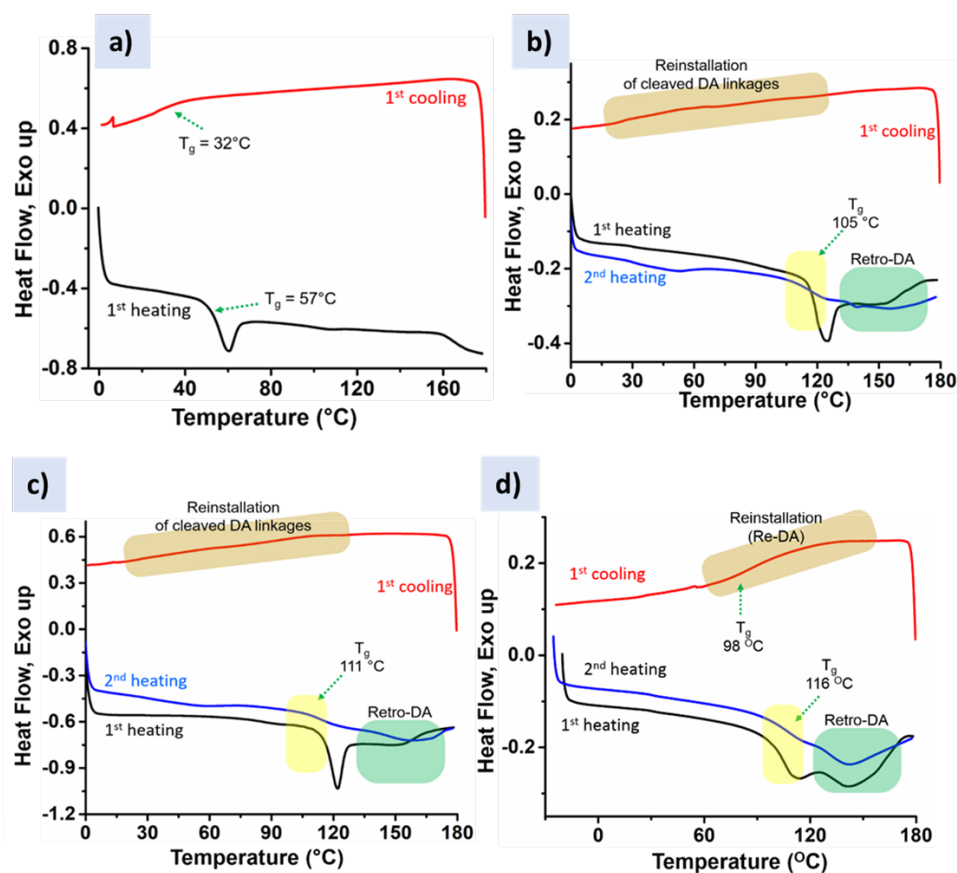


Figure 4.5. DSC analysis of a) P1 and b) P1A and c) P1B d) P1C DA polymer

Table 4.2 An overview of DSC analysis of all polymers

Polymers ^a	T_g (°C) ^b	T_{rDA} (°C) ^b	ΔH (J/g)		
			ΔH_{rDA} (1 st heating)	ΔH_{re-DA} (1 st cooling)	ΔH_{rDA} (2 nd heating)
P1	57	-	-	-	-
P1A	105	153	3.1	1.3	1.6
P1B	111	149	5.6	3.4	3.7
P1C	116	146	10.5	9.5	5.3

An overview of DSC analysis of all polymers is provided in **Table 4.2**. The DSC thermogram of the **P1A**, **P1B** and **P1C** DA polymers are shown in **Figure 4.5 b-d** respectively. The **P1C** DA polymer with the highest molar content of POSS-M exhibited the most elevated T_g , followed by **P1B** and **P1A** DA polymers (as shown in **Table 4.2**). Notably, the thermoreversible nature of the furan-maleimide DA covalent linkages is also confirmed from the DSC curves. The emergence of an additional broad endotherm at T_{rDA} (temperature zone of the retro-DA reaction $\approx 146^\circ\text{C}$) in the 1st heating curve of **P1C** polymer indicates the occurrence of a retro-DA reaction. Interestingly, an exothermic peak emerges within the range of T_{re-DA} (temperature zone of reformation of DA adduct $\approx 60^\circ\text{C}$ to 155°C) in the 1st cooling curve, which is attributed to the re-installation of the cleaved DA linkages. Furthermore, in the 2nd heating curve, the re-emergence of a similar inflexion (assigned to T_g) and endotherm (assigned to T_{rDA}) within the same temperature zone as in the 1st heating cycle confirms the reversible dynamic behaviour of the DA linkages. The ΔH_{rDA} [10.5 J g^{-1} (1st heating curve), 5.3 J g^{-1} (2nd heating curve)], and ΔH_{re-DA} (9.5 J g^{-1}) values of **P1C** DA polymer are comparatively higher (both in 1st and 2nd heating cycles) than the other DA-modified polymers. This indicates that a larger number of DA conjugate species in **P1C** cleave at T_{rDA} and reform subsequently at T_{re-DA} . The DSC analysis results correlate with the FTIR results, which initially provided evidence about the increase in the content of DA functionalities with increased molar content of POSS-M in **P1** polymer.

4.3.6. TGA analysis of Polymers

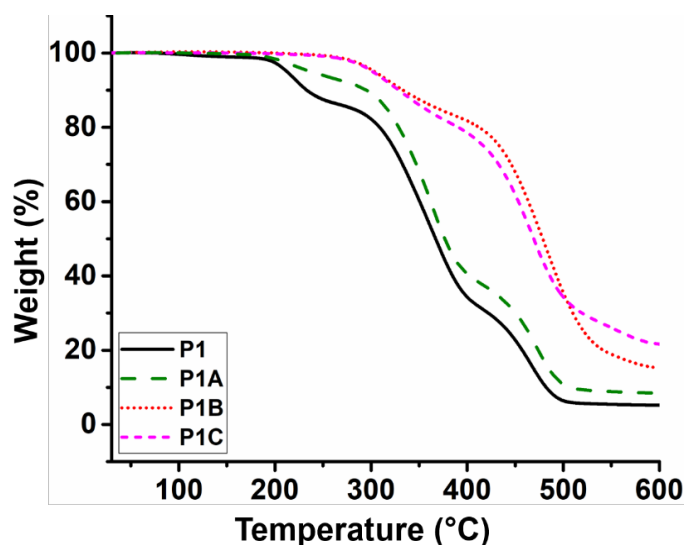


Figure 4.6. TGA analysis of a) P1 and b) P1A and c) P1B d) P1C DA polymer

The thermal stability of the **P1** copolymer and its DA-POSS hybrid adducts was determined via thermogravimetric analysis (TGA). The initial decomposition T_5 (the temperature at 5% weight loss), T_{10} (the temperature at 10% weight loss), and T_{50} (temperature at 50% weight loss) temperatures of POSS-M derived **P1** copolymers were significantly greater than the pristine **P1** copolymer (**Figure 4.6**). Importantly, as the molar content of POSS-M was increased, the decomposition temperature of the DA copolymers significantly improved (*vide infra* **Table 4.3**). However, the T_{10} and T_{50} of the **P1C** copolymer were slightly less compared to **P1B**. As shown by the DSC analysis, the content of DA conjugates was higher in **P1C** than the other DA-modified copolymers. Due to their higher concentration, a greater number of DA conjugates undergo cleavage (with temperature), which subsequently reduces the thermal stability. Nevertheless, the residual content of the POSS-M derived copolymers was higher than the **P1** copolymer, which gradually increased with the molar feed content of

POSS-M. Overall, the thermal stability of the POSS-derived DA copolymers was significantly higher than the **P1** copolymer.

Table 4.3. Summary of TGA analysis of all copolymers

Polymer Samples	Temperature (°C)			Final residue (%)
	5% weight loss (T_5)	10% weight loss (T_{10})	50% weight loss (T_{50})	
P1	212	233	367	5
P1A	236	295	376	9
P1B	301	333	478	15
P1C	304	328	469	17

4.3.7. Self-healing analysis of polymers

The dynamic behaviour of the DA linkages facilitated the POSS-M-derived **P1** polymers to exhibit self-healing characteristics. The self-healing characteristics were studied using optical microscope. The pristine polymer and the POSS-M modified polymers were dissolved and coated over a glass plate. Further, a scratch was deliberately made over the polymer surface using a razor blade and were observed under optical microscope. Then the samples were heated for 5 h at 130 °C (retro-DA temperature), followed by annealing at 65 °C for 24 h and observed again using the optical microscope. The healing efficiency (E_H) was calculated according to the **equation 4.3**. The **P1** polymer (**Figure 4.7a,b**) showed relatively low healing efficiency ($E_H \approx 17\%$). Interestingly, the self-healing efficiency of the DA-modified polymers was significantly improved with increased molar content of POSS-M (as shown in **Table 4.4**, **Figure 4.7**). After heating the notched **P1C** sample for 5 h at 130 °C, followed by annealing at 65 °C for 24 h, the scratch width of 10.1 μm reduced to 2.2 μm (**Figure 4.7**). As the scratched DA polymer sample was heated at a specific temperature (close to T_{IDA}), the DA-covalent bonds undergo cleavage that facilitated the mobility of the polymer chain due to the release of bulky POSS-M molecules, allowing the

flow of the released fluoropolymer as its T_g is significantly lower than the processing temperature of 130 °C. Consequently, at T_{rDA} , the width of the scratched interfaces is minimized due to the flow of the fluoropolymer. Finally, the reconsolidated sample was achieved by further annealing at 65°C for 24 h to re-install the cleaved DA linkages. Because of the higher content of dynamic DA functionalities, the healing behavior of the **P1C** DA polymer ($E_H \approx 78\%$) was noticeably better than the **P1B** ($E_H \approx 53.4\%$) and **P1A** ($E_H \approx 39.3\%$) DA polymers. This highlights the role of dynamic covalent linkages in the DA polymers.

$$\text{Healing efficiency } (E_H)(\%) = \frac{(\text{Original scratch width}) - (\text{Healed scratch width})}{(\text{Original scratch width})} \times 100$$

(Equation 4.3)

Table 4.4. Self-healing analysis of all polymers

Polymers	Scratch width (μm)		Healing efficiency (E_H) (%)
	Original	Healed	
P1	13.8 \pm 0.2	11.4 \pm 0.5	17.3
P1A	15.0 \pm 0.3	9.1 \pm 0.2	39.3
P1B	14.6 \pm 0.3	6.8 \pm 0.1	53.4
P1C	10.1 \pm 0.5	2.2 \pm 0.3	78.2

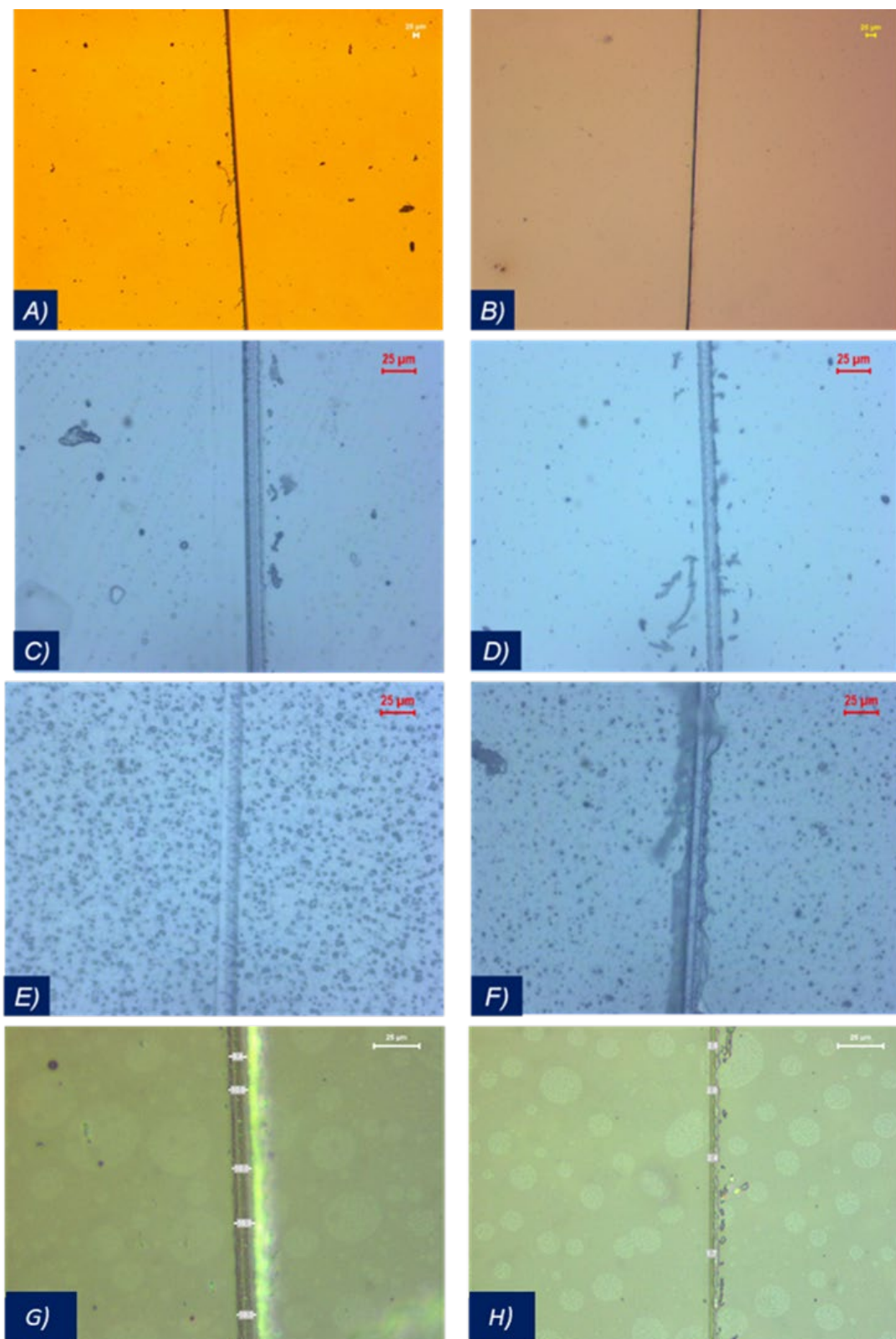


Figure 4.7. Optical microscopy images of scratched and healed samples of P1 (A-B) (unmodified copolymer), and P1A (C-D), P1B (E-F), and P1C (G-H) (POSS-M modified copolymer).

4.3.8. Hydrophobicity and surface morphology of the polymers

The hydrophobic nature of the DA polymer on surfaces was elucidated from the water contact angle (WCA) measurements. A drop of water is placed on the individual polymer surfaces, and the WCA values were determined within a duration of ≈ 10 sec (Figure 4.8).

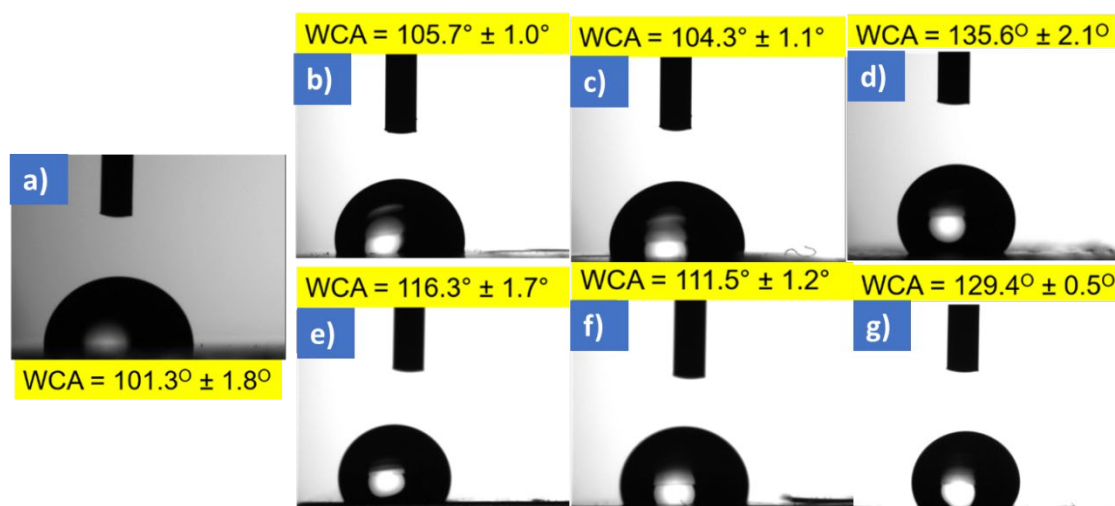


Figure 4.8. WCA values of a) **P1**, b-d) **P1A**, **P1B**, **P1C** (before healing cycle) and e-f) **P1C** (after healing cycle).

Table 4.5. Contact angle value of all polymers

Polymers	Contact Angle Value (°)	
	Before healing	After healing
P1	$101.3^\circ \pm 1.8^\circ$	-
P1A	$105.7^\circ \pm 1.0^\circ$	$104.3^\circ \pm 1.1^\circ$
P1B	$116.3^\circ \pm 1.7^\circ$	$111.5^\circ \pm 1.2^\circ$
P1C	$135.6^\circ \pm 2.1^\circ$	$129.4^\circ \pm 0.5^\circ$

The POSS-M derived DA polymers exhibit higher surface hydrophobicity than the parent **P1** polymer ($WCA = 101.3^\circ \pm 1.8^\circ$) (Table 4.5). The functionalization of **P1** with POSS-M molecules is associated with the remarkable improvement of WCA values, which can be reasoned to the increased micro/nano-surface roughness of the DA polymers (with an increase in the molar content of POSS-M) that has been further endorsed by the AFM analysis.

Figure 4.9 shows the 3D AFM images of the pristine polymer and the POSS-M modified polymer. As evidenced by AFM analysis, the DA modification of the **P1** polymer with POSS-M increases the surface roughness (S_q) of the resultant DA hybrid polymers. The incorporation of different molar contents of POSS-M increases the S_q from 0.67 nm (**P1**) to 190 nm (**P1C**). Interestingly, the notable improvement in the WCA value with increased molar content of POSS-M can be correlated with the increased S_q values of the DA polymers obtained from the AFM analysis (**Figure 4.9**). The higher the level of surface roughness, the higher is the extent of air entrapped beneath the deposited water droplet, and consequently, the polymer surface exhibits higher WCA.

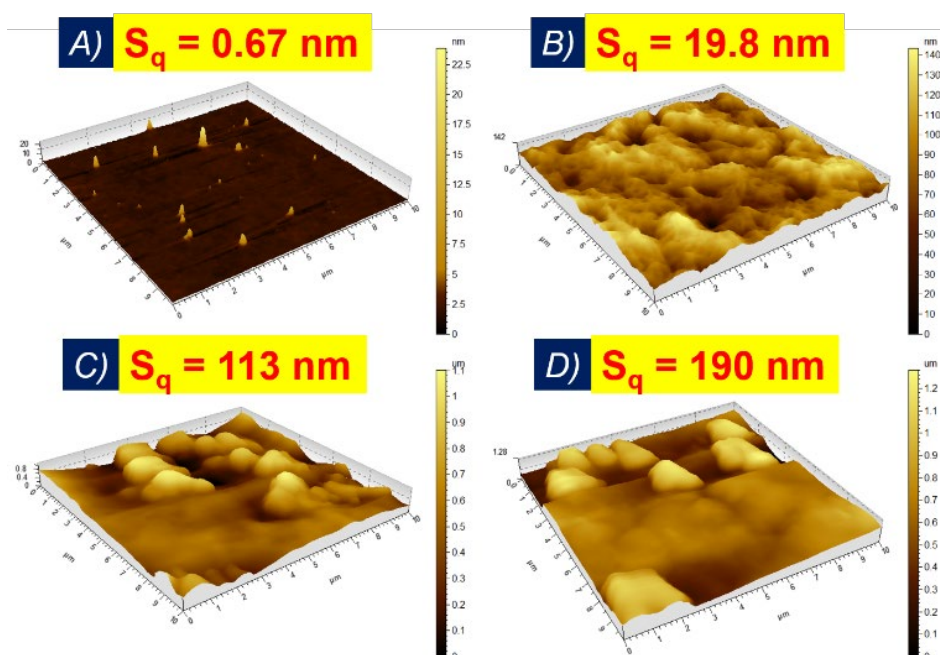


Figure 4.9. AFM 3D height images of (a) **P1**, (b) **P1A**, (c) **P1B**, and (d) **P1C**.

4.4. Conclusion

A random copolymer (**P1**) comprising reactive furfuryl groups (FMA) and fluorinated moiety (TFEMA) were synthesized via RAFT polymerization. The copolymer was successfully modified with different molar contents of maleimide functionalized POSS (POSS-M) via the furan-maleimide Diels-Alder (DA) reaction. The pristine **P1** copolymer and its POSS-M derived DA polymers were characterized by ¹H NMR, FT-IR, and SEC analyses. As evidenced by the DSC analysis, the significant shift in the T_g values (for DA copolymers) compared to **P1** polymer confirmed its successful derivation with POSS-M functionalities. Also, the thermoreversible nature of the furan-maleimide DA covalent linkages was confirmed from the DSC analysis. Interestingly, the WCA of the DA hybrid copolymer(s), in comparison to the pristine **P1** copolymer (WCA $\approx 101^\circ$), was significantly improved on modification with hydrophobic POSS molecules (e.g., for **P1C**, WCA $\approx 135^\circ$). This increase in hydrophobicity is attributed to the rise in the surface roughness values, as observed in the AFM analysis. Moreover, as evidenced by the DSC and optical microscopy analyses, the thermoreversible behaviour of the furan-POSS-M DA covalent linkages facilitated the hybrid copolymers to exhibit excellent self-healing characteristics. Interestingly, there has been a remarkable increase in thermal stability, as evidenced by the TGA analysis. Such POSS-derived DA fluoropolymer conjugates with exceptional thermal stability, ultra-hydrophobic characteristics, and excellent self-healing features can pave a new direction for specialty high-temperature-resistant materials, paints and coatings, and applications.

References

- [1] D.W. Smith, S.T. Iacono, S.S. Iyer, Handbook of fluoropolymer science and technology, John Wiley & Sons, New Jersey, 2014.
- [2] Y. Patil, B. Ameduri, Advances in the (Co) polymerization of Alkyl 2-Trifluoromethacrylates and 2-(Trifluoromethyl) acrylic Acid, Prog. Polym. Sci. 38(5) (2013) 703-739.
- [3] B. Ameduri, H. Sawada, Fluoropolymers: From Fundamentals to Applications, RSC, Oxford, 2016.
- [4] S. van der Zwaag, Self-healing materials: an alternative approach to 20 Centuries of Material Science, Virginia: Springer (2007).
- [5] N. Sottos, S. White, I. Bond, Introduction: self-healing polymers and composites, J R Soc Interface 4(13) (2007) 347-348.
- [6] S.R. White, N.R. Sottos, P.H. Geubelle, J.S. Moore, M.R. Kessler, S. Sriram, E. Brown, S. Viswanathan, Autonomic healing of polymer composites, Nature 409(6822) (2001) 794.
- [7] B. Ghosh, M.W. Urban, Self-repairing oxetane-substituted chitosan polyurethane networks, Science 323(5920) (2009) 1458-1460.
- [8] Y. Amamoto, J. Kamada, H. Otsuka, A. Takahara, K. Matyjaszewski, Repeatable Photoinduced Self-Healing of Covalently Cross-Linked Polymers through Reshuffling of Trithiocarbonate Units, Angew. Chem. 123(7) (2011) 1698-1701.
- [9] X. Chen, M.A. Dam, K. Ono, A. Mal, H. Shen, S.R. Nutt, K. Sheran, F. Wudl, A thermally re-mendable cross-linked polymeric material, Science 295(5560) (2002) 1698-1702.
- [10] A.A. Kavitha, N.K. Singha, "Click chemistry" in tailor-made polymethacrylates bearing reactive furfuryl functionality: a new class of self-healing polymeric material, ACS Appl. Mater. Interfaces 1(7) (2009) 1427-1436.
- [11] P. Mondal, P.K. Behera, N.K. Singha, A healable thermo-reversible functional polymer prepared via RAFT polymerization and ultrafast 'click' chemistry using a triazolinedione derivative, Chem. Comm. 53(62) (2017) 8715-8718.
- [12] P. Cordier, F. Tournilhac, C. Soulié-Ziakovic, L. Leibler, Self-healing and thermoreversible rubber from supramolecular assembly, Nature 451(7181) (2008) 977.
- [13] S. Burattini, B.W. Greenland, D.H. Merino, W. Weng, J. Seppala, H.M. Colquhoun, W. Hayes, M.E. Mackay, I.W. Hamley, S.J. Rowan, A healable

supramolecular polymer blend based on aromatic π - π stacking and hydrogen-bonding interactions, *J. Am. Chem. Soc.* 132(34) (2010) 12051-12058.

[14] J. Jin, L. Cai, Y.-G. Jia, S. Liu, Y. Chen, L. Ren, Progress in self-healing hydrogels assembled by host-guest interactions: preparation and biomedical applications, *J. Mater. Chem. B* 7(10) (2019) 1637-1651.

[15] L. Voorhaar, M.M. Diaz, F. Leroux, S. Rogers, A.M. Abakumov, G. Van Tendeloo, G. Van Assche, B. Van Mele, R. Hoogenboom, Supramolecular thermoplastics and thermoplastic elastomer materials with self-healing ability based on oligomeric charged triblock copolymers, *NPG Asia Materials* 9(5) (2017) e385-e385.

[16] N. Roy, B. Bruchmann, J.-M. Lehn, DYNAMERS: dynamic polymers as self-healing materials, *Chem. Soc. Rev.* 44(11) (2015) 3786-3807.

[17] A.A. Kavitha, N.K. Singha, Smart “all acrylate” ABA triblock copolymer bearing reactive functionality via atom transfer radical polymerization (ATRP): demonstration of a “click reaction” in thermoreversible property, *Macromolecules* 43(7) (2010) 3193-3205.

[18] N.B. Pramanik, G.B. Nando, N.K. Singha, Self-healing polymeric gel via RAFT polymerization and Diels-Alder click chemistry, *Polymer* 69 (2015) 349-356.

[19] K. De Bruycker, S. Billiet, H.A. Houck, S. Chattopadhyay, J.M. Winne, F.E. Du Prez, Triazolinediones as Highly Enabling Synthetic Tools, *Chem. Rev.* 116(6) (2016) 3919-3974.

[20] S.L. Banerjee, K. Bhattacharya, S. Samanta, N.K. Singha, Self-Healable Antifouling Zwitterionic Hydrogel Based on Synergistic Phototriggered Dynamic Disulfide Metathesis Reaction and Ionic Interaction, *ACS Appl. Mater. Interfaces* 10(32) (2018) 27391-27406.

[21] Y.-L. Liu, T.-W. Chuo, Self-healing polymers based on thermally reversible Diels-Alder chemistry, *Polym. Chem.* 4(7) (2013) 2194-2205.

[22] A.K. Padhan, D. Mandal, Thermo-reversible self-healing in a fluorinated crosslinked copolymer, *Polym. Chem.* 9(23) (2018) 3248-3261.

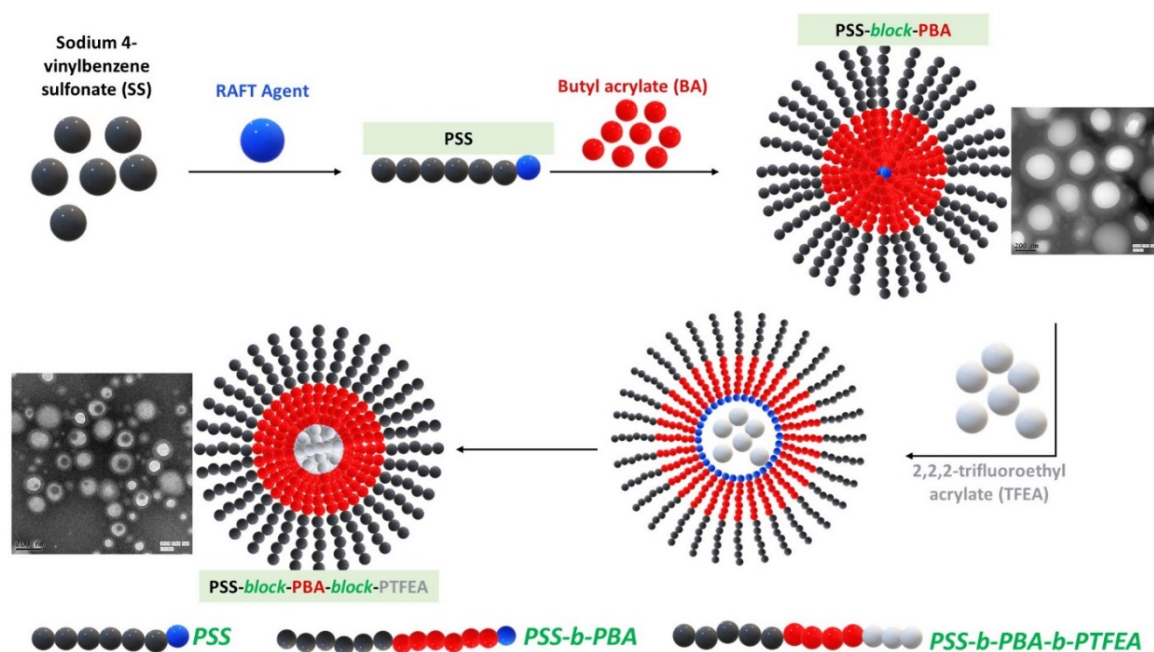
[23] S. Banerjee, B.V. Tawade, B. Améduri, Functional fluorinated polymer materials and preliminary self-healing behavior, *Polym. Chem.* 10(16) (2019) 1993-1997.

[24] A. Amalin Kavitha, N.K. Singha, A tailor-made polymethacrylate bearing a reactive diene in reversible diels-alder reaction, *J. Polym. Sci. A Polym. Chem.* 45(19) (2007) 4441-4449.

- [25] E. Goiti, F. Heatley, M.B. Huglin, J.M. Rego, Kinetic aspects of the Diels–Alder reaction between poly (styrene-co-furfuryl methacrylate) and bismaleimide, *Eur. Polym. J.* 40(7) (2004) 1451-1460.
- [26] K. Matyjaszewski, T.P. Davis, *Handbook of radical polymerization*, John Wiley & Sons, Hoboken, 2003.
- [27] A.A. Kavitha, N.K. Singha, Atom-Transfer Radical Copolymerization of Furfuryl Methacrylate (FMA) and Methyl Methacrylate (MMA): A Thermally-Amendable Copolymer, *Macromol. Chem. Phys.* 208(23) (2007) 2569-2577.
- [28] S. Gu, X. Gao, Improved shape memory performance of star-shaped POSS-poly lactide based polyurethanes (POSS-PLAUs), *RSC Adv.* 5(109) (2015) 90209-90216.
- [29] F. Alves, I. Nischang, A simple approach to hybrid inorganic–organic step-growth hydrogels with scalable control of physicochemical properties and biodegradability, *Polym. Chem.* 6(12) (2015) 2183-2187.
- [30] B. Alvarado-Tenorio, A. Romo-Urbe, P.T. Mather, Nanoscale order and crystallization in POSS–PCL shape memory molecular networks, *Macromolecules* 48(16) (2015) 5770-5779.
- [31] K.Y. Mya, H.B. Gose, T. Pretsch, M. Bothe, C. He, Star-shaped POSS-polycaprolactone polyurethanes and their shape memory performance, *J. Mater. Chem.* 21(13) (2011) 4827-4836.
- [32] M. Joshi, B.S. Butola, Polymeric nanocomposites—Polyhedral oligomeric silsesquioxanes (POSS) as hybrid nanofiller, *J. Macromol. Sci., Part C: Polym. Rev.* 44(4) (2004) 389-410.
- [33] G. Li, L. Wang, H. Ni, C.U. Pittman, Polyhedral oligomeric silsesquioxane (POSS) polymers and copolymers: a review, *J. Inorg. Organomet. Polym.* 11(3) (2001) 123-154.
- [34] P.K. Behera, P. Mondal, N.K. Singha, Self-Healable and Ultrahydrophobic Polyurethane-POSS Hybrids by Diels–Alder “Click” Reaction: A New Class of Coating Material, *Macromolecules* 51 (2018) 4770-4781.
- [35] J. Pyun, K. Matyjaszewski, J. Wu, G.-M. Kim, S.B. Chun, P.T. Mather, ABA triblock copolymers containing polyhedral oligomeric silsesquioxane pendant groups: synthesis and unique properties, *Polymer* 44(9) (2003) 2739-2750.
- [36] A. Franczyk, H. He, J. Burdynska, C.M. Hui, K. Matyjaszewski, B. Marciniak, Synthesis of high molecular weight polymethacrylates with polyhedral oligomeric

silsesquioxane moieties by atom transfer radical polymerization, ACS Macro Lett. 3(8) (2014) 799-802.

A MULTIFUNCTIONAL TRIBLOCK COPOLYMER BASED ON FLUOROACRYLATE VIA POLYMERIZATION-INDUCED SELF-ASSEMBLY (PISA); SYNTHESIS AND APPLICATION AS A THIN FILM DIELECTRIC MATERIAL



This chapter reports the synthesis of a multifunctional triblock copolymer via the polymerization-induced self-assembly (PISA) process. This chapter also delineates the thermal, mechanical and dielectric properties of the thin films formed from the triblock copolymer.

Abstract

Developing a fluoropolymer, especially fluoroacrylate based triblock copolymers, via surfactant-free emulsion polymerization is a challenging goal. This chapter reports the preparation of a triblock copolymer of sodium 4-vinylbenzene sulfonate (SS), butyl acrylate (BA), and 2,2,2-trifluoroethyl acrylate (TFEA) via PISA process using RAFT polymerization technique. Initially, poly(sodium 4-vinylbenzene sulfonate) [PSS] was prepared via RAFT polymerization in DMSO and was used as a macro-RAFT agent to prepare diblock copolymer of SS and BA. During this block copolymerization the PSS macro-RAFT with grown poly(butyl acrylate) moiety acted as surfactant leading to PISA process. This diblock copolymer, poly(sodium 4-vinylbenzene sulfonate-*block*-butyl acrylate) (PSS-*b*-PBA), was used as a macro-RAFT to polymerize the fluoro monomer TFEA. Thus, the triblock copolymer, poly(sodium 4-vinylbenzene sulfonate)-*block*-poly(butyl acrylate)-*block*-poly(2,2,2-trifluoroethyl acrylate) [PSS-*b*-PBA-*b*-PTFEA (TBCP)] was prepared via PISA process. The chemical composition was interpreted from the ^1H NMR and FTIR spectroscopic analyses. The morphology of the diblock and the triblock copolymer was studied by transmission electron microscopy (TEM) analysis.

Interestingly, the TBCP film was highly transparent and showed interesting mechanical properties with a remarkably high elongation of 1500%. Moreover, the TBCP exhibited excellent hydrophobicity having a water contact angle (WCA) of $\sim 122^\circ$. The TBCP films showed dielectric properties, which was analyzed using the AC-impedance analyzer. The prepared TBCP can be used as potential piezoelectric materials and in actuators.

5.1. Introduction

Fluorine is an interesting element because of its high electronegativity leading to higher bond strength with the carbon atom. Polymers containing fluorine atoms, especially with the C-F bond, have unique properties and are widely used in typical day-to-day applications as well as high-end applications. [1, 2] In 1930, Roy J. Plunkett reported the first fluoropolymer based on tetrafluoroethylene (TFE) after a serendipitous discovery. [3] Since then, the interest in the scientific community towards the development of fluoropolymers for a wide array of engineering applications has received significant attention. Because of the unique characteristic of C-F bonds, fluoropolymers have distinct properties like excellent thermal stability, impressive low-temperature properties, high resistance to fuels and corrosive chemicals, good optical clarity, and low surface energy. [4, 5] Owing to these exceptional properties, fluoropolymers have gained attention in the research community with the goal of developing novel materials with remarkable properties and potential high-end applications. [5-8] Fluoropolymers also have excellent dielectric properties including dielectric constant, dielectric strength, and low dissipation factor. This has led to the development of fluoropolymer-based materials for application as ion exchange membranes, insulators in battery application, membranes in the fuel cell, semiconductors, energy storage devices, and photolithographic applications. [5, 8-14] The development of fluorinated ion-exchange membranes became particularly relevant after the introduction of Nafion by the DuPont company, USA [15, 16] in 1972.

Acrylate/methacrylate-based fluorine-containing block copolymers (BCPs) find special attention among general categories in the fluoropolymer family. Compared to conventional fluoropolymers, fluorinated BCPs have been recognized to have a significant potential advantage owing to their unique microphase separation behavior,

and can undergo self-assembly in solution leading to the development of well-defined polymers whose properties can be tuned for usage in a wide range of applications. [17-22] Importantly, fluoroacrylate based BCPs can competently enhance the synergism of the outstanding surface properties afforded by the fluorinated polymer segments and the remarkable film-forming properties offered by the acrylate polymer blocks. [23, 24] Therefore, preparing fluoroacrylate based BCPs with tailored architecture has drawn much attention within the polymer research community. [25, 26] In general, BCPs with tailor-made properties and well-defined architecture are difficult to produce via conventional RP. The introduction of RDRP techniques such as NMP, ATRP, and RAFT have paved the way for the development of numerous BCPs for different applications. [27-29] The PISA process, in combination with RDRP technique, is a valuable for the efficiently synthesis of a BCPs based nanoobjects with different nanostructures of varying morphologies in aqueous and no-aqueous media, thereby having outstanding properties. [30] In principle, BCP based nanoobjects via the PISA process can be produced by any of the RDRP technique. There are numerous studies on the PISA process via NMP [31-34] and ATRP. [35-39] However, RAFT-mediated PISA remains the most commonly employed strategy. [30, 40-44]

A substantial amount of work has been reported on the synthesis of polymers with a fluorinated core via the PISA process. The main motive for the synthesis of this type of material is to develop superhydrophobic surfaces (SHSs). Shen et al. reported the RAFT-mediated PISA process for the synthesis of block copolymers comprising heptadecafluorodecyl methacrylate (HDFDMA) in the core prepared from different macro-RAFT agents such as poly[(ethylene glycol) methyl ether] (PEG), poly(2-(dimethylamino)ethyl methacrylate) (PDMAEMA), poly(methyl methacrylate) (PMMA), and poly(stearyl methacrylate) (PSMA). [45] The property of the prepared

BCPs varied depending on the macro-RAFT agent used. BCPs with PDMAEMA and PMMA exhibited an amorphous nature, whereas the BCPs with PEG and PSMA in the shell were more crystalline. The BCPs with a PHDFDMA core exhibited different nonspherical morphologies upon self-assembly. Bernice et al. reported the synthesis of diblock copolymers comprising poly(2,2,2-trifluoroethyl methacrylate) [PTFEMA] as the core-forming block prepared using poly(glycerol monomethacrylate) [PGMA]. [46] These BCPs exhibited a well-defined spherical morphology. Guo et al. reported a one-pot synthesis of BCPs comprising methacrylic acid (MAA) and TFEMA (PMAA-*b*-PTEFMA) and studied the effects of concentration of the PMAA macro-RAFT agent on the polymerization of TFEMA [47]. Chakraborty et al. reported the synthesis of BCPs comprising core functionalized PTFEMA particles and reactive groups in the shell based on 4-vinyl pyridine (4VP) and vinyltriethoxysilane (VTES) via the PISA process. [48] Here, the 4VP block units of the copolymer of VTES and 4VP were quaternized and employed for the emulsion polymerization of TFEMA. Further, the VTES units were grafted with silica nanoparticles, and Superhydrophobic surfaces (SHSs) were developed on modification with fluorinated trichlorosilane. The coatings based on these hybrid latex materials exhibited a nanostructured surface. Similarly, Ouhib et al. reported the development of transparent superhydrophobic coatings based on amphiphilic BCPs comprising methacrylic acid (MAA), butyl acrylate (BA) and 1H,1H,2H,2H-perfluorodecyl acrylate (FDA) [PMAA-*b*-PBA-*b*-P(BA-co-FDA)]. [49] SHSs were developed by mixing silica nanoparticles with the latex and spin coating them on various substrates. Qiao et al. reported the preparation of triblock copolymer nanoparticles comprising acrylic acid (AA) and 2,2,3,3,4,4,4-hexafluorobutyl acrylate (HFBA) [PAA-*b*-PHFBA-*b*-PAA] via a surfactant-free process. [50] The BCPs exhibited hydrophobicity upon thermal annealing. Recently, Couturaud et al. reported

BCPs based on pentafluorophenyl methacrylate (PFPMA) prepared using linear PEG as a macro-RAFT agent. The prepared BCP nanoparticles exhibited a spherical morphology. Further, the BCPs were core-crosslinked to form micelles which demonstrated cytocompatibility.[51] Busatto et al. reported the dispersion polymerization of 2,3,4,5,6-pentafluorobenzyl methacrylate (PFBMA) using poly[poly(ethylene glycol) methyl ether methacrylate] (PPEGMA) as the macro-RAFT agent [52]. These BCPs exhibited spherical, wormlike, or vesicular morphologies depending on the molar content of the PPEGMA. Although there are numerous reports on the synthesis of BCPs comprising fluorinated blocks via the RAFT mediated PISA process, they emphasize either the effect of macro-RAFT or the morphology of the polymers prepared. There are no reports on the potential application of these types of materials.

This chapter reports synthesis of a new class of hydrophobic fluoroacrylate based triblock copolymer comprising of sodium 4-vinylbenzene sulfonate (SS), butyl acrylate (BA), and 2,2-trifluoroethyl acrylate (TFEA) via polymerization induced self-assembly (PISA) using RAFT polymerization. The self-assembled morphology of these BCPs was studied using TEM analyses. Subsequently, the mechanical and dielectric properties of the films cast from the emulsion of these BCPs were analyzed.

5.2. Experimental section

5.2.1. Synthesis of macro-RAFT (PSS) via RAFT polymerization

In a typical polymerization reaction, the monomer, SS (5.0 g, 24.2 mmol), and the RAFT agent CPDTC (0.09 g, 0.25 mmol) were added to in 10 ml DMF in a Schlenk tube. Then the initiator AIBN (0.01 g, 0.06 mmol) was added to the above mixture, followed by purging with nitrogen for 15 min to remove the oxygen in the reaction medium. The polymerization reaction was carried out for 8 h at 80 °C. The reaction

was terminated by quenching the reaction tube in an ice bath. Methanol was used to precipitate the final polymer product which was dried in a vacuum oven at 45 °C overnight. Subsequently, butyl acrylate (BA) was polymerized using the prepared poly(sodium 4-vinylbenzene sulfonate) (PSS) macro-RAFT agent. The theoretical molecular weight of the BCP was calculated as $M_{n, \text{Theo}} = 17200$ g/mol which was consistent with the molecular weight calculated by $^1\text{H NMR}$, $M_{n, \text{NMR}} = 18400$ g/mol.

5.2.2. Synthesis of the diblock copolymer (PSS-*b*-PBA) via surfactant-free RAFT polymerization

The macro-RAFT agent, PSS (3.68 g, 0.2 mmol), was dissolved in 10 ml of deionized water in a Schlenk tube. The monomer, BA (2.0 g, 15.6 mmol), was added dropwise to the mixture under continuous stirring. Then the initiator, potassium persulphate (KPS) (13.5 mg, 0.05 mmol), was added to the mixture and stirred for 15 mins under nitrogen purging. The mixture was then sonicated for 15 min below room temperature to form a stable emulsion. The Schlenk tube was then placed in an oil bath preheated at 70 °C. The polymerization reaction was carried out for 8 h. The reaction was terminated by quenching the reaction tube in an ice bath, and the final product was dried overnight in a vacuum oven at 45 °C. The percent conversion was calculated gravimetrically, taking an aliquot from the polymer emulsion, and found to be 71 %. The theoretical molecular weight of the diblock copolymer was calculated as $M_{n, \text{Theo}} = 24300$ g/mol.

5.2.3. Synthesis of the triblock copolymer (PSS-*b*-PBA-*b*-PTFEA) (TBCP) via surfactant-free RAFT emulsion polymerization

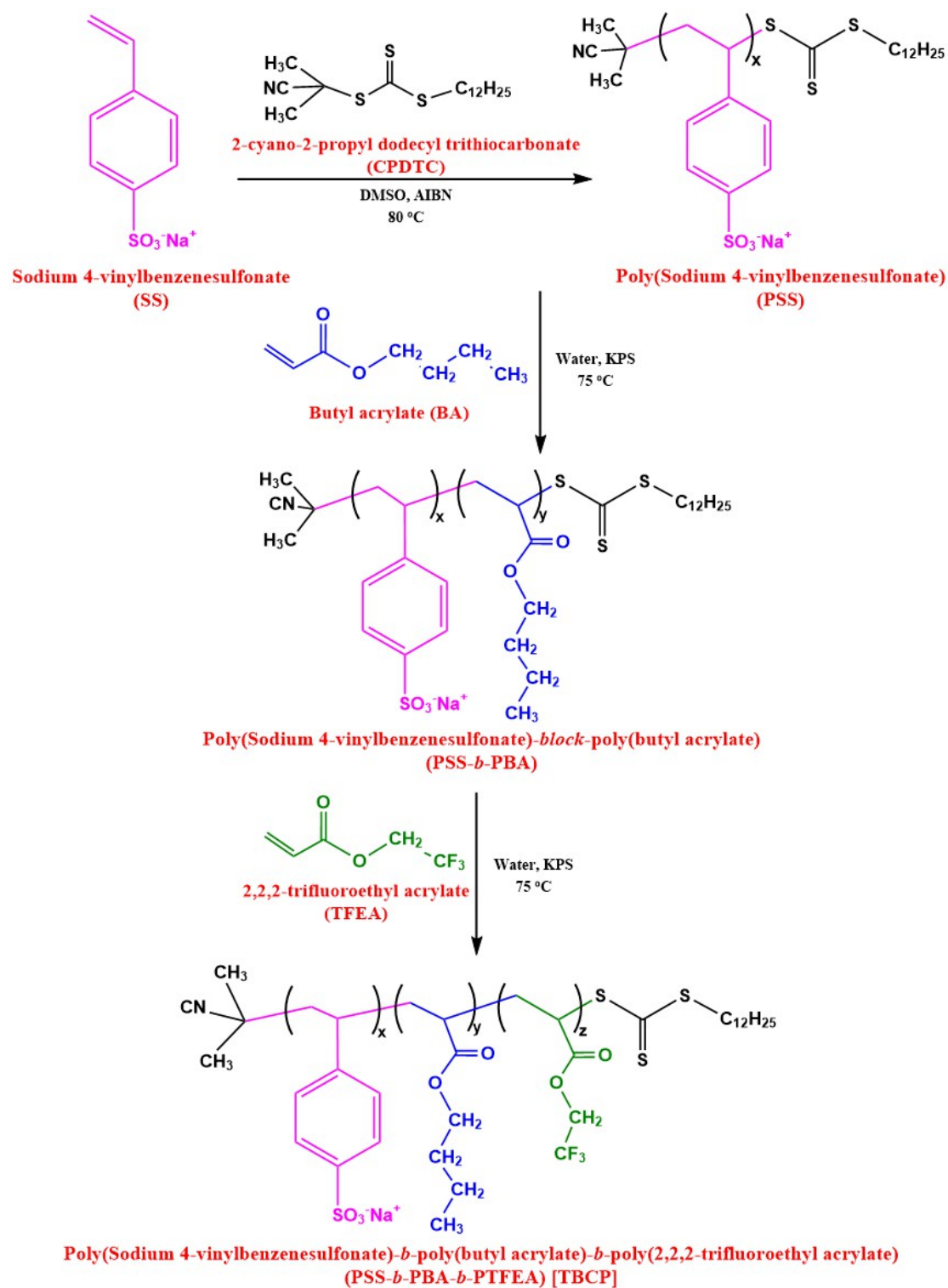
The diblock copolymer, PSS-*b*-PBA, was used as both the macro-RAFT and surfactant to prepare the target triblock copolymer via PISA. In a typical polymerization reaction, the diblock copolymer, PSS-*b*-PBA, (0.64 g, 0.025 mmol),

was dissolved in 5 ml of deionized water in a 50 ml RB flask. Then the monomer, TFEA (3.0 g, 19 mmol), was added dropwise to the mixture under constant stirring. Subsequently, the initiator, KPS (0.027 g, 0.1 mmol), was dissolved in 1 ml of deionized water and added to the mixture and stirred for 15 mins under nitrogen purging. The mixture was then sonicated for 15 min below room temperature to form a stable emulsion. The RB flask was then placed in an oil bath preheated at 70 °C and the polymerization reaction was carried out for 5 h. The reaction was terminated by quenching the reaction flask in an ice bath, and the final product was dried in a vacuum oven at 45 °C overnight. The percent conversion was calculated gravimetrically and found to be 90 %. The theoretical molecular weight of the triblock copolymer was calculated as $M_{n, \text{Theo}} = 51500 \text{ g/mol}$.

5.3. Results and discussion

5.3.1. Synthesis of PSS-*b*-PBA-*b*-PTFEA triblock copolymer (TBCP) via PISA

The synthesis of the PSS-*b*-PBA-*b*-PTFEA (TBCP) triblock copolymer is outlined in **Scheme 5.1**. Initially, the homopolymer, PSS, was prepared via RAFT polymerization of SS using CPDTC as the RAFT agent and AIBN as the thermal initiator at 80 °C in DMSO. This water-soluble macro-RAFT, PSS was subsequently used to prepare PSS-*b*-PBA diblock copolymer. The resultant diblock copolymer was employed to prepare the triblock copolymer PSS-*b*-PBA-*b*-PTFEA (TBCP). The diblock copolymer PSS-*b*-PBA can act as a macro-RAFT and can also self-assemble to form micelles in water which leads to PISA on the addition of the hydrophobic monomer TFEA. Then, the triblock copolymer (TBCP), PSS-*b*-PBA-*b*-PTFEA was prepared and characterized by ¹H NMR and FT-IR spectroscopic analysis.



Scheme 5.1 Preparation of PSS-*b*-PBA-*b*-PTFEA (TBCP) via surfactant-free RAFT emulsion polymerization.

5.3.2. ^1H NMR Spectroscopic analysis

The synthesized macro-RAFT agent (PSS) was characterized by ^1H NMR analysis. **Figure 5.1** shows the ^1H NMR spectrum of the PSS homopolymer in DMSO-

d₆. The resonances at $\delta = 7.5$ and 6.5 ppm are due to the ortho (2H) and meta (2H) protons in the phenyl group (designated as 8 and 9) in the PSS polymer. The small peak at 3.7 ppm is attributed to the $-\text{S}-\text{CH}_2-$ protons, indicating the RAFT end group. The degree of polymerization was calculated to be 100 from the peak ratio of the peaks corresponding to the RAFT end-group, and the molecular weight of the polymer (M_n , NMR) was estimated to be 18400 g/mol. This was in good agreement with the M_n calculated theoretically from the monomer conversion ($M_n = 17300$ g/mol).

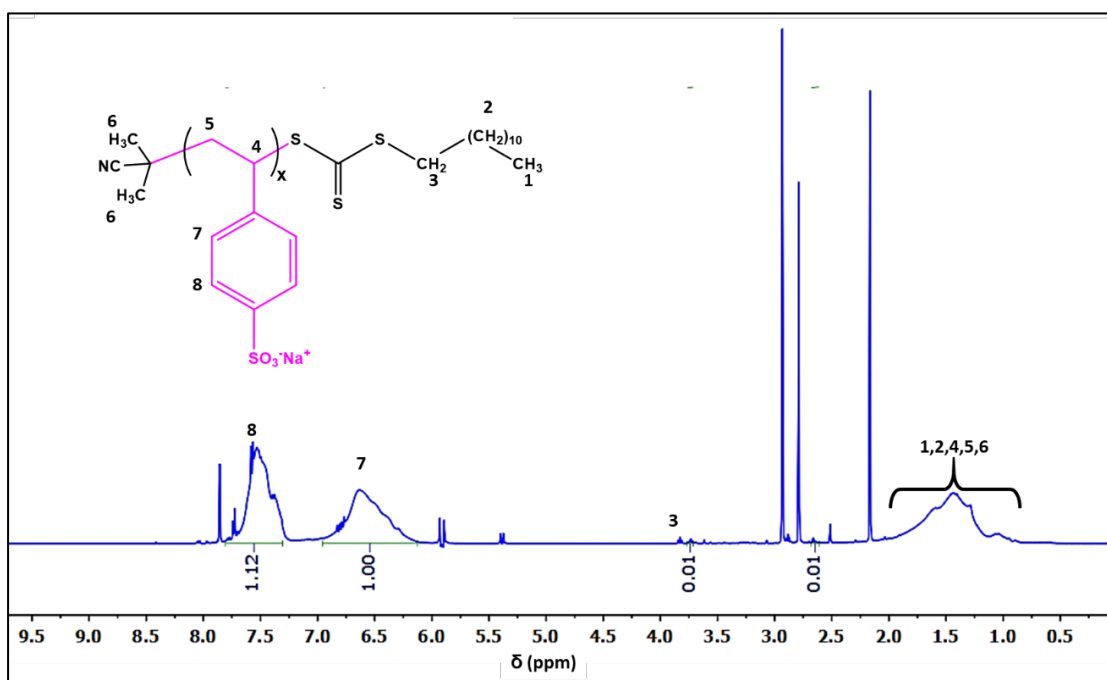


Figure 5.1. ^1H NMR spectrum of **P1** copolymer in CDCl_3 solvent.

^1H NMR spectrum of the triblock copolymer (TBCP) was recorded in D_2O solvent (**Figure 5.2**). It can be observed from the spectrum that only the hydrophilic PSS protons were observed. The absence of the resonating peaks corresponding to the hydrophobic PBA and PTFEA units indicates BCP formation and the amphiphilic self-assembled nature of the BCP in D_2O . [53, 54]

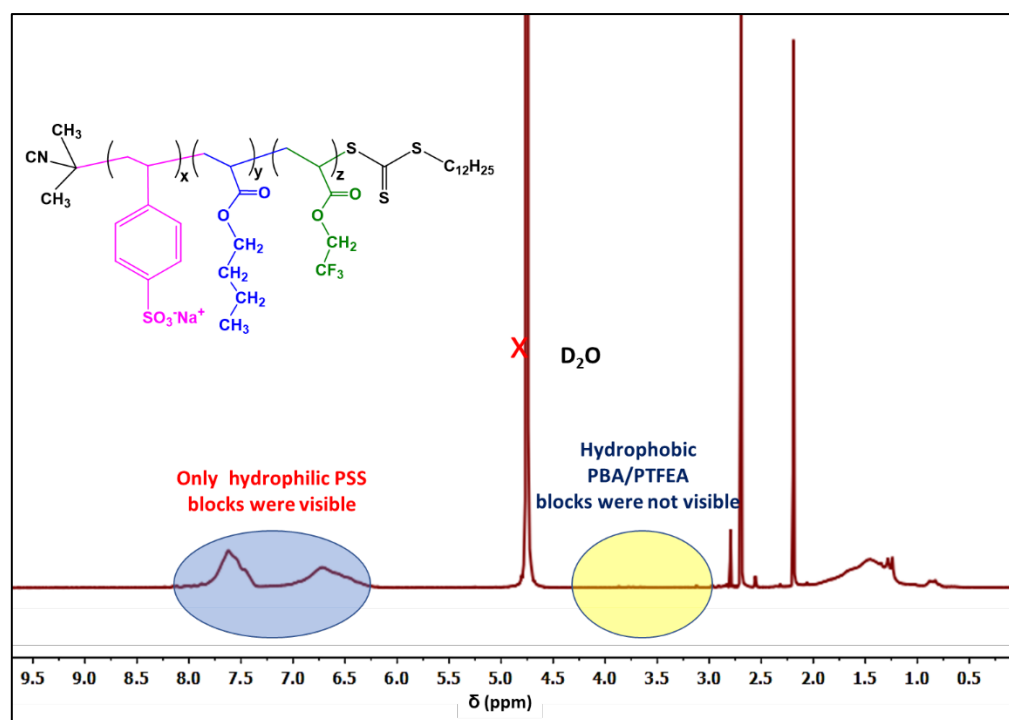


Figure 5.2. ^1H NMR spectrum of TBCP in D_2O .

A summary of the homopolymer, diblock, and the triblock copolymer prepared are shown in **Table 5.1**. The conversion was calculated gravimetrically.

Table 4.1. Summary of the polymers prepared

S. No.	Sample Codes	RAFT Agent	Conv. ^a (%)	$M_{n, \text{theo}}$ (g/mol)
1	PSS	CPDTC	85	17300
2	PSS- <i>b</i> -PBA	PSS as macro RAFT	71	24300
3	PSS- <i>b</i> -PBA- <i>b</i> -PTFEA (TBCP)	PSS- <i>b</i> -PBA as macro RAFT	90	51400

^a Calculated gravimetrically.

$$^b M_{n, \text{theo}} = \left(\frac{[M]_0}{[\text{RAFT}]} \times M_{\text{monomer}} \times X \right) + M_{\text{RAFT}}$$

Where,

$M_{n, \text{Theo}}$ = Theoretical molecular weight.

$[M]_0$ = Initial monomer concentration; $[\text{RAFT}]$ = RAFT concentration.

M_{monomer} = Molecular weight of monomer.

M_{RAFT} = Molecular weight of RAFT (or) macro-RAFT agent.

X = % monomer conversion

5.3.3. FTIR analysis of polymers

The FTIR spectra of the macro-RAFT agent (PSS), PSS-*b*-PBA copolymer, and the final copolymer [PSS-*b*-PBA-*b*-PTFEA, (TBCP)] are shown in **Figure 5.3**. The absorption band at 2954 cm^{-1} is attributed to the stretching vibration of C–H bonds of aromatic ring present in the PSS segment. The absorption bands at $1245\text{--}1154\text{ cm}^{-1}$ and 1043 cm^{-1} are associated with the stretching vibration of S=O and O=S=O, respectively. In the FT-IR spectrum of PSS-*b*-PBA, a new absorption band at 1724 cm^{-1} is observed, which indicates the $>\text{C}=\text{O}$ stretching of the ester group, present in the PBA unit. In the TBCP spectrum, the emergence of the new bands at $1310\text{--}1272\text{ cm}^{-1}$ and 962 cm^{-1} are assigned to the C–F bond stretching and bending vibrations, respectively, and confirm the presence of the PTFEA segment. It is observed from the spectrum of TBCP that the intensity of the absorption band around $3500\text{--}3000\text{ cm}^{-1}$ increased due to the entrapped water present in the TBCP film.

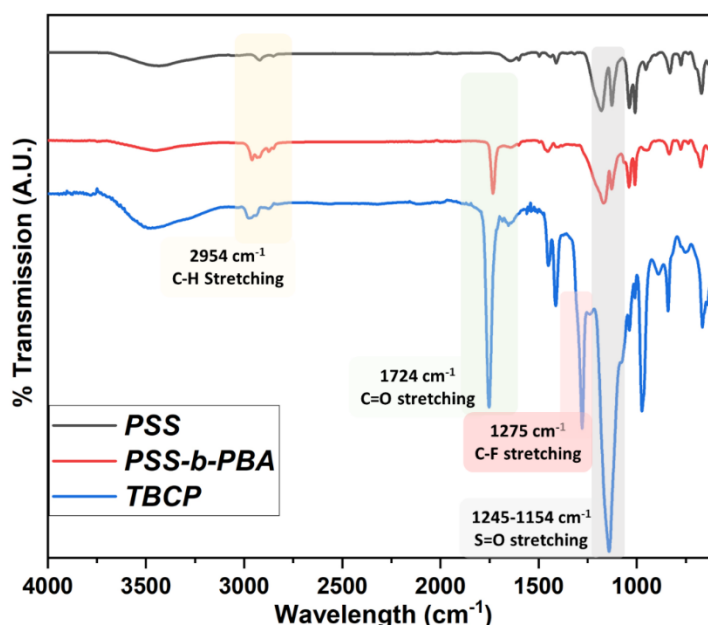


Figure 5.3. FTIR spectra of the macro-RAFT agent (PSS), diblock (PSS-*b*-PBA), and triblock (TBCP) copolymer.

5.3.4. Differential scanning calorimetry (DSC) analysis

Figure 5.4 shows the DSC thermograms of the macro-RAFT agent, diblock, and triblock copolymers. The glass transition temperature (T_g) of the macro-RAFT

agent, PSS, appeared at around 120 °C. It can be observed from the DSC thermogram of the diblock copolymer (PSS-*b*-PBA) that there is no significant change in the T_g of the PSS block. The T_g of the PBA block is not visible due to short length of the PBA segment present in the diblock copolymer. In the case of the triblock copolymer (TBCP), the T_g of the PSS block shifted towards lower temperature (103 °C) due to the soft flexible amorphous matrix of PBA and PTFEA directly affecting the hard PSS segments. The TBCP also showed an inflexion around -7 °C, which is attributed to the T_g of PTFEA part. [55] The presence of a distinct T_g for the individual blocks in the BCPs and the shift in the endotherm in the DSC thermogram of the TBCP indicates the presence of phase separation among the different blocks. This was further confirmed by the TEM analysis.

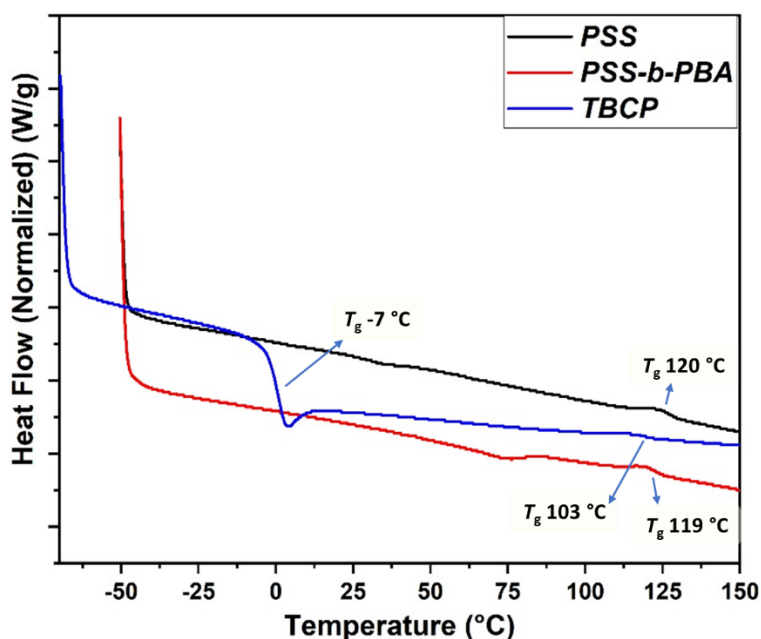


Figure 5.4. DSC traces of PSS, PSS-*b*-PBA, and TBCP.

5.3.5. TGA analysis

Figure 5.5 shows the TGA thermograms of the PSS, diblock and triblock copolymers respectively. The samples were kept in humid conditions for four months to ensure equilibrium moisture prior to TGA analysis. The TGA thermograms show

16%, 3% and 1.5% weight loss up to 170 °C temperature for PSS, the diblock and triblock copolymer respectively, corresponding to evaporation of absorbed water. This initial weight loss indicates the water uptake property of the corresponding polymers. The second stage weight loss at ~380 °C was due to the desulfonation of the PSS polymer while the third stage weight loss at 500- 600 °C was due to the dearomatization of the PSS ring. [56, 57] Importantly, PSS showed a high char yield of ~40%. For the diblock copolymer, the weight loss at ~270 °C was due to the degradation of the butyl acrylate part. For the triblock copolymer, the weight loss at ~720 °C was due to the C-F bond degradation associated with the PTEFA block. Thus, TGA analysis indicates the TBCP has higher thermal stability compared to PSS as well as the diblock copolymer.

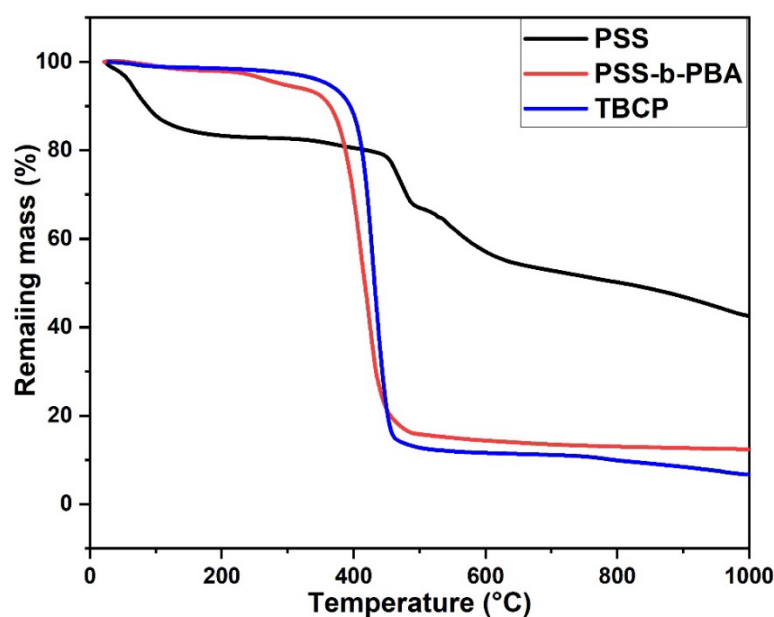


Figure 5.5. TGA thermograms of macro-RAFT, diblock and triblock copolymer.

5.3.6. Transmission electron microscopy (TEM) analysis

Figure 5.6a and **Figure 5.6b** shows the TEM images of the diblock copolymer (PSS-*b*-PBA) and the triblock block copolymer (TBCP), respectively coated over a TEM grid. It can be observed from the TEM images of PSS-*b*-PBA that the diblock copolymer forms vesicles upon self-assembly. The dark spot inside the vesicles in the

TEM images of the TBCP clearly shows that the polymerization of TFEA takes place inside the vesicles leading to the formation of self-assembled triblock copolymer.

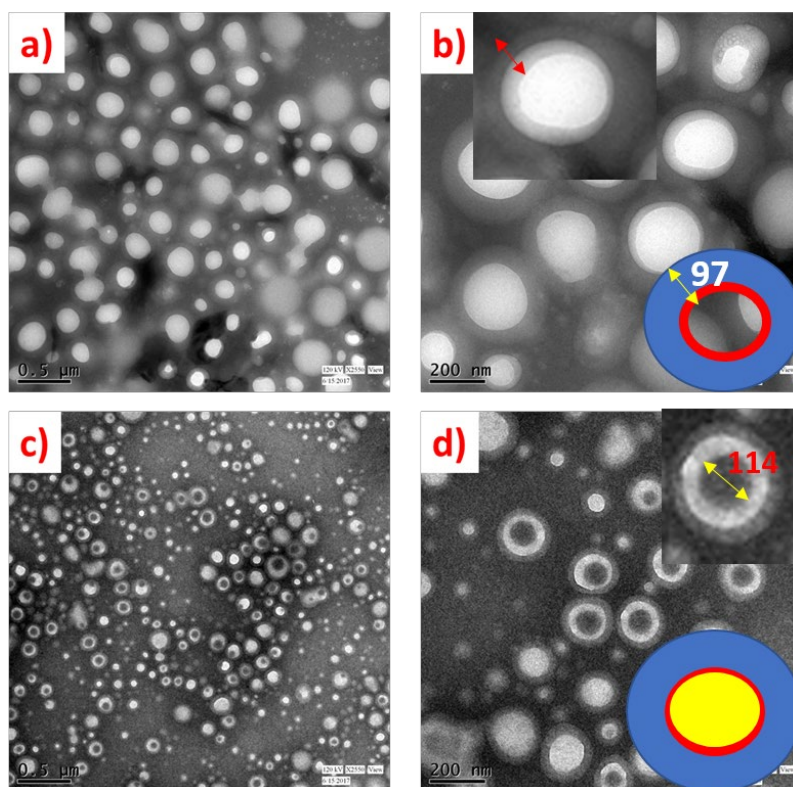


Figure 5.6. TEM images of the diblock (a, b) and triblock TBCP (c, d) at different magnification.

5.3.7. Dynamic light scattering (DLS) study

The stability of the emulsion and the particle size distribution were studied by DLS analysis. **Figure 5.7** shows the DLS curves of the diblock and triblock copolymer emulsion. It can be observed that both the diblock and the triblock copolymer emulsion shows narrow and unimodal distributions of the emulsion particles. The lower particle size distribution indicates the good stability of the emulsions. It is observed that the average particle size of the triblock copolymer is higher than the diblock copolymer which confirms the PISA formation due to incorporation of the hydrophobic fluoroacrylate. [54] It can be observed that the particle size of both the diblock and triblock, obtained from DLS is higher than that calculated from TEM analysis. This can be attributed to the shrinkage of the particles on drying during TEM sample preparation.

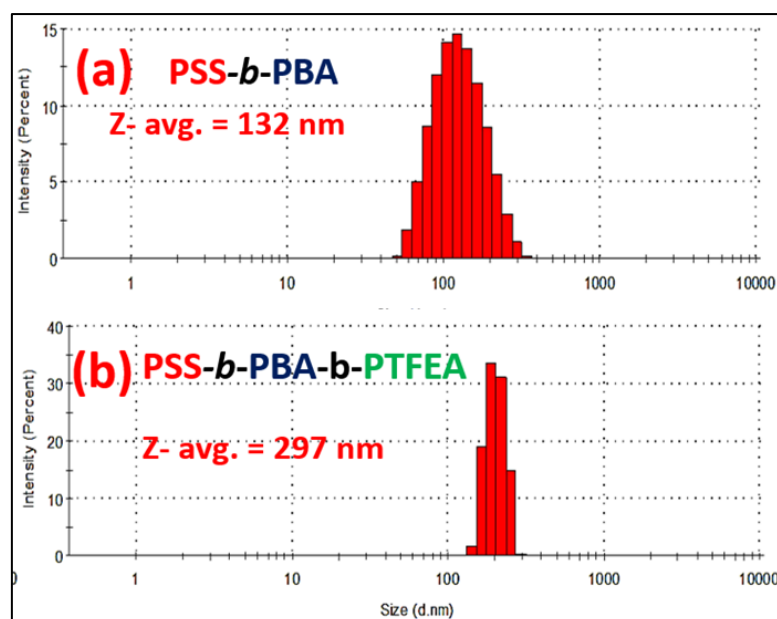


Figure 5.7. DLS analysis of (a) diblock copolymer emulsion and (b) triblock copolymer emulsion.

5.3.8. Analysis of Tensile properties of TBCP

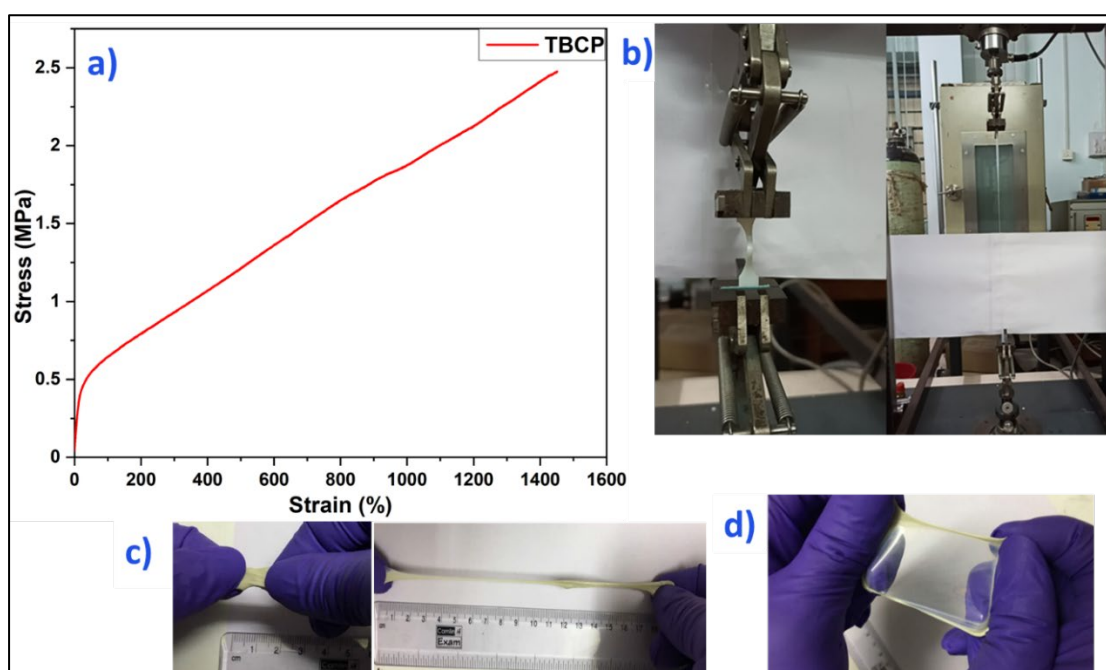


Figure 5.8. Tensile study of the triblock (TBCP) copolymer.

Figure 5.8a shows the tensile stress-strain curve of the triblock copolymer (TBCP) and **Figure 5.8b** shows the photograph of the tensile sample before and after elongation. **Figure 5.8c** shows photographs of elongation of the cut sample upon stretching. The TBCP formed transparent films on stretching as seen in **Figure 5.8d**.

Table 5.2 summarize the values of the tensile test results of the TBCP film. The elastic modulus, tensile stress and elongation at the break are of 0.79 ± 0.11 MPa, 2.50 ± 0.23 MPa and 1400 ± 113 %, respectively. This result indicates the excellent rubbery properties of the TBCP membrane and are better than conventional HCR (high consistency rubber). Because of the very high elongation percentage, the toughness of the TBCP is also high, this delineates that more energy dissipates to resist the rupture, which is an important property for a film to be suitable for membrane application.

Table 5.2. Summary of the tensile property study of the TBCP.

Sample	Thickness of the film (mm)	E_{mod} MPa	TS MPa	EAB %
TBCP	0.57	0.79 ± 0.11	2.50 ± 0.23	1400 ± 113

5.3.9. Water contact angle (WCA) analysis

The hydrophobic nature of the TBCP films was elucidated from the WCA measurements. A drop of water was deposited on the polymer film, and the WCA values were determined within a duration of ~10 sec. **Figure 5.9** shows the image of the water droplet over the polymer film and the corresponding contact angle value. It was observed that the TBCP exhibits high surface hydrophobicity with a measured $WCA = 122.67^\circ \pm 0.15^\circ$.

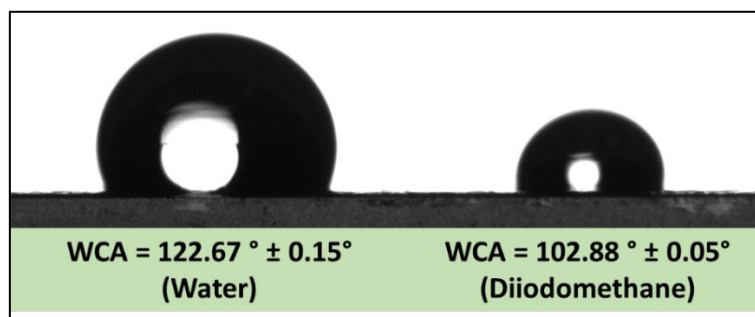


Figure 5.9. Water and diiodomethane contact angle of the TBCP coated on glass slide.

The surface energy of the TBCP film is calculated using water and diiodomethane as polar and non-polar liquids, respectively. From the contact angle

data, the surface energy of the solid polymer film was determined by the following equations.

$$(1 + \cos\theta)\gamma_l = 2(\gamma_s^d \times \gamma_l^d)^{1/2} + 2(\gamma_s^p \times \gamma_l^p)^{1/2} \quad (\text{equation 5.1})$$

$$\gamma_s^d + \gamma_s^p = \gamma_s \quad (\text{equation 5.2})$$

where, θ is the value of contact angle, γ_s is the total surface energy, γ_l is the surface free energy of liquid that can be obtained from $(\gamma_l^d + \gamma_l^p)$, γ_l^d and γ_l^p are the dispersive and polar component of liquid surface energy. For water, $\gamma_l^d = 21.8$ mJ/m² and $\gamma_l^p = 51.0$ mJ/m². For diiodomethane, $\gamma_l^d = 48.5$ mJ/m² and $\gamma_l^p = 2.3$ mJ/m².

The total surface energy of the TBCP film surface was calculated using the contact angle values $122.67^\circ \pm 0.15^\circ$ (water) and $102.88^\circ \pm 0.05^\circ$ (diiodomethane), and was found to be 7.96 ± 0.02 mN/m.

5.3.10. AC impedance spectroscopy

The dielectric properties of the TBCP films were analyzed using AC impedance spectroscopy. **Figure 5.10** shows the dielectric properties of the TBCP. In general, the dielectric permittivity of the polymer depends on two important factors; (i) the polar functional groups present in the polymer chain, and (ii) the close packing, or crystallization, of the polymer chains. [58, 59] Generally, as the crystallization increases, there is only restricted movements or alignment of the polar functional groups in the material which reduces the dielectric constant.[59] Herein, the presence of block polymer chains prevents close packing and allows significant degree of freedom for the polar groups present in the PSS-*b*-PBA-*b*-PTFEA BCP. Hence, the

presence of a broad peak (**Figure 5.10(a)**) in the low frequency range could be due to the block copolymer structure which imparts significant high free volume in the polymer matrix indicating the dielectric nature of the material. This was also evident from the loss tangent curve (**Figure 5.10(b)**) as its very high value of may be attributed to the reduced packing of the polymer chains or a lower degree of crystallinity. The loss tangent, or $\tan \delta$, is a measure of dielectric loss of the material and it is measured as,

$$\tan \delta = \frac{\epsilon''}{\epsilon'} \quad \text{(equation 5.3)}$$

Where ϵ'' and ϵ' are the imaginary and real part of dielectric permittivity, respectively.

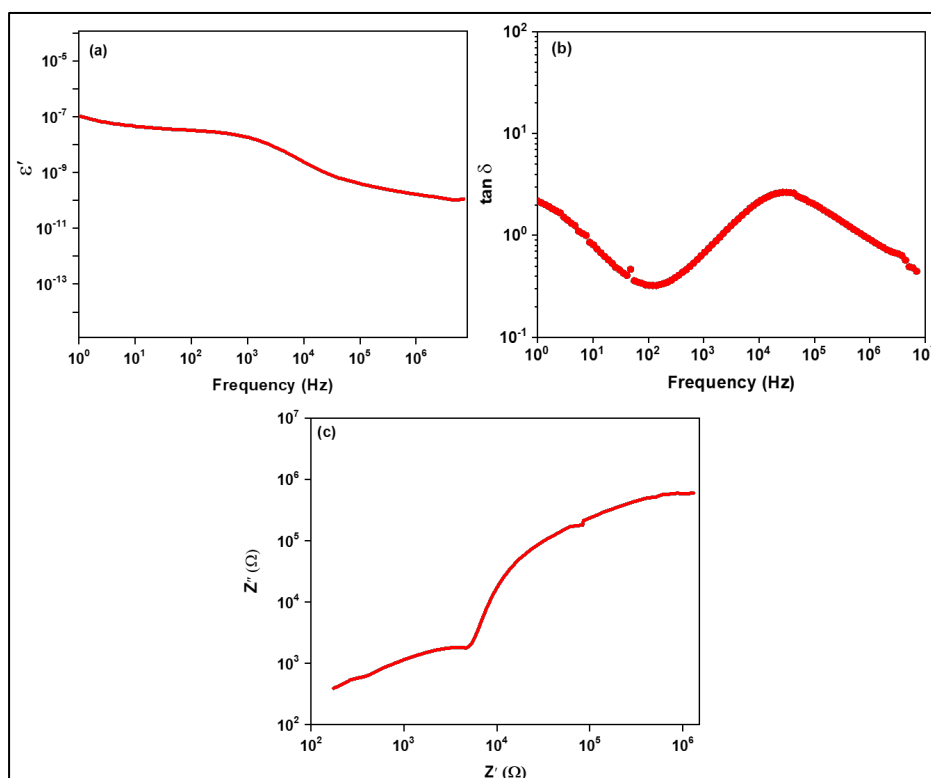


Figure 5.10. Dielectric study of the TBCP thin film. a) dielectric permittivity with reference to frequency b) loss tangent curve ($\tan \delta$) c) impedance curve.

Impedance spectroscopy elucidates the effect of the grain boundary and electrical processes taking place within the materials. Complex impedance is measured in the impedance spectroscopy and it has two parts; real and imaginary impedances and

are recorded simultaneously. Mathematically, the complex impedance is calculated using the following equation, [60]

$$Z = Z' - jZ'' \quad \text{(equation 5.4)}$$

The impedance spectroscopy curve **Figure 5.10(c)** delineates the non-Debye relaxation, and it shows a semicircle at low frequency. The increment in the system resistance as observed from the increase in real-part impedance resistance at low frequency. This increment could be attributed to the complex structure of the block copolymer or due to the polymer/solution interface. [61] The evolution of impedance spectra was characterized by the presence of intermediate states at low and high frequencies. Hence, the prepared copolymer shows dielectric properties attributed to their polar functional groups and chemical structure of the block copolymer chains and elucidate the possibility for the thin film based piezoelectric harvesting applications.

5.4. Conclusions

In conclusion, a new triblock copolymer of sodium 4-vinylbenzene sulfonate (SS), butyl acrylate (BA), and 2,2,2-trifluoroethyl acrylate (TFEA) was synthesised via polymerization induced self-assembly (PISA) using the RAFT polymerization technique. The distinct T_g of the different blocks and the shift in the differential scanning calorimetry (DSC) traces confirms block copolymer formation. The thermogravimetry analysis (TGA) thermogram shows that the water uptake property of the triblock copolymer (TBCP) is less compared to the diblock copolymer. The morphology of the diblock and the triblock copolymer was studied by TEM analysis. The TBCP copolymer showed core-shell type morphology with the fluoro block towards the core. The dynamic light scattering (DLS) analysis showed narrow and unimodal particle distribution for the copolymer emulsion. Interestingly, the prepared

TBCP films showed remarkable mechanical properties with ~ 1500% elongation and form a transparent thin film on stretching. Moreover, the TBCP exhibits excellent hydrophobicity having a water contact angle (WCA) of ~122°. The dielectric properties of the TBCP films were studied using AC-impedance spectroscopy analysis. The presence of a broad peak in the low frequency range of the dielectric permittivity curve indicates the dielectric nature of the TBCP thin film. The prepared TBCP can have a potential application as capacitor, potential piezoelectric harvesting material as well as an actuator.

References

- [1] D.W. Smith, S.T. Iacono, S.S. Iyer, Handbook of fluoropolymer science and technology, John Wiley & Sons, New Jersey, 2014.
- [2] Y. Patil, B. Ameduri, Advances in the (Co) polymerization of Alkyl 2-Trifluoromethacrylates and 2-(Trifluoromethyl) acrylic Acid, Prog. Polym. Sci. 38(5) (2013) 703-739.
- [3] R.J. Plunkett, The history of polytetrafluoroethylene: discovery and development, High Performance Polymers: Their Origin and Development, Springer, New York, 1986, pp. 261-266.
- [4] G. Kostov, A. Rousseau, B. Boutevin, T. Pascal, Novel fluoroacrylated copolymers: synthesis, characterization and properties, Journal of fluorine chemistry 126(2) (2005) 231-240.
- [5] G.G. Hougham, P.E. Cassidy, K. Johns, T. Davidson, Fluoropolymers 2: Properties, Kluwer Academic Publishers, New York, 1999.
- [6] B. Ameduri, H. Sawada, Fluoropolymers: From Fundamentals to Applications, RSC, Cambridge, 2016.
- [7] G.G. Hougham, P.E. Cassidy, K. Johns, T. Davidson, Fluoropolymers 1: synthesis, Kluwer Academic Publishers, New York, 2006.
- [8] B. Ameduri, B. Boutevin, Well-architected fluoropolymers: synthesis, properties and applications, Elsevier, Amsterdam, 2004.
- [9] J.G. Drobny, Applications of Fluoropolymer Films: Properties, Processing, and Products, William Andrew, United Kingdom, 2020.

- [10] T. Nakajima, H. Groult, *Advanced fluoride-based materials for energy conversion*, Elsevier, Amsterdam, 2015.
- [11] M.A. Hickner, H. Ghassemi, Y.S. Kim, B.R. Einsla, J.E. McGrath, *Alternative polymer systems for proton exchange membranes (PEMs)*, *Chemical reviews* 104(10) (2004) 4587-4612.
- [12] W. Grot, *Fluorinated ionomers*, William Andrew, Pennsylvania, 2011.
- [13] K. Sasaki, H.-W. Li, A. Hayashi, J. Yamabe, T. Ogura, S.M. Lyth, *Hydrogen Energy Engineering*, Springer, Japan, 2016.
- [14] M. Toriumi, N. Shida, T. Yamazaki, H. Watanabe, S. Ishikawa, T. Itani, *Fluoropolymer-based resist materials for 157-nm lithography*, *Microelectronic engineering* 61 (2002) 717-722.
- [15] R. Souzy, B. Ameduri, *Functional fluoropolymers for fuel cell membranes*, *Progress in Polymer Science* 30(6) (2005) 644-687.
- [16] S. Banerjee, D.E. Curtin, *Nafion® perfluorinated membranes in fuel cells*, *Journal of fluorine chemistry* 125(8) (2004) 1211-1216.
- [17] M.T. Islam, M.R. Islam, K.T. Lim, *A paradigm shift in morphological architecture of PEO-b-PFOMA semi-fluorinated block copolymer thin films upon facile solvent annealing*, *Polymer* 52(22) (2011) 5212-5220.
- [18] N.M. Hansen, K. Jankova, S. Hvilsted, *Fluoropolymer materials and architectures prepared by controlled radical polymerizations*, *European Polymer Journal* 43(2) (2007) 255-293.
- [19] S. Ponnupandian, A. Chakrabarty, P. Mondal, R. Hoogenboom, A.B. Lowe, N.K. Singha, *POSS and fluorine containing nanostructured block copolymer; Synthesis via RAFT polymerization and its application as hydrophobic coating material*, *European Polymer Journal* (2020) 109679-109689.
- [20] J. He, P. Ni, C. Liu, *Synthesis and characterization of amphiphilic fluorinated pentablock copolymers based on Pluronic F127*, *Journal of Polymer Science Part A: Polymer Chemistry* 46(9) (2008) 3029-3041.
- [21] H. Zhang, P. Ni, J. He, C. Liu, *Novel fluoroalkyl end-capped amphiphilic diblock copolymers with pH/temperature response and self-assembly behavior*, *Langmuir* 24(9) (2008) 4647-4654.
- [22] X. Dong, L. He, N. Wang, J.-Y. Liang, M.-J. Niu, X. Zhao, *Diblock fluoroacrylate copolymers from two initiators: synthesis, self-assembly and surface properties*, *Journal of Materials Chemistry* 22(43) (2012) 23078-23090.

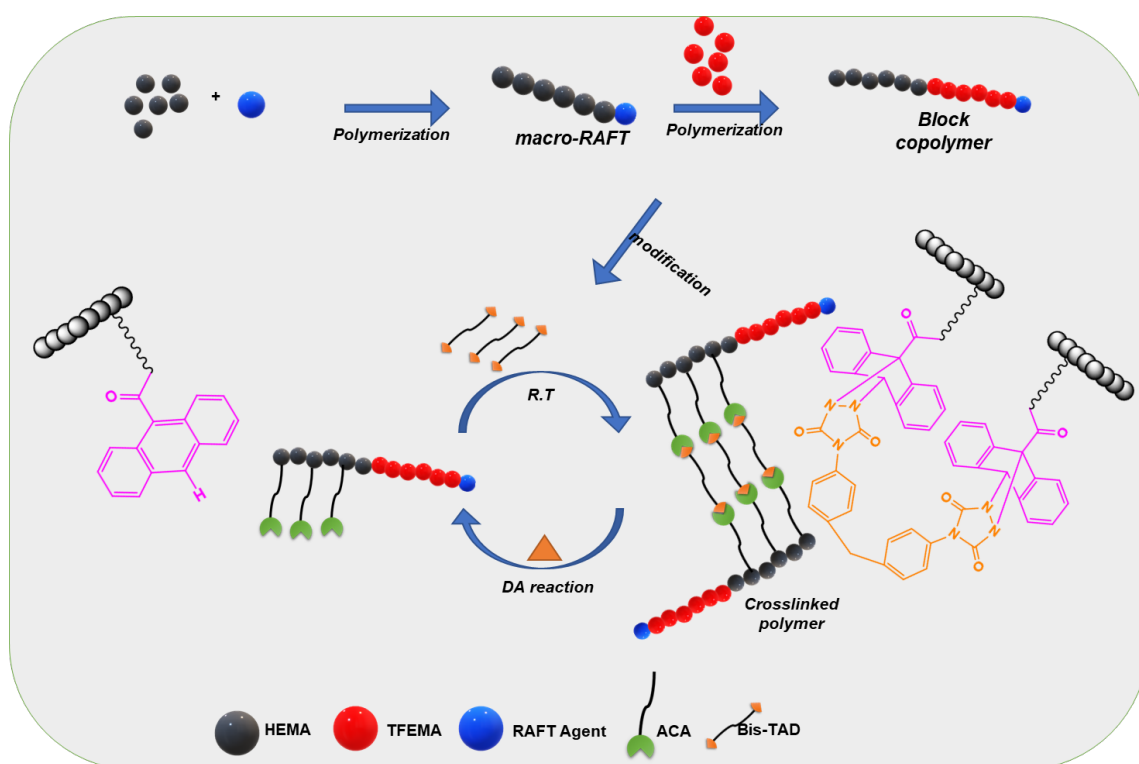
- [23] J. Liang, L. He, X. Zhao, X. Dong, H. Luo, W. Li, Novel linear fluoro-silicon-containing pentablock copolymers: synthesis and their properties as coating materials, *Journal of Materials Chemistry* 21(19) (2011) 6934-6943.
- [24] K.Y. Mya, E.M. Lin, C.S. Gudipati, H.B. Gose, C. He, Self-Assembly of Block Copolymer Micelles: Synthesis via Reversible Addition– Fragmentation Chain Transfer Polymerization and Aqueous Solution Properties, *The Journal of Physical Chemistry B* 114(28) (2010) 9128-9134.
- [25] Y. Zhu, W.T. Ford, Novel fluorinated block copolymer stabilizers for dispersion polymerization of cross-linked poly (2-ethylhexyl methacrylate-stat-chloromethylstyrene) in fluorinated solvents, *Macromolecules* 41(16) (2008) 6089-6093.
- [26] H. Peng, I. Blakey, B. Dargaville, F. Rasoul, S. Rose, A.K. Whittaker, Synthesis and evaluation of partly fluorinated block copolymers as MRI imaging agents, *Biomacromolecules* 10(2) (2009) 374-381.
- [27] D. Bertin, B. Boutevin, Controlled radical polymerization, *Polymer Bulletin* 37(3) (1996) 337-344.
- [28] K. Matyjaszewski, P.J. Miller, E. Fossum, Y. Nakagawa, Synthesis of block, graft and star polymers from inorganic macroinitiators, *Applied organometallic chemistry* 12(10-11) (1998) 667-673.
- [29] K. Matyjaszewski, J. Spanswick, Controlled/living radical polymerization, *Materials Today* 8(3) (2005) 26-33.
- [30] B. Charleux, G. Delaittre, J. Rieger, F. D'Agosto, Polymerization-induced self-assembly: from soluble macromolecules to block copolymer nano-objects in one step, *Macromolecules* 45(17) (2012) 6753-6765.
- [31] G. Delaittre, C. Dire, J. Rieger, J.-L. Putaux, B. Charleux, Formation of polymer vesicles by simultaneous chain growth and self-assembly of amphiphilic block copolymers, *Chemical communications* (20) (2009) 2887-2889.
- [32] G. Delaittre, J. Nicolas, C. Lefay, M. Save, B. Charleux, Surfactant-free synthesis of amphiphilic diblock copolymer nanoparticles via nitroxide-mediated emulsion polymerization, *Chemical communications* (5) (2005) 614-616.
- [33] S. Brusseau, F. D'Agosto, S. Magnet, L. Couvreur, C. Chamignon, B. Charleux, Nitroxide-Mediated copolymerization of methacrylic acid and sodium 4-styrenesulfonate in water solution and one-pot synthesis of amphiphilic block copolymer nanoparticles, *Macromolecules* 44(14) (2011) 5590-5598.

- [34] E. Groison, S.g.n. Brusseau, F. D'Agosto, S.p. Magnet, R. Inoubli, L. Couvreur, B. Charleux, Well-defined amphiphilic block copolymer nanoobjects via nitroxide-mediated emulsion polymerization, *ACS Macro Letters* 1(1) (2012) 47-51.
- [35] W.-M. Wan, C.-Y. Pan, Atom transfer radical dispersion polymerization in an ethanol/water mixture, *Macromolecules* 40(25) (2007) 8897-8905.
- [36] S. Sugihara, K. Sugihara, S.P. Armes, H. Ahmad, A.L. Lewis, Synthesis of biomimetic poly (2-(methacryloyloxy) ethyl phosphorylcholine) nanolatexes via atom transfer radical dispersion polymerization in alcohol/water mixtures, *Macromolecules* 43(15) (2010) 6321-6329.
- [37] G. Wang, M. Schmitt, Z. Wang, B. Lee, X. Pan, L. Fu, J. Yan, S. Li, G. Xie, M.R. Bockstaller, Polymerization-induced self-assembly (PISA) using ICAR ATRP at low catalyst concentration, *Macromolecules* 49(22) (2016) 8605-8615.
- [38] Y. Wang, G. Han, W. Duan, W. Zhang, ICAR ATRP in PEG with Low Concentration of Cu (II) Catalyst: A Versatile Method for Synthesis of Block Copolymer Nanoassemblies under Dispersion Polymerization, *Macromolecular Rapid Communications* 40(2) (2019) 1800140-1800146.
- [39] A. Alzahrani, D. Zhou, R.P. Kuchel, P.B. Zetterlund, F. Aldabbagh, Polymerization-induced self-assembly based on ATRP in supercritical carbon dioxide, *Polymer Chemistry* 10(21) (2019) 2658-2665.
- [40] F. D'Agosto, J. Rieger, M. Lansalot, RAFT-Mediated Polymerization-Induced Self-Assembly, *Angewandte Chemie International Edition* 59(22) (2020) 8368-8392.
- [41] J.-T. Sun, C.-Y. Hong, C.-Y. Pan, Formation of the block copolymer aggregates via polymerization-induced self-assembly and reorganization, *Soft Matter* 8(30) (2012) 7753-7767.
- [42] A.B. Lowe, RAFT alcoholic dispersion polymerization with polymerization-induced self-assembly, *Polymer* 106 (2016) 161-181.
- [43] J.-L. Six, K. Ferji, Polymerization induced self-assembly: An opportunity toward the self-assembly of polysaccharide-containing copolymers into high-order morphologies, *Polymer Chemistry* 10(1) (2019) 45-53.
- [44] Y. Pei, A.B. Lowe, P.J. Roth, Stimulus-Responsive Nanoparticles and Associated (Reversible) Polymorphism via Polymerization Induced Self-assembly (PISA), *Macromolecular rapid communications* 38(1) (2017) 1600528-1600542.

- [45] L. Shen, H. Guo, J. Zheng, X. Wang, Y. Yang, Z. An, RAFT polymerization-induced self-assembly as a strategy for versatile synthesis of semifluorinated liquid-crystalline block copolymer nanoobjects, *ACS Macro Letters* 7(3) (2018) 287-292.
- [46] B. Akpınar, L.A. Fielding, V.J. Cunningham, Y. Ning, O.O. Mykhaylyk, P.W. Fowler, S.P. Armes, Determining the effective density and stabilizer layer thickness of sterically stabilized nanoparticles, *Macromolecules* 49(14) (2016) 5160-5171.
- [47] L. Guo, Y. Jiang, T. Qiu, Y. Meng, X. Li, One-pot synthesis of poly (methacrylic acid)-b-poly (2, 2, 2-trifluoroethyl methacrylate) diblock copolymers via RAFT polymerization, *Polymer* 55(18) (2014) 4601-4610.
- [48] A. Chakrabarty, S. Ponnupandian, N.G. Kang, J.W. Mays, N.K. Singha, Designing superhydrophobic surface based on fluoropolymer–silica nanocomposite via RAFT-mediated polymerization-induced self-assembly, *Journal of Polymer Science Part A: Polymer Chemistry* 56(3) (2018) 266-275.
- [49] F. Ouhib, A. Dirani, A. Aqil, K. Glinel, B. Nysten, A.M. Jonas, C. Jérôme, C. Detrembleur, Transparent superhydrophobic coatings from amphiphilic-fluorinated block copolymers synthesized by aqueous polymerization-induced self-assembly, *Polymer Chemistry* 7(24) (2016) 3998-4003.
- [50] Z. Qiao, T. Qiu, W. Liu, L. Guo, X. Li, Novel tri-block copolymers of poly (acrylic acid)-b-poly (2, 2, 3, 3, 4, 4, 4-hexafluorobutyl acrylate)-b-poly (acrylic acid) prepared via two-step RAFT emulsion polymerization, *Polymer Chemistry* 7(24) (2016) 3993-3997.
- [51] B. Couturaud, P.G. Georgiou, S. Varlas, J.R. Jones, M.C. Arno, J.C. Foster, R.K. O'Reilly, Poly (Pentafluorophenyl Methacrylate)-Based Nano-Objects Developed by Photo-PISA as Scaffolds for Post-Polymerization Functionalization, *Macromolecular Rapid Communications* 40(2) (2019) 1800460-1800466.
- [52] N. Busatto, V. Stolojan, M. Shaw, J.L. Keddie, P.J. Roth, Reactive Polymorphic Nanoparticles: Preparation via Polymerization-Induced Self-Assembly and Postsynthesis Thiol–para-Fluoro Core Modification, *Macromolecular Rapid Communications* 40(2) (2019) 1800346-1800352.
- [53] S.S. Payyappilly, S. Panja, P. Mandal, S. Dhara, S. Chattopadhyay, Organic solvent-free low temperature method of preparation for self assembled amphiphilic poly (ϵ -caprolactone)–poly (ethylene glycol) block copolymer based nanocarriers for protein delivery, *Colloids and Surfaces B: Biointerfaces* 135 (2015) 510-517.

- [54] S. Samanta, S.L. Banerjee, S.K. Ghosh, N.K. Singha, Smart Polyacrylate Emulsion Based on a New ABC-Type Triblock Copolymer via RAFT-Mediated Surfactant-Free Miniemulsion Polymerization: Its Multifunctional Properties, *ACS Applied Materials & Interfaces* 11(47) (2019) 44722-44734.
- [55] Y. Kadoma, Kinetic polymerization behavior of fluorinated monomers for dental use, *Dental materials journal* 29(5) (2010) 602-608.
- [56] S.E. Facchinetto, T. Bortolotto, G.E. Neumann, J.C. Vieira, B.B.d. Menezes, C. Giacomelli, V. Schmidt, Synthesis of Submicrometer Calcium Carbonate Particles from Inorganic Salts Using Linear Polymers as Crystallization Modifiers, *Journal of the Brazilian Chemical Society* 28(4) (2017) 547-556.
- [57] M. Mohy Eldin, M. Abu-Saied, T. Tamer, M. Youssef, A. Hashem, M. Sabet, Development of polystyrene based nanoparticles ions exchange resin for water purification applications, *Desalination and Water Treatment* 57(32) (2016) 14810-14823.
- [58] K. Zhong, B. Li, *Polymer Nanocomposites for Dielectrics*, CRC Press, New York, 2017.
- [59] M. Sharma, G. Madras, S. Bose, Process induced electroactive β -polymorph in PVDF: effect on dielectric and ferroelectric properties, *Physical Chemistry Chemical Physics* 16(28) (2014) 14792-14799.
- [60] J. Joshi, D. Kanchan, M. Joshi, H. Jethva, K. Parikh, Dielectric relaxation, complex impedance and modulus spectroscopic studies of mix phase rod like cobalt sulfide nanoparticles, *Materials Research Bulletin* 93 (2017) 63-73.
- [61] L. Marchesi, F.R. Simões, L. Pocrifka, E. Pereira, Investigation of polypyrrole degradation using electrochemical impedance spectroscopy, *The Journal of Physical Chemistry B* 115(31) (2011) 9570-9575.

SELF-HEALABLE HYDROPHOBIC ANTHRACENYL FUNCTIONALIZED FLUOROUS BLOCK COPOLYMER VIA RAFT POLYMERIZATION AND DIELS-ALDER REACTION USING 1,2,4-TRIAZOLINE-3,5-DIONE (TAD) DERIVATIVE



This chapter reports the synthesis of a hydrophobic self-healing fluoropolymer based on the ultrafast anthracene-TAD Diels-Alder (DA) reaction and RAFT polymerization. Herein, the block copolymer of TFEMA and HEMA were prepared via RAFT polymerization. The hydroxyl group containing BCP was modified with anthracenyl functionality, which was subsequently crosslinked via DA chemistry using a bifunctional TAD derivative. The dynamic DA linkages endow facile healing characteristics on the TAD derived polymers. The hydrophobic characteristics of the copolymers are also analyzed.

Abstract

This chapter delineates the dynamic and ultrafast Diels-Alder (DA) chemistry to develop self-healing hydrophobic fluorinated polymer. For this purpose, a block copolymer (BCP) of 2,2,2-trifluoroethylmethacrylate (TFEMA) and 2-hydroxyethyl methacrylate (HEMA), was prepared via RAFT polymerization using 4-cyano-4-[(dodecylsulfanylthiocarbonyl)sulfanyl]pentanoic acid (CDTSPA) as the RAFT agent. Next, the pendant hydroxyl groups were modified with anthracenyl functionality via esterification with 9-anthracenecarboxylic acid. ¹H NMR and FTIR analyses were used to characterize the pre- and post-modified polymers. The tailor-made polymer bearing anthracenyl pendants was subsequently crosslinked via an ultrafast DA reaction using a bifunctional 1,2,4-triazoline-3,5-dione (TAD) derivative at room temperature (r.t.) within 10 minutes, as evidenced by the disappearance of the red colour of the azo derivative. DSC analysis was carried out to interpret the thermoreversible behaviour of the TAD-derived DA polymer. The dynamic nature of the anthracenyl-TAD σ -conjugates endowed self-healing properties within the DA crosslinked polymer at 130 °C. Interestingly, the TAD conjugated fluoropolymer was hydrophobic, as evidenced by the WCA analysis.

6.1. Introduction

The pioneering work of White et al. to conceptualize biomimetic self-healing materials has led to significant interest in the material research community. [1] Noticeably, the “Self-healing technology” has been announced as one of the top ten emerging technologies by World Economic Forum and Global Agenda Council in 2013. Polymeric materials are often prone to several damages such as, scratches, crack formation, delamination, and puncture, which ultimately lead to catastrophic failure and reduced service life. [2, 3] The inclusion of self-healing characteristics within conventional polymeric materials has been acknowledged as one of the important sustainable approaches to overcome such drawbacks. As such, self-healable materials are being widely developed with tremendous effort. [3-6]

The self-healing ability of a material can be achieved either extrinsically (by incorporating microcapsules comprising healing agents) or intrinsically (by physical or chemical interactions promoted by an external stimulus). [7] Unlike the extrinsic healing approach, intrinsic healing is based on weak non-covalent interactions,[8, 9] reversible covalent bonds, [10] or host-guest interactions. [11-13] This can be inherently achieved multiple times via varied chemical or physical interactions, without any additives. Among such interactions, smart polymeric materials, e.g., thermoresponsive self-healing or dynamers) prepared via Diels–Alder (DA) chemistry (especially based on furan-maleimide cycloaddition) has attracted significant attention due to its straightforward and orthogonal selectivity, high conversion, and excellent (free of by-product) yield. [14-18] Nevertheless, the synthesis of materials based on such versatile conjugation requires a long time (> 24-48 h) and requires elevated reaction temperatures > 50-60 °C. There are a few reports available that describe the application of anthracene–maleimide DA chemistry in preparing polymer materials.

[19-21] However, unlike the furan-maleimide (retro-) DA-cycloaddition reaction, the reversibility of anthracene-maleimide conjugation demands $> 250-300\text{ }^{\circ}\text{C}$. [22-24] Consequently, such chemistry is barely utilized in developing self-mendable materials. Moreover, the anthracene-maleimide cycloaddition requires $>100\text{ }^{\circ}\text{C}$ and a prolonged reaction period, $> 48-72\text{ h}$ to be effective.

Due to its fast reactivity under catalyst-free and ambient conditions, the use of 1,2,4-triazoline-3,5-dione (TAD) heterocyclic derivatives in the rapid modification of functional polymeric materials has gained recent interest. [25-27] For example, Mondal et al. elucidated an ultrafast crosslinking approach to develop healable fluorescent polymethacrylate coatings based on dynamic anthracene-TAD DA ‘click chemistry.’ [28] Unlike the sluggish anthracene-maleimide reversible exchange mechanism, the anthracene-TAD DA conjugates can be readily obtained under ambient conditions (within $< 2\text{ min}$), and, importantly, the bonds are reversible at temperatures $>100\text{ }^{\circ}\text{C}$, which can be exploited to develop re-mendable materials.

Fluoropolymers, especially fluorinated acrylates/methacrylates (FA/FMA) with fluorine atoms as part of pendant groups, have been an attractive research topic in the field of fluoropolymers. (Meth)Acrylic-based fluorinated (co)polymers have been widely used in varied applications, especially in anti-graffiti and easy-clean coatings, release coatings/liners in pressure-sensitive adhesives, treatment for paper, paperboard, and leather, as penetrating sealers for porous surfaces and as protective coatings for electronic applications. Although barely studied, the incorporation of self-healing characteristics in such hi-tech materials is worthwhile. Wang et al. reported polymer and protein repellent antifouling coatings based on self-healing fluoropolymer brushes prepared via ATRP. [29, 30] Li et al. reported sulfonated poly(ether ether ketone) and 1H,1H,2H,2H-perfluorooctyltriethoxysilane based superhydrophobic self-healing

coatings. [31] Wang and co-workers developed fluorinated decyl POSS and hydrolyzed fluorinated alkylsilane based self-healing (super) hydrophobic and oleophobic surfaces. [32] Zhou et al. reported fluoroalkylsilane and modified silica nanoparticles based robust self-healing super amphiphilic fabrics. [33] Padhan et al. [34] and Banerjee et al. [35] successfully utilized dynamic furfuryl and bis-maleimide DA cycloaddition in developing self-healing fluoropolymers. To the best of our knowledge, there have been no reports on the development of self-healing hydrophobic tailor-made fluoropolymer applying dynamic anthracene-TAD DA chemistry.

Herein, the RAFT polymerization was employed to polymerize HEMA, which was subsequently exploited as a macro-RAFT agent to polymerize TFEMA. The methacrylic BCP bearing pendant hydroxyl group was coupled with anthracenyl moiety, which acted as the reaction partner to the TAD moiety. The addition of a bifunctional TAD derivative to the anthracenyl-modified copolymer led to ultrafast crosslinking (as supported by the disappearance of the TAD colour within 10 minutes) under ambient conditions. The dynamic nature of the anthracene-TAD DA conjugates facilitated self-healing behaviour of the tailor-made polymethacrylates, which was analyzed via AFM analysis. Moreover, the TAD derived polymer was hydrophobic and exhibited a water contact angle of 108°.

6.2. Experimental section

6.2.1. Preparation of (4,4'-(4,4'-diphenylmethylene)-bis-(1,2,4-triazoline-3,5-dione)) (bisTAD)

The bisTAD was prepared following the reaction procedure adopted by Mondal et al. In a typical reaction, ethyl carbazide (EC) (4.0 g, 38 mmol) was dissolved in toluene (30 mL) and was taken in a 100 mL 2 neck round-bottomed flask (RBF) placed in an ice bath. Then a mixture of 4,4-methylenebis(phenyl isocyanate) (4.8 g, 19.2

mmol) dissolved in 20 mL of toluene was added dropwise to the RBF under constant stirring and in a nitrogen atmosphere. Further to the complete addition, the mixture was constantly stirred at r.t for 5 h, followed by 2 h at 90 °C. Then, the reaction mixture was cooled to r.t. and filtered. The filtrate was washed thoroughly with toluene to remove unreacted compounds. In another 100 mL RBF, bifunctional semicarbazide (4.1 g, 9 mmol) was dissolved in 20 mL aqueous KOH solution (4 M) under a nitrogen atmosphere and the solution was refluxed at 100 °C for 2 h. Then the solution mixture was filtered when it was still warm and then allowed to cool to r.t. Using conc. HCl, the filtered solution was acidified until the pH of the solution reaches 1. Then, the mixture was cooled to r.t. The white product obtained on cooling ((4,4-diphenylmethylene)-bis-(urazole)) was filtered and dried in a vacuum oven. To obtain bisTAD a mixture of DABCO-Br (2.5 g, 1.6 mmol) and (4,4-diphenylmethylene)-bis-(urazole) (1.0 g, 2.7 mmol) dissolved in 20 mL dichloromethane was combined in a 100 mL round-bottomed flask under a nitrogen atmosphere and was stirred at r.t for 5 h. The mixture was then filtered off, and the residue was washed with dichloromethane. Finally, on drying the residue at 40 °C on a rotary evaporator, the pink coloured bisTAD derivative was obtained.

6.2.2. Preparation of poly(HEMA-*block*-TFEMA) using CDTSPA as the RAFT agent:

The BCP of HEMA and TFEMA was prepared via RAFT polymerization. First, HEMA (7.68 mmol) and the RAFT agent CDTSPA (0.14 mmol) were combined in a Schlenk tube and dissolved in 1 ml of DMF. The initiator, AIBN (0.035 mmol) was then added to the mixture and the Schlenk tube was sealed. The solution was then purged with nitrogen for 30 min. Finally, the Schlenk tube containing the reaction mixture was immersed into an oil bath preheated at 80 °C and the polymerization reaction was carried out for 8 hours. The polymer obtained was precipitated in diethyl

ether. The final precipitated polymer was dried at 60 °C under vacuum overnight. The molecular weight of the polymer was calculated theoretically ($M_{n, \text{Theo}}$) as well as using NMR analysis ($M_{n, \text{NMR}}$). Then the HEMA homopolymer having a reactive end group was employed as a macro-RAFT agent for the polymerization of TFEMA. The macro-RAFT agent (0.071 mmol) and the monomer TFEMA (2.97 mmol) were combined in a Schlenk tube and dissolved in 1 ml of DMF. Finally, initiator AIBN (0.025 mmol) was added to the mixture and the reaction system was purged and the polymerization was carried out at 80 °C for 12 hours. The obtained BCP was isolated by precipitation in diethyl ether and was dried overnight under vacuum at 60 °C.

6.2.3. Modification of PHEMA-*block*-PTFEMA using anthracenecarboxylic acid (ACA) and crosslinking using TAD compound:

The BCP, PHEMA-*b*-PTFEMA was modified with anthracene carboxylic acid (ACA) using 4-dimethylaminopyridine (DMAP) and *N,N'*-dicyclohexylcarbodiimide (DCC) as a coupling agent. In a typical reaction, 0.5 g of BCP (0.06 mmol) was dissolved in 0.2 ml of DMF solvent taken in a 25 ml round-bottomed (RB) flask. In separate vial, DCC (0.4 g, 2 mmol), DMAP (0.02 g, 0.2 mmol) and ACA (0.43 g, 2 mmol) were dissolved in 0.3 ml of DMF. The mixture of DCC, DMAP, and ACA was added to the BCP solution dropwise at 0°C and kept at this temperature for 1h. subsequently, the temperature was gradually raised to r.t. and the reaction was allowed to proceed for 36 hours. The resultant modified polymer was isolated by precipitating in diethyl ether and repeatedly washed to remove residual DCC, DMAP and ACA. The modification of the hydroxyl group in PHEMA-*b*-PTFEMA with anthracenyl group was confirmed by ¹H NMR and FTIR spectroscopic analyses.

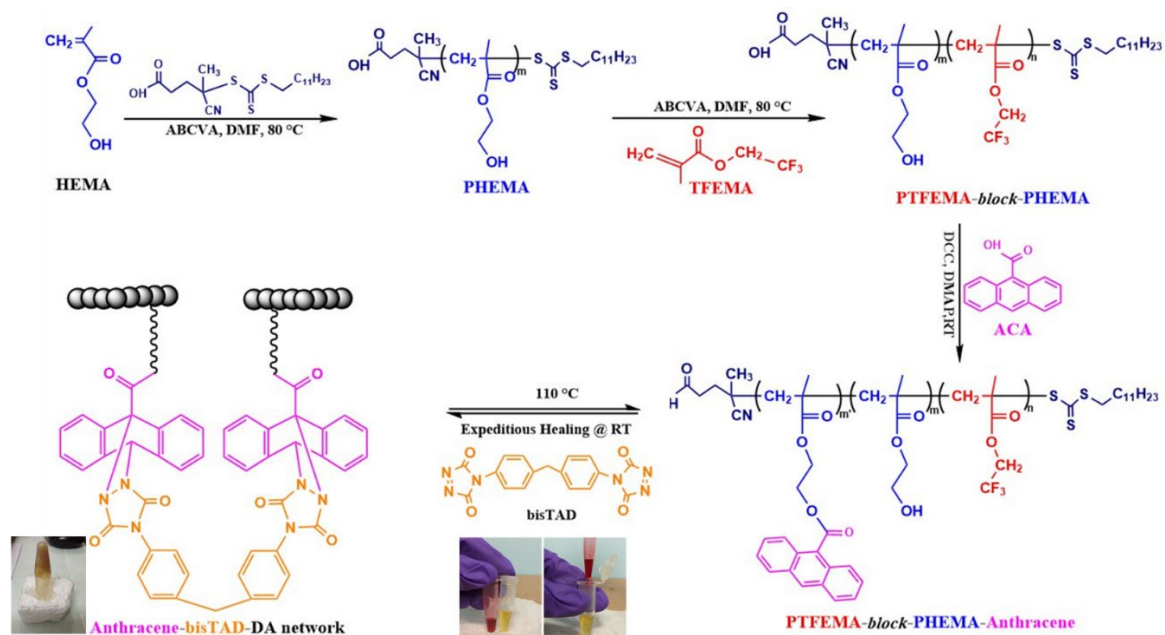
6.2.4. Crosslinking reaction of anthracenyl modified BCP using TAD compound:

To obtain the bisTAD crosslinked adduct, the modified BCP (0.1 g, 0.31 mmol reactive anthracenyl units) and bisTAD (0.0044 g, 0.012 mmol) were taken separately (at a molar ratio of reactive anthracene: bisTAD unit = 24:1) dissolved in 0.1 mL of THF and then mixed at r.t., which resulted in the ultrafast formation of crosslinked polymer within 2 min. This was confirmed by the disappearance of the red colour of bisTAD. The crosslinked polymer was dried overnight at 40 °C in a vacuum oven before further analysis.

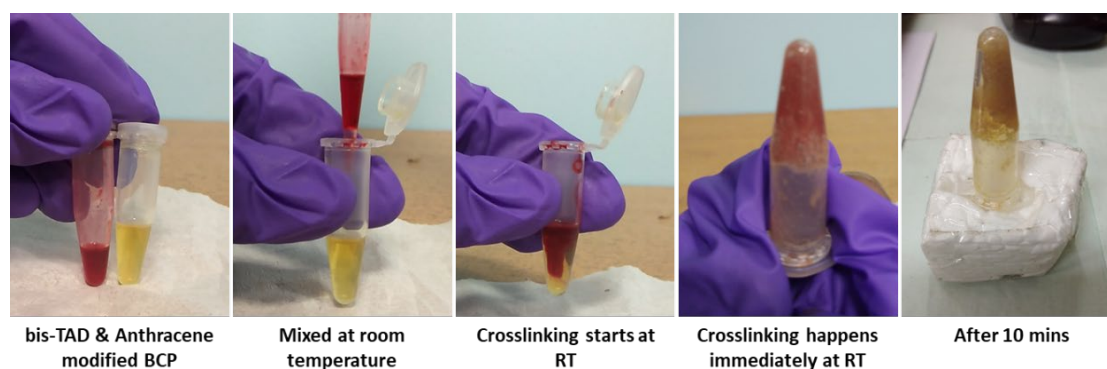
6.3. Results and discussion

6.3.1. Preparation of PHEMA-block-TFEMA and modification of BCP with anthracenyl unit and further crosslinking using bisTAD.

The synthesis of the PHEMA-*b*-PTFEMA BCP, its modification with an anthracenyl derivative and its conjugation with bisTAD is outlined in **Scheme 6.1**. Initially, the PHEMA macro-RAFT agent was prepared via RAFT polymerization of HEMA using CDTSPA as the RAFT agent and ABCVA as a thermal initiator at 85 °C. Then, the BCP was prepared by polymerizing TFEMA monomer using the PHEMA macro-RAFT agent. The preparation of the BCP is summarized in **Table 6.1**. The BCP was further modified with anthracene carboxylic acid to obtain a BCP with pendant anthracenyl units. Further, the modified BCP was crosslinked using bisTAD. The crosslinking DA reaction between anthracenyl units and bisTAD was evidenced by the disappearance of the red colour of bisTAD as shown in **Scheme 6.2**.



Scheme 6.1. Preparation of PHEMA-*block*-PTFEMA and modification of the BCP with anthracenyl units and further crosslinking using bisTAD.



Scheme 6.2. Photographs showing the crosslinking reaction of anthracenyl modified PHEMA-*block*-PTFEMA copolymer via TAD chemistry.

6.3.2. ^1H NMR spectroscopic analysis

The synthesized macro-RAFT agent PHEMA was characterized by ^1H NMR analysis.

Figure 6.1 shows the ^1H NMR spectrum of the PHEMA homopolymer recorded in $\text{DMSO-}d_6$. The characteristic resonances at δ (ppm) 4.94 (H^7), 3.60 (H^6), and 3.95 (H^5) correspond to the $-\text{OH}$, $>\text{CH}_2$, and $-\text{OCH}_2$ protons respectively of the PHEMA pendant chain. The presence of the RAFT agent was confirmed from the resonance at δ (ppm) 3.18 (H^2) attributed to the $-\text{S}-\text{CH}_2-$ methylene protons. The $M_{n,\text{NMR}}$ was calculated from the peak integral ratios of the H^7 protons of the PHEMA chain and H^2 protons of the

terminal RAFT group (**Figure 6.1**). The $M_{n, \text{NMR}}$ value of the macro-RAFT polymer ($M_{n, \text{NMR}} = 7000 \text{ g/mol}$) was consistent with its $M_{n, \text{Theo.}}$ value ($M_{n, \text{Theo.}} = 7500 \text{ g/mol}$).

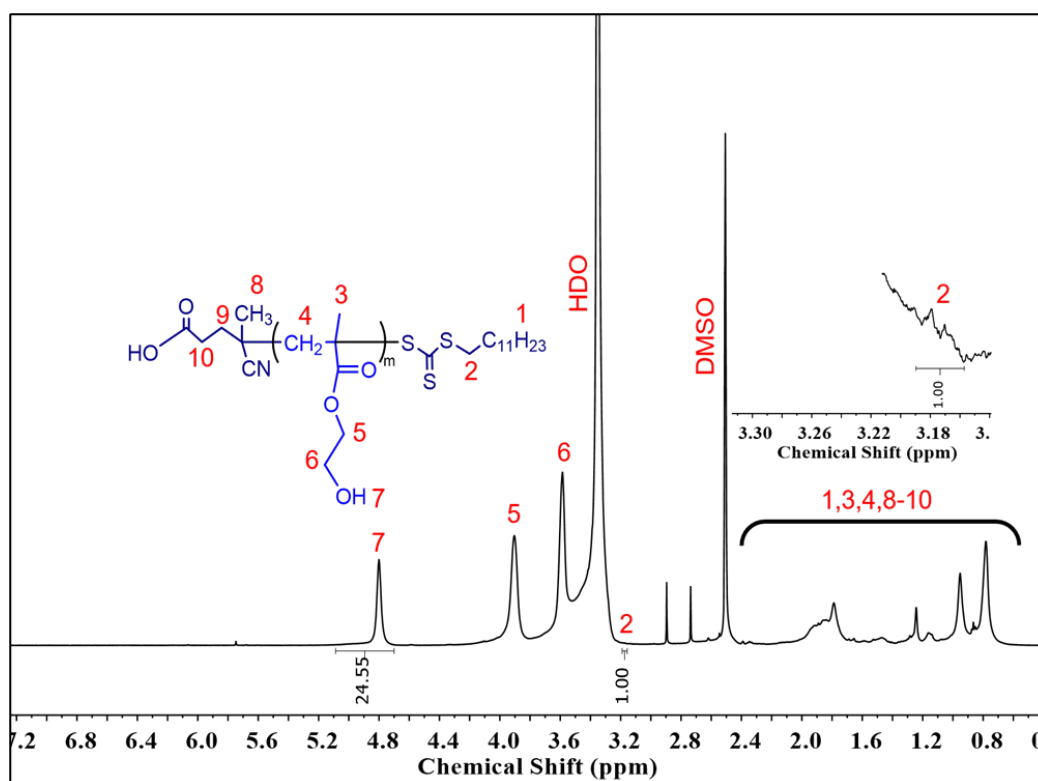


Figure 6.1. ^1H NMR spectrum of PHEMA macro-RAFT agent recorded in $\text{DMSO-}d_6$.

The synthesized macro RAFT agent (PHEMA) was used to polymerize TFEMA monomer. The obtained BCP was characterized by ^1H NMR analysis. The ^1H NMR spectrum of the PHEMA-*b*-PTFEMA BCP recorded in the $\text{DMSO-}d_6$ (**Figure 6.2**). The characteristic resonances at δ (ppm) 4.95 (H^7), 3.53 (H^6), 3.75 (H^5) correspond to the -OH, $>\text{CH}_2$, and $-\text{OCH}_2$ protons respectively of the PHEMA pendant chain. The characteristic broad resonance at δ (ppm) 4.55 (H^{13}) corresponds to the $-\text{OCH}_2$ protons of the PTFEMA pendant chain and indicates the successful polymerization of TFEMA with the PHEMA-macro-RAFT agent. The presence of the RAFT agent was unambiguously observed from the resonance at δ (ppm) 3.27 (H^2) attributed to the $-\text{S}-\text{CH}_2-$ methylene protons. The $M_{n, \text{NMR}}$ and copolymer composition were calculated from the peak integral ratios of the H^7 protons of the PHEMA chain, H^{13} protons of the

PTFEMA chain, and H² protons of the terminal RAFT group (**Figure 6.2**). As depicted in **Table 1**, the $M_{n, \text{NMR}}$ value of PHEMA-*b*-PTFEMA BCP was consistent with its $M_{n, \text{Theo.}}$ values.

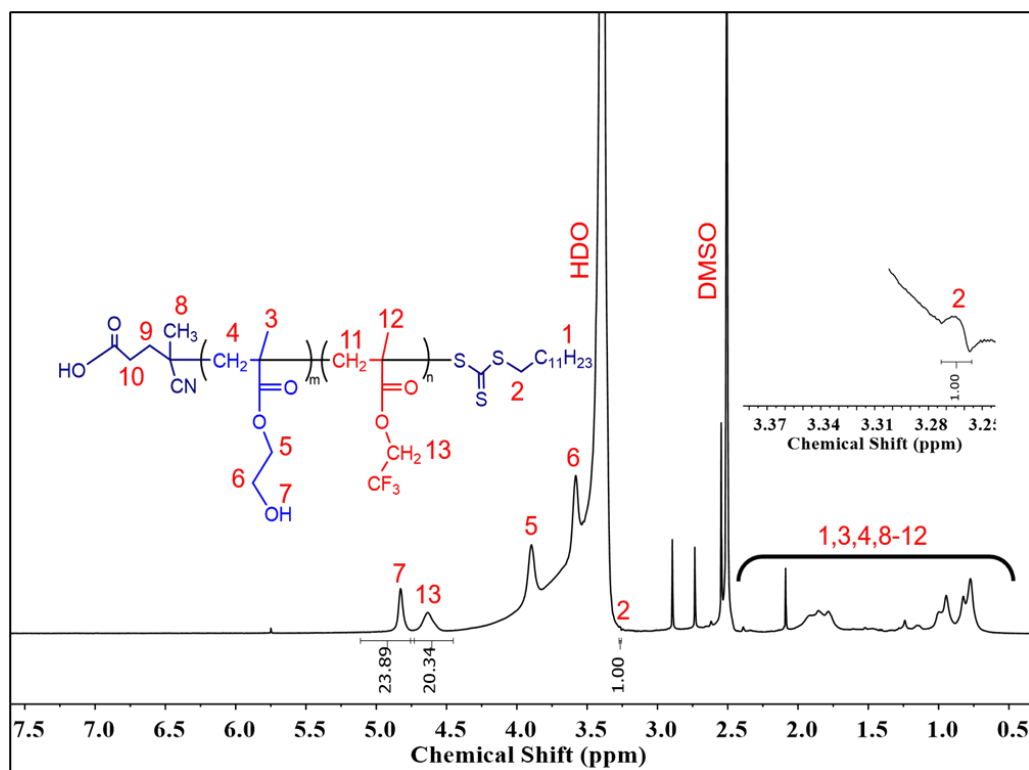


Figure 6.2. ¹H NMR spectrum of PHEMA-*b*-PTFEMA measured in DMSO-*d*₆.

The ¹H NMR spectrum of the anthracene modified BCP was recorded in DMSO-*d*₆ (**Figure 6.3**). The appearance of new broad peaks at $\delta = 7.53$ ppm to 8.88 ppm, associated with the aromatic protons of anthracene species, in the modified copolymer. Importantly, an increase in the integral ratio of H¹³ (-O-CH₂- of TFEMA) and H⁷ (-OH of HEMA) indicates that the hydroxyl groups of the BCP were successfully modified with anthracenyl functionalities (ACA). The incorporation of anthracenyl groups and modification with the TAD derivative was supported via results obtained by FTIR analysis.

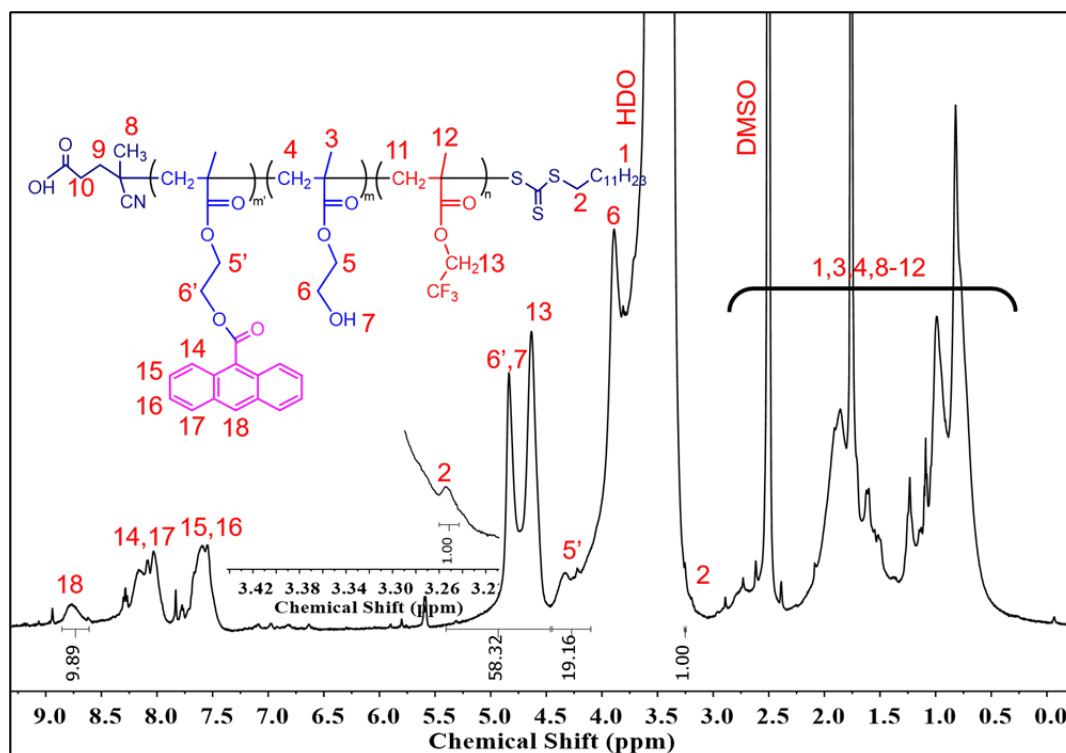


Figure 6.3. ^1H NMR spectrum of the anthracene modified BCP recorded in $\text{DMSO-}d_6$.

An overview of the macro-RAFT, block copolymer and modified BCP prepared are shown in **Table 6.1**.

6.3.3. FTIR analysis of polymers

The preparation of the BCP-TAD adduct via a DA reaction was characterized via IR analysis in ATR mode. The FTIR spectra of the PHEMA-*b*-PTFEMA BCP, the anthracenyl modified BCP, and the bisTAD derived BCP are shown in **Figure 6.4**. The appearance of the characteristic absorption peak at 1790 cm^{-1} due to imide carbonyl stretching of the final DA adduct (as shown in the structure) confirmed the incorporation of the TAD derivative within the BCP. Further, on reaction with bisTAD, the reduction in the absorbance of the peak appearing at 734 cm^{-1} (corresponding to the C-H bending vibration), indicates that the anthracenyl functionality (of BCP) undergo DA conjugation with TAD via its C₉ and C₁₀ centre (as shown in the structure).

Table 6.1. An overview of all polymers

Sample Code	Feed ratio	M_n (g/mol)		Number of HEMA unit/polymer chain	Number of anthracenyl unit/polymer chain	% of anthracenyl grafting w.r.t HEMA
		$M_{n, \text{theo}}$	$M_{n, \text{NMR}}$			
PHEMA ₅₀ (macro-RAFT)	HEMA:RAFT:ABCVA (75:1:0.25)	7500	7000	50	-	-
PHEMA _{50-b} - PTFEMA ₂₀	TFEMA:macro-RAFT:ABCVA (50:1:0.25)	10900	10400	50	-	-
PTFEMA _{20-b} - PHEMA ₃₂ - Anthracene ₁₈	BCP:DCC:DMAP:ACA (1:50:5:50)	21500	13900	32	18	36

^a Calculated gravimetrically.

$$M_{n, \text{theo}} = \left(\frac{[M]_0}{[RAFT]} \times M_{\text{monomer}} \times X \right) + M_{\text{RAFT}}$$

Where,

$[M]_0$ = Initial monomer concentration; [RAFT] = RAFT concentration.

M_{monomer} = Molecular weight of monomer.

M_{RAFT} = Molecular weight of RAFT agent; $M_{n, \text{Theo}}$ of the macro-RAFT agent.

X = % monomer conversion

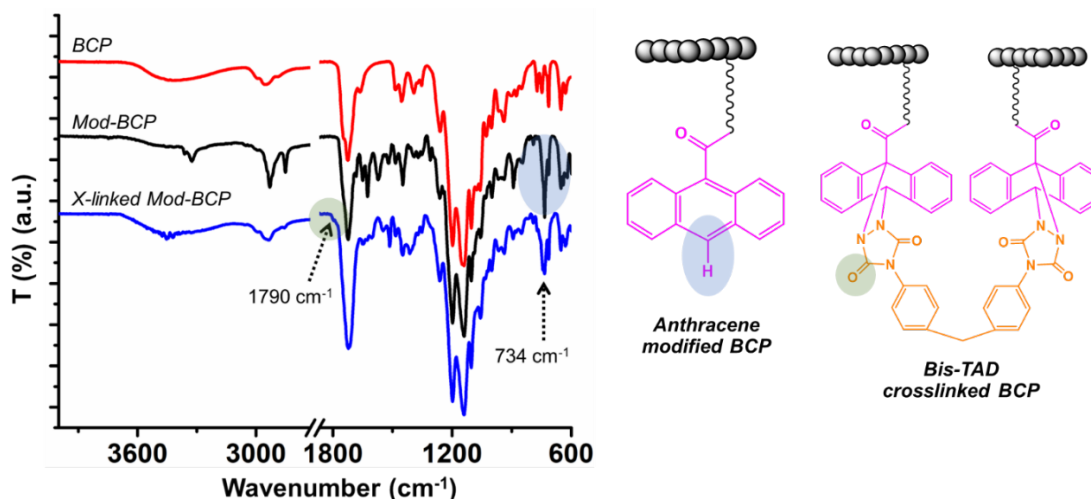


Figure 6.4. FTIR spectra of the BCP, anthracenyl-modified BCP, and TAD-derived BCP.

6.3.4. Differential scanning calorimetry (DSC) analysis

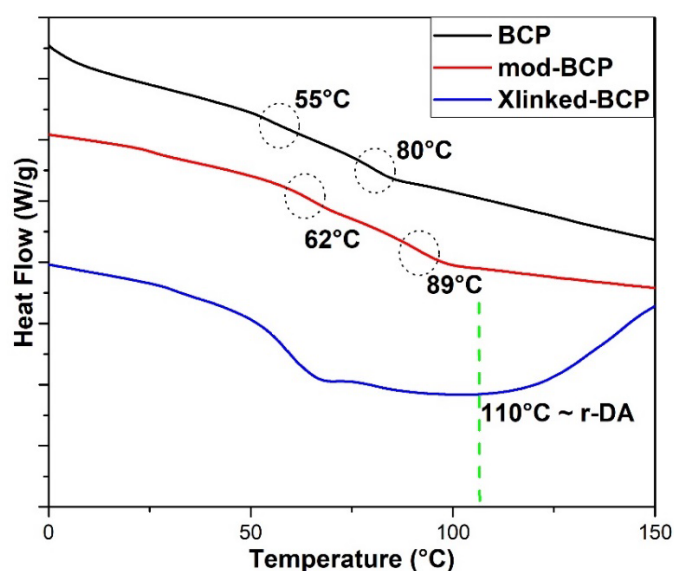


Figure 6.5. DSC thermogram of BCP, modified BCP and crosslinked modified BCP.

Figure 6.5 shows the DSC thermograms of the pristine BCP, anthracenyl modified BCP, and bisTAD derived DA network. The T_g of the PHEMA block and the PTFEMA block in the BCP appear at 55 °C and 80 °C, respectively. The presence of two distinct T_g 's indicates successful BCP formation. On modification with anthracenyl units, the T_g of both the blocks in the BCP shifted to a higher temperature of 62 °C and 89 °C. This indicates the successful incorporation of the anthracenyl groups into the

BCP which restricts segmental mobility due to the bulky nature of the anthracenyl group. Further, in the DSC thermogram of the bisTAD crosslinked BCP, the broad endotherm starting at ≈ 110 °C may be attributed to the retro-DA temperature, i.e. the onset temperature at which the anthracenyl-TAD DA conjugates cleave. [28]

6.3.5. Water contact angle (WCA) analysis

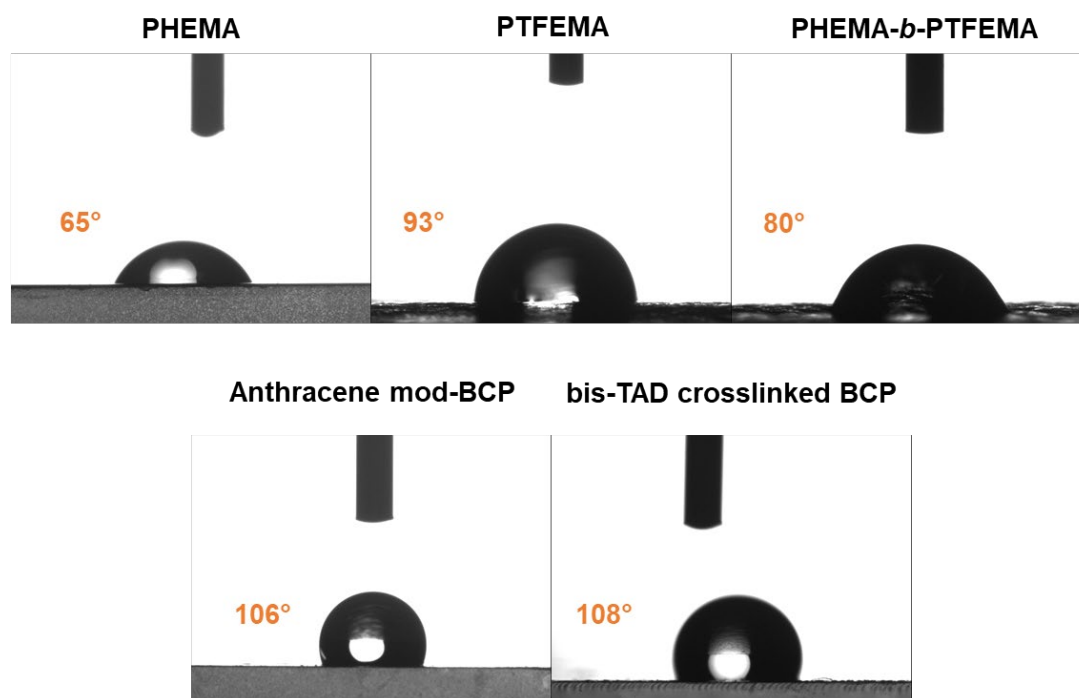


Figure 6.6. Water contact angle analysis of the homopolymers, BCP, modified BCP and crosslinked modified BCP.

The hydrophobic nature of the homopolymers, BCP, modified BCP with anthracenyl moiety, and the bisTAD crosslinked polymer was elucidated from water contact angle (WCA) measurements. A drop of water is placed on the individual polymer surfaces coated over a glass plate, and the WCA values were determined within a duration of ~ 10 sec. **Figure 6.6** shows the images of the water droplets over the polymer film and their WCA value. As shown in **Table 6.2**, it can be observed that the WCA of BCP decreased compared to the homopolymer PTFEMA, which can be attributed to the presence of hydrophilic HEMA units in the BCP. It is observed that the WCA values of the anthracenyl modified BCP increased significantly to 106°

compared to the pristine BCP (WCA = 80°). Interestingly, there is no significant change in the WCA value of the modified polymer after crosslinking with bisTAD.

Table 6.2. Summary of Water contact angle analysis

Sample	Contact Angle
PHEMA	65°
PTFEMA	93°
PHEMA- <i>b</i> -PTFEMA	80°
PHEMA- <i>b</i> -PTFEMA-Anthracene modified BCP	106°
bisTAD Crosslinked BCP	108°

6.3.6. Self-healing analysis

The self-healing characteristics of the bisTAD derived DA crosslinked BCP was studied via AFM analysis. As evidenced by the DSC analysis, the endotherm due to retro-DA reaction appears within the range of ≈ 110 -130°C. The crosslinked BCP was dissolved in DMF by heating at the retro-DA temperature and coated over a glass surface via the drop-casting method, followed by evaporation. Next, the dried polymer surface was deliberately notched using a razor blade with an initial scratch depth of ≈ 2.60 μm , as evidenced by AFM analysis (**Figure 6.7**). Then the notched polymer surface was heated at 130 °C (retro-DA temperature) (**Figure 6.7**), and its healing characteristics monitored via AFM at different time intervals. Following 30 min of heating at the retro-DA temperature, the notched depth of the healed polymer surface reduced to ≈ 1.60 μm . Further, after 1 h heating, the depth of the scratch reduced to ≈ 1.00 μm . At the retro-DA temperature, the anthracene-TAD DA covalent bonds cleaved and facilitated the mobility of polymer chains to heal the scratch depth. Finally, the healed sample was cooled to r.t to ensure the re-reaction of the cleaved DA functionalities. The scratch was still visible on the surface of the healed bisTAD DA crosslinked polymer, which can be reasoned to its relatively lesser content of DA functionalities (number of anthracenyl (in BCP): TAD units = 18:1).

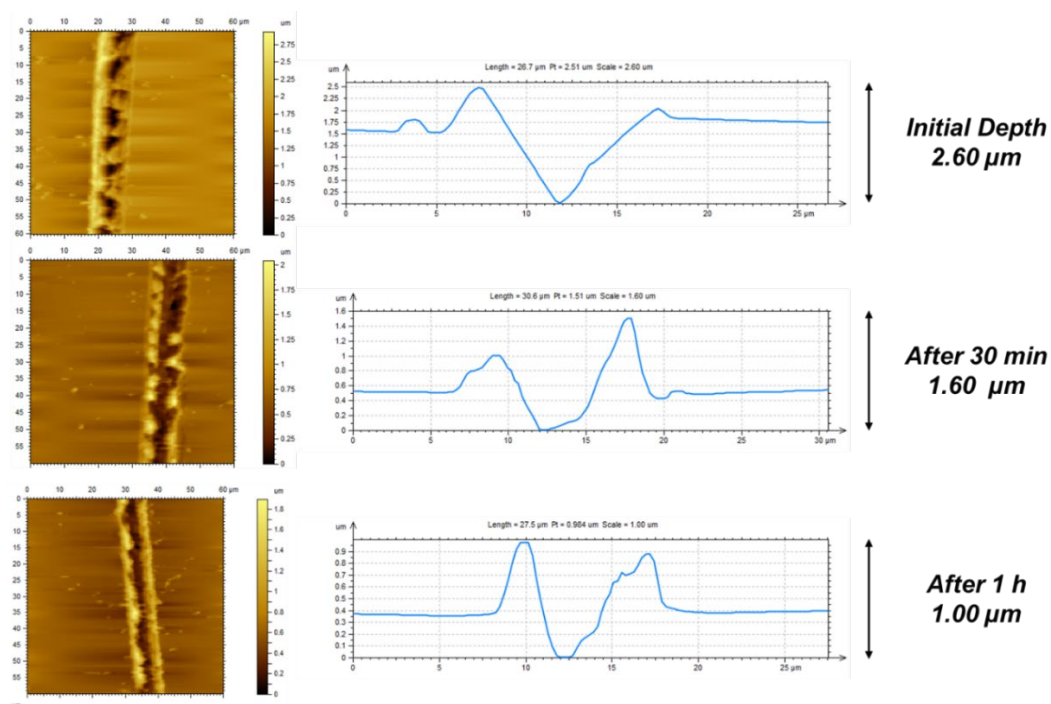


Figure 6.7. Self-healing analysis of crosslinked BCP-TAD conjugate.

6.4. Conclusion

A BCP containing reactive hydroxyl group (HEMA) and a fluorinated species (TFEMA) was successfully synthesized via RAFT polymerization and modified with anthracenyl units. The ultrafast crosslinking of the modified BCP was achieved using a bifunctional TAD via a DA reaction. The emergence of characteristic peaks in the ^1H NMR spectrum and the new absorption bands in the FTIR spectra of the modified BCP validated the successful modification with anthracenyl functionality. Compared to the pristine BCP in the DSC thermogram, the shift in the T_g values towards higher values further confirmed the successful modification of the copolymer and the incorporation of the anthracene functionalities. The thermoreversible nature of the anthracene-TAD DA covalent linkages was also confirmed from the DSC analysis. The thermoreversible behaviour of the anthracene-TAD DA covalent linkages facilitated self-healing characteristics, which was analysed and quantified via AFM analysis. This fluoropolymer with hydrophobic and healing features could be a promising material for specialty coatings and paints applications.

References

- [1] N. Sottos, S. White, I. Bond, Introduction: self-healing polymers and composites, *Journal of The Royal Society Interface* 4(13) (2007) 347-348.
- [2] S.D. Bergman, F. Wudl, Mendable polymers, *Journal of Materials Chemistry* 18(1) (2008) 41-62.
- [3] B.J. Blaiszik, S.L. Kramer, S.C. Olugebefola, J.S. Moore, N.R. Sottos, S.R. White, Self-healing polymers and composites, *Annual review of materials research* 40 (2010) 179-211.
- [4] S. Wang, M.W. Urban, Self-healing polymers, *Nature Reviews Materials* 5 (2020) 1-22.
- [5] C.I. Idumah, Recent advancements in self-healing polymers, polymer blends, and nanocomposites, *Polymers and Polymer Composites* (2020) 0967391120910882.
- [6] N.K. Guimard, K.K. Oehlenschlaeger, J. Zhou, S. Hilf, F.G. Schmidt, C. Barner-Kowollik, Current trends in the field of self-healing materials, *Macromolecular Chemistry and Physics* 213(2) (2012) 131-143.
- [7] Y. Yuan, T. Yin, M. Rong, M. Zhang, Self healing in polymers and polymer composites. Concepts, realization and outlook: A review, *Express Polymer Letters* 2(4) (2008) 238-250.
- [8] P. Cordier, F. Tournilhac, C. Soulié-Ziakovic, L. Leibler, Self-healing and thermoreversible rubber from supramolecular assembly, *Nature* 451(7181) (2008) 977-980.
- [9] E. Formoso, J.M. Asua, J.M. Matxain, F. Ruipérez, The role of non-covalent interactions in the self-healing mechanism of disulfide-based polymers, *Physical Chemistry Chemical Physics* 19(28) (2017) 18461-18470.
- [10] X. Chen, M.A. Dam, K. Ono, A. Mal, H. Shen, S.R. Nutt, K. Sheran, F. Wudl, A thermally re-mendable cross-linked polymeric material, *Science* 295(5560) (2002) 1698-1702.
- [11] Z. Deng, Y. Guo, X. Zhao, P.X. Ma, B. Guo, Multifunctional stimuli-responsive hydrogels with self-healing, high conductivity, and rapid recovery through host-guest interactions, *Chemistry of Materials* 30(5) (2018) 1729-1742.
- [12] S. Nomimura, M. Osaki, J. Park, R. Ikura, Y. Takashima, H. Yamaguchi, A. Harada, Self-healing alkyl acrylate-based supramolecular elastomers cross-linked via host-guest interactions, *Macromolecules* 52(7) (2019) 2659-2668.

- [13] S.L. Banerjee, R. Hoskins, T. Swift, S. Rimmer, N.K. Singha, A self-healable fluorescence active hydrogel based on ionic block copolymers prepared via ring opening polymerization and xanthate mediated RAFT polymerization, *Polymer Chemistry* 9(10) (2018) 1190-1205.
- [14] A. Amalin Kavitha, N.K. Singha, A tailor-made polymethacrylate bearing a reactive diene in reversible diels–alder reaction, *Journal of Polymer Science Part A: Polymer Chemistry* 45(19) (2007) 4441-4449.
- [15] H. Nandivada, X. Jiang, J. Lahann, Click chemistry: versatility and control in the hands of materials scientists, *Advanced Materials* 19(17) (2007) 2197-2208.
- [16] A. Gandini, The furan/maleimide Diels–Alder reaction: A versatile click–unclick tool in macromolecular synthesis, *Progress in Polymer Science* 38(1) (2013) 1-29.
- [17] P.K. Behera, P. Mondal, N.K. Singha, Self-Healable and Ultrahydrophobic Polyurethane-POSS Hybrids by Diels–Alder “Click” Reaction: A New Class of Coating Material, *Macromolecules* 51(13) (2018) 4770-4781.
- [18] N.B. Pramanik, G.B. Nando, N.K. Singha, Self-healing polymeric gel via RAFT polymerization and Diels–Alder click chemistry, *Polymer* 69 (2015) 349-356.
- [19] J. Kötteritzsch, R. Geitner, J. Ahner, M. Abend, S. Zechel, J. Vitz, S. Hoepfener, B. Dietzek, M. Schmitt, J. Popp, Remendable polymers via reversible Diels–Alder cycloaddition of anthracene-containing copolymers with fullerenes, *Journal of Applied Polymer Science* 135(10) (2018) 45916-45930.
- [20] N. Yoshie, S. Saito, N. Oya, A thermally-stable self-mending polymer networked by Diels–Alder cycloaddition, *Polymer* 52(26) (2011) 6074-6079.
- [21] Y. Heo, M.H. Malakooti, H.A. Sodano, Self-healing polymers and composites for extreme environments, *Journal of Materials Chemistry A* 4(44) (2016) 17403-17411.
- [22] Y.-L. Liu, T.-W. Chuo, Self-healing polymers based on thermally reversible Diels–Alder chemistry, *Polymer Chemistry* 4(7) (2013) 2194-2205.
- [23] J.R. Jones, C.L. Liotta, D.M. Collard, D.A. Schiraldi, Cross-Linking and Modification of Poly (ethylene terephthalate-co-2, 6-anthracenedicarboxylate) by Diels–Alder Reactions with Maleimides, *Macromolecules* 32(18) (1999) 5786-5792.
- [24] M. Grigoras, G. Colotin, Copolymerization of a bisanthracene compound with bismaleimides by Diels–Alder cycloaddition, *Polymer international* 50(12) (2001) 1375-1378.

- [25] K. De Bruycker, S. Billiet, H.A. Houck, S. Chattopadhyay, J.M. Winne, F.E. Du Prez, Triazolinediones as highly enabling synthetic tools, *Chemical reviews* 116(6) (2016) 3919-3974.
- [26] O. Roling, K. De Bruycker, B. Vonhören, L. Stricker, M. Körsgen, H.F. Arlinghaus, B.J. Ravoo, F.E. Du Prez, Rewritable polymer brush micropatterns grafted by triazolinedione click chemistry, *Angewandte Chemie International Edition* 54(44) (2015) 13126-13129.
- [27] P. Mondal, G. Jana, P.K. Behera, P.K. Chattaraj, N.K. Singha, Fast “ES-Click” Reaction Involving Furfuryl and Triazolinedione Functionalities toward Designing a Healable Polymethacrylate, *Macromolecules* 53(19) (2020) 8313-8323.
- [28] P. Mondal, G. Jana, P.K. Behera, P.K. Chattaraj, N.K. Singha, A new healable polymer material based on ultrafast Diels–Alder ‘click’ chemistry using triazolinedione and fluorescent anthracyl derivatives: a mechanistic approach, *Polymer Chemistry* 10(37) (2019) 5070-5079.
- [29] Z. Wang, H. Zuilhof, Self-healing fluoropolymer brushes as highly polymer-repellent coatings, *Journal of Materials Chemistry A* 4(7) (2016) 2408-2412.
- [30] Z. Wang, H. Zuilhof, Self-healing superhydrophobic fluoropolymer brushes as highly protein-repellent coatings, *Langmuir* 32(25) (2016) 6310-6318.
- [31] Y. Li, L. Li, J. Sun, Bioinspired self-healing superhydrophobic coatings, *Angewandte Chemie* 122(35) (2010) 6265-6269.
- [32] H. Wang, Y. Xue, J. Ding, L. Feng, X. Wang, T. Lin, Durable, self-healing superhydrophobic and superoleophobic surfaces from fluorinated-decyl polyhedral oligomeric silsesquioxane and hydrolyzed fluorinated alkyl silane, *Angewandte Chemie* 123(48) (2011) 11635-11638.
- [33] H. Zhou, H. Wang, H. Niu, A. Gestos, T. Lin, Robust, self-healing superamphiphobic fabrics prepared by two-step coating of fluoro-containing polymer, fluoroalkyl silane, and modified silica nanoparticles, *Advanced Functional Materials* 23(13) (2013) 1664-1670.
- [34] A.K. Padhan, D. Mandal, Thermo-reversible self-healing in a fluorinated crosslinked copolymer, *Polymer Chemistry* 9(23) (2018) 3248-3261.
- [35] S. Banerjee, B.V. Tawade, B. Améduri, Functional fluorinated polymer materials and preliminary self-healing behavior, *Polymer Chemistry* 10(16) (2019) 1993-1997.

SUMMARY AND CONCLUSIONS



This chapter delineates the outcomes and future scope of the work reported in this thesis

7.1. Summary and Conclusions

This chapter summarizes the conclusions and future perspectives of the work reported in this thesis. In brief, a different class of tailor-made functional fluoropolymers based on fluoroacrylates and fluoromethacrylates were prepared via RAFT polymerization. Their potential applications were explored in various areas ranging from the development of hydrophobic surface coatings, development of hydrophobic self-healing materials, and the development of thin films for dielectric applications. The content of the thesis also examines post-polymerization modification adopting different Diels-Alder (DA) reactions based on furan-maleimide DA coupling as well as anthracene-triazolinedione (TAD) chemistry for the synthesis of novel functional materials. A new multifunctional triblock copolymer, based on a fluoroacrylate, was developed adopting polymerization-induced self-assembly (PISA). The applications of these functional poly(fluoroacrylates) were explored as potential self-healable coatings, hydrophobic dielectric thin films, and specialty functional materials with a fluorescence-active anthracenyl moiety.

In Chapter 3, diblock copolymers (AB-type) based on hybrid POSS moiety (MA*ib*POSS) and a fluorinated monomer (TFEMA) was successfully synthesized via RAFT polymerization. The block copolymers were characterized by ¹H NMR and FT-IR spectroscopic analyses. SEC analysis results indicated controlled molecular weights and the low dispersities of the polymers. The morphology of the BCPs in varying the solvent was studied by preparing BCP coatings from different solvents and observed by SEM and TEM analyses. The BCP thin films showed core-shell type morphology when cast from chloroform, and lamellar type morphology when cast from THF as the solvent. The cluster profiling data from XPS analysis revealed that the PTFEMA segments are located in the shell, and the PMA*ib*POSS segments

resides in the core. Further, the effect of thermal annealing on the coating surface was studied using AFM analysis. Owing to the crystallization of the PMA*ib*POSS block, the surface roughness of the coated BCP film increased from 2.89 nm before annealing to 10.5 nm after annealing at 120 °C. The water contact angle of the BCP also increased to 128° from 115°. The potential application of the BCPs as a hydrophobic coating material for paints and coating application was studied by coating the BCPs over different substrates such as glass, cotton fabric and an aluminium metal plate via dip-coating. The resulting BCP coated substrates showed significantly improved hydrophobicity as determined by WCA measurements.

In Chapter-4, a random copolymer comprising the reactive furfuryl group (FMA) and a fluorinated segment (TFEMA) was synthesized via RAFT polymerization. Further, the copolymer was successfully modified with different molar contents of maleimide functionalized POSS (POSS-M) via the furan-maleimide DA reaction. The emergence of new peaks in the ¹H NMR and FT-IR spectra, compared to the pristine copolymer, and its POSS-M derived DA polymers confirmed successful modification. This was further corroborated by the increase in the molecular weight as determined by SEC analyses. The significant shift in the *T_g* values (for DA copolymers) towards higher values as evidenced in the DSC analysis results, confirmed its successful derivation with POSS-M functionalities. Also, the thermoreversible nature of the furan-maleimide DA covalent linkages was confirmed from the DSC analysis. Interestingly, the WCA of the DA hybrid copolymer(s), in comparison to the pristine copolymer (WCA ≈101°), was increased significantly on modification with hydrophobic POSS molecules (WCA ≈135°). This increase in hydrophobicity is attributed to the rise in the surface roughness values, as observed in the AFM analysis. In addition, to the increase in hydrophobicity, the copolymers exhibited good self-

healing property with efficiencies of ~78 % due to the dynamic DA covalent bonds between the reactive furan group in the copolymer and the maleimide group in POSS-M. Interestingly, there was a remarkable increase in thermal stability, as evidenced by the TGA analysis. Such POSS-derived DA fluoropolymer conjugates with exceptional thermal stability, ultra-hydrophobic characteristics, and excellent self-healing features open a new direction for specialty high-temperature-resistant materials, paints and coatings applications.

In Chapter-5, a new class of triblock copolymer (TBCP) comprising sodium 4-vinylbenzene sulfonate (SS), butyl acrylate (BA), and 2,2,2-trifluoroethyl acrylate (TFEA) was synthesized via the PISA process using RAFT polymerization. The ^1H NMR results showed the amphiphilic nature of the prepared TBCP. The distinct T_g of the different blocks and the shift in the DSC traces confirmed block copolymer formation. The TGA thermogram showed the reduction in the water uptake properties after incorporation of the fluoroacrylate block which is good for the proposed membrane application. The morphology of the diblock and the triblock copolymers was studied by TEM analysis. The TBCP copolymer showed a core-shell morphology with fluoro block in the core. Interestingly, the prepared TBCP films showed remarkable mechanical properties with 1500% elongation and formed a transparent thin film upon stretching. Moreover, the TBCP exhibited excellent hydrophobicity having a water contact angle of $\sim 122^\circ$. The dielectric properties of the TBCP films were studied by AC-impedance spectroscopy. The presence of a broad peak in the low-frequency range of the dielectric permittivity curve indicated the dielectric nature of the TBCP thin film. The prepared TBCP can be used in capacitors, potential piezoelectric harvesting applications and as actuators.

In Chapter-6, a BCP containing reactive hydroxyl groups (HEMA) and a

fluorinated species (TFEMA) was successfully synthesized via RAFT polymerization and modified with anthracenyl units. The incorporation of a bifunctional TAD facilitated an ultrafast crosslinking via the DA reaction in the modified BCPs. The successful modification of the BCP with anthracenyl units was confirmed by the emergence of characteristic peaks in the ^1H NMR spectrum and with new absorption bands in the FTIR spectra of the modified BCP. The shift in the T_g values towards higher temperature in the DSC thermogram of the BCP compared to the pristine confirmed successful modification of the copolymer and the incorporation of the anthracene functionalities. The thermoreversible nature of the anthracene-TAD DA covalent linkages was also confirmed from the DSC analysis. The self-healing characteristics facilitated by the thermoreversible behaviour of the anthracene-TAD DA covalent linkages was analysed via AFM analysis. This fluoropolymer with hydrophobic and healing features could be promising for specialty coatings and paints applications.

7.2. Contribution of the thesis

This thesis reports the preparation of a new class of functional fluoropolymers based on fluoroacrylates bearing different functionalities such as POSS, anthracene, and sulfonate moieties, prepared by RAFT polymerization, and their potential application in the development of hydrophobic surface coating and self-healable hydrophobic thin film materials.

7.3. Future scope of the thesis

In this thesis work preparation of different types of functional fluoropolymers based on fluoroacrylates/fluoromethacrylates along with different comonomers via RAFT polymerization and their applications in the development of hydrophobic surface coating and self-healable hydrophobic thin film materials were studied. This opens up future opportunities for the development of fluoropolymer coatings based on FA/FMA with tunable properties and speciality functions such as self-cleaning surfaces with self-healing property, chemical and environmental resistant fluorescence micro-pattern designing, conductive inks and sensor applications.

List of Publications

- **P. Siva**, P. Mandal, T. Becker, R. Hoogenboom, AB Lowe, NK Singha, *Self-Healing Ultrahydrophobic POSS-Functionalized Fluorinated Copolymer via RAFT Polymerization and Dynamic Diels-Alder Reaction*, **Polymer Chemistry**, (2021), DOI: <https://doi.org/10.1039/D0PY01522A>.
- **P. Siva**, A. Chakrabarty, P. Mandal, R. Hoogenboom, AB Lowe, NK Singha, *POSS and fluorine containing nanostructured block copolymer; Synthesis via RAFT polymerization and its application as hydrophobic coating material*, **European Polymer Journal**, 131 (2020), 51-58.
- **P. Siva**, P. Mandal, SK Raut, NK Singha, polyhedral oligomeric silsesquioxane (POSS) polymer nanocomposites, **Elsevier**, 2020. (Accepted for publication)
- **P. Siva**, P. Mandal, AB Lowe, NK Singha, *Self-healable Hydrophobic Anthracenyl Functionalized Fluorous Block Copolymer via RAFT Polymerization and Diels-Alder Reaction using 1,2,4-triazoline-3,5-dione (TAD) Derivative (Under communication)*.
- **P. Siva**, S. Samanta, AB Lowe, NK Singha, *A Multifunctional Triblock Copolymer Based on Fluoroacrylate via Polymerization-Induced Self-Assembly (PISA); Synthesis and Application as A Thin Film Dielectric Material (Under preparation)*.
- A. Chakrabarty, **P. Siva**, NG Kang, JW Mays, NK Singha, *Designing superhydrophobic surface based on fluoropolymer–silica nanocomposite via RAFT-mediated polymerization-induced self-assembly*, **Journal of Polymer Science Part A: Polymer Chemistry**, 56 (2018) 266–275.
- P. Mandal, **P. Siva**, S. Choudhury, N. K. Singha, *Tuning properties and morphology in high vinyl content SBS block copolymer, a thermoplastic elastomer via thiol-ene modification*. **Rubber Chemistry and Technology**, 90 (2017), 550-561.
- BP Koiry, **P. Siva**, C. Soumyadip, N. k. Singha, *Syntheses, and morphologies of fluorinated diblock copolymer prepared via RAFT polymerization*. **Journal of Fluorine Chemistry**, 189 (2016), 51-58.
- A. Chakrabarty, **P. Siva**, K. Naskar, N. K. Singha, *Nanoclay Stabilized Pickering Miniemulsion of Fluorinated Copolymer with Improved Hydrophobicity via RAFT Polymerization*. **RSC Advances**, 6 (2016), 34987-34995.

Curriculum Vitae

Siva Ponnupandian

sivaponnupandian@gmail.com

+91-6374014076



Academic qualification:

Course	Name of the Institution	Board of Study	Month & Year of Passing	CGPA (Out of 10)
PhD.	Indian Institute of Technology Kharagpur, India and Curtin University, Australia	Thesis Submitted by November 2020		
M. Tech. (Polymer Technology)	Kamaraj College of Engineering and Technology, Virudhunagar.	Anna University, Chennai.	June 2014	8.9
B. Tech. (Polymer Technology)	Kamaraj College of Engineering and Technology, Virudhunagar.	Anna University, Chennai.	April 2012	7.46

Scholarships Received:

- **Senior Research Fellowship** funded by **Council of Scientific & Industrial Research (CSIR), India**, from August 2014 till May 2017.
- **Curtin International Postgraduate Research Scholarship (CIPRS) and Research Stipend Scholarship** funded by the Office of research and Development, Curtin University, Perth, Western Australia from October 2017 till September 2018.

Publication details:

Publications during PhD Tenure

- **P. Siva**, P. Mandal, T. Becker, R. Hoogenboom, AB Lowe, NK Singha, *Self-Healing Ultrahydrophobic POSS-Functionalized Fluorinated Copolymer via RAFT Polymerization and Dynamic Diels-Alder Reaction*, **Polymer Chemistry**, (2021), DOI: <https://doi.org/10.1039/D0PY01522A>.
- **P. Siva**, A. Chakrabarty, P. Mandal, R. Hoogenboom, AB Lowe, NK Singha, *POSS and fluorine containing nanostructured block copolymer; Synthesis via RAFT polymerization and its application as hydrophobic coating material*, **European Polymer Journal**, 131 (2020), 51-58.
- A. Chakrabarty, **P. Siva**, NG Kang, JW Mays, NK Singha, *Designing superhydrophobic surface based on fluoropolymer-silica nanocomposite via RAFT-mediated polymerization-induced self-assembly*, **Journal of Polymer Science Part A: Polymer Chemistry**, 56 (2018) 266-275.
- P. Mandal, **P. Siva**, S. Choudhury, N. K. Singha, *Tuning properties and morphology in high vinyl content SBS block copolymer, a thermoplastic elastomer via thiol-ene*

modification. Rubber Chemistry and Technology, 90 (2017), 550-561.

- BP Koiry, **P. Siva**, C. Soumyadip, N. k. Singha, *Syntheses, and morphologies of fluorinated diblock copolymer prepared via RAFT polymerization. Journal of Fluorine Chemistry*, 189 (2016), 51-58.
- A. Chakrabarty, **P. Siva**, K. Naskar, N. K. Singha, *Nanoclay Stabilized Pickering Miniemulsion of Fluorinated Copolymer with Improved Hydrophobicity via RAFT Polymerization. RSC Advances*, 6 (2016), 34987-34995.
- **P. Siva**, P. Mandal, R. Hoogenboom, AB Lowe, NK Singha, *Self-healable Hydrophobic Anthracenyl Functionalized Fluorous Block Copolymer via RAFT Polymerization and Diels-Alder Reaction using 1,2,4-triazoline-3,5-dione (TAD) Derivative (Under communication)*.
- **P. Siva**, S. Samanta, AB Lowe, NK Singha, *A Multifunctional Triblock Copolymer Based on Fluoroacrylate via Polymerization-Induced Self-Assembly (PISA); Synthesis and Application as A Thin Film Dielectric Material (Under preparation)*.

Other Publications

- B. Meenarathi, **P. Siva**, S. Palanikumar, L. Kannammal, R. Anbarasan, *Synthesis, characterization, and drug release activity of poly (ϵ -caprolactone)/ Fe_3O_4 -alizarinred nanocomposites. Nanocomposites*, 2 (2016), 98-107.
- B. Meenarathi, **P. Siva**, M. Jeyapriya, R. Baskaran, R. Anbarasan. *Synthesis, Characterization, Catalytic Reduction, and Splinting Activity of Poly(ϵ -caprolactone-co-morpholine)/Ag Nanocomposite. Advances in Polymer Technology*, (2016), 21678.
- S. Palanikumar, **P. Siva**, B. Meenarathi, L. Kannammal, R. Anbarasan. *Effect of Fe_3O_4 on the sedimentation and structure-property relationship of starch under different pHs. International Journal of Biological Macromolecules*, 67 (2014), 91-98.

Book Chapters:

- **P. Siva**, P. Mandal, SK Raut, NK Singha, polyhedral oligomeric silsesquioxane (POSS) polymer nanocomposites, **Elsevier**, 2020. (Accepted for publication)